Quantum Mechanical Assessment of Stereoelectronic Profile of Phosphines and N-Heterocyclic Carbenes and Applications in Grubbs Olefin Metathesis Catalysis

Thesis submitted to the
UNIVERSITY OF KERALA
for the award of Degree of

DOCTOR OF PHILOSOPHY
in Chemistry under the Faculty of Science

By

JOMON MATHEW

Computational Modeling and Simulation Section
Process Engineering and Environmental Technology Division
National Institute for Interdisciplinary Science and Technology (CSIR)
Thiruvananthapuram – 695 019
Kerala, India

2011

DECLARATION

I hereby declare that the Ph.D. thesis entitled "**Quantum Mechanical Assessment of Stereoelectronic Profile of Phosphines and N-Heterocyclic Carbenes and Applications in Grubbs Olefin Metathesis Catalysis**" is an independent work carried out by me at the Computational Modeling and Simulation Section, Process Engineering and Environmental Technology Division, National Institute for Interdisciplinary Science and Technology (NIIST-CSIR), Trivandrum, under the supervision of Dr. C. H. Suresh and it has not been submitted elsewhere for any other degree, diploma or title.

Jomon Mathew

National Institute for Interdisciplinary Science & Technology
(Formerly Regional Research Laboratory)
(Council of Scientific & Industrial Research) India

Industrial Estate P.O., Pappanamcode, Trivandrum – 695 019

Dr. Cherumuttathu H. Suresh
Scientist

E-Mail: sureshch@gmail.com
Phone: 0471 – 2515264, 9446552294

April 6, 2011

CERTIFICATE

This is to certify that the work embodied in the thesis entitled "**Quantum Mechanical Assessment of Stereoelectronic Profile of Phosphines and N-Heterocyclic Carbenes and Applications in Grubbs Olefin Metathesis Catalysis**" has been carried out by Mr. Jomon Mathew under my supervision and guidance at the Computational Modeling and Simulation Section, Process Engineering and Environmental Technology Division, National Institute for Interdisciplinary Science and Technology (NIIST-CSIR), Trivandrum and this work has not been submitted elsewhere for a degree.

Dr. C. H. Suresh
(Thesis Supervisor)

ACKNOWLEDGEMENT

I wholeheartedly extend my thanks to all my friends at NIIST.

I am deeply grateful to my family for their constant love and care.

Jomon Mathew

Contents

List of Tables

List of Figures

List of Schemes

List of Abbreviations

CI	: Configuration Interaction
CCSD	: Coupled Cluster Single and Double
DFT	: Density Functional Theory
ECP	: Effective Core Potential
GGA	: Generalized Gradient Approximation
G03	: Gaussian 03
HF	: Hartree-Fock
HK	: Hohenberg-Kohn
LDA	: Local-Density Approximation
MP	: Moller-Plesset Perturbation Theory
CC	: Coupled Cluster
MESP	: Molecular Electrostatic Potential
MO	: Molecular Orbital
ONIOM	: Our N-layered Integrated Molecular Orbital + Molecular Mechanics
PES	: Potential Energy Surface
STO	: Slater-Type Orbitals
GTO	: Gaussian-Type Orbitals
DZ	: Double Zeta
TS	: Transition State
XC	: Exchange Correlation
QSAR	: Quantitative Structure Activity Relationship
LKB	: Ligand Knowledge Base
QM	: Quantum Mechanics
MM	: Molecular Mechanics
UFF	: Universal Force Field
MD	: Molecular Dynamics
NHC	: N-Heterocyclic Carbene
G1R	: First Generation Grubbs Catalyst
G2R	: Second Generation Grubbs Catalyst
IMes	: N,N-bis(mesityl)imidazol-2-ylidene
H_2IMes	: N,N-bis(mesityl)-4,5-dihydroimidazol-2-ylidene
TEP	: Tolman Electronic Parameter

Preface

With the development of transition metal based Schrock catalysts and Grubbs catalysts, olefin metathesis has emerged as one of the most powerful tool in organic synthesis. Olefin metathesis reaction is successfully employed for the synthesis of wide variety of like fused ring systems, bridged bicycloalkenes, alkaloids, heterocyclic compounds, polymers, biologically important compounds like m macrolactones interlocked macrocyclic compounds etc.

Computational chemistry is one of the most rapidly expanding and exciting area of scientific endeavours. Nowadays quantum chemistry has provided the most important approach to study a wide range of chemical problems, including enzymology, thermochemistry, material science, catalysis and reaction mechanisms.

In this research, we have employed the quantum chemical methods to develop stereoelectronic descriptors for phosphines (PR_3) and N-heterocyclic carbenes (NHC). These descriptors are applied for the assessment of stereoelectronic and structural effects on the activity of first generation (G1R) and second generation (G2R) Grubbs olefin metathesis catalysts. The thesis entitled "**Quantum Mechanical Assessment of Stereoelectronic Profile of Phosphines and N-Heterocyclic Carbenes and Applications in Grubbs Olefin Metathesis Catalysis**" is divided into four chapters.

The first part of the Chapter 1 summarizes the development of Schrock and Grubbs olefin metathesis catalysts and gives a brief account of various experimental and theoretical studies to introduce the mechanism and activity of these catalysts. The second part of the Chapter 1 gives a brief account of various computational methods and their theoretical basis.

Chapter 2 of the thesis deals with the development of stereoelectronic descriptors of phosphines and N-heterocyclic carbene (NHC) ligands. Molecular electrostatic potential

(MESP) based steric and electronic parameters for free phosphines are developed using Quantum Mechanical (QM) and hybrid Quantum Mechanical-Molecular Mechanical (QM-MM) methods. Based on these parameters, phosphine ligands are classified as electron donating and electron withdrawing with respect to the steric and electronic effects. Further, MESP-based descriptor for the electronic effect of NHCs is established.

In the third chapter, the role of steric and electronic effects of phosphines on G1R and NHCs on G2R catalysis is analyzed. MESP-based quantum chemical discriptors for the steric and electronic effects of phosphines and NHCs in the active form as well as in the olefin coordinated complex for various G1R and G2R catalyst systems were developed. These descriptors were used to assess the stereoelectronic control of phosphines and NHCs in first and second generation Grubbs olefin metathesis catalysis.

A detailed mechanistic investigation on the decomposition of a Grubbs second generation olefin metathesis catalyst is the subject of fourth chapter. Various factors leading to the decomposition of Grubbs catalyst is analyzed for the designing of catalyst systems which can withstand the tendecy of decomposition.

Chapter 1

Introduction

Part A - Olefin Metathesis Catalysts
&
Part B - Computational Chemistry

Part A - Olefin Metathesis Catalysts

1.1 Olefin Metathesis Catalysts

1.1.1 Olefin Metathesis

Olefin metathesis is an organic reaction in which the exchange of double bonds between olefins takes place. A schematic representation of olefin metathesis reaction between two olefins is depicted below (Scheme 1.1).
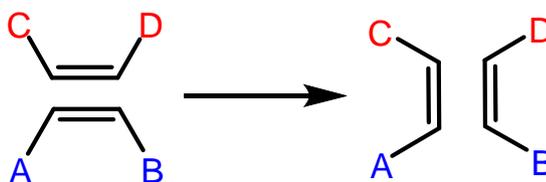
Scheme 1.1 Olefin metathesis reaction.

A direct breaking and reformation of CC double bond as depicted in Scheme 1.1 is not feasible and hence the development of catalysts for olefin metathesis became a major concern among researchers for utilizing the great synthetic potential of metathesis. A number of chemists made major contributions to the development of metathesis catalysts and their applications; but the crucial progress in this area was made by Grubbs and Schrock. In 2005, Nobel Prize in Chemistry was awarded to Yves Chauvin, Robert H. Grubbs and Richard R. Schrock for the development of olefin metathesis catalysts and for the elucidation of the mechanism for olefin metathesis. Yves Chauvin in 1972 proposed a plausible mechanism for olefin metathesis which involves the reaction between a metal carbene complex and olefin [Hérrison and Chauvin 1971] (Scheme 1.2). The metal carbene reacts with an olefin in a concerted way and forms a metallacyclobutane ring. Subsequent ring opening of metallacyclobutane could produce

either the initial reactants or a new olefin and a metal carbene. The reaction is characterized by a series of reversible steps, which lead to a thermodynamic equilibrium of the reaction products.
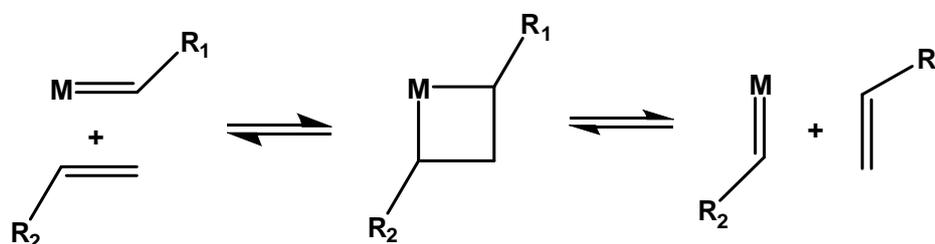
Scheme 1.2 Mechanism of olefin metathesis proposed by Chauvin.

Richard R. Schrock was awarded the Nobel Prize for being the first to discover an alkylidene complex for olefin metathesis and for developing a whole family of tungsten and molybdenum alkylidene complexes [Schrock *et al*. 1980; Schrock *et al*. 1991] (Figure 1.1a). Robert H. Grubbs was honored with the Nobel Prize for the development of ruthenium based olefin metathesis catalysts, which are highly tolerant to functional groups and moisture and showed activity similar to that of Schrock catalysts (Figure 1.1b).

M = Mo, W
R, Ar - bulky substituents

L = Phosphine,
N-heterocyclic carbene

(a)   **(b)**
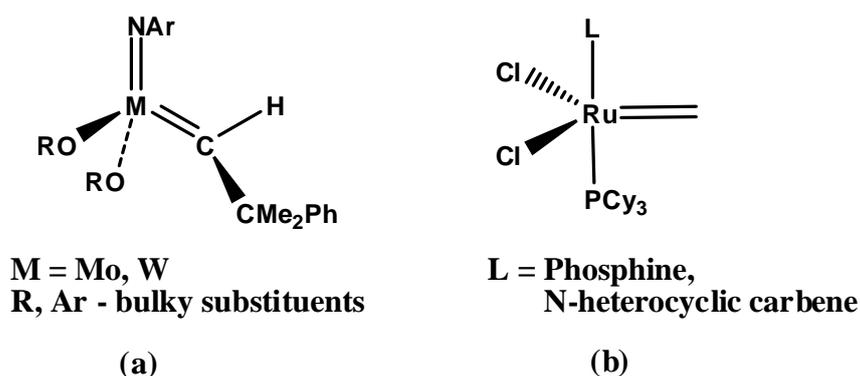
Figure 1.1 (a) Schrock catalyst (b) Grubbs catalyst

The metathesis reaction is a versatile tool with a large variety of applications in both polymer chemistry and organic synthesis. The basic transformation reactions include Ring Opening Metathesis polymerization (ROMP), Ring Closing Metathesis

(RCM), Acyclic Diene Metathesis Polymerization (ADMET), Ring Opening Metathesis

(ROM) and Cross Metathesis (CM) (Scheme 1.3).

Ring closing metathesis   **Ring opening metathesis polymerization**

Cross metathesis   **Acyclic Diene Metathesis Polymerization**
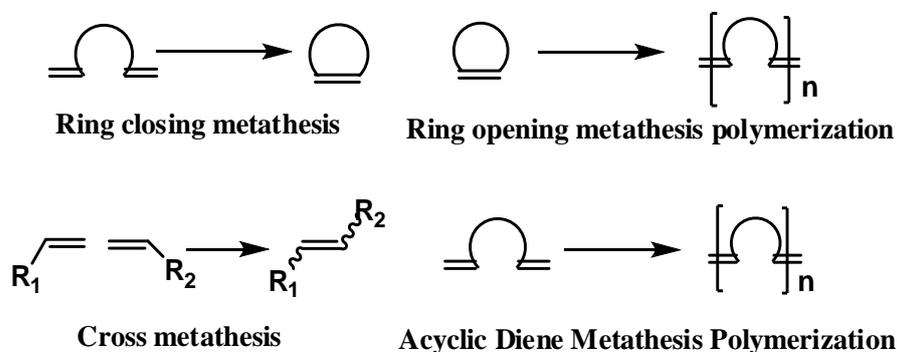
Scheme 1.3 Fundamental olefin metathesis reactions.

These metathesis reactions are successfully employed for the synthesis of wide

variety of organic compounds which includes fused ring systems, bridged

bicycloalkenes, alkaloids (pyrrolidine, pyrrolizidine, piperidine, indolizidine and

quinolizidine), heterocyclic compounds, polymers, biologically important compounds

like macrolactones, antibiotic macrolides, interlocked macrocyclic compounds like

catenanes etc.

1.1.2 Evolution of High Oxidation State Schrock Catalysts

The introduction of olefin polymerization catalyst based on transition metal salts

and main group alkylating agents by Karl Zeigler and Giulio Natta in early 1950s

initiated the development of transition metal based catalysts for molecular catalysis

[Ziegler *et al*. 1955; Natta *et al*. 1964]. In 1956, Herbert S. Eleuterio observed the

formation of polyethylene from propylene in the presence of a heterogeneous Mo catalyst

and proposed that propylene was initially converted into 2-butene and ethylene, followed

by the polymerization of ethylene [Ivin and Mol 1997]. Robert L. Banks and Grant C.

Bailey, of Phillips Petroleum in 1964 reported the formation of ethylene and butane from

the disproportionation of propylene using molybdenum hexacarbonyl supported on

alumina [Banks and Bailey 1964]. In 1967, Nissim Calderon and his group at Goodyear

Tire & Rubber observed the metathesis of 2-pentene in the presence of a catalyst based

on tungsten hexachloride, ethanol and $EtAlMe_2$. They found that one carbon of the

double bond of one olefin exchanges its place with one carbon of the double bond of

other olefin and named the reaction as "Olefin Metathesis" which had been formerly

called "olefin disporportionation" [Calderon *et al.* 1967]. The initial assumption on the

mechanism of olefin metathesis consists of the formation of a cyclobutane intermediate

complexed to metal [Calderon *et al.* 1968]. But in 1971 Yves Chauvin and Jean-Louis

Hérisson from French Petroleum Institute suggested that olefin metathesis is initiated by

a metal carbene. The metal carbene reacts with olefin leading to the formation of

metallacyclobutane intermediate which breaks up to form new olefin and new metal

carbene and propagates the reaction [Hérrison and Chauvin 1971]. This mechanism was

more accepted and directed the researchers to focus on metal carbenes. Supporting

Chauvin's mechanism Robert H Grubbs in 1973 succeeded in isolating the metallacycle

with   platinum   by   the   reaction   of   dilithiobutane   with   *cis*-

bis(triphenylphosphine)dichloroplatinum(II) [Biefeld *et al*. 1973]. In 1974 Charles P.

Casey and Terry J. Burkhardt from the University of Wisconsin, observed the formation

of a new olefin 1,1-diphenylethene from the reaction of isobutene and a metal carbene

(diphenylcarbene)pentacarbonyltungsten which was the first implementation of metal

carbenes in olefin metathesis [Casey and Burkhardt 1974]. In 1975 Thomas J. Katz and

coworkers analyzed the kinetics of olefin metathesis reaction and substantiated the

carbene mechanism [Katz and McGinnis 1975]. Tebbe reported the fully characterized

Tebbe complex in 1978 which could catalyze the degenerate metathesis of terminal

olefins [Tebbe *et al*. 1978; Tebbe *et al*. 1979; Grubbs 2003] (Scheme 1.4). Later they

reported the synthesis of Titanium-cyclobutane species [Tebbe *et al*. 1980].
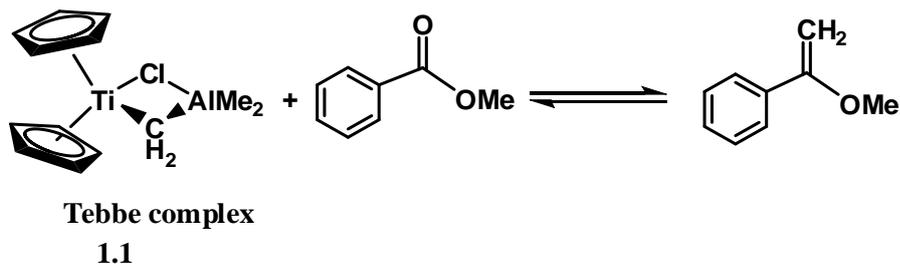
Tebbe complex
1.1

Scheme 1.4 Metathesis with Tebbe complex.

The discovery of Tebbe complex triggered the metal carbene chemistry for the synthesis of practical catalysts. Various tantalum alkylidene complexes were synthesized and tested for their use as metathesis catalysts, but were found to be inactive even though they form tantalacyclobutane intermediates [McLain *et al*. 1979]. In 1980 Schrock and coworkers reported the metathesis of *cis*-2-pentene using the tantalum complex Ta(CH-t-Bu)Cl(PMe$_3$)(O-t-Bu)$_2$. This was the first report on the metathesis of simple olefin using a high oxidation state alkylidene complex and identified alkoxide ligands as suitable ligand systems for olefin metathesis catalysts [Schrock *et al*. 1980; Rocklage *et al*. 1981; Schrock 1995]. Development of this well characterized catalyst offered more insights into the metathesis reaction and in later years Mo, W and Re based alkylidenes catalysts were synthesized by various groups for olefin metathesis reaction [Oskam *et al*. 1993; Schrock *et al*. 1991; Fox *et al*. 1993; Bell *et al*. 1994; de la Mata *et al*. 1998; Blosch *et al*. 1991; de la Mata *et al*. 1996; Vaughan *et al*. 1995; Cai *et al*. 1996; Schofield *et al*. 1991]. Among these the most effective and versatile class of catalysts are Mo and W based imido alkylidene bisalkoxide complexes M(NR)(CHR')(OR")$_2$ (Figure 1.2). One advantage of Mo versus W is that molybdenum intermediates generally lose olefin more readily than the tungsten intermediates and consequently show better activity at lower temperatures.

1.2   **1.3**
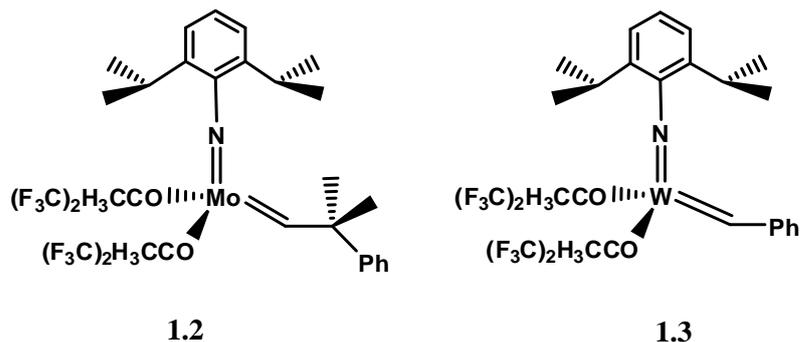
Figure 1.2 Mo and W based olefin metathesis catalyst.

In recent years efficient chiral Mo catalysts were synthesized by the incorporation of bidendate alkoxide ligands and various imido ligands for many enantioselective ring opening, ring closing and cross metathesis reactions [La *et al.* 1998; Zhu *et al.* 1999] (Figure 1.3).

1.4   **1.5**
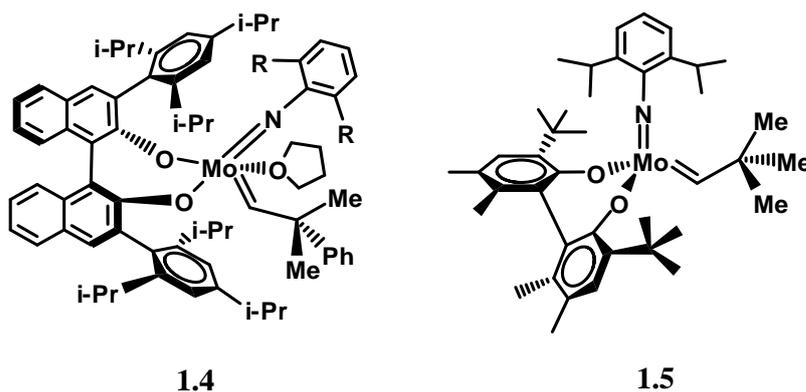
Figure 1.3 Chiral Mo catalysts for olefin metathesis.

1.1.3 Development of Grubbs Catalysts

Along with the ill-defined Mo and W based heterogeneous olefin metathesis catalysts, RuCl$_3$ in ethanol was found to be an initiator for metathesis [Michelotti and Keaveney 1965; Rinehart and Smith 1965]. Earlier efforts for the development of metathesis catalysts were focused on the development of high oxidation state metal carbenes from early transition metals and therefore it took three decades to synthesize a well characterized Ru based olefin metathesis catalyst. In 1992 Grubbs and co-workers reported the synthesis of first metathesis active 16 –electron Ru(II) alkylidene complex

$(PPh_3)_2Cl_2Ru=CH-CH=CPh_2$ from $RuCl_2(PPh_3)_3$ [Nguyen *et al*. 1992] (Scheme 1.5). This

catalyst was found to be effective in ring opening metathesis polymerization (ROMP) of

norbornene and was remarkably stable to water, acid and many other functional groups.

1.6   **1.7**
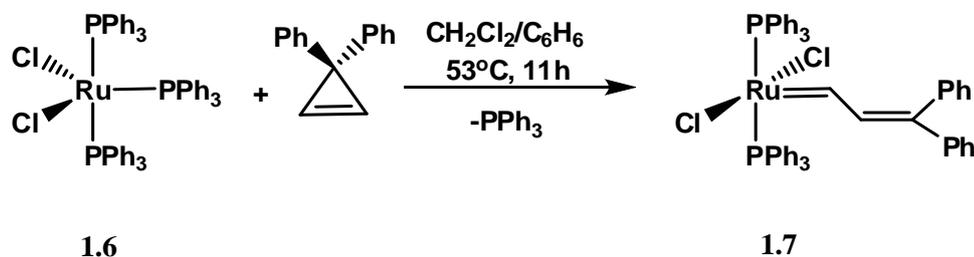
Scheme 1.5 Synthesis of first stable Ru based olefin metathesis catalyst.

Later Grubbs' group modified the $(PPh_3)_2Cl_2Ru=CH-CH=CPh_2$ complex by

replacing PPh_3 with a better σ-donating phosphine, PCy_3 which could catalyze the

metathesis reaction more effectively and was found to be working well for the metathesis

of less strained olefins also [Nguyen *et al*. 1993; Fu *et al*. 1993]. For the large scale

synthesis a new pathway was developed using $RuCl_2(PPh_3)_3$ and phenyldiazomethane

and these diphosphine Ru(II) alkylidene metathesis catalysts are knows as first

generation Grubbs catalysts [Schwab *et al*. 1995; Schwab *et al*. 1996] (Scheme 1.6).

1.6   **1.8**
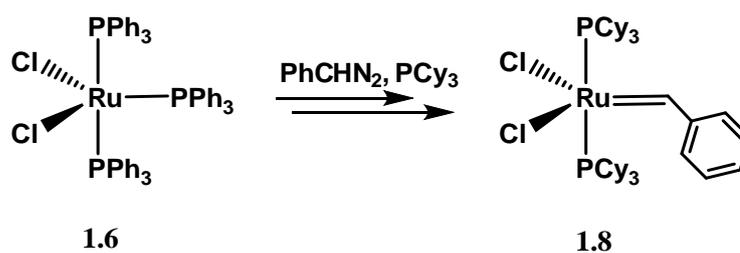
Scheme 1.6 Synthesis of first generation Grubbs catalyst.

In 1968 Öfele and Wanzlick independently reported the metal coordinated N-

heterocyclic carbenes (NHC), but the real breakthrough in N-heterocyclic carbene

chemistry was invoked after the synthesis of first stable N-heterocyclic carbene by

Arduengo *et al* in 1991 [Öfele 1968; Wanzlick and Schönherr 1968; [a]Arduengo *et al*.

1991; [b]Arduengo *et al*. 1991]. Understanding the outstanding potential of NHCs,

Herrmann *et al*. synthesized the first NHC coordinated Grubbs catalyst by replacing one PCy$_3$ of Grubbs first generation catalyst with 2-imidazolin-2-ylidene [Weskamp *et al*. 1998] (Scheme 1.7). Complex 1.9 was found to be more active than the first generation system for the polymerization of cyclooctadiene as well as ring closing metathesis.

1.8   **1.9**
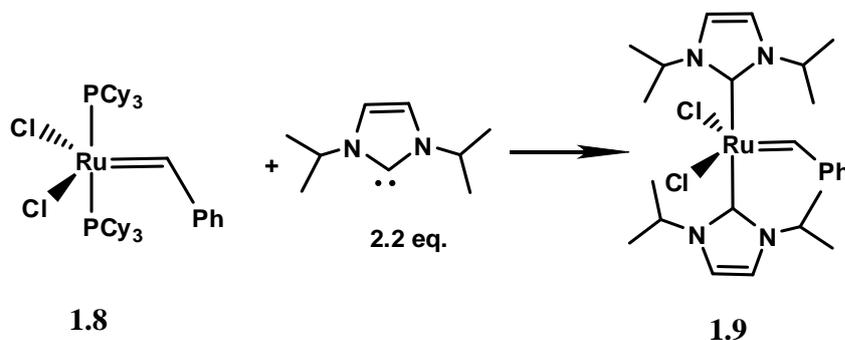
Scheme 1.7 NHC substitution on Grubbs first generation catalyst.

In 1999 both Herrmann's group [Weskamp *et al*. 1999; Ackermann *et al*. 1999] and Nolan's group [[a]Huang *et al*. 1999; [b]Huang *et al*. 1999] independently reported the introduction one unsaturated NHC ligand in a ruthenium biphosphine benzylidene and the NHC-coordinated Grubbs catalysts are generally known as Grubbs second generation catalysts (Scheme 1.8).

1.8   **1.10**
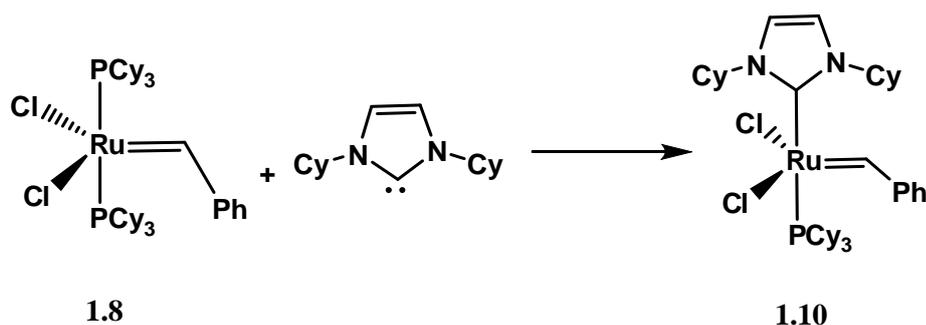
Scheme 1.8 First mono NHC coordinated Grubbs catalyst.

In the same year Grubbs and co-workers reported the synthesis of N,N-dimesityl-4,5-dihydroimidazol-2-ylidene (H$_2$IMes) coordinated Grubbs catalyst 1.11 which is the commercially available 2nd generation Grubbs catalyst [Scholl *et al*. 1999] (Scheme 1.9). They also showed that the substitution with H$_2$IMes improved the catalyst activity

compared to the introduction of the unsaturated analogue IMes (N,N-bis(mesityl)imidazol-2-ylidene) [Huang *et al*. 1999; Bielawski and Grubbs 2000].

1.8   **1.11**
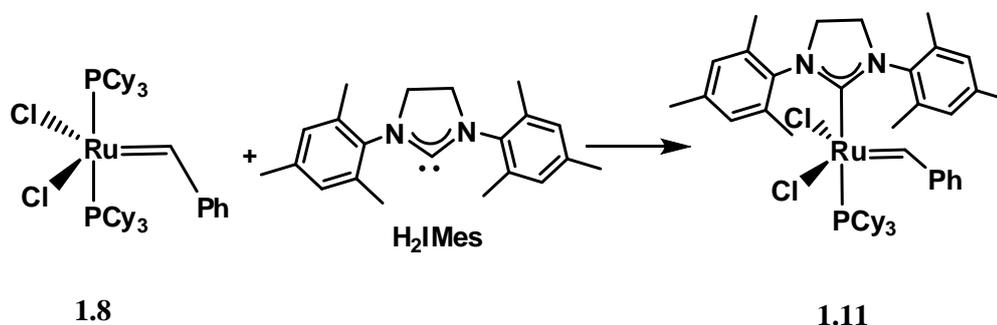
Scheme 1.9 Synthesis of second generation Grubbs catalyst.

The most significant modification of the Grubbs catalyst was achieved by Hoveyda and co-workers [Kingsbury *et al*. 1999] by the incorporation of chelating carbene ligand in the first generation Grubbs catalyst. They reported the synthesis of complex 1.12 by the reaction between (2-isopropoxyphenyl)-diazomethane and PCy_3 with $Cl_2Ru(PPh)_3$. The complex was found to offer good activity and excellent stability to air and moisture. Similar catalysts with a chelating carbene ligand are referred as Grubbs-Hoveyda catalysts. Blechert and Hoveyda concurrently reported the second generation analogue 1.13 in 2000 [Garber *et al*. 2000; Gessler *et al*. 2000] (Figure 1.4). The extra stability of this catalyst is obtained through the chelating character of the carbene that assists the oxygen donor in its recoordination to form the 16 electron complex. Due to the slow initiation rate of 1.13 several steric and electronic modifications on the chelating carbene ligand were reported. A successful tuning of the electronic nature of chelate carbene was achieved by Grela and co-workers by the introduction of an electron withdrawing group on the benzylidene fragment [Michrowska *et al*. 2004].
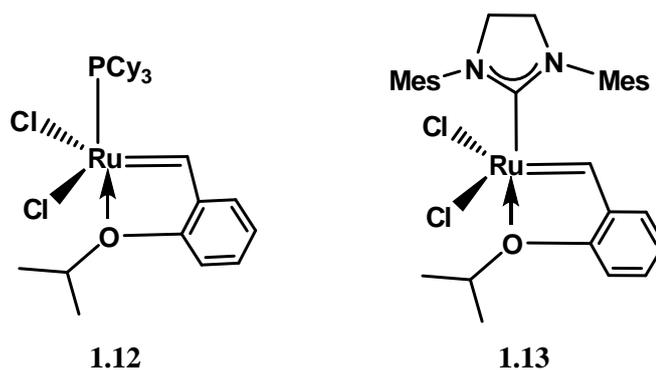
Figure 1.4 Grubbs-Hoveyda catalysts.

A number of modifications on the second generation Grubbs catalyst and Grubbs-Hoveyda catalysts were achieved by introducing different NHCs. A representative set of NHC ligands used in Grubbs catalysts are depicted in Figure 1.5 (Furstner *et al*. 2001; [a]Ritter *et al*. 2006; [a]Ledoux *et al*. 2007; Vehlow *et al*. 2006; [b]Ledoux *et al*. 2007; Kingsbury and Hoveyda 2005].
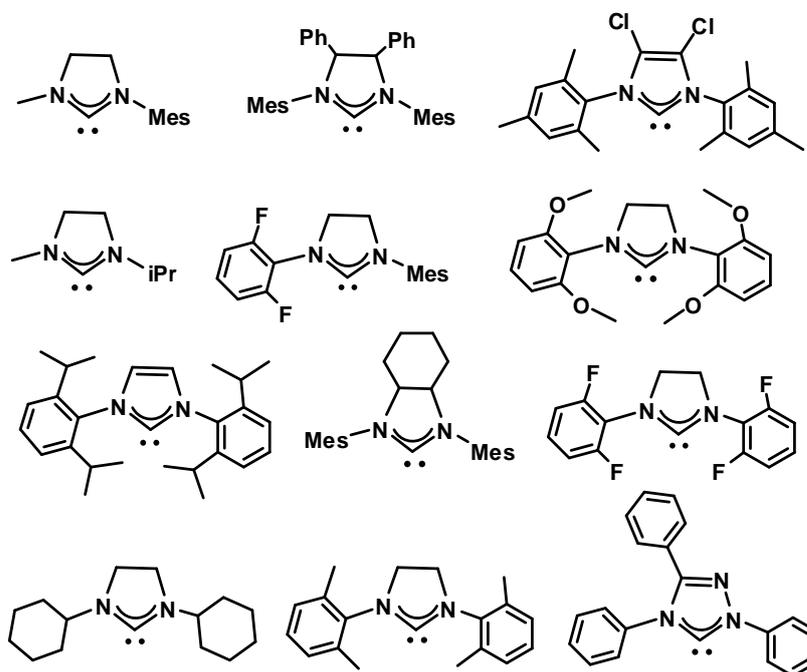
Figure 1.5 NHC ligands used in Grubbs catalysts.

The synthesis of chiral compounds is one of the most important and rapidly progressing areas of organic chemistry and the introduction of chirality in the ligand framework has become a most important aspect in the design of olefin metathesis

catalyst systems. Various research groups synthesized a number of complexes which are potent catalyst showing enantiomeric selectivity for the ring closing metathesis (RCM) (Figure 1.6). The synthesis of chiral Grubbs-Hoveyda catalyst systems for the enantioselective synthesis was achieved by Hoveyda and co-workers and Fournier *et al.* (Figure 1.6) [Weskamp *et al.* 1998; Seiders *et al.* 2001; Van Veldhuizen *et al.* 2005; Fournier and Collins 2007]
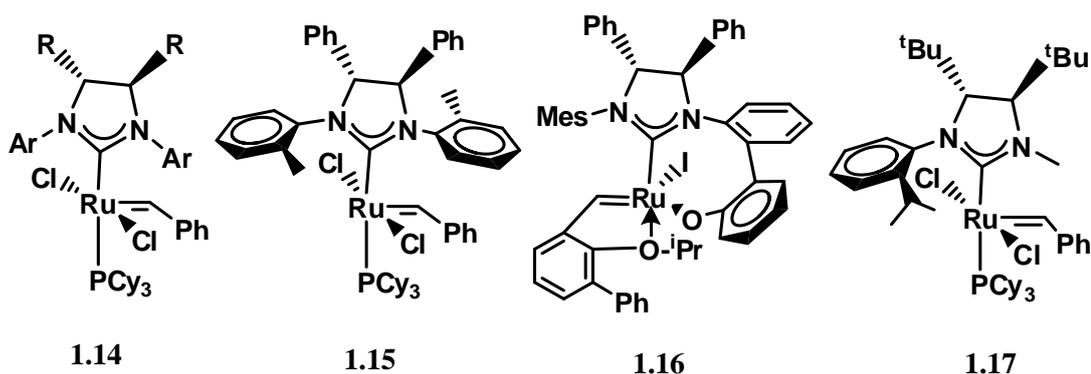
Figure 1.6 Ruthenium based chiral olefin metathesis catalysts.

1.1.4 Mechanism and Activity of Grubbs catalysts

High activity and stability of the first generation $(PCy_3)_2Cl_2Ru=CHPh$ (1.8) and second generation $(PCy_3)(H_2IMes)Cl_2Ru=CHPh$ (1.11) Grubbs catalysts have made them an efficient and powerful tool in organic and polymer chemistry for performing metathesis transformations. A huge amount of experimental and theoretical investigations were devoted to understand the mechanism and activity of these complexes and its analogues with an ultimate goal to design and develop more active catalysts. Scheme 1.10 depicts the complete mechanism of olefin metathesis by Grubbs first generation catalyst.
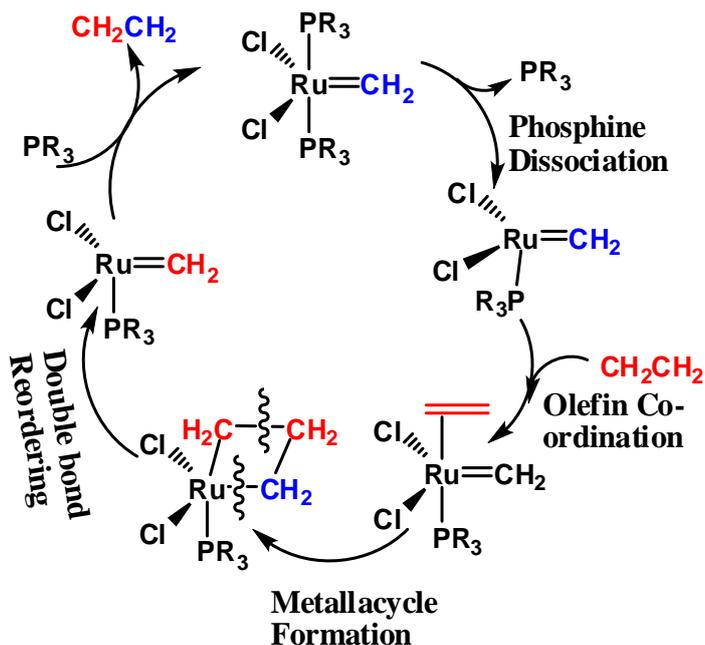
Scheme 1.10 Mechanism of olefin metathesis by Grubbs first generation catalyst.

Grubbs and co-workers in 1997 carried out a detailed experimental analysis to explore the effect of ligand variation on the mechanism and activity of first generation catalyst [Dias *et al*. 1997]. They synthesized a series of ruthenium complexes of general formula $(PR_3)_2X_2Ru=CHCHCPh_2$ and their activities were determined by monitoring ring closing metathesis of acyclic diene, diethyl diallylmalonate. They found that two competing pathways can exist for the reaction; the dominant one in which phosphine dissociates from the 16-electron bisphosphine complex to form a 14-electron complex to which olefin coordinates, while in the minor one olefin coordinates to bisphosphine ruthenium complex which is followed by phosphine dissociation (Scheme 1.11). The catalytic activity was analyzed with different combinations of halogens and phosphines and concluded that larger and more electron donating phosphines and smaller and electron withdrawing halogens on the complex produce active catalysts.
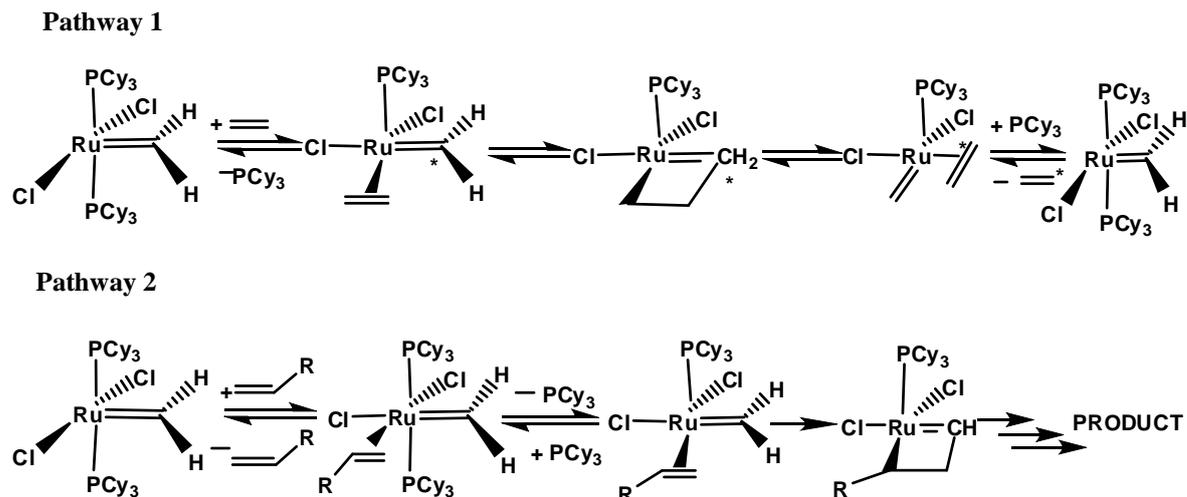
Pathway 1

Pathway 2

Scheme 1.11 Two possible pathways for Grubbs olefin metathesis catalysis.

Later Grubbs' group carried out a detailed investigation on the mechanism and ligand effects on the catalytic activity of both first generation and second generation systems [Sanford *et al.* 2001]. They noticed that the initial phosphine dissociation takes place at higher rate in first generation systems compared to that of second generation systems which resulted from the higher steric effect of phosphine at the ruthenium center. They considered the phosphine dissociation as the rate limiting step in second generation systems while the formation of metallacyclobutane in first generation systems and the enhanced activity of second generation systems originates from the ease of olefin coordination to the 14-electron intermediate.

Buda and coworkers in 1998 performed a quantum molecular dynamics study (Car-Parinello dynamic simulations) of olefin metathesis catalyzed by first generation bisphosphine ruthenium complex $Cl_2(PH_3)_2Ru=CH_2$. They observed the relative easiness of Cl-Ru-Cl cis-trans configurartional exchange, carbene rotation, loss of one phosphine, and formation of metallacyclobutane which are supporting the experimental results reported from Grubbs' group [Aagaard *et al.* 1998]. They also noticed that the bisphosphine complex is active and stericaly crowded system shows higher metathesis activity.

Adlhart and Chen carried out density functional analysis on the role of ligands and substrates on the mechanism and activity of ruthenium olefin metathesis catalysts using gradient corrected BP86 functional [Adlhart and Chen 2004]. They studied the possibility of various mechanistic pathways for the reaction of first generation Grubbs catalyst $(PCy_3)_2Cl_2Ru=CH_2$ with ethylene and found the dissociative mechanism with trans olefin as the most favorable one. They extended their analysis on second generation $(H_2IMes)PCy_3Cl_2Ru=CH_2$ and observed that when the substrate was changed from ethylene to ethyl vinyl ether and norbornene the reaction became more exergonic by 8-15 kcal/mol. Further, the energy barrier for [2+2] cycloreversion is vanished in exergonic reactions. They proposed that the difference in the activity of first and second generation systems is associated with their different stability for the 14-electron carbene species with respect to the 14-electron metallacyclobutane intermediate and that electronic effect plays a major role.

Jensen and co-workers presented a multivariate quantitative structure-activity relationship (QSAR) model for a set of 14-electron complexes $LCl_2Ru=CH_2$ with different dative ligands L [Occhipinti *et al*. 2006]. The dependent and independent variables used in the QSAR model is derived from density functional theory (DFT) calculations. Based on the QSAR analysis, they suggested that ligands which can stabilize the high oxidation state (+4) metallacyclobutane intermediate and its accompanying transition states can promote the catalytic activity. Since the stabilization can be achieved by ligand-to-metal σ-donation, the catalytic activity correlates with σ-donation property of the ligand L, while metal-to-ligand π back donation lower the catalytic activity. Further the steric repulsion between ligand and alkylidene moiety also correlates with catalytic activity and a bulky ligand L forces the reaction to a less stericaly congested metallacyclobutane species.

Metallacyclobutane is the most important intermediate in olefin metathesis reaction. Suresh and Koga in 2004 carried out a density functional analysis on the structural and bonding interaction of ruthenacyclobutane that would govern metathesis route [Suresh and Koga 2004]. They observed the existence of two α-C-C agostic interaction between the d_{y2} orbital on the metal and the orbitals of $-CH_2CH_2CH_2$-fragment. They also identified the existence of strong π-orbital interactions between $Ru=CH_2$ and olefin moiety in the transition state for the formation of metallacyclobutane. These orbital interactions facilitate the olefin metathesis reaction by flattening the potential energy surface of $PH_3RuCl_2=CH_2(C_2H_4)$ − $PH_3Cl_2Ru(C_2H_4)(=CH_2)$. Later Suresh and Baik identified that both the α and β C-C bonds are interacting with the metal simultaneously in the metallacyclobutane which leads to the formation of a unique α,β-(C-C-C) agostic interaction. This interaction substantially stabilizes the 14-electron metallacyclobutane and brings down the energy to a value lower than the energy of the 16-electron alkylidene analogue [Suresh and Baik 2005]. Further exploration on the structural and electronic nature of metallacyclobutane in different metal complexes allowed the quantification of agostic bond strength ($E_{agostic}$) [Suresh 2006]. The $E_{agostic}$ of α,β-(C-C-C) agostic interaction in metallacyclobutanes was found to be much higher than the strength of C-H agostic bonds and they proposed that this interaction would play an important role in the C-C bond activation of metathesis reaction.

A detailed theoretical investigation on the origin of enhanced activity of second generation Grubbs olefin metathesis catalysts compared to the first generation was carried out by Straub [Straub 2005; Straub 2007]. He identified four possible binding mode of olefin to the 14-electron alkylidene complex in the formation of alkene carbene intermediates depicted in Scheme 1.12.
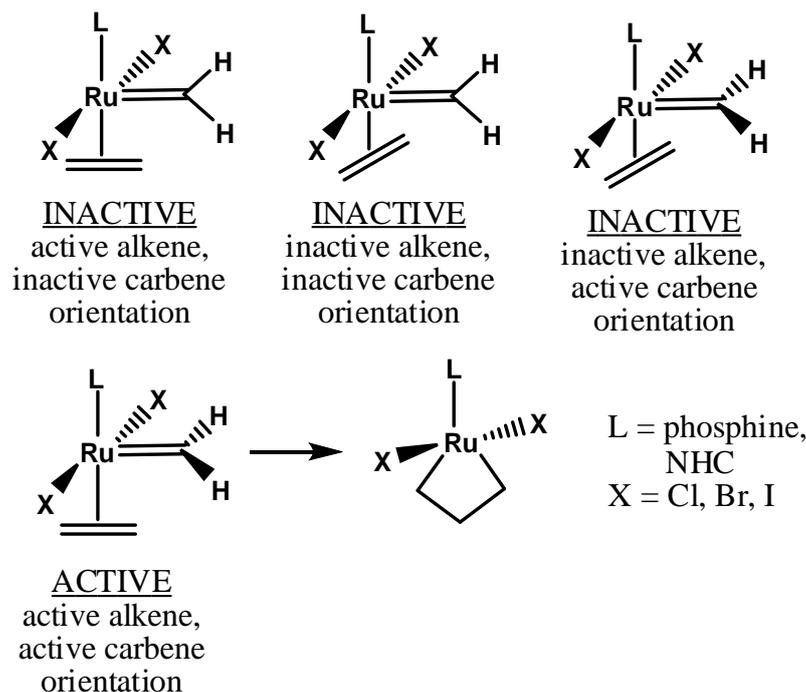
Scheme 1.12 Possible binding modes of olefin to the 14-electron ruthenium complex.

Among this, three conformers are inactive and only one conformation is active in which the both carbene and alkene are in active orientation. Therefore the ligand effects which could keep the alkene and carbene in active orientation will enhance the catalytic activity. He proposed that enhanced electron donating nature of NHC actually stabilizes the active conformation for the formation of metallacyclobutane and therefore the enhanced activity of second generation systems originate mainly from the electronic effect of NHCs.

Cavallo presented a detailed density functional analysis on the various aspects of ruthenium catalyzed olefin metathesis reaction [Cavallo 2002]. They observed that the binding energy of PCy_3 in first generation systems is lower than that in second generation systems which is in agreement with the earlier experimental reports by Grubbs *et al*. Further, they found that solvent effects could reduce the absolute binding energies of phosphines and NHCs while, the binding energy of apolar ethane is not much affected. The activation energy for the formation of metallacyclobutane was found to be lower for

NHC coordinated second generation systems compared to first generation systems. The metallacyclic structures of first generation systems have slightly higher energy with respect to the corresponding olefin-bound intermediate, while the metallacyclic structures of second generation systems is more stable than its olefin bound complex. The steric effect was identified as the major factor for the enhanced activity when the substituents on N in NHC are mesityl groups. These systems do not promote the phosphine dissociation, but enhances the olefin coordination and lowers the activation barrier for the formation of metallacyclobutane and thus increases the overall activity.

It is generally accepted that in (NHC)Ru based catalysts, the coordination of olefin can be preferentially trans to the NHC ligand. But there exists a possibility of side bound coordination and the two pathways are depicted in Scheme 1.13.
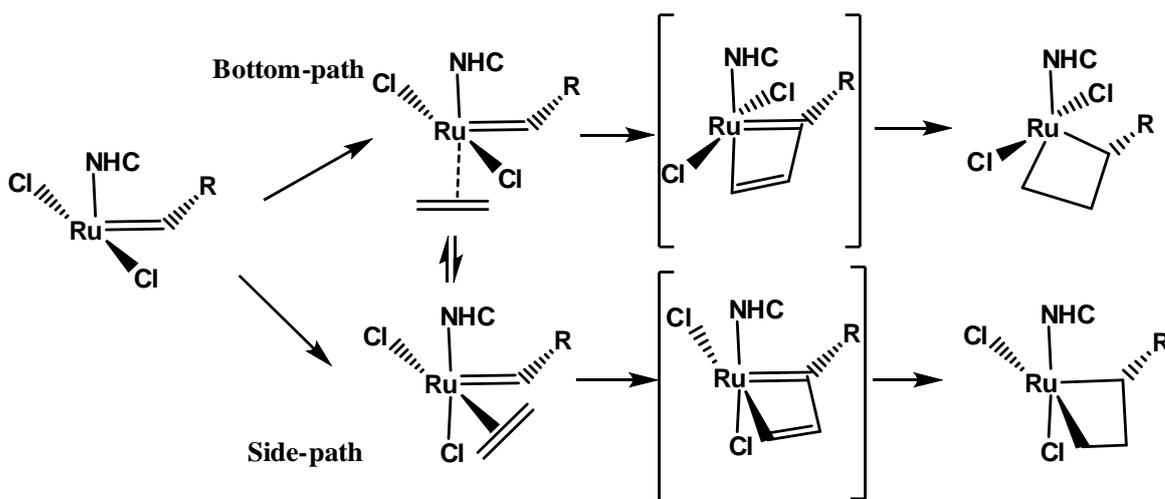
Scheme 1.13 Two pathways for olefin metathesis reaction based on olefin coordination.

Based on density functional analysis on the two reaction pathways, Correa and Cavallo suggested that the preferred reaction pathway is a delicate balance between steric, electronic and solvent effects. They found that, in general, polar solvents push toward the side reaction pathway and the absence of strong steric effects can also make the side reaction path competitive, but the bulkier NHC ligands and substrates strongly favor the bottom reaction pathway [Correa and Cavallo 2006].

1.1.5 Grubbs Catalysts for Enyne Metathesis

Along with various olefin metathesis reactions, Grubbs ruthenium catalysts were identified as potential catalysts for enyne metathesis in which an alkene and an alkyne yield a 1,3-diene product. Both intramolecular and intermolecular enyne metathesis using first generation as well as second generation ruthenium catalysts were reported [Movassaghi *et al*. 2009; Renaud *et al*. 2000; Diver and Giessert 2004]. Lippstreu and Straub carried out a detailed density functional analysis on the mechanism of enyne metathesis and identified that the binding of alkyne to the 14-electron catalyst is stronger than the binding of alkene [Lippstreu and Straub 2005]. The insertion of alkyne into ruthenium carbon double bonds displayed higher intrinsic barrier than the alkene insertion and the alkyne insertion was found to be the only one irreversible step in the catalytic cycle.

1.1.6 Development of New Ligands

The introduction of an NHC ligand in place of a phosphine was major breakthrough in the development of ruthenium olefin metathesis catalysts and therefore the design and synthesis of new ligands which could further improve the catalytic activity is a major concern among researchers. The greater stability of NHC compounds and their bonding properties as ligands in transition metal complexes are partially due to the ability of nitrogen to act as a π-donor which decreases the electron deficiency at the adjacent carbene center. Since the π-donor capabilities of the heavier elements are as large as or even larger than their second row homologues, the use P stabilized carbenes and in particular, P-heterocyclic carbenes (PHC) got more interest as ligands in organometallic systems. Bertrand and coworkers in 2005 reported a stable P-heterocyclic carbene which is an analogue of NHC reported by Martin *et al* [Martin *et al*. 2005] (Figure 1.7).
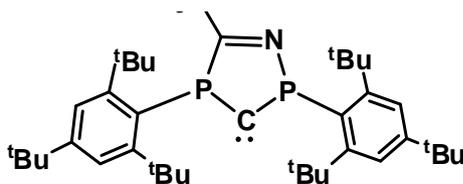
Figure 1.7 First isolated PHC.

Density functional calculations on the use of PHC coordinated ruthenium complexes suggested that PHCs exert small singlet-triplet energy separation compared to NHCs which could stabilize the active form of the catalyst. As a result, the olefin coordination became less favorable but the formation of metallacyclobutane became more facile [Schoeller *et al*. 2005]. Further, theoretical calculations by Jacobson revealed that the PHC coordinated catalysts follow a dissociative reaction pathway in accordance with NHC coordinated systems. They found that the ring opening of the ruthenacyclobutane is the rate limiting step and the initial phosphine dissociation is more favorable in PHC coordinated systems than NHC coordinated systems. Further, the ruthenacyclobutane of PHC coordinated system is in a deeper potential minimum than that of NHC coordinated system and showed agostic interaction in metallacyclobutane [Jacobsen 2006].

Another important class of ligands which has got wide attention is divalent carbon(0) compounds also known as carbones. They are carbon compounds with a general formula CL_2 in which the carbon atom carries two electron pairs unlike carbene which have one electron lone pair. The divalent carbon(0) atom in carbones is stabilized by two donor ligands L and they are known as carbodiphopshoranes (CDP) when the donor ligands L are phosphines. McKelvie in 1961 synthesized the first carbodiphosphoranes but it was considered as a carbene or allene or ylide [Ramirez *et al*.1961]. Such a wrong assumption prevented further development of these species for a long time even though there were some reports on CDPs and carbodiarsoranes [Schubert

et al. 1981; Schmidbaur and Nusstein 1985]. An extensive theoretical investigation on the nature and bonding properties of carbones were performed by Frenking and co-workers and they observed that carbones are capable of acting as both σ- and π- donor ligands using both electron lone pairs [Tonner *et al*. 2006; Deshmukh *et al*. 2008]. They also carried out theoretical investigations on the nature of carbodicarbenes (CDC) by substituting the phosphines at the carbon atom of CDPs by NHCs. Their calculations suggested that CDCs are experimentally accessible and should have interesting properties [Tonner and Frenking 2007]. Further they analyzed the activity of CDP coordinated ruthenium complex in olefin metathesis reaction and found that their catalytic activity might be higher than that of NHC coordinated systems. Later Bertrand and coworkers synthesized CDCs and analyzed the nature and its coordination chemistry [Dyker *et al*. 2008; Fürstner *et al*. 2008; Kaufhold and Hahn 2008]. Various CDPs and CDCs are depicted in Figure 1.8.
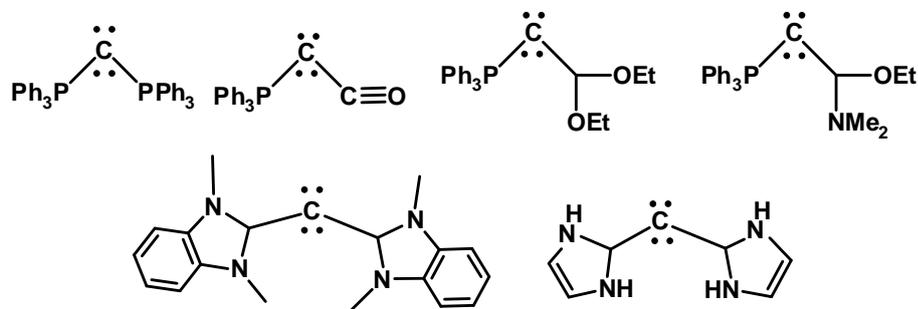
Figure 1.8 Examples of carbodiphosphoranes and carbodicarbenes.

1.1.7 Ligand Knowledge Base

An ion or molecule that coordinates to a central metal to form a coordination complex is considered as a ligand in coordination chemistry. The steric and electronic nature of ligands is crucial in deciding the geometry, properties and functions of organometallic complexes. Therefore the quantification of steric and electronic effects of ligands is necessary in the designing and synthesis of new organometallic catalysts and

complexes. Further, the coordination of a ligand to a metal center would alter the nature and reactivity of ligands. Therefore it is challenging to provide efficient descriptors for the steric and electronic effects of ligands in its free form as well as in the coordinated form. Phosphines were recognized as good 2-electron donor ligand in the early development of organometallic chemistry and therefore initial attempts on the quantification steric and electronic effects of ligands were focused on phosphine ligands. Tolman succeeded in designing a method for the quantification of steric and electronic effects of phosphines. He introduced Tolman electronic parameter (TEP) as a measure of electronic effect of phosphines and cone angle (θ) as a measure of steric effect of phosphines [Tolman 1970; Tolman 1977]. Later a number of descriptors were introduced by various groups to assess the stereoelectronic effects of phosphines and other ligands [Brown 1993; Lever 1990; Suresh and Koga 2002].

A prototype collection of knowledge on ligands in metal complexes is known as ligand knowledge base (LKB). LKBs can be developed using computationally derived chemically robust descriptors of ligands and explored with multivariate statistical methods. The most important part of the development of an LKB lies in deriving simple and efficient descriptors of ligands. LKBs allow the use of a ligand with a desired amount of property and thus highly useful in the designing and synthesis complexes for specific applications.

Fey *et al*. developed a ligand knowledge base for phosphorous donor ligands using computationally derived descriptors and structural parameters. They used a large set of monodendate phosphines and various available steric and electronic parameters along with a number of computationally descriptors such as energy of highest occupied molecular orbital (E_{HOMO}), energy of lowest unoccupied molecular orbital (E_{LUMO}), NBO charge on P, proton affinity etc. The LKB was used to map chemical space and visualize clustering of ligands in chemically meaningful subsets. They also developed linear

regression models that describe the relationship between the descriptors and experimental parameters and the evaluation of the models suggested that the LKB descriptors are competent to predict a substantial range of ligand behavior [Fey *et al*. 2006; Mansson *et al*. 2006; Jover *et al*. 2010]. Later they extended the LKB of monodendate phosphines by adding more number of ligands. They also developed LKB for P, P and P, N donor bidendate ligands and for C-donor ligands (carbenes) [Fey *et al*. 2009; Fey *et al*. 2008]. All these LKBs were highly applicable in the designing of new organometallic catalysts such as Grubbs olefin metathesis catalysts and other complexes.

Part B - Computational Chemistry

1.2 Computational Chemistry

Various scientific discoveries in the late 19th century and in the first part of the 20th century by Michael Faraday, Gustav Kirchoff, Ludwig Boltzman, Albert Einstein, Max Plank, Neils Bohr, Erwin Schrödinger and others marked the emergence of quantum mechanics. Quantum mechanics surpass the inadequacy of classical mechanics to describe motion on an atomic scale. It deals with electronic processes and hence is capable of giving descriptions of energies and distributions of the electrons which determine chemical structures and processes of arbitrary accuracy with the limitations which are technological rather than theoretical. Schrödinger equation is the basic governing equation in quantum mechanics and an exact solution to the Schrödinger equation leads to prediction of the behavior of matter at microscopic level [Schrödinger 1926]. However, an exact solution is almost impossible for systems having more than one electron. A tremendous amount of effort, over several decades, has taken to devise methods that can solve, in principle, the time-independent Schrödinger equation for many electron systems, but high quality numerical solutions have proved elusive. Thus the practical applications of the Schrödinger equation seems to be restricted which necessitates the formulation of approximate methods for many electron systems. Recently developed mathematical tools for computing in high dimensions have revealed a new path toward such solutions which will enable accurate computation of chemical and physical properties of molecules and materials, and thus have an impact on many problems in chemistry, physics, biology, and materials science. Improvement of computational performance and the availability of a variety of softwares have made it

possible to deal with the complex mathematical problems. Now quantum chemistry calculations are applicable to a wide range of chemical problems, including enzymology, thermochemistry, material science, catalysis, cluster science, and reaction mechanisms. Several packages are available with varying capabilities, ease of use, and performance which includes Gaussian, GAMESS, MOPAC, Spartan, Sybyl, Hyperchem, Amsterdam Density Functional (ADF), CASTEP etc. In addition, the molecular visualization programs Gauss View, PCMODEL, MolDen, Molekel, RasMol, Chemcraft and Moplot are available.

Computational chemistry methods range from highly accurate to very approximate; highly accurate methods are typically feasible only for small systems. For computational quantum chemical calculations one may employ different methods based on (a) Molecular mechanics (MM) (b) ab-initio quantum chemical methods (c) semi-empirical quantum chemical methods (d) the density functional methods (e) molecular dynamics and Monte Carlo simulations or (f) hybrid quantum mechanics/molecular mechanics (QM/MM) methods. The MM methods [Boyd and Lipkowitz 1982; Weiner and Kollman 1981; Bowen and Allinger 1991; Dinur and Hagler 1991] apply the laws of classical physics to molecular nuclei without explicit consideration of electrons. Molecular Mechanics computations are quite inexpensive, while it can handle chemical systems containing many thousands of atoms such as proteins, enzymes and other macromolecular systems. Semi-empirical quantum methods [Pople and Beveridge 1970; Stewart 1990], represents a middle road between the mostly qualitative results available from molecular mechanics and the high computationally demanding quantitative results from *ab initio* methods. Semi-empirical techniques are much faster, use approximations from empirical (experimental) data to provide the input into the mathematical models, and are generally applicable to very large molecular systems. *Ab initio* (Latin for "from

the beginning" or "from first principle") methods provide a mathematical description of the chemical system by solving the Schrödinger equation, using rigorous mathematical approximations, without employing any empirical data except the universal constants. Hence, the results obtained from these sophisticated *ab initio* methods are known to be accurate and generally are in good agreement with the experimental results [Szabo and Ostlund 1996] and these methods are generally used for small systems. Molecular dynamics (MD) uses Newton's laws of motion to examine the time-dependent behavior of systems, including vibrations or Brownian motion, using a classical mechanical description [Rapaport 2004; Schlick 2002]. The molecular dynamics and Monte Carlo based methods can be used to investigate the macroscopic properties of a system [Doll and Freeman 1994].

DFT-based methods promise to provide reliable predictions of the structure and properties of chemical systems with lesser computational effort and are presently the most successful approach to compute the electronic structure of matter. The Hohenberg-Kohn [Hohenberg and Kohn 1964] and Kohn-Sham [Kohn and Sham 1965] formalisms have shown that the physical observables of a system in its ground state can be expressed as functionals of the electron density (ED) and led to the development of density functional theory (DFT) [Parr and Yang 1989]. The hybrid QM/MM approach combines the strength of both QM (accuracy) and MM (speed) calculations, are generally applicable for the calculation of ground and excited state properties like molecular energies and structures, energies and structures of transition states, atomic charges, reaction pathways etc.

1.2.1 Quantum Chemical Methods

1.2.1.1 Ab initio Molecular Orbital Theory

All quantum chemical methods describe the electronic structure of matter in terms of Schrödinger equation. The term *ab-initio* suggests that the chemical phenomena are explained in terms of fundamental physical constants such as Planck's constant, velocity of light, mass of electrons and nuclei. Other than the determination of these constants, *ab-initio* methods are independent of experiments. Since most of the chemical phenomena are due to the time-independent interactions, one may write time-independent Schrödinger equation, which in its simplest form is

$$\mathbf{H}\Psi = E\Psi \qquad \qquad \text{… (Eq. 1.1)}$$

where $\mathbf{H}$ is the Hamiltonian operator comprising of the nuclear and electronic kinetic energy operators and the potential energy operators corresponding to the nuclear-nuclear, nuclear-electron and electron-electron interactions. The many-particle wavefunction Ψ describes the system, while E is the energy eigen value of the system. The Hamiltonian operator for N electron and M nucleus can be written as

$$\mathbf{H} = -\sum_{i=1}^{N}\frac{1}{2}\nabla_i^2 - \sum_{A=1}^{M}\frac{1}{2M_A}\nabla_A^2 - \sum_{i=1}^{N}\sum_{A=1}^{M}\frac{Z_A}{r_{iA}} + \sum_{i=1}^{N}\sum_{j>i}^{N}\frac{1}{r_{ij}} + \sum_{A=1}^{N}\sum_{B>1}^{M}\frac{Z_A Z_B}{R_{AB}} \qquad \text{… (Eq. 1.2)}$$

where R_A and r_i are the position vectors of nuclei and electrons. The distance between the ith electron and A^{th} nucleus is r_{iA}; the distance between i^{th} and j^{th} electron is r_{ij} and the distance between the Ath nucleus and B^{th} nucleus is R_{AB}. M_A is the ratio of the mass of the nucleus A to the mass of an electron and Z_A is the atomic number of nucleus A.

Born and Oppenheimer (BO) proposed an approximation [Born and Oppenheimer 1927] to solve the Schrödinger equation based on the concept that the nuclear and electronic motions take place at different time scales, the latter being much smaller than the former. Thus, an electron in motion sees relatively static nuclei, while a moving

nucleus feels averaged electronic motion. From this, the separation of the electronic and nuclear Hamiltonians are possible and to make their corresponding wavefunctions as well. The molecular wavefunction can then be represented as a product of electronic and nuclear counterparts.

$$\Psi(\{\mathbf{r}_i\};\{\mathbf{R}_A\}) = \Phi_{elec}(\{\mathbf{r}_i\};\{\mathbf{R}_A\})\Phi_{nuc}(\{\mathbf{R}_A\}) \qquad \text{... (Eq. 1.3)}$$

Here, $\{\mathbf{r}_i\}$ and $\{\mathbf{R}_A\}$ are the positions of electrons and nuclei, respectively. The eigenvalue equation for the electronic case is then written as

$$\mathbf{H}_{elec}\Phi_{elec}(\{\mathbf{r}_i\};\{\mathbf{R}_A\}) = E_{elec}\Phi_{elec}(\{\mathbf{r}_i\};\{\mathbf{R}_A\}) \qquad \text{... (Eq. 1.4)}$$

The electronic Hamiltonian depends explicitly on the electronic coordinates and parametrically on nuclear coordinates. Since the chemical phenomena occur primarily due to various interactions between electrons of the systems, explicit treatment of the electronic Hamiltonian generally suffices to investigate chemical properties and reactions.

The system of atomic units (a.u.), also referred as Hartree units, has been conveniently adopted as a convention in QM wherein the mass of an electron, Planck's constant, charge of a proton, the length corresponding to radius of first Bohr orbit in hydrogen atom and 4π times the permittivity in free space ($4\pi\varepsilon_0$) are all set to unity and the unit of energy in a.u. numerically turns out to be one-half the energy of a hydrogen atom in its ground state (GS). The use of atomic units leads to a simplified and convenient electronic Hamiltonian (excluding the internuclear repulsion) as shown Eq. 1.5.

$$\mathbf{H}_{elec} = -\sum_{i=1}^{N}\frac{1}{2}\nabla_i^2 - \sum_{i=1}^{N}\sum_{A=1}^{M}\frac{Z_A}{r_{iA}} + \sum_{i=1}^{N}\sum_{j>i}^{N}\frac{1}{r_{ij}} \qquad \text{... (Eq. 1.5)}$$

The first term is the electronic kinetic energy operator summed over the number of electrons, N. The second term represents Coulombic attraction between electrons i and

M nuclei A, while Z_A are the nuclear charges. The last term attributes to the Coulombic repulsion between electrons. Once the wavefunction Ψ is obtained by solving the Schrödinger equation, any experimental observable can be computed as the expectation value of appropriate operator, $\langle \Psi | O | \Psi \rangle$. In the case of total electronic energy, the operator is electronic Hamiltonian.

1.2.1.2 Hartree-Fock Theory

The acceptable solutions of Eq. (1.1) need to be necessarily well-behaved, i.e. wavefunction is finite, single valued, continuous, quadratically integrable and obeying the appropriate boundary conditions. Thus

$$\int \Psi^*(\mathbf{r}_1, \mathbf{r}_2 \ldots, \mathbf{r}_N) \Psi(\mathbf{r}_1, \mathbf{r}_2 \ldots, \mathbf{r}_N) d^3 r_1 d^3 r_2 \ldots d^3 r_N = 1 \qquad \ldots \text{(Eq. 1.6)}$$

Hartree [Hartree 1928] devised an approximate wavefunction of many-electron systems known as Hartree product (HP) function, which is a product of the one-electron functions and normally referred as orbitals. In this function, the spatial distribution of electrons has been defined in terms of spatial orbitals. These spatial orbitals are functions of the position vectors of electrons. But the spin of electron is also required to define an electron completely. Thus the notion of electronic spin is introduced in the one-electron function (orbital) by means of the spin functions $\alpha(\omega)$ and $\beta(\omega)$ that correspond to the up and down spin electrons, respectively. This leads to the spin orbitals, $\{\chi_j\}$ defined below.

$$\begin{aligned} \chi_{2i-1}(\mathbf{x}) &= \psi_i(\mathbf{r})\alpha(\omega) \\ \chi_{2i}(\mathbf{x}) &= \psi_i(\mathbf{r})\beta(\omega) \end{aligned} \qquad \ldots \text{(Eq. 1.7)}$$

where each electron is defined in terms of combined spatial and spin coordinates, $\mathbf{x}$. Thus, the HP function can be written as

$$\Psi^{HP}(\mathbf{x}_1, \mathbf{x}_2, \ldots, \mathbf{x}_N) = \chi_i(\mathbf{x}_1)\chi_j(\mathbf{x}_2)\ldots\chi_k(\mathbf{x}_N) \qquad \ldots \text{(Eq. 1.8)}$$

Since the HP function is an independent-electron wavefunction it do not satisfy the antisymmetry principle. According to the Pauli's exclusion principle [Pauli 1925], no two electrons of an atom shall have identical value of all the four quantum numbers *viz.* n, l, m and s. Slater [Slater 1930] and Fock [Fock 1930] independently proposed that an antisymmetrized sum of all the permutations of HP functions would solve this problem for many-electron systems.

$$\Psi(\mathbf{x}_1,\mathbf{x}_2,...\mathbf{x}_i,...\mathbf{x}_j,...\mathbf{x}_N) = -\Psi(\mathbf{x}_1,\mathbf{x}_2,...\mathbf{x}_j,...\mathbf{x}_i,...\mathbf{x}_N) \qquad \text{... (Eq. 1.9)}$$

This is achieved by using a determinant form of function, later came to be known as the Slater determinant. Thus, an N-electron wavefunction within the HF formulation can be written as

$$\Psi(\mathbf{x}_1,\mathbf{x}_2,....,\mathbf{x}_N) = \frac{1}{\sqrt{N!}} \begin{vmatrix} \chi_i(\mathbf{x}_1) & \chi_j(\mathbf{x}_1) \cdots & \chi_N(\mathbf{x}_1) \\ \chi_i(\mathbf{x}_2) & \chi_j(\mathbf{x}_2) \cdots & \chi_N(\mathbf{x}_2) \\ . & . \quad \cdots & . \\ \chi_i(\mathbf{x}_N) & \chi_j(\mathbf{x}_N) \cdots & \chi_N(\mathbf{x}_N) \end{vmatrix} \qquad \text{... (Eq. 1.10)}$$

The factor $1/\sqrt{N!}$ is a normalization factor. The spin orbitals are denoted as χ's, while $\mathbf{x}_1$, $\mathbf{x}_2$...*etc.* represent the combined spatial and spin coordinates of the respective electrons. The normalized Slater determinant can also be represented in a shorter notation as

$$\Psi(\mathbf{x}_1,\mathbf{x}_2......,\mathbf{x}_N) = \left| \chi_i\chi_j.....\chi_N \right\rangle \qquad \text{... (Eq. 1.11)}$$

In this notation it is presumed that electrons 1,2...*etc.* sequentially occupy the spin orbitals. The simplest antisymmetric wave function which can be used to describe the ground state of an N–electron system is a single slater determinant,

$$\left| \Psi_0 \right\rangle = \left| \chi_i\chi_j.....\chi_N \right\rangle \qquad \text{... (Eq. 1.12)}$$

According to variation principle the best wave function of this functional form is one which gives the lowest possible energy

$$E_0 = \langle \psi_o \mid \mathbf{H} \mid \psi_o \rangle$$

.... (Eq. 1.13)

where H is the full electronic Hamiltonian. By minimizing E_0 with respect to the choice

of spin orbitals, one can derive an equation called the Hartree–Fock (HF) equation which

determines the optimal spin orbitals. Hartree-Fock equation is an eigen value equation of

the form

$$f(i)\chi(x_i) = \varepsilon\chi(x_i)$$

.... (Eq. 1.14)

where f(i) is a one electron operator called the Fock operator of the form

$$f(i) = -\frac{1}{2}\nabla_i^2 - \sum_{A=1}^{M}\frac{Z_A}{r_{iA}} + V^{HF}(i)$$

... (Eq. 1.15)

Where $V^{HF}(i)$ is the Hartree-Fock potential which is the average potential experienced

by the ith electron due to the presence of other electrons. Thus, the HF approximation

replaces the complicated many electron problem by a one electron problem in which

electron-electron repulsion is treated in an average way. The procedure of solving the

Hartree-Fock equation is called the self –consistent-filed (SCF) method and is given

below.

An initial guess at the spin orbital is made to calculate the average field ($V^{HF}(i)$)

seen by each electron and then solve the eigen value equation (Eq. 1.14) for a new set of

spin orbitals. These new spin orbitals are used to obtain new fields and repeat the

procedure repeats until the self-consistency is reached (until fields no longer change and

the spin orbitals used to construct the Fock operator are same as its eigen functions). The

solution of HF eigen value problem yields a set $\{\chi_k\}$ of orthonormal HF spin orbitals

with orbital energies $\{\varepsilon_k\}$. The N spin orbitals with the lowest energies are called the

occupied orbitals and the remaining members of the set $\{\chi_k\}$ are called virtual or

unoccupied orbitals.

In the one-electron Fock operator defined for each electron i

$$f(i) = -\frac{1}{2}\nabla_i^2 - \sum_{A=1}^{M}\frac{Z_A}{r_{iA}} + V^{HF}(i) \qquad \dots \text{(Eq. 1.15)}$$

the first two terms represent the one-electron operator, called the core-Hamiltonian and is a sum of kinetic energy and nuclear-electron attraction energy operators while the final term, the HF potential, is defined as for the electron (1)

$$V^{HF}(1) = \sum_{j}^{N}\left(J_j(1) - K_j(1)\right) \qquad \dots \text{(Eq. 1.16)}$$

Coulomb operator, $J_j(1) = \int \chi_j(2)\frac{1}{r_{12}}\chi_j(2)dx_2$ \qquad ... (Eq. 1.17)

And the exchange operator can only be written through its effect when operating on a spin orbital

$$K_j(1)\chi_i(1) = \left[\int \chi_j(2)\frac{1}{r_{12}}\chi_i(2)dx_2\right]\chi_j(1) \qquad \dots \text{(Eq. 1.18)}$$

Derivation of the HF equations for the closed shell systems was proposed by Roothaan and Hall [Roothaan 1951; Hall 1951]. The HF equation Eq. 1.14 may be rewritten by substituting Eq. 1.19, where the spin orbital is expressed as the linear combination of basis functions, leads to 1.20

$$\psi_i = \sum_{\mu=1}^{K}C_{\mu i}\phi_\mu \qquad i = 1, 2,\dots, K \qquad \dots \text{(Eq. 1.19)}$$

Where ϕ_μ are the basis functions corresponding to atomic orbitals and $C_{\mu i}$ are the coefficients of ϕ_μ and K is the total number of basis functions.

$$f_{(i)}\sum_{\mu=1}^{K}C_{\mu i}\phi_\mu = \varepsilon\sum_{\mu=1}^{K}C_{\mu i}\phi_\mu \qquad \dots \text{(Eq. 1.20)}$$

Premultiplying on both sides of eq.1.20 by ϕ_{μ}^{*} and integrating gives the Roothaan Hall

equation 1.21

$$FC=SC\varepsilon \qquad\qquad ...\ (Eq.\ 1.21)$$

Where ε are orbital energies, S is the overlap matrix and F is the Fock matrix. The Fock

matrix F is the matrix representation of the Fock operator (Eq. 1.15) in the basis ϕ_{μ}.

The Fock matrix must be diagonalized to find out the unknown molecular orbital

coefficients in order to determine the eigen values from Roothaan Hall equation (Eq.

1.21). The MO coefficients of the Fock matrix are determined by the SCF procedure,

where first we guess the orbital coefficients (e.g. from an effective Hamiltonian method)

and then we iterate to convergence.

The one-electron nature of Fock operator results certain limitations to Hartree-

Fock theory constructed using the Roothaan approach since all electron correlation is

ignored other than exchange. Further, the choice of basis set was challenging to early

computational chemists. Eve though the LCAO approach using hydrogenic orbitals

remains attractive, this basis set requires numerical solution of the four index integrals

appearing in the Fock matrix elements which is a tedious process. Since each index runs

over the total number of basis functions, there are in principle N^4 total integrals to be

evaluated, and this quartic scaling behavior with respect to basis set size proves to be a

bottleneck in HF theory applied to essentially any molecules.

1.2.1.3 Basis Sets

Basis set refers to the set of non-orthogonal one-particle wavefunctions used to

build molecular orbitals, which are expanded as a linear combination of atomic orbitals

with the weights or coefficients to be determined. Since it is not possible to obtain the

exact AOs for many-electron atoms, Slater type orbitals (STOs) [Allen and Karo 1960]

were used to mimic AOs in the early days [Clementi 1964]. Francis S. Boys suggested

the use of standard Gaussian functions centered on atoms (Gaussian type orbitals, GTO) to overcome the difficulty in computing two- and other multi-center integrals using STOs [[a]Boys 1950; Feller and Davidson 1990]. A Cartesian Gaussian function used in electronic structure calculations has the form:

$$g\left(\alpha, l, m, n; x, y, z\right) = N_{lmn}\left(x - x_A\right)^l \left(y - y_A\right)^m \left(z - z_A\right)^n e^{-\alpha |r - r_A|^2} \qquad \dots \text{(Eq. 1.22)}$$

where, α is the orbital exponent and l, m, n are the powers of Cartesian components x, y and z respectively. The center of a Gaussian function is denoted by $r_A = (x_A, y_A, z_A)$. The computational advantage of GTOs over STOs is primarily due to the Gaussian product theorem [Shavitt 1963], *viz.* the product of two GTOs is also a Gaussian function centered at the weighted midpoint of the two functions. In addition, the resulting integrals can be evaluated analytically. However, for the sake of computational convenience, it is a common practice [Stewart 1970] to bunch together a set of GTOs with fixed coefficients, d_i (Eq. 1.23). Such a linear combination is termed the contracted GTO (CGTO).

$$g^{CGTO}(l, m, n, x, y, z) = \sum_i d_i\, g(\alpha_i, l, m, n, x, y, z) \qquad \dots \text{(Eq. 1.23)}$$

The orbital exponent and contraction coefficients are determined from appropriate atomic calculations. There are varieties of Gaussian basis sets available now, which have been continuously improved over the years. The single-zeta Gaussian basis sets, also known, as minimal basis set, are the simplest GTOs. In the most popular single-zeta basis set STO-3G [Hehre *et al.* 1969] each Slater type orbital consists of 3 primitive Gaussian type orbitals (PGTO). A basis set which doubles the number of functions in the minimal basis set is described as a double zeta (DZ) basis and the split valence basis sets are produced when the doubling or tripling is restricted only to valence orbitals. Pople and coworkers designed the split valence basis sets of type 'k-nlmG' where 'k' indicates how many PGTOs are used for representing the core orbitals and 'nlm' indicates both

how many functions the valence orbitals are split into and how many PGTOs are used for their representation [Ditchfield *et al.* 1971]. 3-21G and 6-31G basis sets are examples of split valence basis sets [Binkley *et al.* 1980; Hehre *et al.* 1972]. Functions of higher angular momentum than the occupied atomic orbitals known as polarization functions are added to the basis sets. The polarization functions are indicated after the G in the notation for basis sets with a separate designation for heavy atoms and hydrogens. Diffuse functions are added to the basis set to spread the electron density over the molecule and are denoted by + or ++ signs. The most frequently used being the Pople's split valence basis set (multiple CGTOs for valence shells only) with a varying number of polarization functions such as 6-31G(d,p), 6-311++G(2d,2p) *etc.*, Dunning [Dunning Jr 1970; Woon and Dunning Jr 1993] basis set and the correlation consistent [Dunning Jr 1989] valence double and triple zeta basis functions (cc-pvdz, cc-pvtz).

1.2.2 Post HF Methods

Post Hartree-Fock methods are the set of methods developed to improve the Hartree-Fock method. They add electron correlation which is a more accurate way. The post-HF methods try to obtain the correlation energy E_{corr}, defined [[b]Boys 1950] as the difference between the exact *ab initio* energy and exact (complete basis) HF energy, *viz.*

$$E_{corr} = \varepsilon_0 - E_0 \qquad \qquad \text{... (Eq. 1.24)}$$

where, ε_0 is the exact eigenvalue of H_{elec} and E_0 the "best" HF energy with the basis set extrapolated to completeness. The popular approaches that try to compute E_{corr} are the configuration interaction [Pople *et al.* 1976; Foresman *et al.* 1992] (CI), coupled cluster (CC) [Kümmel 2002; Cramer 2004] and many body perturbation theory (MBPT) [Kelly 1969, Brillouin 1934] methods.

1.2.2.1 Configuration Interaction

A popular approach to incorporate the correlation effects into an ab initio molecular orbital calculation is configuration interaction (CI), in which excited states are included in the description of an electronic state. In principle, CI provides an exact solution of the many electron problem. The HF wavefunction is used as the reference determinant and the energy is minimized variationally with respect to the determinant expansion coefficients.

The complete CI wavefunction is a linear combination of Slater determinants with all the permutations of electron occupancies expanded as shown below.

$$\left|\Phi_0\right\rangle = c_0\left|\Psi_0\right\rangle + \sum_{ar} c_a^r\left|\Psi_a^r\right\rangle + \sum_{\substack{a<b \\ r<s}} c_{ab}^{rs}\left|\Psi_{ab}^{rs}\right\rangle + \sum_{\substack{a<b<c \\ r<s<t}} c_{abc}^{rst}\left|\Psi_{abc}^{rst}\right\rangle + \dots \qquad \dots \text{(Eq. 1.25)}$$

The first term in Eq. (1.25) represents the Slater determinant corresponding to the HF wavefunction and rest of the terms constitute singly, doubly, triply... n-tuply excited determinants with appropriate expansion coefficients. The indices a,b,r,s, *etc*. signify the occupied and virtual orbitals involved in the electron excitations. It is a convention to use the indices a, b, c... for occupied orbitals and r, s, t... for the virtual ones.

The number of excitations used to make each determinant classifies configuration interaction calculations. If only one electron has been moved from each determinant, it is called a configuration interaction single-excitation (CIS) calculation. CIS calculations give an approximation to the excited states of the molecule, but do not change the ground-state energy. Single-and double excitation (CISD) calculations yield a ground-state energy that has been corrected for correlation. Triple-excitation (CISDT) and quadruple-excitation (CISDTQ) calculations are done only when very-high-accuracy results are desired. The configuration interaction calculation with all possible excitations is called a full CI. The full CI calculation using an infinitely large basis set will give an

exact quantum mechanical result. However, full CI calculations require immense amount of computer power and therefore very rarely done.

1.2.2.2 Coupled Cluster Methods

The coupled cluster method is one of the most important practical advancement over the CI method [Čizek 1966]. It is the more mathematically refined technique for estimating the electron correlation energy. The CC method assumes the full CI wavefunction

$$\psi_{CC} = e^T \psi_{HF} \qquad \text{... (Eq. 1.26)}$$

ψ_{HF} is a Slater determinant constructed from Hartree-Fock molecular orbitals and

$$e^T = 1 + T + \frac{1}{2}T^2 + \frac{1}{6}T^3 + ... = \sum_{k=0}^{\infty} \frac{1}{k!}T^k \qquad \text{… (Eq. 1.27)}$$

T is known as cluster operator which when acting on ψ_{HF} produces a linear combination of excited slater determinants and can be given as

$$T = T_1 + T_2 + T_3 + ….+ T_n \qquad \text{... (Eq. 1.28)}$$

where n is the total number of electrons and various T_i operators generate all possible determinants having i excitation from the reference.

$$T_2 = \sum_{i<j}^{occ.} \sum_{a<b}^{vir.} t_{ij}^{ab} \psi_{ij}^{ab} \qquad \text{... (Eq. 1.29)}$$

where the amplitudes t are determined by the constraint that Eq. 1.26 be satisfied.

When considering the double excitation $T=T_2$ and the Taylor expansion of the exponential function in (Eq. 1.26) gives

$$\Psi_{CCD} = \left(1 + T_2 + \frac{1}{2!}T^2 + \frac{1}{3!}T^3 + ...\right)\Psi_{HF} \qquad \text{… (Eq. 1.30)}$$

Where CCD implies coupled cluster with only the double excitation operator. The first two terms in parenthesis $(1+T_2)$ defines the configuration double excitation method and the remaining terms involve the product of excitation operators. Solving for the unknown

coefficients t_{ij}^{ab} is necessary for finding the approximate solution $\left|\psi_{CC}\right\rangle$. The coupled cluster correlation energy is determined completely by the singles and doubles coefficients and the two electron MO integrals. The cost of including single excitations (T_1) in addition to doubles is worth to increase in accuracy and this defines CCSD models. Inclusion of connected triple excitations arising with their amplitudes from T_3 defines CCSDT and if the singles/triples coupling term is included then it is called CCSD(T).

1.2.2.3 Perturbation Theory

Möller and perturbation theory improves the Hartree-Fock method by adding electron correlation effects by means of Rayleigh-Schrodinger perturbation theory (RS-PT) [Krishnan and Pople 1978; Bartlett and Silver 1975], usually to second (MP2), third (MP3) and fourth (MP4) order. In RS-PT the true Hamiltonian operator H is expressed as the sum of a 'zeroth order' Hamiltonian H_0 and a perturbation U:

$$H = H_0 + \lambda U \qquad \qquad ... \text{(Eq. 1.31)}$$

The eigenfunctions of the zeroth order Hamiltonian are written $\psi_i^{(0)}$ with energies $E_i^{(0)}$. The ground state wavefunction is thus $\psi_0^{(0)}$ with energy $E_0^{(0)}$. λ is a parameter that can vary between 0 and 1; when λ is zero then H is equal to the zeroth-order Hamiltonian but when λ is one then H equals its true value. The eigen functions ψ_i and eigenvalues E_i of H are then expressed in powers of λ

$$\psi_i = \psi_i^{(0)} + \lambda\psi_i^{(1)} + \lambda^2\psi_i^{(2)} ... = \sum_{n=0}\lambda^n\psi_i^{(n)} \qquad \qquad … \text{(Eq. 1.32)}$$

$$E_i = E_i^{(0)} + \lambda E_i^{(1)} + \lambda^2 E_i^{(2)} + ... = \sum_{n=0}\lambda^n E_i^{(n)} \qquad \qquad ... \text{(Eq. 1.33)}$$

$E_i^{(1)}$ is the first order correction to the energy, $E_i^{(2)}$ is the second order correction and so on. These energies can be calculated from the eigenfunctions as follows.

$$E_i^{(0)} = \int \psi_i^{(0)} \, H_0 \, \psi_i^{(0)} d\tau \qquad \qquad \text{... (Eq. 1.34)}$$

$$E_i^{(1)} = \int \psi_i^{(0)} \, U \, \psi_i^{(0)} d\tau \qquad \qquad \text{... (Eq. 1.35)}$$

$$E_i^{(2)} = \int \psi_i^{(0)} \, U \, \psi_i^{(1)} d\tau \qquad \qquad \text{... (Eq. 1.36)}$$

$$E_i^{(3)} = \int \psi_i^{(0)} \, U \, \psi_i^{(2)} d\tau \qquad \qquad \text{... (Eq. 1.37)}$$

To determine the corrections to the energy, it is necessary to determine the wavefunctions to a given order. In Möller-Plesset perturbation [Möller and Plesset 1934] theory the unperturbed Hamiltonian H_0 is the sum of the one-electron Fock operator for the N electron. In order to calculate higher order wavefunctions we need to establish the form of the perturbation, U. This is the difference between the 'real' Hamiltonian H and the zeroth order Hamiltonian, H_o,

The Hamiltonian is equal to the sum of the nuclear attraction terms and electron repulsion terms:

$$H = \sum_{i=1}^{N} (H^{core}) + \sum_{i=1}^{N} \sum_{j=i+1}^{N} \frac{1}{r_{ij}} \qquad \qquad \text{... (Eq. 1.38)}$$

Hence the perturbatioin U is given by

$$U = \sum_{i=1}^{N} \sum_{j=i+1}^{N} \frac{1}{r_{ij}} - \sum_{j=1}^{N} (J_i + K_i) \qquad \qquad \text{... (Eq. 1.39)}$$

The first order energy $E_0^{(1)}$ is given by

$$E_0^{(1)} = -\frac{1}{2} \sum_{i=1}^{N} \sum_{j=1}^{N} [(ii \mid jj) - (ij \mid ij)] \qquad \qquad \text{... (Eq. 1.40)}$$

The sum of the zeroth order and first order energies thus corresponds to the Hartree-Fock energies

$$E_0^{(0)} + E_0^{(1)} = \sum_{i=1}^{N} \varepsilon_i - \frac{1}{2} \sum_{i=1}^{N} \sum_{j=1}^{N} [(ii \mid jj) - (ij \mid ij)] \qquad \text{... (Eq. 1.41)}$$

To obtain an improvement on the Hartree-Fock energy it is therefore necessary to use Moller-Plesset perturbation theory to at least second order. This level of theory is referred to as MP2 and involves the integral $\int \psi_0^{(0)} U \psi_0^{(1)} d\tau$

The higher order wavefunction $\psi_0^{(1)}$ is expressed as linear combinations of solutions to the zeroth –order Hamiltonian:

$$\psi_0^{(1)} = \sum_j c_j^{(1)} \psi_j^{(0)} \qquad \text{... (Eq. 1.42)}$$

The $\psi_j^{(0)}$ in Eq. 1.42 will include single, double etc. excitations obtained by promoting electrons into virtual orbitals obtained from a Hartree-Fock calculation.

The second order energy is given by

$$E_0^{(2)} = \sum_i^{\text{occupied}} \sum_{j>i} \sum_a^{\text{virtual}} \sum_{b>a} \frac{\iint d\tau_1 d\tau_2 \chi_i(1)\chi_j(2)\left(\frac{1}{r_{12}}\right)[\chi_a(1)\chi_b(2) - \chi_b(1)\chi_a(2)}{\varepsilon_a + \varepsilon_b - \varepsilon_i - \varepsilon_j} \qquad \text{.... (Eq. 1.43)}$$

These integrals will be non zero only for double excitations, according to the Brillouin theorem.

Möller-Plesset calculations are computationally intensive and so their use is often restricted to single point calculations at geometry obtained using a lower level of theory. They are at present the most popular way to incorporate electron correlation in molecular quantum mechanical calculations, especially at the MP2 level.

1.2.3 Density Functional Theory (DFT)

Density functional theory (DFT) is one of the most popular approaches to quantum mechanical many-body electronic structure calculations of molecular and condensed matter systems. DFT has been very popular for calculations in solid state physics since the 1970s. However, it was not considered accurate enough for calculations

in quantum chemistry until the 1990s, when the approximations used in the theory were greatly refined. DFT is now a leading method for electronic structure calculations in both fields.

The basic idea of DFT is to describe an interacting system of electrons via its density ($\rho(\mathbf{r})$) which is a function of its many body wave-function and the major advantage is that the wavefunction for an N-elelctron system is a function of 3N spatial co-ordinates whereas the density $\rho(\mathbf{r})$ is dependent only on three independent spatial co-ordinates (or four, if the spin is included). Further, the density $\rho(\mathbf{r})$ is an observable, subject to a measurement experimentally while the many-particle wavefunction is an intangible entity and the density is a very conventional parameter for a collective description of many-electron system wherein single particle co-ordinates lose their identity.

The first true density functional theory was developed by Thomas and Fermi (TF model) in 1920s [Thomas 1927; Fermi 1927; Fermi 1928]. They derived a kinetic energy functional $T_{TF}[\rho]$ based on uniform electron gas.

$$T_{TF}[\rho] = \frac{3}{10}(3\pi^2)^{2/3}\int d^3 r\, \rho^{5/3}(\mathbf{r}) \qquad\qquad \dots \text{(Eq. 1.44)}$$

The Thomas-Fermi kinetic energy functional is the only density functional that has an elegant mathematical derivation, but unfortunately, it is not accurate enough to be chemically useful. Also, it was the first DFT functional as such, because it showed that non-electrostatic energy terms can be expressed in terms of the electron density.

The key variable in DFT is $\rho(\mathbf{r})$ can be given as

$$\rho(\vec{r}) = N\int d^3 r_2 \int d^3 r_3 \dots \int d^3 r_N \psi^*(\vec{r}_1, \vec{r}_2 \dots \vec{r}_N)\psi(\vec{r}_1, \vec{r}_2 \dots \vec{r}_N) \qquad \dots \text{(Eq. 1.45)}$$

Though the TF model has been improved with corrections in the later years, it remained as a simple qualitative model until the formulation of Hohenberg-Kohn (HK) theorems in

1964 which is the foundation of DFT. In this theory, the electron density plays the role of basic variable. The HK theorems may be stated as (i) the external potential and hence the total energy is a unique functional of electron density and (ii) the ground state energy can be obtained variationally: the density that minimizes the total energy is the exact ground state density. A straightforward consequence of the first Hohenberg and Kohn theorem is that the ground state energy E is also uniquely determined by the ground-state charge density.

According to HK theorem, it is in principle possible to calculate the ground state wave function $\psi_0(\vec{r}_1 ... \vec{r}_N)$ for a given ground state electron density $\rho_0(\vec{r})$. In other words ψ_0 is a unique function of ρ_0. ie,

$$\Psi_0 = \Psi_0[\rho_0] \qquad\qquad\qquad ...(\text{Eq. 1.46})$$

and consequently all the ground state observables O are also functionals of ρ_0.

$$\langle \mathbf{O} \rangle[\rho_0] = \langle \psi_0[\rho_0]\mathbf{O}\psi_0[\rho_0] \rangle \qquad\qquad ... (\text{Eq. 1.47})$$

From this, the ground state energy is a functional of ρ_0.

$$E_0 = E[\rho_0] = \langle \psi_0[\rho_0] | T + V + U | \psi_0[\rho_0] \rangle \qquad ... (\text{Eq. 1.48})$$

where the contribution of the external potential $\langle \psi_0[\rho_0] | V | \psi_0[\rho_0] \rangle$ can be written explicitly in terms of density.

$$V[\rho] = \int V(\vec{r})\rho(\vec{r})d^3r \qquad\qquad ... (\text{Eq. 1.49})$$

Having a specified system, ie, V is known one then has to minimize the functional

$$E[\rho] = T[\rho]U[\rho] + \int V(\vec{r})\rho(\vec{r})d^3r \qquad ... (\text{Eq. 1.50})$$

with respect to, assuming one has got reliable expressions for $T[\rho]$ and $U[\rho]$. A successful minimization of the energy functional will yield the ground state density ρ_0 and all other ground state observables. The variational problem of minimizing the energy

functional $E[\rho]$ can be solved by applying the Lagrangian method of undetermined multipliers, which was done by Kohn and Sham in 1965. Hereby, one uses the fact that the functional in the equation above can be written as a fictitious density functional of a non-interacting system.

$$E_S[\rho] = \left\langle \psi_S[\rho] \middle| T_S + V_S \middle| \psi_S[\rho] \right\rangle \qquad \qquad \dots \text{(Eq. 1.51)}$$

where T_S denotes the non interacting kinetic energy and V_S is an external effective potential in which the particles are moving. Therefore, $\rho_S(\vec{r}) \equiv \rho(\vec{r})$ if V_S is chosen to be

$$V_{S=} V + U + (T_S - T) \qquad \qquad \dots \text{(Eq. 1.52)}$$

Thus, one can solve the Kohn-Sham equation of this non-interacting system

$$\left(-\frac{\hbar^2}{2m} \nabla^2 + V_S(\vec{r}) \right) \varphi_i(\mathbf{r}) = \varepsilon_i \varphi_i(\vec{r}) \qquad \qquad \dots \text{(Eq. 1.53)}$$

which yields the orbitals ϕ_i that reproduce the density $\rho(\vec{r})$ of the original many body system

$$\rho(\vec{r}) \equiv \rho_S(\vec{r}) = \sum_i^N \left| \varphi_i(\vec{r}) \right|^2 \qquad \qquad \dots \text{(Eq. 1.54)}$$

The effective single- particle potential V_S can be written more detail as

$$V_S = V + \int \frac{e^2 \rho_S(\vec{r}')}{\left| \mathbf{r} - \mathbf{r}' \right|} d^3r' + V_{XC}\left[\rho_S(\vec{r}) \right] \qquad \qquad \dots \text{(Eq. 1.55)}$$

The second term denotes the Hartree term describing the electron-electron Coulumb repulsion while the last term V_{XC} is called the exchange correlation potential. V_{XC} includes all the many particle interactions. Since the Hartree term and V_{XC} depends on $\rho(\vec{r})$, which depends on ϕ_i, which in turn depends on V_S, the problem of solving Kohn-Sham equations for the ϕ_i. From these one calculated a new density and starts again. This procedure is repeated until the convergence is reached.

Even the HK and KS formalisms do not lead to the exact form of exchange-

correlation functional V_{XC}, much of it is left to a systematic search and guesswork. Therefore approximations are required for the calculation physical quantities. The most widely used approximation in physics is local density approximation (LDA) where the functional depends only on the density at the coordinate where the functional is evaluated.

$$E_{XC}[\rho] \equiv \int \varepsilon_{XC}(\rho)\mathbf{d^3r} \qquad \qquad \text{... (Eq. 1.56)}$$

The local spin density approximation (LSDA) is a straight forward generalization of LDA to include electron spin:

$$E_{XC}[\rho_\uparrow, \rho_\downarrow] \equiv \int \varepsilon_{XC}(\rho_\uparrow, \rho_\downarrow)\mathbf{d^3r} \qquad \qquad \text{... (Eq. 1.57)}$$

Highly accurate formulae for the exchange-correlation energy density $\varepsilon_{XC}(\rho_\uparrow, \rho_\downarrow)$ have been constructed from simulations of a free electron gas. This had been the most successful method for decades until newer functionals within KS formalism were introduced. A notable difference came with the generalized gradient approximation (GGA) where, in addition to the density values, the functionals are dependent on the gradient of densities. GGA are local but also take into account the gradient of the density at the same coordinate.

$$E_{XC}[\rho_\uparrow, \rho_\downarrow] \equiv \int \varepsilon_{XC}(\rho_\uparrow, \rho_\downarrow, \vec{\nabla}\rho_\uparrow, \vec{\nabla}\rho_\downarrow)\mathbf{d^3r} \qquad \qquad \text{... (Eq. 1.58)}$$

The most widely used exchange functionals are Slater's X_α [Slater 1951], B88 [Becke 1988] (Becke's 1988 functional that includes Slater's exchange with gradient corrections), having the form as

$$E_{XC}^{Becke88} = E_{XC}^{LDA} - \gamma \int \frac{\rho^{4/3}x^2}{(1 + 6\gamma\sinh^{-1}x)}\mathbf{d^3r} \qquad \qquad \text{... (Eq. 1.59)}$$

where $x = \rho^{-4/3|\nabla\rho|}$ and γ is a parameter chosen to fit the exchange energy of inert gas atoms (0.0042 a.u. as defined by Becke). Similarly, there exist local and gradient-

corrected correlation functionals. Amongst the other functionals, widely used are P86 and PW91 by Perdew and Wang [Perdew *et al.* 1992] etc.

There also exists another type of functional, which offers some improvement over the corresponding pure DFT functional. This includes a mixture of HF and DFT exchange along with DFT correlation. The popular functional BLYP is obtained by coupling of Becke's generalized gradient corrected exchange functional with the gradient corrected correlation functional of Lee, Yang and Parr [Lee *et al.* 1988]. A popular hybrid functional is B3LYP, Becke-3 parameters non-local exchange functional, with the non-local correlation functional of Lee *et al.*, functional having the form [Becke 1993; Lee *et al.* 1988] :

$$E_{xc}^{B3LYP} = (1-a)E_x^{LSDA} + aE_x^{HF} + b\Delta\Delta_x^{B88} + E_c^{VWN3} + (1-c)E_c^{LSDA} + cE_c^{LYP} \qquad ... \text{(Eq. 1.60)}$$

Recently Truhlar *et al.* developed a M05 and M06 class hybrid meta functionals which are readily recognized for a more accurate prediction of various properties of transition metal based systems as well as main group elements [Zhao and Truhlar 2008].

The disadvantage of DFT is the exchange-correlation functional, which cannot be derived rigorously from first principles. But DFT still remains as an economical alternative for treating molecules at correlated level of theory.

1.2.4 Potential Energy Surface

Representation of chemical reactions can be explained by potential energy surface (PES). Potential energy surfaces form a central concept in the theoretical description of molecular structures, properties, and reactivities. The PES arises upon the application of the BO approximation to the solution of the Schrodinger equation. Considering the general Hamiltonian

$$H = T_r + T_R + V(r, R) \qquad\qquad ... \text{(Eq. 1.61)}$$

where T_r is the operator for the kinetic energy of electronic motion, T_R is the operator for the kinetic energy of nuclear motion, and V(r,R) is the potential energy due to electrostatic interactions between all of the charged particles (electrons and nuclei). On applying the BO approximation the nuclear kinetic energy term, T_R; in the molecular Hamiltonian vanishes and the electronic and nuclear degrees of freedom can be separated. This yields the time-independent Schrödinger equation for the electronic degrees of freedom.

$$\left[T_r + V(r,R)\right]\psi(r;R) = E(R)\psi(r;R) \qquad \ldots \text{(Eq. 1.62)}$$

In eq. (1.62) $\psi(r;R)$ is the electronic wavefunction which depends parametrically on the nuclear positions, and the energy of the system, E(R), is a function of the nuclear degrees of freedom. A plot of E versus R gives the PES.

The study of most chemical processes and properties by computational chemists begins with the optimization of one or more structures to find minima on PESs, which correspond to equilibrium geometries. A simplified PES can be represented as a topographic surface with valleys and saddle points in Figure 1.9. A common analogy compares the topology of PESs to mountainous landscapes. Molecular structures correspond to the positions of minima in the valleys. Reaction rates can be determined from the height and profile of the pathway connecting reactant and product valleys. From the shape of a valley, the vibrational spectrum of a molecule can be computed, and the response of the energy to electric and magnetic fields determines molecular properties such as dipole moment, polarizability, NMR shielding, etc [Pulay 1995; Dykstra 1988; Jørgensen *et al*. 1986; Jensen 1999].
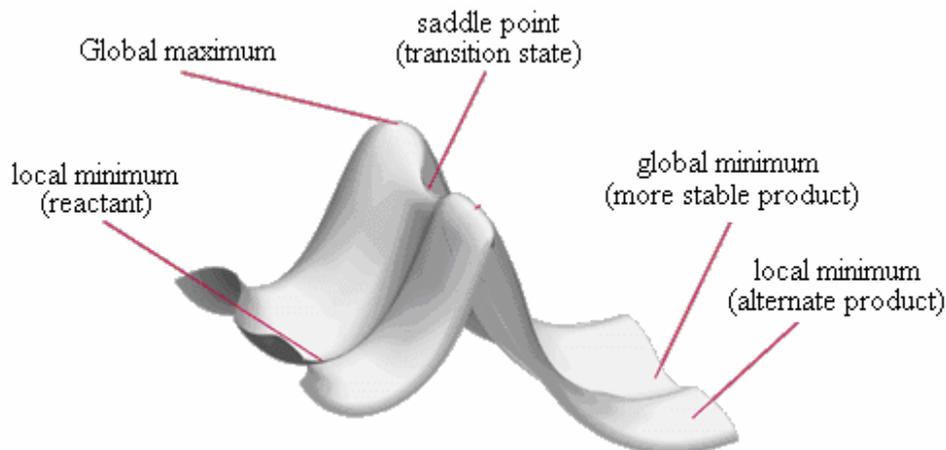
Figure 1.9 Representation of a model potential energy surface.

To obtain reaction barriers and to calculate reaction rates using transition state theory (TST), it is necessary to locate first-order saddle points on the PES, which correspond to transition states (TS). A transition structure is the highest point on the reaction path that requires the least energy to get from the reactant to the product. In other words, it is a stationary point that is an energy maximum in one direction and a minimum in all others. For a point to be considered to be a transition state structure the first derivatives must be zero and the energy must be a maximum along the reaction path connecting the valley of reactants with the valley of products on the potential energy surface.

1.2.5 Molecular Electrostatic Potential

The most fundamental quantitative law in electrostatics describing the force of attraction or repulsion between two point charges was given by Coulomb in 1784 which can be mathematically expressed as

$$F = \frac{q_1 q_2 \hat{\mathbf{r}}}{4\pi\varepsilon_0 r^2} \qquad \qquad ... \text{(Eq. 1.63)}$$

where q_1 and q_2 are point charges separated by a distance r in vacuum; $\hat{r}$ is a r unit vector joining the position vectors of q_1 and q_2 and $4\pi\varepsilon_0$ is the constant of proportionality. The

intensity of an electric field is the force acting on a unit test charge placed at a reference point in the field. The field due to a fixed point charge q produced at a site **r** is

$$\mathbf{E} = \frac{q\mathbf{r}}{4\pi\varepsilon_0 |\mathbf{r}|^3} \qquad \dots \text{(Eq. 1.64)}$$

Applying the principle of superposition, for a system of two more charges $\{q_\alpha\}$, the electric field is the vector sum of the fields $\mathbf{E}_\alpha$ produced by the individual charges and can be given as

$$\mathbf{E}(\mathbf{r}) = \sum_\alpha \mathbf{E}_\alpha(\mathbf{r}) = \frac{1}{4\pi\varepsilon_0}\sum_\alpha \frac{q_\alpha(\mathbf{r}-\mathbf{r}_\alpha)}{|\mathbf{r}-\mathbf{r}_\alpha|^3} \qquad \dots \text{(Eq. 1.65)}$$

The classical Coulombic electrostatic potential, V(**r**) at the point **r** due to a discrete point charge q_α placed at $\mathbf{r}_\alpha$ is given by

$$V(\mathbf{r}) = \frac{1}{4\pi\varepsilon_0}\frac{q_\alpha}{|\mathbf{r}-\mathbf{r}_\alpha|} \qquad \dots \text{(Eq. 1.66)}$$

Since electrostatic potential (ESP) obeys the principle of superposition, the ESP at a point **r** due to a collection of discrete charges $\{q_\alpha\}$ located at $\{\mathbf{r}_\alpha\}$ can be written as

$$V(\mathbf{r}) = \frac{1}{4\pi\varepsilon_0}\sum_\alpha \frac{q_\alpha}{|\mathbf{r}-\mathbf{r}_\alpha|} \qquad \dots \text{(Eq. 1.67)}$$

If instead of discrete charges, consider a continuous distribution of charge over space, $\rho(\mathbf{r}')$ is the continuous charge distribution. The charge contained in an infinitesimal volume element $d^3\mathbf{r}'$ around a point $\mathbf{r}'$ is $\rho(\mathbf{r}')d^3\mathbf{r}'$. This generates a potential of $\rho(\mathbf{r}')d^3\mathbf{r}'/|\mathbf{r}-\mathbf{r}'|$ at a reference point **r**. Then the potential generated by the entire charge distribution is obtained by integration over the entire space, i.e.

$$V(\mathbf{r}) = \frac{1}{4\pi\varepsilon_0}\int \frac{\rho(\mathbf{r}')d^3\mathbf{r}'}{|\mathbf{r}-\mathbf{r}'|} \qquad \dots \text{(Eq. 1.68)}$$

The electrostatic potential for a combination of discrete charges q_α placed at r_α and a smeared distribution $\rho(\mathbf{r})$ can be written by employing superposition principle and

combining eqs. 1.66 and 1.68 as

$$V(\mathbf{r}) = \frac{1}{4\pi\varepsilon_0}\left\{\sum_\alpha \frac{q_\alpha}{|\mathbf{r}-\mathbf{r}_\alpha|} + \int \frac{\rho(\mathbf{r'})}{|\mathbf{r}-\mathbf{r'}|}d^3\mathbf{r'}\right\} \qquad \text{... (Eq. 1.69)}$$

In a molecular charge distribution which is a collection of positive discrete charges $\{Z_\alpha\}$ and a continuous negative electron density distribution described by $\rho(\mathbf{r})$ the molecular electrostatic potential (MESP) [Gadre and Shirsat 2000] is given as

$$V(\mathbf{r}) = \sum_\alpha^N \frac{Z_\alpha}{|\mathbf{r}-\mathbf{R}_\alpha|} - \int \frac{\rho(\mathbf{r'})d^3\mathbf{r'}}{|\mathbf{r}-\mathbf{r'}|} \qquad \text{... (Eq. 1.70)}$$

The two terms refer to the bare nuclear potential and the electronic contributions, respectively. Effective localization of electron-rich regions in the molecular system thus emerges through a balance of these two terms. The above equation shows that the electrostatic potential is certainly specific to a given molecular geometry, and the value of V($\mathbf{r}$) in any particular region depends on whether the effect of nuclei or electrons is dominant there. Thus MESP is positive in the region close to nuclei and negative in the electron-rich region. The MESP, $V(\mathbf{r})$, is a real physical property of a molecule, which can attain positive, zero or negative values. This is in contrast to the behavior of electron densities in position, which can attain only non-negative values. The ESP at nuclear sites shows a discontinuity and negative value since the nuclear contribution from the corresponding atom is dropped out. The MESP at a nucleus of A molecule $V_{0,A}$ can be give as

$$V_{0,A} = \sum_{B\neq A} \frac{Z_B}{|\mathbf{R}_B-\mathbf{R}_A|} - \int \frac{\rho(\mathbf{r'})d^3\mathbf{r'}}{|\mathbf{r}-\mathbf{r'}|} \qquad \text{... (Eq. 1.71)}$$

Nevertheless, every atom is considered to possess a MESP maximum at its center. The monotonic decreasing atomic ESP is expected to achieve zero at infinite distance from the atom center and this feature is referred to as an asymptotic CP (minimum), which has greater significance in the case of molecules.

The topography of molecular electrostatic potential can be characterized in terms of critical point *viz.* minima, saddle and maxima [Gadre and Pathak 1990; Pathak and Gadre 1990; Gadre *et al.* 1992, Shirsat *et al.* 1992; Gadre and Shirsat 2000]. A nondegenerate CP is denoted as (*R*, *S*, where *R* (rank) is the number of nonzero eigenvalues of the Hessian matrix at the CP and *S* (signature) is the algebraic sum of the signs of the eigenvalues. All chemical notations such as lone pairs, bonds, and π-bonds (aromatic, delocalized, and localized) have their topographical manifestations in MESP. MESP brings out electron rich regions like lone-pairs of electrons and π-bonds in the form of a negative valued (3, +3) minima. Any bonding (covalent/weak) interaction between atoms is featured by the presence of a positive valued (3, −1) CP (BCP) and a positive valued (3, +1) CP is the manifestation of a ring. The absence of *non-nuclear maxima* is a main feature of MESP topography over other scalar fields in the interpretation of electronic mechanisms. Similar to the molecular electron density (MED) topography, BCPs bring out the strain in bonds by deviating from the line joining the corresponding atoms. The significance of the negative-valued MESP and their critical points in molecules and their anionic species have been widely addressed in the literature [Politzer and Truhlar 1981, Gadre and Shrivastava 1993; Luque *et al*. 1994; Gadre *et al*. 1996].

1.2.6 Hybrid Quantum Mechanical-Molecular Mechanical Methods

Quantum chemical methods are generally applicable and allow the calculation of ground and excited state properties such as molecular energies and structures, energies and structures of transition states, atomic charges, reaction pathways etc. while molecular mechanics uses Newtonian mechanics and the potential energy is calculated using force fields. It is possible to combine these two methods into one calculation known as hybrid

QM/MM method, which models a very large compound using molecular mechanics and one active site of the molecule with quantum mechanics [Gao 1996, Warshel and Levitt 1976; . Singh and Kollman 1986; Field *et al*. 1990; Mordasini and Thiel 1998]. Among various hybrid methods the ONIOM (Our N-layered Integrated molecular Orbital + molecular Mechanics) method developed by Morokuma and coworkers is more general, that allows to combine a variety of quantum mechanical methods as well as a molecular mechanics method in multiple layers [Maseras and Morokuma 1995; Humbel *et al*. 1996; [a]Svensson *et al*. 1996; [b]Svensson *et al*. 1996; Dapprich *et al*. 1999; Vreven and Morokuma 2000; Vreven *et al.* 2001]

First Layer
Bond-formation/breaking takes place
Use the "High level" (H) method.

Second Layer
Electronic effect on the first layer
Use the "Medium level" (M) method

Third Layer
Environmental effects on the first layer
Use the "Low level" (L)method.
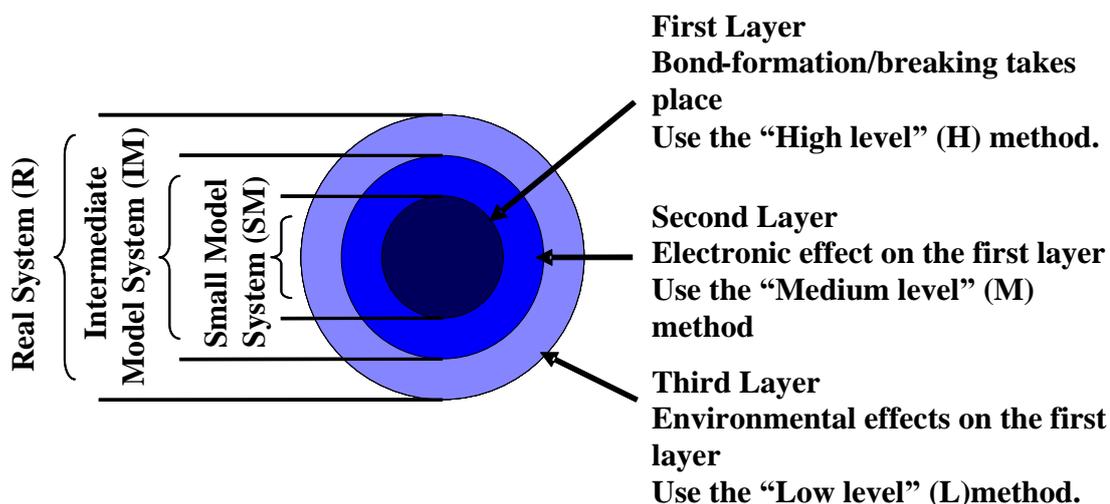
Figure 1.10 The onion skin-like layers and models in ONIOM method.

Figure 1.10 is a pictorial representation of three layer ONIOM method in which the system is divided into three layers. The inner part is the smaller part where the chemical reaction occurs and is treated with an accurate level of theory such as QM with a higher computational cost. The second layer is treated with a medium level method and the third layer which is not directly involved in the chemical reaction is treated with a low cost level of theory such as MM. Implementation of two layer ONIOM method is depicted in Figure 1.11 and the three layer ONIOM method in Figure 1.12.
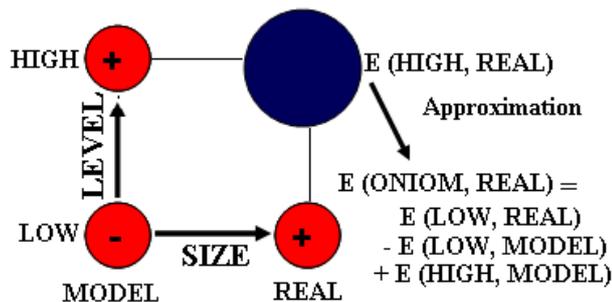
Figure 1.11 Tow-layer ONIOM method.
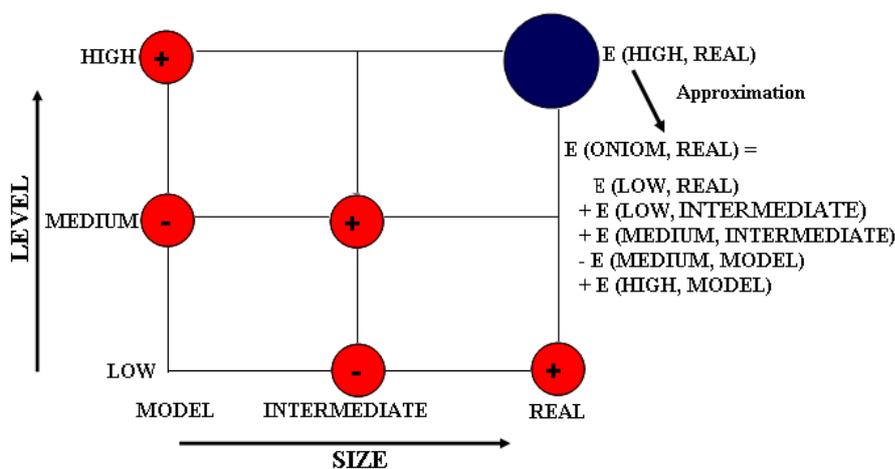
Figure 1.12 Three-layer ONIOM method.

The target calculation is the high level calculation for a large real system, E(high, real), which is prohibitively expensive. It is possible to perform an inexpensive low level calculation for the real system E(low, real) that may not be sufficiently accurate for the property. An accurate high level calculation for a smaller model system E(high, model) is also possible. Starting from E(low, model), if one assumes that the correction for the high level, E(high, model) - E(low, model), and the correction for the real system, E(low, real) - E(low, model), to be additive, as illustrated in Figure 1.22, the energy of the real system at the high level can be estimated extrapolatively from three independent calculations as:

E(ONIOM, real) = E(high, model) + E(low, real) - E(low, model).   ... (Eq. 1.72)

and for a three layer ONIOM calculation (Figure 1.11)

E(ONIOM, real) = E(high, model) - E(medium, model) + E(medium, intermediate) + E(low, intermediate) + E(low, real)   ... (Eq. 1.73)

ONIOM method offers a wide application in thermo chemistry analysis of metal complexes and organic systems, chemical reactions in cluster and solution, material and nanochemistry, in enzymatic reactions and molecular dynamics simulations [Froese and Morokuma 1999; Liu *et al.* 2002; Torrent *et al.* 2002; Choi and Gordon 1999; Re and Morokuma 2001; Irle *et al*. 2002; Kerdcharoen and Morokuma 2002].

1.3 Conclusion

The first part of Chapter 1 describes the development of Schrock and Grubbs catalysts from an ill-defined form to a well characterized form. Both Schrock and Grubbs catalysts are successfully employed for the synthesis of a wide variety of organic compounds and still known to be one of the most important tools in organic synthesis. A detailed literature survey on the experimental and theoretical studies on the mechanism and activity of Grubbs catalysts is also presented. The second part of Chapter 1 deals with the theoretical background of the computational methods which are commonly used in computational chemistry calculations. This part includes a brief account of the Hartree-Fock theory which is the fundamental of much of the electronic structure methods, the Post HF methods, Density Functional Theory, Hybrid QM-MM methods and some specific electronic properties and computational methods.

Chapter 2

Quantitative Assessment of Stereoelectronic Effects of Phosphines and N-Heterocyclic Carbene Ligands
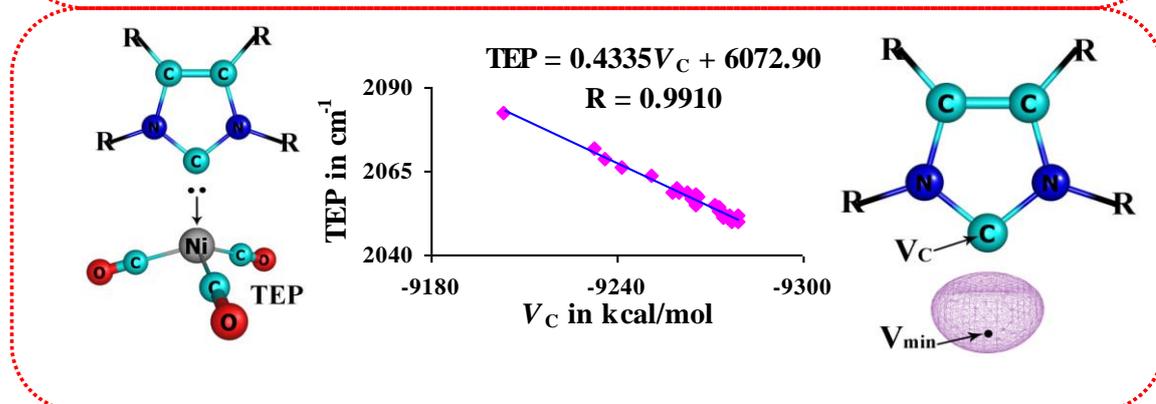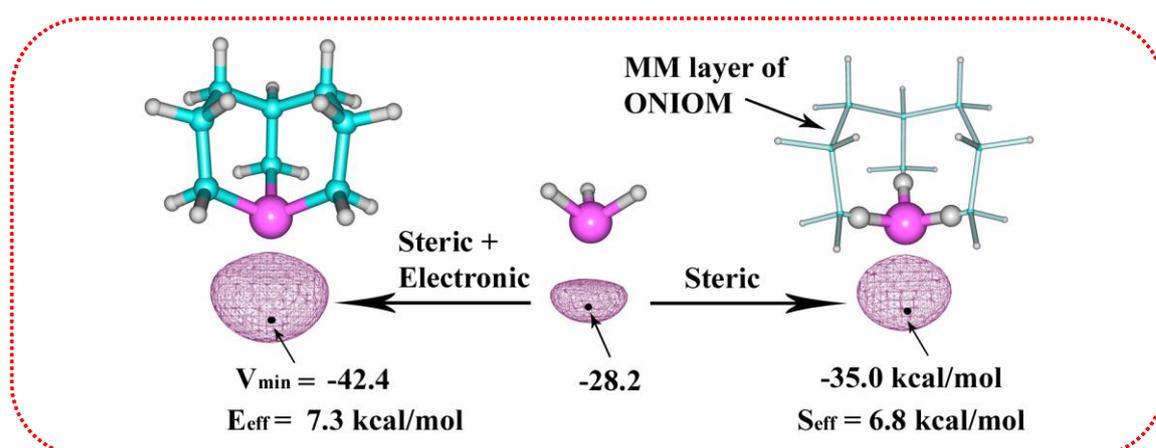
2.1 Abstract

*The stereoelectronic profile of a variety of phosphine ligands (PR_3) have been estimated using a combined approach of quantum mechanics (QM) and molecular mechanics (MM). Quantum mechanically derived molecular electrostatic potential minimum (V_{min}) of a PR_3 ligand at the phosphorus lone pair region provides a direct measure of the total electronic (E_{eff}) and steric effects (S_{eff}) of the ligand.   The difference between the V_{min} of unsubstituted PH_3 ($V_{min}(PH_3)$) and V_{min} of PR_3 is considered as $E_{eff} + S_{eff}$. It is found that a two layer QM-MM ONIOM method comprising of PH_3 in the inner QM layer and the R groups in the outer MM layer is useful to locate the structure of a PR_3 ligand in an 'electronic effect free' environment of the substituents. The V_{min} of the ONIOM optimized PR_3 at the phosphorus lone pair region thus provides the quantification of the steric effect as $S_{eff} = V_{min}(PH_3) - V_{min}(ONIOM\_PR_3)$. Since $V_{min}(PR_3)$ contains both E_{eff} and S_{eff}, the E_{eff} can be easily defined as $E_{eff} = V_{min}(ONIOM\_PR_3) - V_{min}(PR_3)$. A modified form of the symmetric deformation coordinate (S4) (Orpen et al. J. Chem. Soc., Dalton Trans. **1991**, 653) is calculated for all the fully optimized and ONIOM optimized free phosphines to obtain their S4 based steric effect values. Good linear correlation between S4 of ONIOM optimized phosphines and the MESP based S_{eff} values was obtained. Further, the determination of the stereoelectronic profile of PR_3 ligands has been achieved leading to a general classification of the ligands into four categories, viz, ligands with (i) ($+E_{eff}$, $+S_{eff}$), (ii) ($+E_{eff}$, $-S_{eff}$), (iii) ($-E_{eff}$, $+S_{eff}$), and (iv) ($-E_{eff}$, -*

S_{eff}) *where plus and minus signs indicate electron donating and electron withdrawing properties, respectively.*

Topographical analysis of molecular electrostatic potential (MESP) has been carried out for a variety of N-heterocyclic carbenes at B3LYP, BP86, and M05 levels of DFT using 6-311++G** basis set. The electron rich character of the carbene carbon is assessed in terms of the absolute minimum of MESP at the carbene lone pair region (V_{min}), as well as MESP at the carbene nucleus (V_C). A linear relationship is established between the V_C and Tolman electronic parameter (TEP) which suggested the use of the former as a simple and efficient descriptor for the electron donating power of N-heterocyclic carbene ligands towards metal coordination. The V_{min} of the carbene also showed good correlation with TEP. However, the deviation from linearity was higher than V_C – TEP correlation, and the reason for this was attributed to the steric effect of N-substituents at the lone pair region. The greater coordinating power of N-heterocyclic carbenes over phosphines is explained on the basis of deeper V_{min} values obtained for the former and in fact even the V_{min} of the least electron rich N-heterocyclic carbene is comparable to the highly electron rich phosphine ligands. Thus the MESP topographical approach presented herein offers quantification of the inherent electron donating power of a free N-heterocyclic carbene ligand.

2.2 Introduction

2.2.1 Steric and Electronic Effects of Phosphine Ligands

Phosphine ligands (PR_3) are considered as one of the most important ligands in organometallic catalyst systems since they allow the tuning of catalysts in terms of steric and electronic effects by the appropriate use of various R groups [Baber *et al.* 2007; Bunten *et al.* 2002; Cavallo and Sola 2001; Gonsalvi *et al.* 1999; White and Coville 1994; Wilson *et al.* 1993; Brown and Lee 1993; Tolman 1977; Martorell *et al.* 2001]. They are easy to synthesize and their ability to stabilize and solubilize transition metal complexes in low oxidation state [Collman *et al.* 1987] is advantageous for the designing of a variety of catalytic systems, such as the famous Grubbs ruthenium based metathesis catalysts [Grubbs and Coates 1996].

Rapid progress in homogeneous catalysis is expected when well defined steric and electronic parameters of a ligand are known before hand when one is targeting the designing of a new catalyst or targeting further improvement on an existing catalyst. Initial efforts on understanding the electron donating and accepting nature of ligands in organometallic complexes made by various groups in 1959 and in early 1960s suggested the use of nitrosyl and carbonyl stretching frequency as a measure of electronic effect [Abel *et al.* 1959; Meriwether and Fiene 1959; Chatt and Hart 1960; Poilblanc and Bigorgne 1966; Bigorgne 1958; Bigorgne 1963]. Horrocks and Taylor in 1963 proposed a "spectrochemical series" for π-bonding ligands based on cobalt nitrosyl carbonyl complexes [Horrocks and Taylor 1963; Hecke and Horrocks 1966].

Strohmeier *et al.* in 1967 performed a detailed investigation on the σ-donor ability and π-acceptor strength of various classes of ligands which include nitriles,

phosphines, sulfoxides, and isonitriles [Strohmeier and Muller 1967] using the photochemical ligand exchange reaction of arene chromium (0) tricarbonyl complexes (Eq 2.1).

$$[ArCr(CO)_3] + L \xrightarrow{h\nu} [ArCr(CO)_2L] + CO \qquad \text{... (Eq. 2.1)}$$

They recognized that the electron density at the metal increases with the increase in the electron density on the arene ligand which in turn favor the backbonding towards the CO groups and the coordinated ligand. Increase in the electron density on the metal results a smaller wave number for the corresponding $\nu(CO)$ frequency. Further, the ligating atom or the functional group of the ligand involved in bonding with the metal has a significant influence on the electronic nature of ligands. They established a series for the electronic effect of ligands *viz.* pyridine $<$ nitrile $<<$ PR$_3$ $\approx$ R$_2$SO $\approx$ isonitrile $<$ CO.

Chadwick A. Tolman in 1970 carried out a comprehensive analysis of electronic effect of phosphine ligands using Ni(CO)$_3$PR$_3$ complexes [Tolman 1970]. They synthesized Ni carbonyl complexes of 70 phosphine ligands and calculated the A$_1$ stretching frequency of CO. They identified that it should be possible to assign to each substituent on phosphorous a contribution to the CO stretching frequency given by the ligand and that the $\nu(CO)$ for Ni complexes of the form Ni(CO)$_3$PX$_1$X$_2$X$_3$ can be written as

$$\nu_{CO}(A_1) = 2056.1 + \sum_{i=1}^{3} \chi_i \ cm^{-1} \qquad \text{... (Eq. 2.2)}$$

where the frequency 2056.1 cm^{-1} is that of tri-t-butylphosphine which is the most basic ligand in the series taken for the analysis. χ_i is the substituent contribution to the $\nu(CO)$ and for t-butyl $\chi_i = 0$. They also observed that the χ_i values are correlating well with

Kabachnik's σ parameters [Kabachnik 1956] which are based on ionization constants of phosphorous acids. The electronic parameter based on the carbonyl stretching frequency in Ni carbonyl complex is known as Tolman Electronic Parameter (TEP). TEP comprises both the σ-donating and π-accepting ability of tertiary phosphines or the net donating ability of phosphines.

The introduction of TEP as a measure of electronic effect of phosphine set off the research on the quantification of the electronic effect of ligands. The use of carbon 13 NMR chemical shifts of nickel carbonyl complexes as well as C-P and M-P coupling constants were proposed as a measure of σ-donor and π-acceptor properties of phosphines [Bodner *et al.* 1980; [a]Bodner 1975, [b]Bodner 1975; Bodner and Todd 1974; [c]Bodner 1975; Allen and Taylor 1982]. Allman and Goel in 1982 demonstrated that the pKa value of phosphines if measured in $HClO_4$/nitromethane correlate with the Hammett, Taft and Kabachnik constants but phosphites showed deviation. Further the pKa value is sensitive to the choice of solvent and acid [Allman and Goel 1982]. Angelici *et al.* in 1988 reported that the basicity of a phosphine ligand can be calculated from the heat of protonation of the phosphine coordinated metal complex [Angelici 1995; Sowa *et al.* 1991; Sowa *et al.* 1992].

Giering *et al.* established a new approach for the quantification of the ligand effects known as quantitative analysis of ligand effects (QALE) by means of a combination of regression and graphical analysis of the experimental data. These data include Tolman's electronic and steric parameters, χ and θ, respectively, as well as thermodynamic (ΔH^0, ΔS^0, and ΔG^0), kinetic (reaction rates), and electrochemical (ΔE^0) entities. Based on the experimental data, QALE provides the resolution of the net electron donating ability into four parameters χ_d (corrected TEP), γ (the steric switch based on Tolman steric parameter θ, E_{ar} (aromatic effect) and π_p (π acidity). The most

noticeable achievement of QALE is the separation of TEP into σ-donor and π acceptor components. Initially QALE was based on χ and θ alone but later the addition of new parameters made QALE an efficient method for the analysis of ligand effects [Bartholomew 1996; Rahman *et al.* 1987; Eriks *et al.* 1989; Rahman *et al.* 1989; Fernandez *et al.* 2001]. Based on experimental and computational analysis, Crabtree *et al.* proved that the choice of transition metal carbonyl for the calculation of TEP is arbitrary. They proposed that any transition metal carbonyl complex for which enough experimental data are available can be used as a valid scale for the electronic effect. They established computationally derived electronic parameter (CEP) from the ab- *initio* calculations on nickel carbonyl complexes [Anton and Crabtree 1983; Perrin *et al.* 2001].

Lever in 1990 introduced an alternative series of electronic parameters of ligands based on the electrochemical E_0 values for various redox couples, especially Ru(III)/Ru(II), for a series of complexes containing the ligands to study [Lever 1990; Lever 2003]. Lever parameters can be calculated for anionic and O- and N- donor ligands. Cundari *et al.* had done the assessment of electronic profile of phosphines on the basis of semi empirical electronic parameter (SEP) on Rh Vaska complexes [Cooney *et al.* 2003].

An extensive theoretical analysis on the stereoelectronic effects of phosphines was performed by Suresh *et al.* [Suresh and Koga 2002]. They calculated the molecular electrostatic potential (MESP) minimum (V_{min}) at the lone pair region of P for a series of phosphines. Since the lone pair regions of molecule posses a high electron density, the MESP at the lone pair region shows a high negative value and the deepest value of MESP at the lone pair region was taken as V_{min}. The MESP is a physical property and can be determined experimentally by X-ray diffraction techniques and theoretically it can be rigorously calculated from its electron density $\rho(\mathbf{r})$ using the equation (Eq. 2.3)

$$V(\mathbf{r}) = \sum_{A}^{N} \frac{Z_A}{|\mathbf{r} - \mathbf{R}_A|} - \int \frac{\rho(\mathbf{r}')\,d^3\,r'}{|\mathbf{r} - \mathbf{r}'|} \qquad\qquad \text{... (Eq. 2.3)}$$

where Z_A is the charge on the Ath nucleus located at R_A [Gadre and Shirsat 2000].

They found that V_{min} values are correlating excellently with pKa value of the conjugate acid of the phosphine ligand and also with TEP. For further validation of MESP, they calculated the energy released (ΔE) in the complex formation following the reactions

$$PR_3 + Ni(CO)_3 \longrightarrow Ni(CO)_3PR_3 \qquad\qquad \text{... (Eq. 2.4)}$$

$$PR_3 + ScH_3 \longrightarrow ScH_3PR_3 \qquad\qquad \text{… (Eq. 2.5)}$$

In both the cases (Eq. 2.4 and Eq. 2.5), π-back bonding is not significant in the product complexes, and they observed that V_{min} is correlating well with ΔE. They also observed a good correlation of V_{min} with ΔH^0 and E^0 reported by Fernandez et al [Fernandez *et al.* 1998] for the following electrochemical reaction

$$Cp(CO)(PR_3)(COMe)Fe^+ + e^- \longrightarrow \eta\text{-}Cp(CO)(PR_3)(COMe)Fe \qquad \text{... (Eq. 2.6)}$$

In the case of complexes having strong back bonding between metal and phosphine, V_{min} cannot be used as a good indicator of ΔE and this was demonstrated by considering the reaction

$$PR_3 + MnH_3NH_3 \longrightarrow MnH_3NH_3PR_3 \qquad\qquad \text{… (Eq. 2.7)}$$

Later they extended the MESP approach for the separation and quantification of steric and electronic effect of phosphines using a two-layer ONIOM method [Suresh 2006]. They established a good correlation of the electronic effect with the Hammett σ_p values.

As an extension to the TEP analysis, Tolman carried out a phosphine exchange reaction on Ni(0) complexes. He observed that the ability of phosphorous ligands to

compete for coordination position in Ni(0) could not be explained based on TEP values which lead to the introduction of a measure of steric effect of phosphorous ligands, the Cone Angle (θ) [Tolman 1977]. For the calculation of cone angle, Ealing CPK model was used for the phosphorous ligand and the cone angle of a symmetric phosphine is the apex angle of a cylindrical cone, centered at 2.28 Å from the center of the P atom, which just touches the van der Waal's radii of the outermost atoms of the model (Figure 2.1a).

(a) Cone angle   (b) Cone angle for unsymmetrical ligands
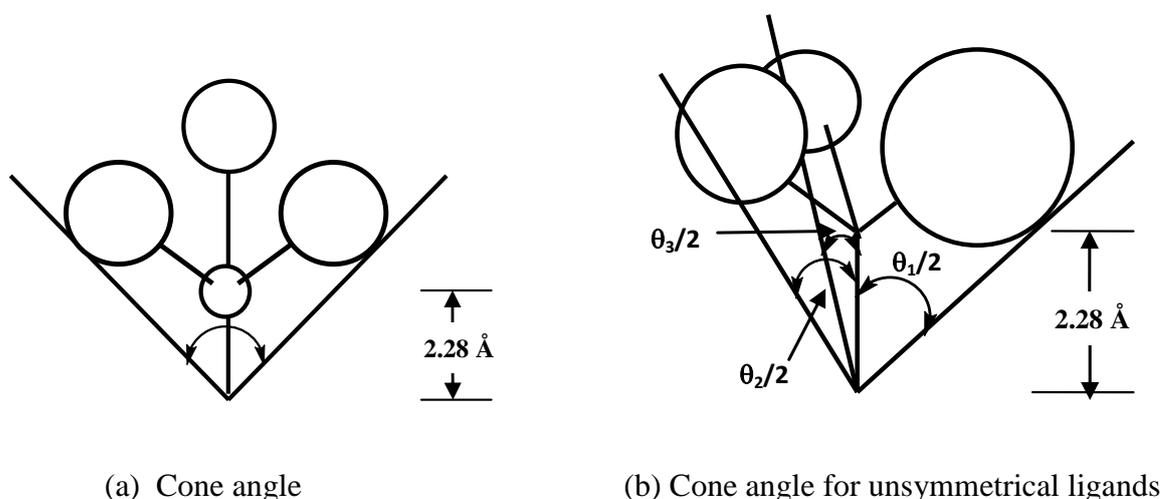
Figure 2.1 Representation of cone angle

It is possible to calculate the effective cone angle of unsymmetrical phosphine $PX_1X_2X_3$ by using a model to minimize the sum of half angles using the equation

$$\theta = \left(\frac{2}{3}\right)\sum_{i=1}^{3}\frac{\theta_i}{2} \qquad \qquad ...\ (Eq.\ 2.8)$$

where θ_i is the angle formed by the substituent X_i (Figure 2.1b). Further, there exists an approximate group additivity relationship for cone angles of unsymmetrical $PX_1X_2X_3$ ligands which considers $\frac{\theta_i}{2}$ will be the same as in $PX_{i3.}$ This allows an easy calculation of the cone angle of $PX_1X_2X_3$ ligand if one has the cone angle value of $P(X_1)_3$, $P(X_2)_3$, and $P(X_3)_3$.

Orpen *et al.* introduced a simple method for the quantification steric effect of phosphines in complexes using crystal structure data retrieved from Cambridge Structural Database (CSD) known as symmetric deformation coordinate (S4') [Dunne *et al.* 1991]. For a complex of the type ZPR_3 (Z=any element) S4' can be defined as the sum of three Z-P-R angles minus sum of three R-P-R angles. The structural parameters used in the calculation of S4' is depicted in Figure 2.2.
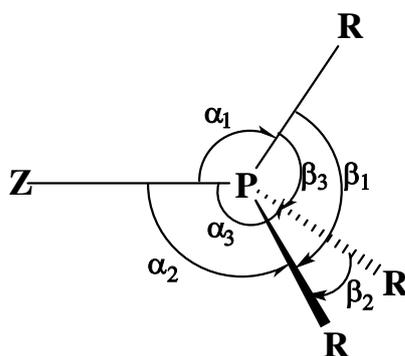
Figure 2.2 Structural parameters in the calculation of S4' of ZPR_3 complex

Using the angles α1, α2, α3, β1, β2, and β3 as defined in Figure 2.2, the S4' can be written as

$$S4' = (\alpha 1 + \alpha 2 + \alpha 3) - (\beta 1 + \beta 2 + \beta 3) \qquad \qquad ... \text{ (Eq. 2.9)}$$

Bulkier phosphines give relatively small S4' values since phosphines with large cone angles tend to give relatively small value for the sum of Z-P-R angles and relatively large value for the sum of R-P-R angles.

Brown and coworkers introduced the ligand repulsive energy parameter, E_R as a measure of the steric effect of phosphines based on a molecular mechanics (MM) model [Brown 1992; Caffery and Brown 1991]. For the calculation of E_R, a phosphine coordinated chromium complex $Cr(CO)_5PR_3$ is modeled and optimized to the lowest energy structure based on a set of force field parameters. Keeping all the coordinates of

the energy minimized structure as frozen the metal-ligand distance is varied from the equilibrium value. For each value of metal-ligand distance, the repulsive van der Waal's energy in the $Cr(CO)_5$ complex is computed. The variation in this quantity with the metal-ligand distance, $dE_{VDW(repulsive)}/dr$ is the van der Waal's repulsive force acting between ligand and the metal complex. E_R is the product of this force and the equilibrium metal-ligand bond distance (r_e) which can be shown as

$$E_R = r_e[dE_{VDW(repulsive)}/dr] \qquad\qquad \text{... (Eq. 2.10)}$$

Cundari *et al.* calculated the S4' values of Rh Vaska complexes using PM3(tm) calculations and found that this quantity correlates strongly with the S4' calculated from crystal structure [Cooney *et al.* 2003]. Other useful parameters for steric effect are solid angle and Taft-Dubois parameters [Komatsuzaki *et al.* 1989; Komatsuzaki *et al.* 1990; Hirota *et al.* 1991; Dubois and Mouvier 1963; Taft 1956; Bellon *et al.* 1980].

Suresh *et al.* extended the MESP approach to the quantification of steric effect of phosphines. They optimized free phosphine ligands in full QM level and computed the molecular electrostatic potential (MESP) minimum V_{min} at the lone pair region of P. This V_{min} was considered as a resultant of both steric and electronic effect induced by the substituents on P. An ONIOM optimization was performed in such a way that the substituents were put in the MM layer (treated with UFF) and the P in the QM layer and the MESP was computed. Since the substituents are treated with MM, the V_{min} reflects only the steric effect of phosphines ($MESP_{steric}$) and the difference between the V_{min} of the fully optimized and ONIOM optimized phosphines will give the electronic effect of phosphines. $MESP_{steric}$ showed excellent correlations with cone angle and H-P-H angles and thus verified the reliability of the MESP approach on the quantification steric effect of phosphines.

2.2.2 Steric and Electronic Effects of N-Heterocyclic Carbene Ligands

In recent years, a large variety of organometallic complexes have been synthesized with the use of strong σ-donating N-heterocyclic carbenes (NHC) as two electron donors [Nolan 2006; Seiders *et al.* 2001; Jafarpour *et al.* 2000]. In many catalytic systems, the use of NHCs is found to be more effective than the previously used phosphines. The increased reactivity of second generation Grubb's catalyst $(PR_3)(NHC)Cl_2Ru=CHR$ compared to the phosphine coordinated first generation system $(PR_3)_2Cl_2Ru=CHR$ is a classical example of the impact of NHCs in catalysis [Grubbs 2003; Crudden and Allen 2004]. The NHCs are attractive choice for the fine tuning of steric and electronic requirement of a catalyst through substitutions at the N-center or through proper modification of the conjugation features of the cyclic moiety. The lone pair in the sp^2 orbital of the carbon can be used for making strong coordination to late transition metals and heavy main group elements, and also to bind to early transition metals and the lanthanoids to produce divalent carbon(II) compounds [Herrmann and Köcher 1997]. Very recently, Frenking and co-workers [Tonner and Frenking 2007; Tonner *et al.* 2006; Deshmukh *et al.* 2008] established the existence of a new class of carbon compounds named as carbones where the carbon atom carries two lone pairs rather than one and they often yield divalent carbon(0) compounds.

There are several attempts to quantify the stereoelectronic features of various types of NHCs. Cavallo *et al.* introduced the buried volume (%V_{Bur}) as a measure of steric size of NHC ligands (Figure 2.3) [Hillier *et al.* 2003; Cavallo *et al.* 2005]. It is the percent of volume occupied by ligand atoms in a sphere centered on the metal. It represents the space around the metal atom that must be shared by different ligands upon

coordination. A bulkier ligand will occupy larger amount of space leading to a greater

%V_{Bur} value. The radius of the sphere is taken as 3 Å which is roughly the distance

between the N atoms of NHC ring and the putative metal atom in an NHC coordinated

metal complex. Later they developed Samb*V*ca, web application for the calculation of

buried volume of organometallic ligands [Poater *et al.* 2009].
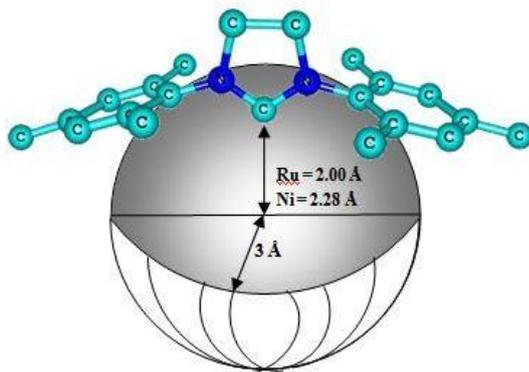
Figure 2.3. Schematic representation of sphere dimension used for determination of

%V_{Bur}

Nolan *et al.* synthesized six different NHC coordinated complexes of the type

(NHC)Cp*RuCl (Cp*=η^5-C$_5$Me$_5$) and calculated bond disruption enthalpy (BDE) of

NHC in the complex [Hillier *et al.* 2003]. They observed a good correlation of BDE with

the theoretically calculated %V_{Bur} value. They extended the stereoelectronic analysis of

NHCs by analyzing the interaction of NHCs with Ni(CO)$_4$. The %V_{Bur} values of NHCs

showed good agreement with the experimentally determined BDE. Further QM-MM

analysis also showed that the steric effects of NHCs are quite important in deciding the

nature of NHC coordinate nickel carbonyl complexes [Kelly *et al.* 2008; Huang *et al.*

1999; Dorta *et al.* 2003; Dorta *et al.* 2005]. Gusev introduced 'r' repulsiveness as a

descriptor of the steric effect of NHCs which is based on the enthalpy for

decarbonylation of Ni(CO)$_3$NHC to form Ni(CO)$_2$NHC [Gusev 2009].

Identifying the possibility of the Tolman electronic parameter (TEP) as a measure of electron donating nature of NHCs, Nolan *et al.* synthesized Ni(CO)$_3$NHC complexes for a series of NHC ligands and calculated the IR stretching frequency of CO. TEP values showed that NHCs are highly electron donating compared to that of phosphines. But they failed to synthesize nickel tricarbonyl complexes of bulkier NHCs like IAd (adamentyl groups as N-substituents) and I^{t}Bu (t-butyl groups as N substituents) because of the high steric nature the NHC ligands and this prevented the comparison of the electronic effect of commonly encountered NHCs [Dorta *et al.* 2005]. In order to place all commonly used NHCs on the same stereoelectronic scale, they analyzed various NHC coordinated carbonyl complexes and found that Ir complexes of the type (NHC)Ir(CO)$_2$Cl would be suitable for the TEP calculation. They observed a good correlation of the TEP calculated from (PR$_3$)Ir(CO)$_2$Cl with that calculated from nickel carbonyl complexes. Thus the use of iridium complex allowed a direct comparison of electronic effect of phosphines and NHCs. Iridium complex based TEP values also showed the higher electron donating nature of NHCs over phoshines. They also found that the difference in the TEP values among various NHCs is not high [Kelly *et al.* 2008]. Gusev calculated conventional TEP values of 76 NHCs with the help of density functional theory calculations. Their TEP values suggested that the electronic effect of NHCs would depend on various factors such as NHC ring size, nature of substituents on N and C4, C5 positions and annulation [Gusev 2009].

In the present work, we explore the MESP based technique to unravel the stereoelectronic profile of a variety of phosphine ligands including some of the typically used phosphite ligands and the electronic effect of a set of typical N-heterocyclic carbene ligands.

2.3 Quantification of Stereoelectronic Effects of Phosphine Ligands

2.3.1 Methodology

2.3.1.1 Selection of Ligands

We have taken cyclic and heterocyclic phosphines and phosphites along with some commonly known non cyclic phosphines for this study and they are shown in Figure 2.4. Also included in this study is the "bowl shaped" phosphine ligands TRMP and TRIP designed by Kawashima and co-workers [Goto *et al.* 2002; Matsumoto *et al.* 2002; Ohta *et al.* 2007; Ohzu *et al.* 2003] which bear m-terphenyl-based P substituents. In many of the ligands, phosphorus atom is connected to saturated/conjugated/partially conjugated units showing four-, five-, six-, and eight-membered ring structures. Cyclic three membered phosphines are exempted from the study due to the lack of adequate force fields to model them. Some of the recently synthesized bulky phosphine systems are also included. A compilation of many of these structures can be seen in the work of Cundari *et al.* [Cooney *et al.* 2003]. The X-ray structures of all the reported ligands are known in their metal complexes and in some cases, the X-ray structure of free forms is also available. Herein, each ligand is named with the CCDC database [Allen 2002] code which has been used to locate the X-ray structures of its metal complex. For some commonly encountered ligands, their typical names are also given (Figure 2.4).

PH₃   PMe₃   PEt₃   P(iPr)₃   P(tBu)₃   P(CF₃)₃   PH₂Ph   PEtPh₂   P(tBu)Ph₂
XIBVUZ   AGEWUE   BILMIS   FUWMAL   BCBPRU   LADZAR   GOJVEG   CPEPPT   XIRQIY

PMe₂Ph   PMePh₂   PCy₃   PPh₃   P(m-C₆H₄F)₃   NOHCOC   GILHOY   KUHZUI
BAXLER   AFUMIX   BABNEY   ACPMNA   SIFBAK

NESNII   CIYTAF   QAHCOR   WILPUC   BEVLUJ   KANMER

PARCIU   RIJLEB   BOHZON   JAJWIA   JEDLAF   JOQKIJ

JOTQAK   QEQJAX   COXRAI   TUDDUR   GEHCAX   KOYGUA

DODKAI   VAKXOU   MASRAZ   FIDDOL   QIVLOW   HAZXOV   JUVNET

HOZSOE   BIYKEZ   TRMP   TRIP

Figure 2.4 Ligands used in the present study.

2.3.1.2 Optimization of Ligands

The X-ray structure of all the PR_3 ligands are located from the CCDC database [Allen 2002] (the name used to identify each structure in the database is given in Figure 2.4) and they are used as input for geometry optimization. Two levels of optimization procedures are used. In the first one, full optimization of a PR_3 structure is carried out with the B3LYP/6-31G(d,p) level of density functional theory (DFT) method [Becke 1993; Lee *et al.* 1988]. In the second method, the hybrid QM-MM method known as ONIOM (Our own n-layered integrated molecular orbital + molecular mechanics), developed by Morokuma and co-workers [Vreven and Morokuma 2000; Dapprich *et al.* 1999] is used [Ananikov *et al.* 2005; Carbo *et al.* 2001; Nozaki *et al.* 1997; Ujaque *et al.* 1998]. The attractive feature of ONIOM method is that a chemical system can be partitioned into two or three layers so that each layer can be treated at different computational levels. Hence, the most critical part of the system can be treated with a high level of QM method while reaming part of the system can be calculated at a low level of theory, often a MM method. In the present work, we have adopted a two layer ONIOM technique which is illustrated in Figure 2.5. The outer layer contains the substituent R groups and the inner layer comprises of PH_3. For the outer layer, the MM method utilizing the universal force field (UFF) [Rappé *et al.* 1992] is selected while for the inner layer, the QM method of B3LYP/6-31G(d,p) is chosen. Since the R groups are treated with the MM force field, we consider that the optimized geometry of PR_3 is obtained in the 'electronic effect' free environment of the 'R' substituents. For all the calculations Gaussian 03 [Frisch *et al.* Gaussian 03 2004] suite of programs are used.
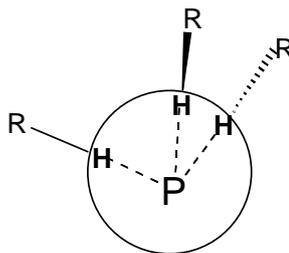
Figure 2.5 The two layer ONIOM method. H atoms are the link atoms.

2.3.1.3 Calculation of Molecular Electrostatic Potential Minimum (V_{min})

For all the ligands optimized at the B3LYP/6-31G(d,p) level, the same level of wave function is used to calculate the molecular electrostatic potential (MESP). The MESP is rigorously calculated using eq. (Eq. 2.3).

In general, electron dense π- and lone pair regions are expected to show high negative MESP whereas electron deficient regions are characterized by positive MESP. In the case of phosphine ligands, a negative-valued MESP minimum (V_{min}) is expected at the lone pair region of the phosphorus atom and it is calculated in all the cases (Figure 2.6) [Suresh and Koga 2002; Suresh 2006]. In the case of ONIOM level optimized PR_3, the V_{min} always corresponds to the MESP minimum of the inner QM layer, viz. PH_3. From the visual inspection of the calculated MESP data using a freely available graphical interface such as MOLEKEL program [Flükiger *et al.* 2000], one can easily find out the V_{min} values. If a guess point near the V_{min} is used along with the Prop =(potential, opt) keyword in Gaussian 03, the exact location and the value of V_{min} can be obtained from a rigorous calculation.
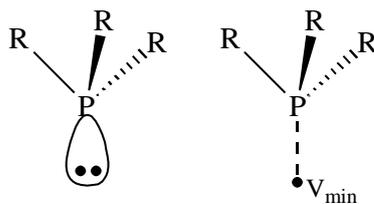
Figure 2.6 Phosphine ligand with its lone pair and V_{min} in the lone pair region.

2.3.1.4 Calculation of Modified Symmetric Deformation Coordinate (S4)

The quantity known as symmetric deformation coordinate (S4') was introduced by Orpen *et al.* as an alternative to the cone angle to measure the steric bulk of phosphines [Dunne *et al.* 1991]. It is a numerical quantity derived from geometrical calculations and can be calculated from the difference between the sum of angles between the substituents and the coordinated atom (a transition metal, a main group metal or a non metal) and the angles between substituents (Figure 2.2). In the present work, since we are dealing only with the PR$_3$ ligands, the definition of α1, α2 and α3 angles are not possible. However, angles that can closely resemble to that of α1, α2, and α3 can be defined as given in Figure 2.7.
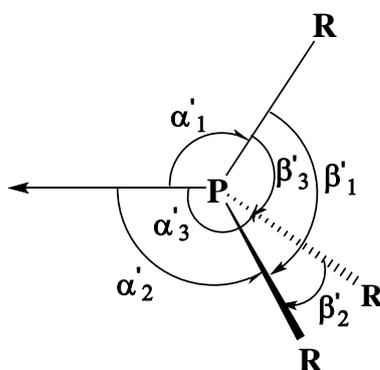
Figure 2.7 Definition of angles used for the calculation of S4 in the present work.

In Figure 2.7, in order to define α' angles for a PR_3 ligand, a line passing through the phosphorus atom is drawn in such a way that it is perpendicular to a plane containing the three atoms directly connected to the phosphorus atom. In the case of phosphine-metal complexes, the metal center is expected on this line at the appropriate bonding distances from the phosphorus atom. Therefore, for free ligands, on the basis of α' and β' angles, a modified symmetric deformation coordinate named S4 is defined as given in Eq. 2.11.

$$S4 = (\alpha'1 + \alpha'2 + \alpha'3) - (\beta'1 + \beta'2 + \beta'3) \qquad \text{... (Eq. 2.11)}$$

In the present work, S4 values are measured for all the fully optimized and the ONIOM level optimized geometries.

2.3.2 Results and Discussion

2.3.2.1 MESP Analysis of Fully Optimized Phosphine Ligands

The V_{min} values of MESP calculated for the fully optimized PR_3 ligands are given in Table 2.1. As expected, all of them show negative value for V_{min}. It can be seen that the V_{min} value of the unsubstituted phosphine PH_3 is -28.22 kcal/mol and the value for other ligands lie in the range of -44.9 to -5.95 kcal/mol. A pictorial illustration of the MESP is depicted in Figure 2.8 using an isosurface of value -18.83 kcal/mol for a representative set of systems. This value is chosen because even for the most electron deficient system in Figure 2.8 (GEHCAX), the visual inspection of the isosurface is possible. The position of the V_{min} corresponding to the lone pair region of the phosphorus atom is also depicted for each ligand in Figure 2.8.
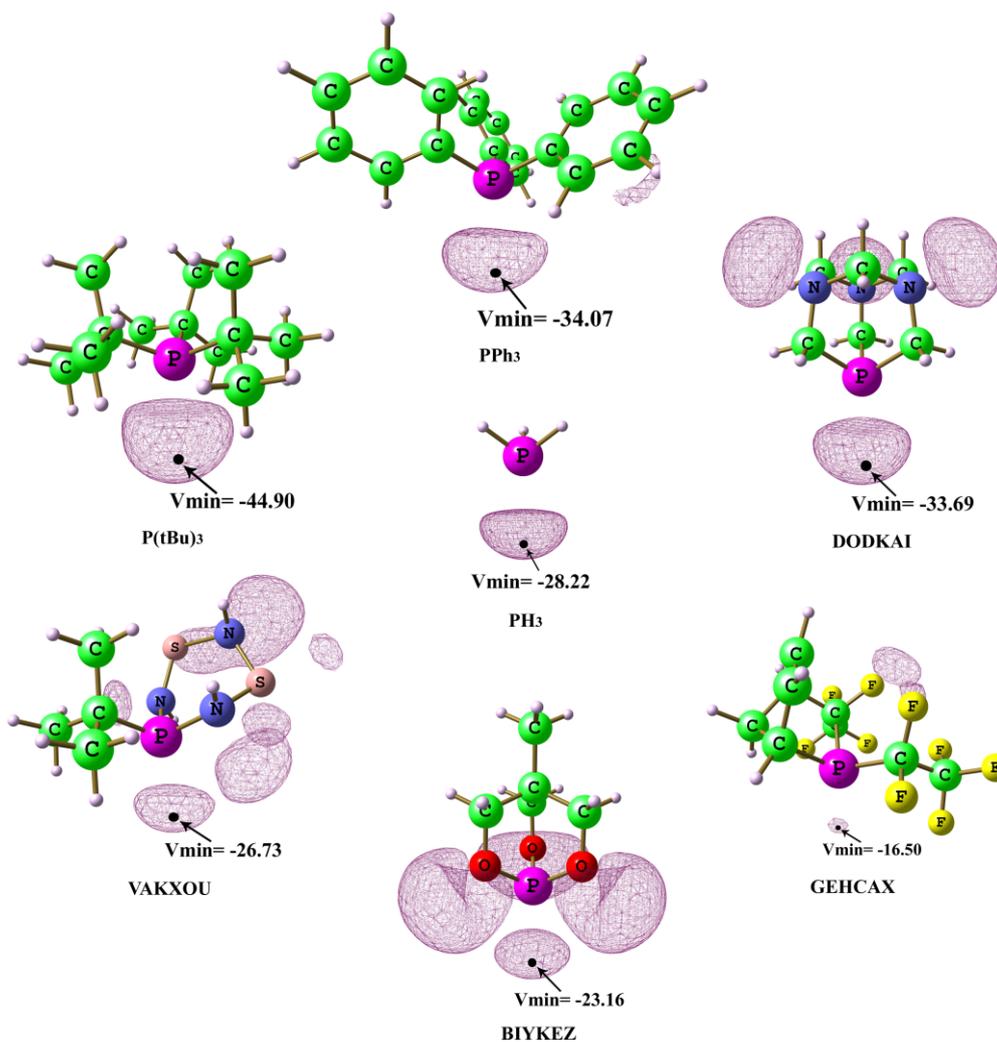
Figure 2.8 V_{min} points (black dots) located for a representative set of PR_3 ligands. The MESP isosurface of -18.83 kcal/mol is also plotted.

There are twenty nine PR_3 ligands showing higher negative value for V_{min} than $V_{min}(PH_3)$ and hence they may be classified as electron donating and the remaining sixteen ligands are expected to behave as electron withdrawing ligands. This classification is meaningful as the MESP is often used as a direct measure of electron donating and electron withdrawing ability of substituents, functional groups and ligands [Politzer and Murray 2002; Suresh and Gadre 2007; Suresh and Gadre 1998; Gadre and Suresh 1997; Suresh *et al.* 2000; Phukan *et al.* 2004]. It may be noted that both steric and electronic effect of the substituent 'R' is contributing to the electron

donating/withdrawing effect of the PR_3 ligand. For instance, the changes in the bulkiness

of R groups can alter the 'p' character of the sp^3 hybridized lone pair orbital of the

phosphorus atom which in turn would lead to a corresponding increase/decrease in the

negative character of the V_{min} at the lone pair. Since the P-R connection is through single

bond, the electronic effect is mainly inductive in nature. Considering the V_{min} of PH_3 as a

reference point, the difference of $V_{min}(PH_3)$ and $V_{min}(PR_3)$ can be taken as the combined

effect of the electronic and steric effect of the PR_3 ligand. We propose the notations E_{eff}

and S_{eff} to designate the electronic and steric effects, respectively. Therefore,

$$E_{eff} + S_{eff} = V_{min}(PH_3) - V_{min}(PR_3) \qquad \qquad ... (Eq.\ 2.12)$$

The values for $E_{eff} + S_{eff}$ is calculated for all PR_3 ligands which are given in Table 2.1

along with $V_{min}(PR_3)$ values.

Table 2.1 MESP $V_{min}(PR_3)$ values of fully optimized geometries of PR_3 ligands (X-ray

IDs are given for most of the ligands). See Figure 2.3 for each structure. All values are in

kcal/mol.

Ligand	$V_{min}(PR_3)$	$E_{eff} + S_{eff}$	Ligand	$V_{min}(PR_3)$	$E_{eff} + S_{eff}$
PH_3	-28.22	0.00	PARCIU	-36.52	8.30
PMe_3	-43.02	14.8	RIJLEB	-17.63	-10.59
PEt_3	-43.55	15.33	BOHZON	-15.31	-12.9
$P(^iPr)_3$	-44.18	15.96	JAJWIA	-33.57	5.35
$P(^tBu)_3$	-44.9	16.68	JEDLAF	-30.12	1.90
$P(CF_3)_3$	-5.95	-22.27	JOQKIJ	-22.78	-5.44
PH_2Ph	-31.05	2.83	JOTQAK	-31.94	3.72
PMe_2Ph	-40.41	12.19	QEQJAX	-35.52	7.29
$PEtPh_2$	-37.23	9.01	COXRAI	-22.90	-5.31
$P(^tBu)Ph_2$	-38.86	10.64	TUDDUR	-33.89	5.67
$PMePh_2$	-36.76	8.54	GEHCAX	-16.50	-11.72
PCy_3	-44.99	16.77	KOYGUA	-42.36	14.14

PPh$_3$	-34.07	5.85	DODKAI	-33.69	5.48
P(m-C$_6$H$_4$F)$_3$	-27.77	-0.45	VAKXOU	-26.73	-1.44
NOHCOC	-25.48	-2.74	MASRAZ	-26.48	-1.74
GILHOY	-32.07	3.84	FIDDOL	-30.12	1.90
KUHZUI	-36.77	8.55	QIVLOW	-16.30	-11.9
NESNII	-38.91	10.68	HAZXOV	-12.17	-16.04
CIYTAF	-25.48	-2.74	JUVNET	-23.16	-5.06
QAHCOR	-32.94	4.72	HOZSOE	-16.57	-11.65
WILPUC	-39.97	11.75	BIYKEZ	-23.16	-5.06
BEVLUJ	-33.07	4.85	TRMP	-31.75	3.53
KANMER	-39.53	11.31	TRIP	-33.69	5.47

It can be seen from the Table 2.1 that $E_{eff} + S_{eff}$ values are ranging from -22.27 to 16.77 kcal/mol. Among these PCy$_3$ is the most electron donating ($V_{min}= -44.99$ kcal/mol) and P(CF$_3$)$_3$ is the most electron withdrawing ligand ($V_{min}= -5.95$ kcal/mol). Among phosphites, HAZXOV (Figure 2.4) is found to be the most electron withdrawing ligand. All phosphites have negative values for $E_{eff} + S_{eff}$, indicating their electron withdrawing nature due to the presence of the electronegative oxygen attached to phosphorus. The higher electron donating tendency observed for PMe$_3$, P(^{t}Bu)$_3$, PEt$_3$, P(^{i}Pr)$_3$, and PCy$_3$ can be attributed to the presence of electron donating alkyl groups whereas the presence of electron withdrawing fluorine in P(CF$_3$)$_3$ makes it highly electron withdrawing in nature. The V_{min} value of -42.36 kcal/mol observed for the caged ligand KOYGUA is comparable to the V_{min} value of PCy$_3$ as the former has cyclohexyl-type R group connections to phosphorus. But in another caged ligand with six membered rings (DODKAI), the presence of nitrogen in the ring structure caused the formation of a less negative V_{min} (-33.69 kcal/mol).

The lesser electron donating tendency of PPh$_3$ can be observed from its low V_{min} value of -34.07 kcal/mol compared to alkyl phosphines such as PEt$_3$ ($V_{min} = -43.55$ kcal/mol). This is expected because the phenyl ring is normally assigned higher group

electronegativity when compared to an alkyl group. In general, the V_{min} values are more influenced by the type of R groups than the steric bulkiness of the R group. Thus in GEHCAX the presence of fluorine drastically reduces the negative value of V_{min} (-16.50 kcal/mol) while PARCIU has appreciable amount of electron donating ability as its V_{min} is -36.52 kcal/mol.

2.3.2.2 MESP Analysis of ONIOM Optimized Phosphine Ligands

The V_{min} values of the ONIOM optimized PR_3 ligands are given in Table 2.2 which always correspond to the PH_3 unit of the QM layer. In the QM layer, the H-P-H angle of the PH_3 will increase when the steric effect of the R groups in the outer layer increases. In other words, the steric effect of the R groups are causing the shrinking or the expansion of the H-P-H angle which in turn will cause a change in the electron density at the lone pair region when compared to that of the fully optimized PH_3 ligand. Therefore, the difference between the $V_{min}(PH_3)$ and the $V_{min}(ONIOM\_PR_3)$ is considered as a measure of the steric effect provided by the substituents (Eq. 2.13).

$$S_{eff} = V_{min}(PH_3) - V_{min}(ONIOM\_PR_3) \quad\quad\quad \dots \text{(Eq. 2.13)}$$

Table 2.2 MESP $V_{min}(ONIOM\_PR_3)$ values of ONIOM-level optimized geometries of PR_3 ligands. All values are in kcal/mol.

Ligand	$V_{min}(ONIOM\_PR_3)$	Ligand	$V_{min}(ONIOM\_PR_3)$
PH_3	-28.22	PARCIU	-28.68
PMe_3	-30.62	RIJLEB	-29.93
PEt_3	-33.01	BOHZON	-29.12
$P(^iPr)_3$	-37.46	JAJWIA	-30.99
$P(^tBu)_3$	-42.90	JEDLAF	-29.30
$P(CF_3)_3$	-33.68	JOQKIJ	-22.21
PH_2Ph	-28.63	JOTQAK	-28.61
PMe_2Ph	-32.83	QEQJAX	-27.29

PEtPh$_2$	-35.12	COXRAI	-28.70
P(^{t}Bu)Ph$_2$	-36.58	TUDDUR	-27.86
PMePh$_2$	-32.47	GEHCAX	-31.50
PCy$_3$	-37.83	KOYGUA	-35.01
PPh$_3$	-34.20	DODKAI	-30.62
P(m-C$_6$H$_4$F)$_3$	-33.82	VAKXOU	-28.61
NOHCOC	-25.16	MASRAZ	-28.18
GILHOY	-22.46	FIDDOL	-28.18
KUHZUI	-28.61	QIVLOW	-31.60
NESNII	-28.18	HAZXOV	-25.10
CIYTAF	-25.92	JUVNET	-26.86
QAHCOR	-24.22	HOZSOE	-24.54
WILPUC	-27.11	BIYKEZ	-26.04
BEVLUJ	-27.36	TRMP	-32.13
KANMER	-30.99	TRIP	-35.77

From eqs 2.12 and 2.13, the electronic effect of a PR$_3$ ligand (E$_{eff}$) can be defined as the difference between V_{min}(ONIOM_PR$_3$) and V_{min}(PR$_3$)

$$E_{eff} = V_{min}(ONIOM\_PR_3) - (V_{min}(PR_3) \qquad \ldots \text{(Eq. 2.14)}$$

The calculated values of E$_{eff}$ and S$_{eff}$ values are summarized in Table 2.3.

Table 2.3 E$_{eff}$ and S$_{eff}$ values of PR$_3$ ligands. All values are in kcal/mol.

Ligand	E$_{eff}$	S$_{eff}$	Ligand	E$_{eff}$	S$_{eff}$
PH$_3$	0.00	0.00	PARCIU	7.84	0.46
PMe$_3$	12.40	2.40	RIJLEB	-12.29	1.71
PEt$_3$	10.54	4.79	BOHZON	-13.81	0.89
P(^{i}Pr)$_3$	6.71	9.24	JAJWIA	2.57	2.78
P(^{t}Bu)$_3$	1.95	14.70	JEDLAF	0.82	1.08
P(CF$_3$)$_3$	-27.73	5.46	JOQKIJ	0.56	-6.01
PH$_2$Ph	2.42	0.41	JOTQAK	3.33	0.39
PMe$_2$Ph	7.58	4.61	QEQJAX	8.22	-0.92
PEtPh$_2$	2.11	6.90	COXRAI	-5.80	0.52
P(^{t}Bu)Ph$_2$	2.28	8.36	TUDDUR	6.02	-0.36

PMePh$_2$	4.29	4.25	GEHCAX	-14.99	3.28
PCy$_3$	7.16	9.61	KOYGUA	7.34	6.79
PPh$_3$	-0.13	5.98	DODKAI	3.07	2.40
P(m-C$_6$H$_4$F)$_3$	-6.05	5.19	VAKXOU	-1.88	0.39
NOHCOC	0.31	-3.06	MASRAZ	-1.69	-0.04
GILHOY	9.60	-5.76	FIDDOL	1.94	-0.04
KUHZUI	8.16	0.39	QIVLOW	-15.2	3.30
NESNII	10.73	-0.04	HAZXOV	-12.92	-3.12
CIYTAF	-0.44	-2.30	JUVNET	-3.70	-1.36
QAHCOR	8.72	-3.99	HOZSOE	-7.97	-3.68
WILPUC	12.86	-1.11	BIYKEZ	-2.89	-2.18
BEVLUJ	5.71	-0.86	TRMP	-0.38	3.91
KANMER	8.53	2.78	TRIP	-2.07	7.55

2.3.2.3 Symmetric Deformation Coordinate

The symmetric S4' deformation coordinates as defined by Orpen *et al.* (Figure 2.2) are calculated for all the ligands in their respective metal complexes and they are presented in Table 2.4. Further, the modified symmetric deformation coordinates S4 (Figure 2.7) are calculated for all the fully optimized geometries of PR$_3$ ligands at the B3LYP/6-31G(d,p) as well as at the ONIOM(B3LYP/6-31G(d,p):UFF) levels and are given in Table 2.4.

Table 2.4 S4 values of X-ray structure, B3LYP/6-31G(d,p) level optimized and ONIOM level optimized PR$_3$ ligands. All values are in degrees.

Ligand	X-ray structure S4'	Fully optimized PR$_3$ S4	ONIOM Optimized PR$_3$ S4
PH$_3$	102.3	88.1	88.1
PMe$_3$	44.1	41.7	74.3
PEt$_3$	42.7	49.3	90.8
P(^{t}Pr)$_3$	25.3	31.1	35.9
P(^{t}Bu)$_3$	15.5	12.0	4.2

P(CF$_3$)$_3$	63.0	64.4	58.0
PH$_2$Ph	59.0	72.7	86.6
PMe$_2$Ph	61.0	50.6	64.1
PEtPh$_2$	41.8	37.4	51.8
P(^{t}Bu)Ph$_2$	34.5	27.1	42.5
PMePh$_2$	39.9	45.7	65.9
PCy$_3$	26.1	39.2	34.1
PPh$_3$	40.0	39.6	56.9
P(m-C$_6$H$_4$F)$_3$	22.0	40.3	40.3
NOHCOC	51.7	60.3	98.1
GILHOY	80.0	87.6	118.4
KUHZUI	57.3	55.7	82.1
NESNII	54.7	62.9	80.2
CIYTAF	57.2	57.3	98.1
QAHCOR	61.1	72	105.8
WILPUC	56.7	64.1	82.1
BEVLUJ	70.0	72.3	90.8
KANMER	49.2	63.3	72.6
PARCIU	63.9	74.9	84.7
RIJLEB	40.3	22.2	73.9
BOHZON	29.7	24.7	78.4
JAJWIA	31.7	36.4	76.5
JEDLAF	61.9	76.0	78.8
JOQKIJ	101.4	111.0	114.9
JOTQAK	41.6	53.3	74.3
QEQJAX	44.4	51.3	80.4
COXRAI	63.8	67.3	78.9
TUDDUR	50.9	57.1	82.9
GEHCAX	62.8	64.8	65.3
KOYGUA	42.9	54.6	51.4
DODKAI	67.6	82.0	71.1
VAKXOU	43.2	38.2	73.2
MASRAZ	31.0	55.1	73.4
FIDDOL	42.4	57.1	73.3
QIVLOW	30.5	45.3	60.7
HAZXOV	53.6	68.0	85.7
JUVNET	38.7	52.9	77.9
HOZSOE	55.3	65.0	85.4
BIYKEZ	42.0	55.0	76.0
TRMP	26.8	39.3	56.8
TRIP	8.9	27.5	40.9

Since the S4 values represent a steric measure of phosphine, correlation between the S4 values of the DFT level optimized structures and the S4' values of the X-ray structures were studied and it is presented in Figure 2.9. The deviation from linearity in the correlation diagram given in Figure 2.9 is expected since there is no metal in optimized geometry of phosphine ligands. But it can be seen that there is an acceptable agreement between the S4' values of X-ray structures and the S4 values of the optimized geometries since the correlation coefficient (r) here is 0.889, which suggests that the S4 definition given in Figure 2.7 is reasonable for assessing the steric effect.
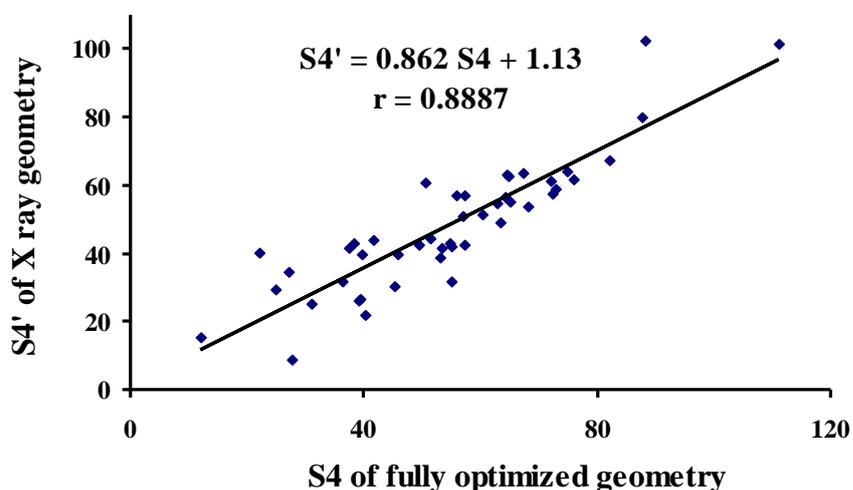
Figure 2.9 Correlation between S4 values of the fully optimized structures and X-ray structures of PR_3 ligands.

It may be noted that in a $(PR_3)ML_n$ complex, the metal to PR_3 interaction can also be influenced by interactions of the other ligands 'L_n' in it. The effect of these interactions will be different in different complexes and so the S4' calculated for a particular PR_3 ligand from X-ray structure may not be the same in all the complexes. To account for this, Orpen *et al.* have calculated S4' for a particular ligand in various complexes and calculated the mean S4' [Dunne *et al.* 1991]. Since then a large number of X-ray structures were added to Cambridge Structural Database (CSD) [Allen 2002]

and the mean S4' calculated by Orpen *et al.* has been found to vary when more structures were included [Cooney *et al.* 2003]. Thus S4' of a phosphine calculated from a single structure may not produce actual steric effect defined by Orpen *et al.* but can be considered as a measure of steric effect only within that complex. However, S4' values can provide a general trend in the steric effect when considering a series of phosphine ligand and Cundari *et al*. have successfully used S4' values from PM3 calculations as a measure of steric effect [Cooney *et al.* 2003]. Compared to the S4' values, the modified S4 values calculated in the present work can be considered as a measure of the steric effect of only the isolated PR_3 ligand in the 'electronic effect included' atmosphere of the R moieties. The usage 'electronic effect included' means that the optimization of PR_3 is carried out using a full QM approach and therefore, the R-P-R angles in the definition of S4 is determined by both the electronic and steric effects of the R moieties. In this spirit, even the S4' values obtained from the X-ray geometries is also truly not representing the steric effect as the electronic effect is not separated out.

The S4 values of the ONIOM level optimized structures may be considered as a measure of the steric effect of the PR_3 ligand in an 'electronic effect free' environment of the R moieties. The correlation between the S4 values of the QM level optimized structures and ONIOM level optimized structures of PR_3 ligands are depicted in Figure 2.10. There is apparently no correlation between the two quantities which is expected because the electronic effects provided by the substituents in phosphines were absent in the ONIOM level calculation whereas both steric and electronic effects were present in the QM level optimized structures.
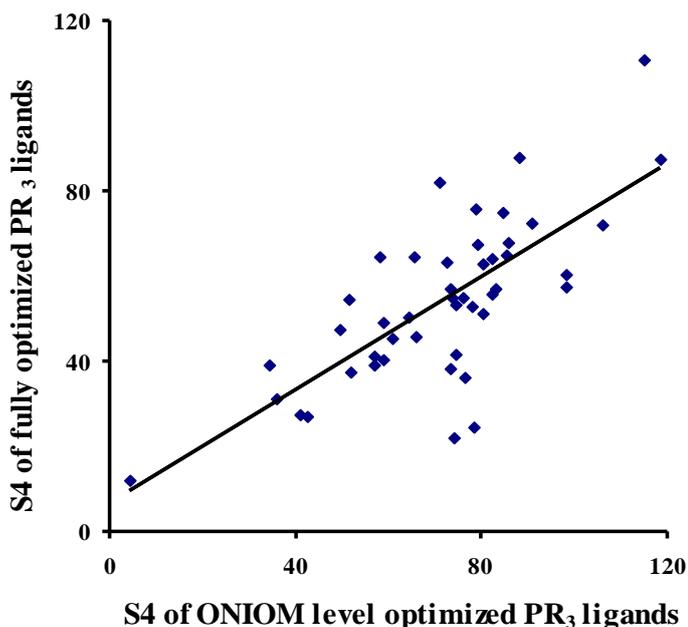
Figure 2.10 Correlation between the S4 values of fully optimized and ONIOM level optimized PR₃ ligands.

2.3.2.4 Comparison of Steric Effect Calculated from MESP and S4

The S4 values calculated for ONIOM level optimized geometries may be considered as a geometric parameter for the quantification of the steric effect in the 'electronic effect free' atmosphere of R moieties. Therefore, it can be compared with the steric effect (S_{eff}) calculated using the MESP approach. There is in fact good agreement between the S4 and the corresponding MESP based S_{eff} values as they show a good linear dependency (correlation coefficient = 0.959) (Figure 2.11).

It may be noted that a positive value of S_{eff} represents higher steric effect and a negative value shows lesser steric effect provided by that ligand when compared to the reference point of PH₃. Cundari *et al*. have reported that phosphites cannot be treated along with phosphines while measuring S4' values because of its conformational flexibility. But from the above correlation which includes phosphites, it is clear that MESP based approach to the steric effect can incorporate a wider range of ligands.

Further, the correlation confirms that the present approach is advantageous because the steric effect based on S4' value depends on various other electronic factors in a complex. In other words, the combination of QM and QM-MM method augmented with the MESP based analysis of the electronic variations around the phosphorus lone pair makes it possible the separation of electronic and steric effect from one another.
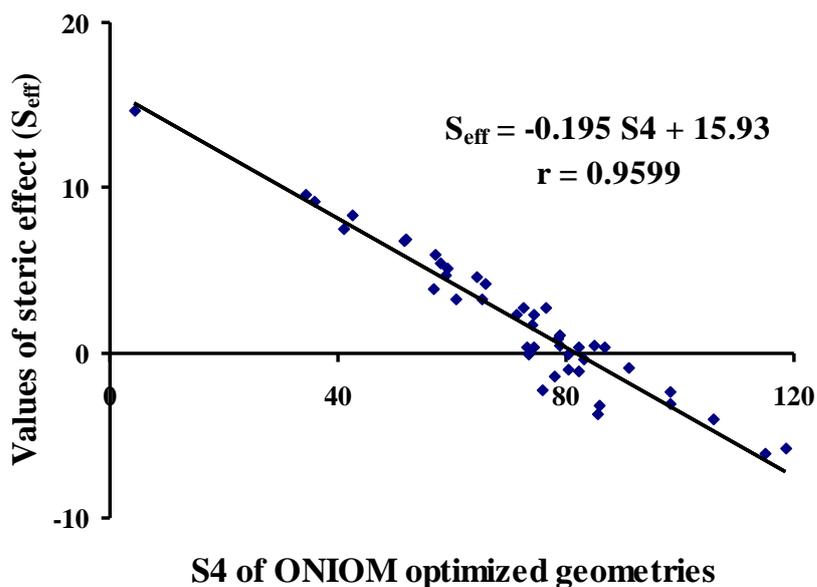
Figure 2.11 Correlation between S4 values of ONIOM optimized geometries and calculated S_{eff}

2.3.2.5 Stereoelectronic profile of ligands

Since the steric effect and electronic effect of phosphines can be separated using MESP, it is possible to construct a stereoelectronic plot of the ligands using the values in Table 2.3 and such a plot is depicted in Figure 2.12.
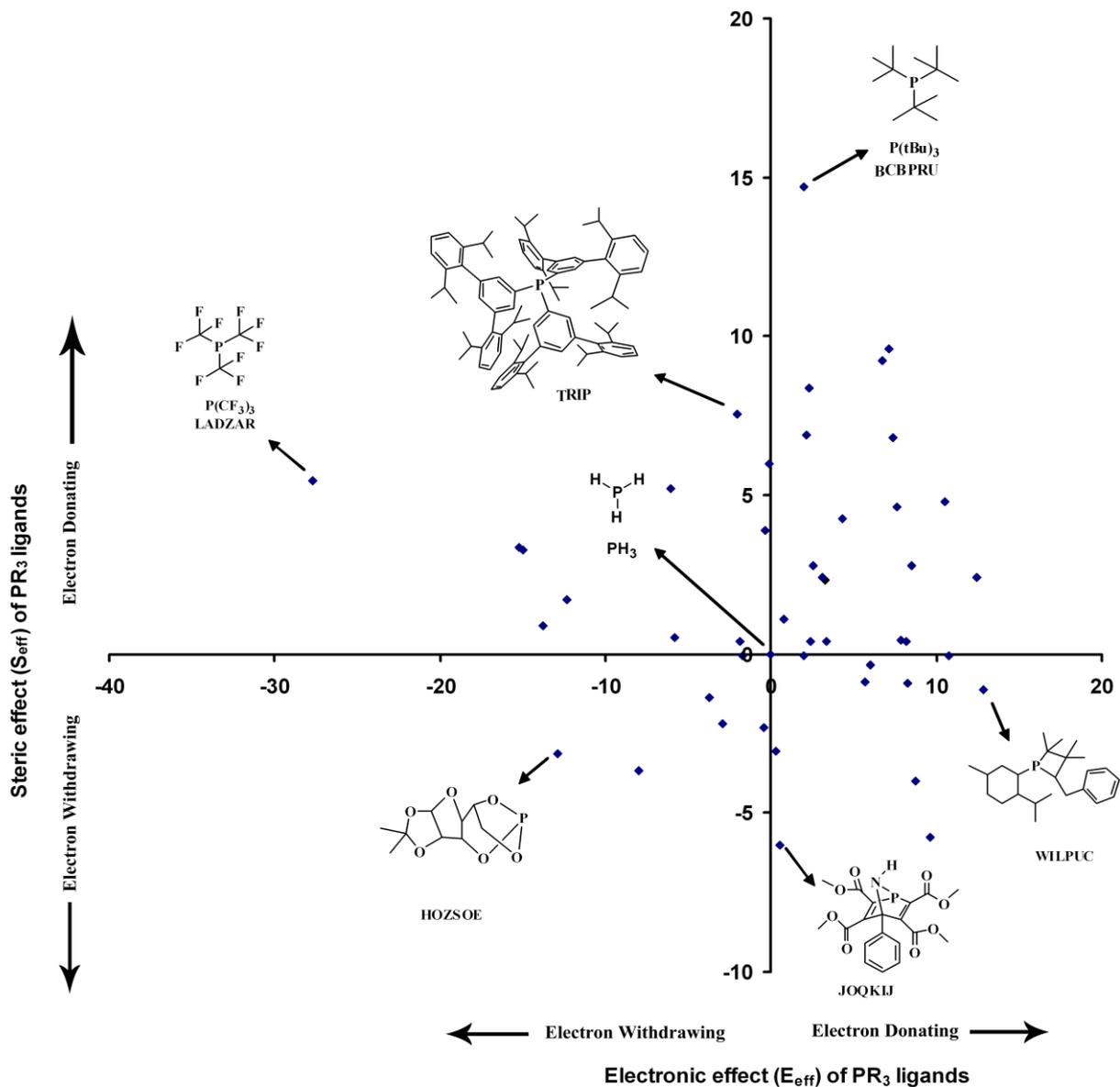
Figure 2.12 Stereoelectronic plot of PR$_3$ ligands.

The stereoelectronic correlations plotted above provides both steric and electronic measures of various types of phosphine ligands which include cyclic, non cyclic and heterocyclic structures and the method adopted for their determination is simple and less expensive in terms of computational cost. Such a stereoelectronic profile could be highly useful in the designing of catalysts since phosphine ligands constitute the major class of co-ligands in inorganic and organometallic chemistry. Positive values of both E$_{eff}$ and S$_{eff}$

indicate electron donating ability whereas their negative values suggest electron withdrawing tendency of the ligands. Therefore, the ligands can be classified in to four categories, viz. , ligands with (i) ($+E_{eff}$, $+S_{eff}$), (ii) ($+E_{eff}$, $-S_{eff}$), (iii) ($-E_{eff}$, $+S_{eff}$), and (iv) ($-E_{eff}$, $-S_{eff}$) where plus and minus signs indicate electron donation and electron withdrawal properties, respectively. It can be seen that PR_3 ligands are distributed in all the four quadrants of the coordinate system and the number of ligands in first quadrant is the highest where both S_{eff} and E_{eff} are positive. Among all the ligands $P(CF_3)_3$ has the highest negative E_{eff} value (-27.73 kcal/mol) meaning that it has the maximum electron withdrawing effect and among phosphites, QIVLOW ($E_{eff} = -15.20$ kcal/mol) is the most electron withdrawing. All other phosphites fall on the third quadrant where both S_{eff} and E_{eff} are negative. WILPUC has the maximum positive value for E_{eff} (12.86 kcal/mol) and so it is the most electron donating. The ligand which has the maximum steric effect is $P(^tBu)_3$ (S_{eff}= 14.70 kcal/mol) and the ligand which has minimum steric effect is JOQKIJ (S_{eff}= -6.01). The 'bowl' shaped ligand TRIP possesses large positive steric effect of 7.55 kcal/mol while its electronic effect has a moderate negative value of -2.07 kcal/mol. It can also be noted that there are ligands in which the steric bulkiness of the substituents makes it electron donating though the electronic effect of it is electron withdrawing in nature and vice versa. Thus in JOQKIJ the electronic effect of the substituents favors the donation of electrons but a higher negative value for S_{eff} make the ligand as electron withdrawing in nature. In $P(CF_3)_3$ (LADZAR), the steric effect favors the electron donating nature but it remains the most electron withdrawing because of the high negative value for E_{eff}. The S_{eff} value for FIDDOL, MASRAZ and NESNII is near to zero and so the nature of the ligand is decided by the electronic effect of substituents. Similarly in PPh_3, the value for E_{eff} is close to zero but the ligand is electron donating because of the positive value for S_{eff}.

2.4 Quantification of Electronic Effect of N-Heterocyclic Carbene (NHC) Ligands

2.4.1 Methodology

2.4.1.1 Topographical analysis of molecular electrostatic potential

It was already described in section 1.2.5 that MESP is a fundamental quantity, widely used to study chemical and biological reactivity as well as the stereoelectronic properties of organic molecules and organometallic ligands [Suresh and Koga 2002; Suresh 2006; Mathew *et al.* 2007; Deshmukh *et al.* 2008; Galabov *et al.* 2006; Politzer and Truhlar 1981; Politzer and Murray 1996; Politzer and Murray 2002; Murray and Politzer 1988]. This three dimensional property of the molecule can be rigorously calculated by using equation (Eq. 2.3). The MESP at nucleus A of a molecule V_A can be obtained by dropping out the nuclear contribution due to Z_A from the definition of MESP, *via* eqn (Eq. 2.15)

$$V_A = \sum_{B \neq A} \frac{Z_B}{|R_B - R_A|} - \int \frac{\rho(r')d^3r'}{|r - r'|} \qquad \dots (2.15)$$

Investigation of the topography of the MESP is an efficient way to understand the electronic distribution in molecules through critical points (CPs) at which all partial derivatives of the function vanish [Pathak and Gadre 1990; Gadre *et al.* 1992; Gadre and Suresh 1997; Suresh and Gadre 1998]. A CP is usually represented as an ordered pair of (*rank*, *signature*). The absolute minimum of the MESP (denoted as V_{min}) has a *rank* 3 and *signature* +3 [Gadre and Shirsat 2000]. The V_{min} points are often located at lone-pair regions and π-bonded regions and they represent centers of negative charge on the

molecule. We have used the UNIVIS program developed by Gadre and Limaye [Limaye and Gadre 2001] to calculate the V_{min} on the lone pair region of the NHC.

It may be noted that there is no local maximum, a (3, -3) CP, in MESP topography [Pathak and Gadre 1990] and therefore the quantity V_A defined in equation (Eq. 2.15) is often used as a convenient parameter to describe the local reactivity [Sayyed and Suresh 2009; Dimitrova and Galabov 2009; Koleva *et al.* 2009; Galabov *et al.* 2008; Liu and Pedersen 2009] of a molecule. The V_A value observed for the carbene carbon atom (designated as V_C) will be used in the present work as an electronic descriptor. The V_C values can be directly obtained from the Gaussian 03 [Frisch *et al.* Gaussian 03 2004] output of a MESP calculation. The V_{min} can also be calculated numerically by the 'cube' calculation in Gaussian 03.

2.4.1.2 Computational Methods

All the systems are optimized at B3LYP/6-311++G** level of density functional method [Becke 1993; Lee *et al.* 1988] using Gaussian03 suite of programs and the wave function generated using the same method is used for the calculation of MESP. For a comparison of the MESP results, all the systems are also optimized and MESP computed using a non hybrid functional BP86 [Becke 1988; Perdew 1986] and a hybrid meta functional M05 [Zhao *et al.* 2005]. At all the levels, a negative valued (3, +3) MESP minimum (V_{min}) is located at the lone pair region of the N-heterocyclic carbene carbon.

2.4.2 Results and Discussion

A set of twenty eight typically used NHC ligands are considered in the present study (Figure 2.13) to evaluate their V_{min} and V_C values. The abbreviations of the names of ligands used herein are the same as that used by Gusev [Gusev 2009]. In the naming of NHC ligands, NHCs with unsaturated imidazole ring are represented by 'Im' and NHCs with saturated imidazole are represented using 'sIm'. The substituents on N are

given after Im or sIm. For instance, ImNMe2 represents the unsaturated NHC ligand with Me substituents on N and sImNMe2 represents the saturated NHC ligand with Me substituents on N. Substituents on C4 and C5 positions are given before NR$_2$. Therefore, the unsaturated NHC ligand with Me substituents on C4, C5 and both N atoms is named as ImMe$_2$$NMe_2$.

Figure 2.13 Schematic structures of the N-heterocyclic carbene ligands and the abbreviations used to represent them.

MESP of a representative set of six ligands are presented in Figure 2.14 wherein the V_{min}, V_C and a negative-valued MESP isosurface are depicted to indicate the lone pair

region of the carbene. For the isosurface, the value -28.24 kcal/mol (-0.045 a.u.) is chosen because it can show the progressive decrease in the negative character of the MESP when going from the electron rich to the electron poor ligands. The choice of the isosurface is arbitrary and if we want to see the lone pair using the same isosurface value for all the molecules, we have to select a value available for the least electron rich ligand (the ligand showing the lowest negative character for V_{min}).

Figure 2.14 Representation of MESP isosurface at -28.24 kcal/mol. V_{min} and V_C in kcal/mol.

The V_{min} and V_C values at BP86, M05 and B3LYP along with TEP values are summarized in Table 2.5.

Table 2.5. MESP values of NHCs (V_{min} and V_C) and the corresponding TEP values

System	V_{min} in kcal/mol			V_C in kcal/mol			TEP (cm^{-1})
	BP86	**M05**	**B3LYP**	**BP86**	**M05**	**B3LYP**	
ImN(CF$_3$)$_2$	-54.51	-53.13	-55.97	-9239.21	-9236.95	-9232.49	2072.0
ImNH$_2$	-76.35	-76.08	-79.07	-9270.14	-9269.26	-9265.13	2058.1
ImNMe$_2$	-78.41	-77.30	-80.43	-9277.17	-9276.35	-9273.06	2054.1
ImNEt$_2$	-79.00	-77.94	-81.01	-9278.30	-9277.55	-9274.32	2052.8
ImN(^{i}Pr)$_2$	-79.47	-78.11	-81.68	-9279.49	-9277.23	-9275.36	2051.5
ImNCy$_2$	-80.28	-79.48	-82.79	-9280.68	-9280.06	-9276.91	2049.7
ImN(^{t}Bu)$_2$	-77.07	-76.53	-78.98	-9281.81	-9281.88	-9278.44	2050.6
ImNMe(^{t}Bu)	-76.62	-76.41	-80.16	-9279.56	-9279.37	-9275.90	2051.7
ImN(CH=CH$_2$)Me	-73.38	-73.29	-75.42	-9270.02	-9269.39	-9265.37	2058.1
Im(NO$_2$)$_2$$N$(CF$_3$)$_2$	-31.80	-31.40	-33.47	-9210.59	-9208.58	-9203.34	2082.6
Im(CF$_3$)$_2$$NMe_2$	-59.86	-59.49	-62.16	-9255.21	-9255.27	-9250.95	2063.9
Im(NO$_2$)$_2$$NMe_2$	-47.65	-48.56	-50.75	-9239.52	-9240.34	-9235.71	2068.6
Im(CN)$_2$$NMe_2$	-51.18	-51.52	-54.80	-9244.35	-9244.10	-9241.25	2066.2
ImF$_2$$NMe_2$	-67.11	-66.67	-69.46	-9264.49	-9262.49	-9258.89	2059.1
ImCl$_2$$NMe_2$	-65.98	-65.94	-69.20	-9263.80	-9262.99	-9259.65	2059.0
ImMe$_2$$NMe_2$	-82.39	-81.53	-84.79	-9282.82	-9282.13	-9278.80	2051.7
Im(NMe$_2$)$_2$$NMe_2$	-82.21	-81.50	-84.57	-9282.57	-9281.94	-9278.64	2050.2
Im(CO$_2$Me)$_2$NMe$_2$	-68.97	-69.12	-71.79	-9265.56	-9266.19	-9262.24	2058.7
DPylm	-72.16	-71.81	-74.54	-9269.39	-9269.33	-9265.40	2055.9
BImNMe$_2$	-73.67	-72.88	-76.02	-9268.13	-9266.69	-9263.77	2057.0
BImNEt$_2$	-74.24	-73.75	-76.74	-9269.51	-9268.13	-9265.30	2055.2
PerNMe$_2$	-69.72	-67.83	-71.50	-9261.61	-9259.91	-9257.44	2058.5
sDPylm	-81.02	-80.73	-83.72	-9277.99	-9276.35	-9273.85	2051.3
Py[c]ImNMe$_2$	-71.13	-70.33	-73.48	-9263.55	-9261.98	-9259.11	2060.0
sImNH$_2$	-78.53	-77.87	-80.87	-9270.96	-9269.26	-9266.10	2057.5
sImNMe$_2$	-78.47	-77.90	-81.38	-9275.98	-9274.03	-9271.35	2054.7
sImNEt$_2$	-79.34	-78.33	-81.70	-9277.11	-9275.04	-9272.50	2053.1
sImN(^{i}Pr)$_2$	-80.04	-78.91	-82.13	-9278.11	-9276.48	-9273.92	2051.9

The V_{min} and V_C values calculated at BP86 and M05 levels showed nearly same

trend to those calculated by B3LYP functional. Compared to B3LYP, both BP86 and

M05 level values showed ~3.00 kcal/mol less negative character for V_{min} and ~0.5 % higher values for V_C. It may be noted that being a one electron property, MESP is not significantly influenced by basis set effects and changes in methodology [Pathak and Gadre 1990; Gadre *et al.* 1995]. Therefore, B3LYP functional is adequate enough for the analysis of V_{min} and V_C of all the N-heterocyclic carbene systems and it is used for further discussions.

The ligand $Im(NO_2)_2N(CF_3)_2$ showed the least negative V_{min} (-33.47 kcal/mol) while the deepest V_{min} is observed for $Im(Me_2)_2NMe_2$ (-84.79 kcal/mol). Similarly the V_C value is the least negative for $Im(NO_2)_2N(CF_3)_2$ (-9203.34 kcal/mol) and the most negative for $Im(Me_2)_2NMe_2$ (-9278.80 kcal/mol). When going from the electron deficient $ImN(CF_3)_2$ to the electron rich ImN^tBu_2, a gradual increase in the negative character of V_C, from -9232.49 kcal/mol to -9278.44 kcal/mol is observed (entries 1 to 7 in Table 2.5) and this reflects the increasing effect of inductive influence of the N-substituent towards electron donation. A very similar trend is also observed for the V_{min} values of entries 1 to 7, except for ImN^tBu_2. A lower V_{min} value of -78.98 kcal/mol for ImN^tBu_2 is observed compared to $ImNMe_2$ because in the former the bulky ^tBu exert significant through space effect which comes from the interaction of its C–H bonds and the lone pair electron density. The effect of substitution at the C4 and C5 position of the imidazole ring is showing a significant change in the electronic effect of NHCs (entries 10 to 18 in Table 2.5). The presence of electron donating Me substituents on C4 and C5, as well as at the N-centers make the $Im(Me_2)_2NMe_2$ ligand the most electron rich among all while the NO_2 substituents on C4 and C5 positions and CF_3 substituents on N-centers bring down the electronic effect of $Im(NO_2)_2N(CF_3)_2$ ligand to the lowest. Ligands with saturated imidazole ring are slightly more electron donating compared to their unsaturated analogues.

The coordinating power of N-heterocyclic carbene ligands is assessed in terms of V_{min}, as well as V_C by correlating these quantities with the TEP values. The correlation coefficient (r) for the V_{min} plot (TEP = $0.594V_{min}$ + 2101.30) is 0.9638 (Figure 2.15) and that for the V_C plot (TEP = $0.433Vc$ + 6072.90) is 0.9910 (Figure 2.16) (V_{min} and V_C values at B3LYP level).
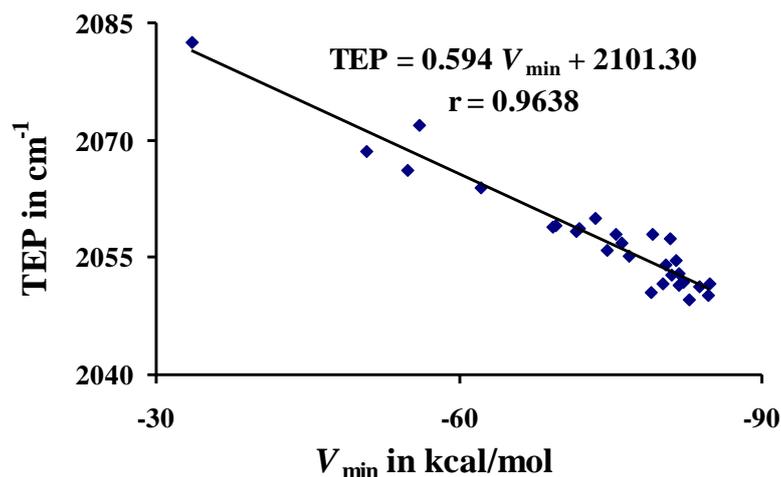
Figure 2.15 Correlation between V_{min} at the lone pair of N-heterocyclic carbene carbon and TEP.
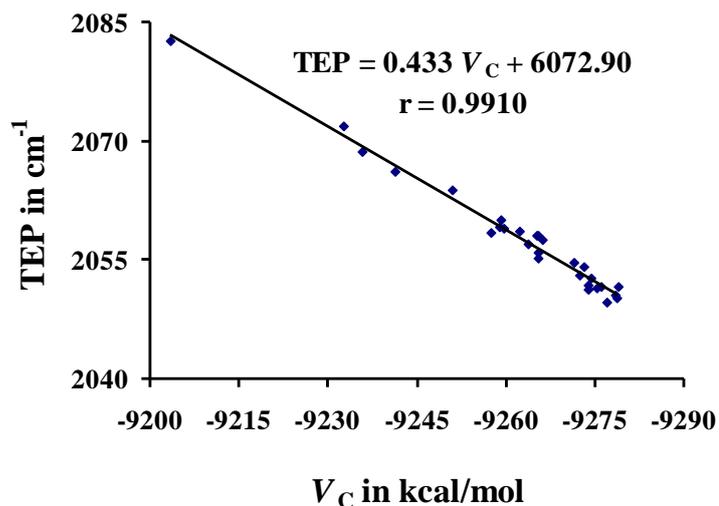
Figure 2.16 Correlation between MESP at the N-heterocyclic carbene carbon nucleus and TEP.

In the case of V_{min} and V_C data obtained using the BP86 method, the slope, intercept and r values are 0.591, 2099.70, 0.9590, respectively for the V_{min} − TEP correlation whereas the corresponding values of the V_C − TEP correlation are 0.446, 6195.40 and 0.9885 (Figure 2.17).
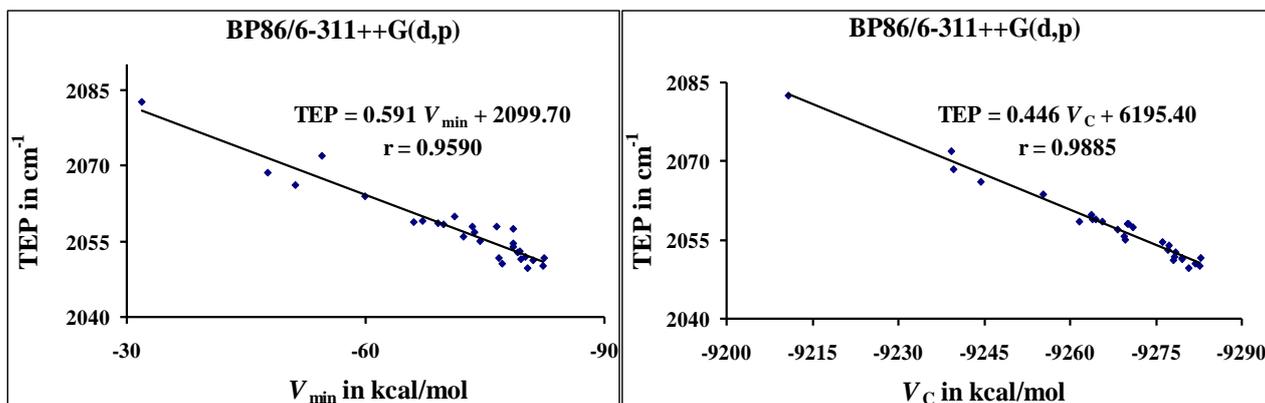
Figure 2.17 Correlation between TEP with V_{min} (left) and TEP with V_C (right). V_{min} and V_C values at BP86/6-311++G(d,p) level

Similarly, using the M05 method, the calculated slope, intercept and R values are 0.605, 2100.30, 0.9629, respectively for the V_{min} − TEP correlation while the corresponding values of the V_C − TEP correlation are 0.444, 6180.10 and 0.9883 (Figure 2.18).
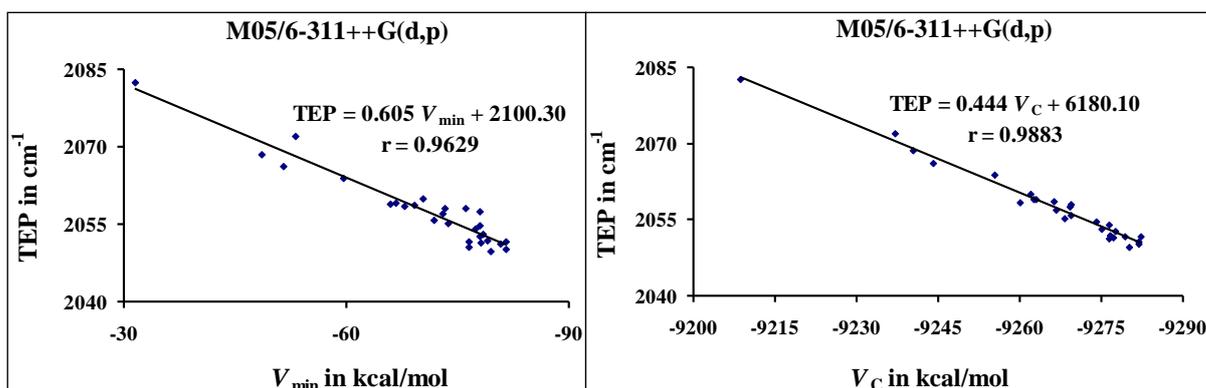
Figure 2.18 Correlation between TEP with V_{min} (left) and TEP with V_C (right). V_{min} and V_C values at M05/6-311++G(d,p) level.

These correlations strongly suggest the use of the MESP-derived quantities as simple and efficient measure of the inherent tendency of an N-heterocyclic carbene ligand towards metal coordination. The V_C − TEP correlation is superior to the V_{min} − TEP correlation. The V_{min} is more sensitive than V_C to the subtle electronic variations in the region surrounding the lone pair and therefore, the values of V_{min} will be more influenced by bulky N-substituents (ImN^tBu_2) and N-substituents having lone pair centers ($Im(NO_2)_2N$ $(CF_3)_2$). On the other hand, V_C will not be influenced significantly by such factors as the referred carbene nucleus is away from the substituent and moreover, the nuclear contribution from the carbene center is not considered in the definition of V_C (eq. 2.15). We may also note that the lone pair electron density is utilized when the ligand is coordinated to a metal and therefore the through space effect of the N-substituent on the lone pair is insignificant in the complexed state of the ligand. The through space interactions will have a shielding effect on the lone pair which in turn will influence the preparation energy required for the ligand to go from the ground state electronic configuration to the configuration it adopts in the complex. Hence, we propose that the V_{min} is appropriate to be used as a measure of the electron rich character of the free uncoordinated N-heterocyclic carbene ligand while V_C is more suited for the quantification of the coordinating power of the ligand.

Our previous studies [Mathew *et al.* 2007] showed that PCy_3 is one of the most electron donating phosphine ligands but the V_{min} value of this ligand (-42.56 kcal/mol at B3LYP/6-311++G**) is very close to the V_{min} value of some of the poorly electron donating N-heterocyclic carbene ligands (entries 1, 10, 12, and 13 in Table 2.5). This suggests that, in general, the N-heterocyclic carbene ligands have much more metal-coordinating power than the phosphines. A similar conclusion was obtained earlier by Nolan *et al.* [Hillier *et al.* 2003].

2. 5 Conclusions

The work presented here describes a method for the separation of the steric effect of a PR_3 ligand from its electronic effect. It may be noted that the steric and electronic effects are intermingled and nearly inseparable in every system and therefore only the combined effect is always observed in their associated electronic properties. The present approach combining both the QM and QM/MM method is attractive as it gives a simple and effective way to assess the amount of steric effect induced electronic variations of the PR_3 ligand. The variation in the electron donating ability with bulkiness in substituents of phosphines is quantified from the MESP minimum (V_{min}) values in the lone pair region of phosphorus atom. A method for the calculation of symmetric deformation coordinates (S4) of free phosphines was introduced and the steric effect of phosphines was measured using a two layer ONIOM level QM/MM method. A good linear correlation between MESP based S_{eff} values and the S4 based steric parameters provided a direct support for the relevance of this method. A stereoelectronic plot was made using the calculated E_{eff} and S_{eff} values and from this plot it is very easy to find the ligands with desired amounts of electronic and steric effects. Such a stereoelectronic plot will be useful in selecting the ligands in the designing of catalyst systems in organometallic chemistry.

Three different DFT methodologies (B3LYP, BP86 and M05) have been used to study the topological properties of the MESP at the lone pair region of NHCs. The MESP showed very similar values and trends for V_{min} and V_C at the three DFT levels. Further, these quantities showed good linear relationship to the TEP, suggesting that the inherent electron donating power of the N-heterocyclic carbene to a metal center can be directly assessed from the electronic property of the uncoordinated ligand itself. On the basis of

the strong correlation between V_C and TEP, we suggest the use of V_C as a simple and efficient measure of the electron donating power of the N-heterocyclic carbene. The use of V_{min} is more appropriate to compare the electron rich character of the lone pair of various carbenes which may also be affected by the through space interaction between the N-substituents and the lone pair electron density. The present MESP-based approach may find use in the fine tuning of the electron donating power of the N-heterocyclic carbene ligands to design new organometallic catalysts.

Chapter 3

Assessment of Stereoelectronic Effects of Phosphines in Grubbs First Generation and N-Heterocyclic Carbenes in Grubbs Second Generation Olefin Metathesis Catalysis
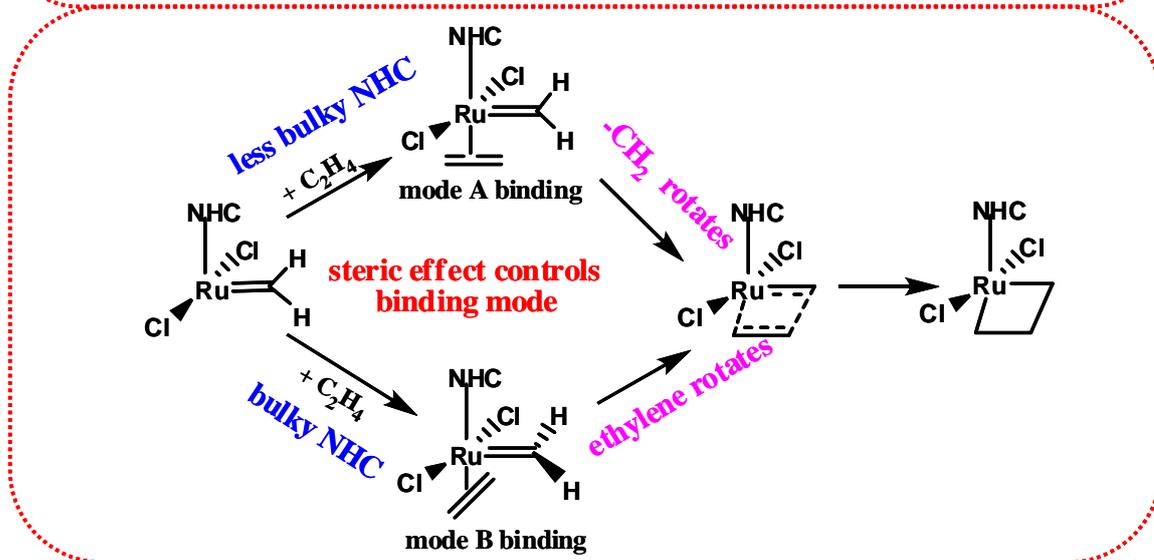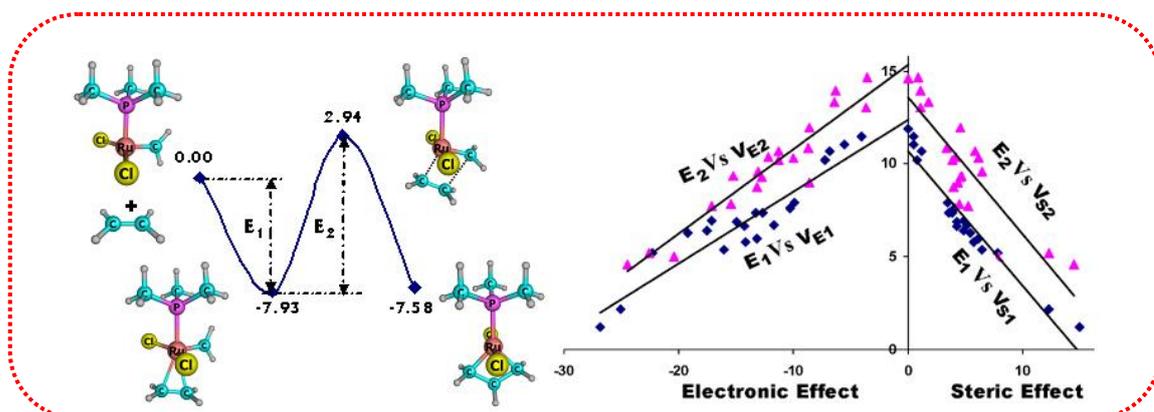
3.1 Abstract

*Quantum mechanically derived molecular electrostatic potential (MESP)-based descriptors have been proposed for the assessment of both the steric and electronic effects of phosphines in several first generation Grubbs olefin metathesis catalysts. The MESP at the P nucleus of the active form of the catalyst $Cl_2(PR_3)Ru=CH_2$ (**1a**) and its ethylene coordinated complex (**2a**) are determined. Further, frozen structures corresponding to **1a** and **2a** are located by replacing the P-R bonds with P-H bonds. The MESP at the P of a frozen geometry is free from the electronic effect of R, but influenced by steric effects due to the structural restrictions imposed in the geometry. The difference between the MESP at the P nucleus of $Cl_2(PH_3)Ru=CH_2$ and $Cl_2(PR_3)Ru=CH_2$ is taken as a measure of the combined steric and electronic effects of PR_3 (V_{SE1}) in **1a**. Similarly, the combined steric and electronic effect of PR_3 in **2a** (V_{SE2}) is also calculated. The frozen structures allowed the calculation of steric-only effects for **1a** (V_{S1}) as well as **2a** (V_{S2}). Thus, the electronic effect of PR_3, V_{E1} in **1a** is (V_{SE1} - V_{S1}) and that of PR_3, V_{E2} in **2a** is (V_{SE2} - V_{S2}). Both the V_{S1} and V_{S2} showed impressive linear correlations with popular geometric steric parameters, viz. the Tolman cone angle (θ) and the symmetric deformation coordinate (S4'). Moreover, V_{E1} and V_{S1} showed linear relationships to the binding energy of ethylene (E_1), suggesting that the steric effect is 1.88 times more dominant than the electronic effect in the olefin binding process. Similarly, both V_{E2} and V_{S2} showed linear correlation with the activation energy (E_2) for the formation of metallacyclobutane. In both the olefin*

binding process and the transition state formation leading to C-C bond coupling, drastic reduction in E_1 as well as in E_2 is observed with an increase in the steric bulkiness of PR_3 while only a moderate decrease in energy parameters is observed with the increase in the electron rich character of PR_3. The stereoelectronic correlation studies presented herein demonstrate that the success of the first generation Grubbs catalysts is primarily due to the choice of the right mix of steric (bulky R substituents on P) and electronic (electron donating R substituents on P) effects of PR_3 ligand.

*The steric and electronic effects of N-heterocyclic carbenes in the second-generation Grubbs olefin metathesis catalysts are quantified on the basis of molecular electrostatic potential at the carbene carbon of both the NHC ligand (V_{C1}) and the alkylidene moiety (V_{C2}). The quantity (V_{C1} + V_{C2}), calculated separately for the active form of the catalyst, $(sImR_2NR_2)Cl_2Ru=CH_2$ (**1b**) and the ethylene bound complex, $(sImR_2NR_2)Cl_2Ru=CH_2(C_2H_4)$ (**2b**) reflected the combined steric and electronic effects of the NHC. For every **1b** and **2b** systems, R is replaced with H and all other nuclear coordinates are frozen to obtain **1b'** and **2b'** respectively. The quantity (V_{C1}' + V_{C2}') of **1b'** and **2b'** served as a good measure of the steric effect of the NHC. For a normalization procedure, (V_{C1} + V_{C2}) and (V_{C1}' + V_{C2}') for any R is considered relative to R = H to define the combined steric and electronic effect of NHCs in the complexes **1b** (V_{SE3}) and **2b** (V_{SE4}) as well as the steric effect in **1b** (V_{S3}) and **2b** (V_{S4}). Thus the electronic effect of the active form, V_{E3} is ($V_{SE3} − V_{S3}$) and that of the olefin bound complex, V_{E4} is ($V_{SE4} − V_{S4}$). Both V_{S3} and V_{S4} showed good linear correlation with the*

volume based steric parameter, the buried volume (%V_{Bur}) developed by Cavallo et al. In complexes with less bulky NHCs, ethylene is coordinated to the active form with an orientation parallel to the alkylidene moiety (mode A binding; binding energy, E_3 is 5 - 9 kcal/mol), whereas in complexes with stericaly bulky NHCs ethylene is coordinated to the active form only in a plane perpendicular to the alkylidene moiety (mode B binding; E_3 is ~10.0 kcal/mol). In mode A binding, the binding energy, E_3 as well as the activation energy, E_4 for the metallacyclobutane formation decreased with an increase in both the steric and electron donating effects of the NHC ligand. The systems with $-CF_3$ as the N-substituent deviated significantly from the (E_3, V_{E3}) correlation line due to the presence of Ru...F interaction. In mode B binding, E_3 and E_4 increased with increase in the steric effect, while the electronic effect showed no correlation to either E_3 or E_4. Thus, if the NHC is bulky, the steric effect will dominate over the electronic effect and will control the metathesis, whereas the electronic and steric effect will have almost equal importance in metathesis activity of catalyst with less bulky NHCs. Lone pair interactions of the type Ru...F have the ability to significantly alter the catalytic activity.

3.2 Introduction

Olefin metathesis is considered as a major breakthrough in transition metal-based catalysis and has become one of the most powerful synthetic methods in organic chemistry. The first synthesized Mo and W-based Schrock catalysts were known for their robust nature and efficiency [Schrock *et al.* 1988; Schaverien *et al.* 1986; [a]Schrock *et al.*

1990; [b]Schrock *et al*. 1990; Murdzek and Schrock 1987; Schrock 1986] and catalysts with higher degree of tolerance towards air, moisture and sensitive functionalities were achieved due to the synthesis of ruthenium based catalysts by Grubbs *et al.* [Schwab *et al.* 1996; Nguyen and Grubbs 1993; Nguyen *et al.* 1992; Trnka and Grubbs 2001]. The first generation Grubbs catalyst (G1R) is a bisphosphine ruthenium carbene complex, while the second generation catalyst (G2R) [Glorius 2007] uses an N-heterocyclic carbene (NHC) in the place of a phosphine ligand. G2R systems exhibited improved catalytic activity compared to that of G1R systems (Figure 3.1). [Schwab *et al.* 1996; Trnka and Grubbs 2001; Grubbs 2003; Scholl *et al.* 1999; Huang *et al.* 1999]. Hoveyda and co-workers reported the synthesis of isopropoxystyrene–coordinated catalyst, [Kingsbury *et al.* 1999] a modified analogue of G1R and later synthesized the isopropoxystyrene–coordinated NHC containing catalyst (Figure 3.1c) [Garber *et al.* 2000; Gessler *et al.* 2000]. Improvement in the metathesis activity is mainly achieved by proper modifications on the steric and electronic requirements of the phosphines in G1R and NHCs in G2R systems which led to the synthesis of several other metathesis catalysts [Berlin *et al.* 2006; [a]Clavier *et al.* 2009; Conrad *et al.* 2003; [b]Clavier *et al.* 2009; Samojłowicz *et al.* 2009; Vougioukalakis and Grubbs 2010; Hong and Grubbs 2006].
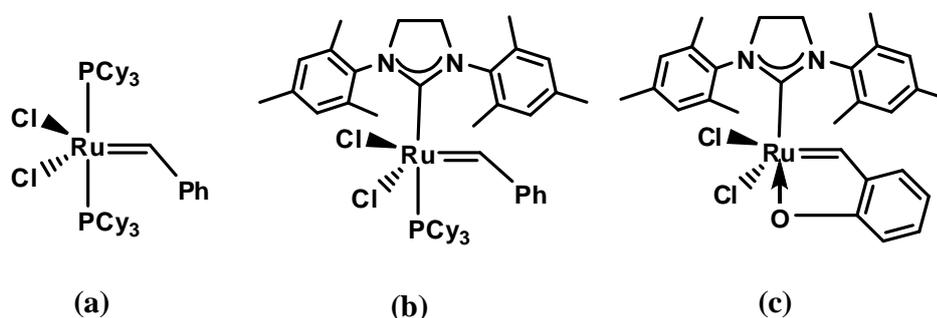
Figure 3.1 (a) Grubbs first generation catalyst (b) Grubbs second generation catalyst (c) Grubbs-Hoveyda catalyst.

A huge amount of theoretical and experimental studies have been devoted to the elucidation of the complete reaction path of olefin metathesis reaction [Straub 2007; Bernardi *et al.* 2003; Cavallo 2002; van der Eide and Piers 2010; Dölker and Frenking 2001; Mathew *et al.* 2008]. In the generally accepted Chauvin [Hérisson and Chauvin 1970] mechanism for the olefin metathesis, the phosphine or the NHC-coordinated 16-electron alkylidene complex is the pre-catalyst. A 14-electron active form of the catalyst is formed from the dissociation of the phosphine from the pre-catalyst [Suresh and Koga 2004; Tsipis *et al.* 2005; Suresh and Baik 2005]. Olefin then binds to the active form and passes through a [2+2] cycloaddition pathway to yield the metallacyclobutane intermediate. The metathesis is completed when the intermediate undergoes cycloreversion to generate the alkene and the alkylidene (Scheme 3.1).

L = PR₃, NHC
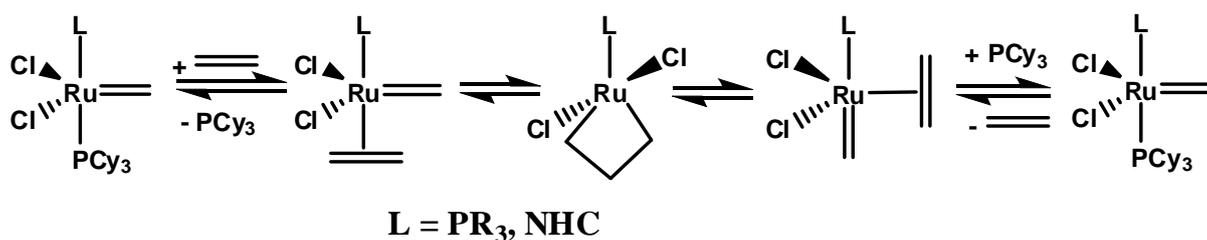
Scheme 3.1 Mechanism of Grubbs olefin metathesis catalysis.

The activity of the catalyst is mainly decided by the steric and electronic effects of the coordinated ligands. Grubbs *et al.* analyzed the activity of the G1R systems with different combinations of phosphines and halogen ligands. They noticed that larger and more electron donating phosphines and smaller and electron withdrawing halogens can lead to more active first generation catalysts [Dias *et al.* 1997]. It was considered that the enhanced activity of the G2R catalysts originates from the higher *trans* influence of NHC over phosphine, PR₃, leading to an easy dissociation of the *trans* ligand. Grubbs *et al.* [Sanford *et al.* 2001] performed a detailed analysis on the kinetics of the initial dissociation of the phosphines in the G1R and G2R catalysts. They observed that the

phosphine dissociation takes place easily in the G1R systems due to higher steric interaction of the two *trans* oriented PR$_3$ ligands around the core unit of the RuCl$_2$(CHR) than the steric interaction due to the NHC and another PR$_3$. Therefore, the dissociation of phosphine is considered as the rate limiting step in the G2R systems, whereas for the G1R systems, the rate limiting step is the formation of the metallacyclobutane. Jensen and co-workers presented a multivariate QSAR model for both the first and second generation olefin metathesis catalysts and showed that ligands which could stabilize the metallacyclobutane intermediate can promote the activity of the catalyst [Occhipinti *et al.* 2006].

Cavallo [Cavallo 2002] proposed that the steric interaction of mesityl substituents on the alkylidene moiety is responsible for the higher activity of IMes and H$_2$IMes coordinated systems compared to the G1R catalyst (PCy$_3$)$_2$Cl$_2$Ru=CHPh. Later they analyzed the reaction pathway of G2R systems and found that that the reaction pathway involving the G2R systems shows a delicate balance between the steric, electronic and solvent effects [Correa and Cavallo 2006]. But Adlhart and Chen [Adlhart and Chen 2004] argued that the electronic effect of NHCs is the major reason for the higher catalytic activity of G2R systems.

Straub [Straub 2005, Straub 2007] analyzed various possible conformations of alkene-carbene complex and suggested that the higher electron donating nature of NHCs forces the alkene-carbene complex to adopt the active conformation leading to an easy [2+2] cycloaddition for the formation of the metallacyclobutane intermediate. Based on the Ru K–edge X-ray absorption spectroscopy analysis of G1R and G2R catalysts, Kennepohl *et al.* [Getty *et al.* 2007] suggested that the NHC ligation can produce an electron deficiency in ruthenium centre even though the NHC is a strong σ-donor ligand and the high activity of NHC-coordinated systems results from the strong binding of the

olefin with the electron deficient metal. Poblet and co-workers [Antonova *et al*. 2009] used energy decomposition analysis (EDA) to quantify the donor-acceptor properties of PR_3 and NHCs in Grubbs catalysts and provided a theoretical basis for Kennepohl's observation.

Even though the role of ligand effects on the initial dissociation of phosphine in G1R systems and NHCs in G2R systems are well studied, the role of the steric and electronic effects of ligands on the two important steps of the catalysis, *viz*. the binding of olefin to the active form and the formation of metallacyclobutane is not well understood. A study in this direction can be conducted by monitoring the steric and electronic effects of phosphines through the variations observed in a sensitive molecular descriptor.

Numerous methods [Brown 1992; Fey 2010; Fey *et al.* 2006; Fey *et al.* 2009; Fey *et al.* 2006] are currently available to determine the steric parameters of free phosphines as well as their metal complexes. Among them, the Tolman cone angle (θ) [Tolman 1970; Tolman 1977] is the most used steric parameter for free phosphines. Orpen *et al.* [Dunne *et al.* 1991] introduced the symmetric deformation coordinate (S4') defined by the M-P-R and R-P-R angles (M is metal and R is substituent) for the evaluation of the steric effect of phosphines in metal complexes ($LnMPR_3$). Cundari *et al.* used the S4' values of phosphines, calculated from PM3(tm) optimized rhodium Vaska complexes as a measure of steric effect [Cooney *et al.* 2003].

Quantification and development of stereoelectronic parameters of NHCs are important in the analysis of the role of steric and electronic effects of G2R metathesis catalysis. Cavallo *et al*. [Cavallo *et al*. 2005] introduced the buried volume, %V_{Bur}, a measure of the volume occupied by NHC ligand in the first coordination sphere of the metal centre to quantify the steric effect. Nolan *et al*. [Kelly III *et al*. 2008; Dorta *et al*.

2005; Dorta *et al*. 2003] and others [Chianese *et al*. 2003] extended the use of the Tolman Electronic Parameter (TEP) for the evaluation of electronic effect of NHCs. Using computational methods, Gusev [Gusev 2009] calculated the TEP values of 76 NHCs from $Ni(CO)_3NHC$ complexes. Fey *et al*. [Fey *et al*. 2009; Fey 2010] developed a ligand knowledge base (LKB) for carbenes using quantum mechanically derived descriptors. Recently, we showed that the molecular electrostatic potential (MESP) at the NHC carbon nucleus and at the C-lone pair is a simple and efficient descriptor of the electronic effect of free NHCs [Mathew and Suresh 2010].

Though the stereoelectronic parameters of phosphines and NHCs are useful measures of the steric size and electronic effect of phosphines and NHCs, the use of such parameters to study the course of a reaction are rather difficult and the use of a sensitive electronic parameter which depends directly on the subtle electronic changes due to steric interaction of the ligand can provide more insights on the various stages of catalytic activity.

The molecular electrostatic potential (MESP) is one of the most widely used electronic property in chemistry for understanding molecular reactivity as it reflects the subtle changes in electron density associated with structural and electronic changes in the system [Bonaccorsi *et al.* 1970; Galabov *et al.* 2006; Sayyed and Suresh 2009; Deshmukh *et al.* 2008; Galabov *et al.* 2008; Politzer 2004; Murray *et al.* 1991; Murray and Politzer 1988; Suresh *et al.* 2000; Dimitrova and Galabov 2009; Murray and Sen 1996; Bonaccorsi *et al.* 1972]. Studies from our laboratory showed that in the case of phosphine ligands, the MESP at the lone pair region of the phosphorus is a good measure of its electronic donating ability in coordination complexes [Suresh and Koga 2002; Suresh 2006]. Further, a MESP-based design for the separation and quantification of the steric and electronic effects of phosphines using a combined QM and QM/MM method

was proposed [Mathew *et al.* 2007]. Recently, we showed that the MESP at the lone pair region of the carbene carbon in N-heterocyclic carbenes can be used as a simple and efficient parameter for their electronic effect [Mathew and Suresh 2010].

In the present work, we further explore the use of MESP in describing stereoelectronic features of first generation and second generation metathesis catalysts. The MESP-based descriptors are derived from quantum chemical calculations and applied to understand the role of steric and electronic effects of PR_3 and NHC in the olefin (ethylene) binding process as well as in the formation of metallacyclobutane in first generation and second generation olefin metathesis catalysis.

3.3 Computational Methods

All the calculations were carried out using density functional theory (DFT), employing gradient-corrected BP86 functional [Becke 1988; Perdew 1986] in combination with def2-TZVPP [Weigend and Ahlrichs 2005] basis set which is a triple zeta quality basis set with two sets of polarization functions. The effective core potential (ECP) associated with def2-TZVPP is used for the ruthenium. Gaussian 03 [Frisch *et al.* Gaussian 03 2004] suite of programs is employed for all the computations. All the transition states were optimized using Synchronous Transit-Guided Quasi Newton (STQN) method [Peng *et al.* 1996] and were characterized by identifying a single imaginary frequency. The MESP [Gadre and Shirsat 2000; Politzer and Truhlar 1981] was calculated using Gaussian03 program at BP86/def2-TZVPP level. For selected systems, electron density critical point analysis was carried out for the optimized geometries using the Bader's atoms in molecule analysis employing the AIM2000 program [Bader 1990; König *et al.* 2001].

3.4 Results and Discussion

3.4.1 Stereoelectronic Effects of Phosphines in First Generation Olefin Metathesis Catalysis

In the present study, we have selected the active form of twenty one first generation catalysts ($Cl_2(PR_3)Ru=CH_2$) in which the coordinated phosphine ranges from the smallest PH_3 to the stericaly bulky $P(^tBu)_3$. For each of the $Cl_2(PR_3)Ru=CH_2$ systems (**1a**), a corresponding system $Cl_2(PH_3')Ru=CH_2$ (**1a'**) is also located by replacing the R substituents with H. In **1a'**, all the structural parameters are kept to a value same as that of **1a**, except the P–H distances. The P–H distances in **1a'** must reflect the steric size of the R group. In order to achieve this, the different P–H distances in **1a'** are determined by a normalization procedure using the standard P-R distance in the Lewis acid-base complex, AlH_3-PH_2R. The aluminum complex is selected for this purpose because the atomic radius of Al (1.25 Å) is only 0.05 Å smaller than that of Ru [Slater 1964]. The normalization procedure is described below.

Six AlH_3-PH_2R systems, *viz.* AlH_3-PH_3, AlH_3-PH_2Me, AlH_3-PH_2Et, AlH_3-$PH_2(^iPr)$, AlH_3-PH_2Ph, AlH_3-$PH_2(^tBu)$ systems were optimized. In these complexes, the H, Me, Et, ^iPr, Ph and ^tBu substituents respectively are assumed to be in a steric free environment because the neighboring interactions are from the smallest atom H and therefore the P–H distance in the AlH_3-PH_3 and P–C distances in AlH_3-PH_2Me, AlH_3-PH_2Et, AlH_3-$PH_2(^iPr)$, AlH_3-PH_2Ph and AlH_3-$PH_2(^tBu)$ systems are taken as good approximations to the standard P–R distances in the absence of steric effect. In the next step, we have calculated the percentage increase in the P-R distance in comparison with the P-H distance. For instance, the P–H distance in AlH_3-PH_3 is 1.419 Å and the P–C distance in AlH_3-$PH_2(^tBu)$ is 1.877 Å, meaning that the latter is increased by 32.2% when

compared to the former (Figure 3.2). On the other hand, the P–H distance in

$Cl_2(PH_3)Ru=CH_2$ system is 1.422 Å while the $P(^tBu)$ distance of 1.966 Å in

$Cl_2P(^tBu)_3Ru=CH_2$ is 38.3% higher than the former (Figure 3.2). We assume that if there

was no steric effect on the P–C bond length in $Cl_2P(^tBu)_3Ru=CH_2$, compared to the P–H

distance of 1.422 Å, the $P(^tBu)$ distance must have shown only an increase by 32.2%. It

means that $Cl_2(^tBu)Ru=CH_2$ showed 6.1% higher bond distance changes than the Al

complexes, which can be attributed to the steric effect of ^tBu on the bond lengths.

Therefore, in order to normalize the P–H distance in the case of **1a'** corresponding to

$Cl_2P(^tBu)_3Ru=CH_2$, we have fixed the P–H bond length to 1.509 Å, a value calculated by

increasing the P–H distance of 1.422 Å by 6.1 % (the steric correction to the bond

length). In the same manner, the P–H distance of **1a'** and **2a'** corresponding to all other

systems has been calculated to normalized values. The percentage of increase in P–H

distance for PMe_3, PEt_3, $P(^iPr_3)$, PPh_3 coordinated active forms are -0.70, 0.50, 1.39, 1.05

respectively.
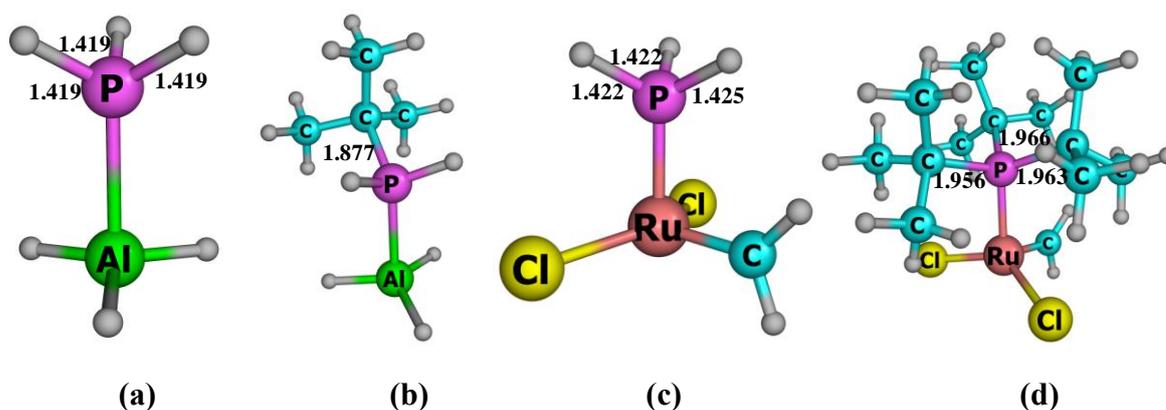
Figure 3.2 (a) AlH_3-PH_3 complex (b) AlH_3-$PH_2(^tBu)$ complex (c) $Cl_2(PH_3)Ru=CH_2$ and

(d) $Cl_2P(^tBu)_3Ru=CH_2$ complexes (All bond lengths are given in Å).

For both **1a** and **1a'**, the MESP at the P nucleus is determined which is -33952.11 kcal/mol for the fully optimized $Cl_2(PH_3)Ru=CH_2$ and all the other systems with PR_3 ligand showed more negative MESP values. The change in the MESP at the P nucleus of **1a** can be attributed to the steric and electronic contributions of the R substituents. Thus, the difference between the MESP at the P nucleus of $Cl_2(PR_3)Ru=CH_2$ and $Cl_2(PH_3)Ru=CH_2$ can be taken as a descriptor for the combined effect of the steric and electronic effects of PR_3 over PH_3. This parameter is designated as V_{SE1}. Similarly, the difference between the MESP at the P nucleus of $Cl_2(PH_3')Ru=CH_2$ and $Cl_2(PH_3)Ru=CH_2$ can be taken as a good measure of the steric effect of PR_3. This assumption is reasonable because an indirect effect of the R substituent is preserved in $Cl_2(PH_3')Ru=CH_2$ due to its frozen structure adopted from $Cl_2(PR_3)Ru=CH_2$. This indirect effect of R is largely steric in nature because the electronic effect of 'H' is nearly identical in both the $Cl_2(PH_3')Ru=CH_2$ and $Cl_2(PH_3)Ru=CH_2$. A notation V_{S1} is used for this parameter. The definitions of V_{SE1} and V_{S1} suggest that the difference between these two must give the electronic effect of PR_3 (V_{E1}) in the complex.

In Table 3.1, V_{SE1}, V_{S1} and V_{E1} values are given along with the θ and S4' values. It is gratifying that the MESP based steric parameter V_{S1} showed good linear correlation with both the geometric steric parameters, θ and S4' (Figure 3.3). Also noticed that an increase in the Ru–P distance d (Table 3.1) corresponds to an increase in the steric effect in terms of V_{S1} as both quantities can be correlated with an equation, *viz.* $V_{S1} = 143.32d - 308.92$ (correlation coefficient, r = 0.9873).
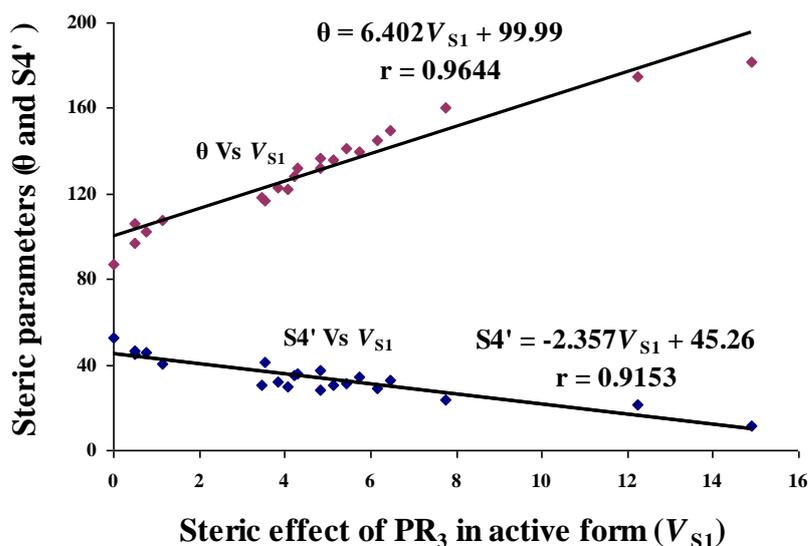
Figure 3.3 Correlation plots showing the relationship of θ with V_{S1} (top) and S4' with V_{S1} (bottom).

Coordination of olefin to the $Cl_2(PR_3)Ru=CH_2$ (**1a**) is a key step in olefin metathesis process and the binding energy of the olefin (E_1) in the complex is a direct indicator of the power of the metal centre to accept the olefin. The value of E_1 can be highly influenced by the stereoelectronic properties of the phosphine ligand in the active form of the complex. Since we have the V_{S1} and V_{E1} parameters, stereoelectronic relationship to the olefin binding power of the active catalyst can be verified. Ethylene is used for the complexation with **1a** and the coordination energy E_1 is calculated for the twenty one systems selected for this study. The binding of the olefin to the active form of the catalyst can yield two different conformations; in the first case, the ethylene C–C bond possesses a perpendicular orientation with respect to the $Ru=CH_2$ plane while in the second case the C–C bond aligns in the $Ru=CH_2$ plane. However, five systems containing the phosphine ligands PH_3, PH_2Me, PH_2Et, PH_2Ph and $PHMe_2$ gave only the first conformation. Structural drawings for the two possible modes of the olefin binding is depicted in Figure 3.4 using $Cl_2(PMe_3)Ru=CH_2(CH_2CH_2)$. For majority of the systems, the first conformation is slightly more stable ($\sim$1 kcal/mol) than the second except for the

cases of P(^{i}Pr)(^{t}Bu$_2$) and P(^{t}Bu$_3$) coordinated systems. For instance, in the most bulky

P(^{t}Bu)$_3$ coordinated system, the second conformation is ~3 kcal/mol more stable than the

first. For the metathesis catalytic activity, the second conformation is more suited than

the first [Straub 2005] (Scheme 3.1) to yield the metallacyclobutane intermediate and

hence, whenever possible, the second conformation is considered as the reactant

complex. E_1 values of all the systems are given in Table 3.1 and it varies from 1.21

kcal/mol for PR$_3$ = P(^{t}Bu)$_3$) to 11.90 kcal/mol for PR$_3$ = PH$_3$.
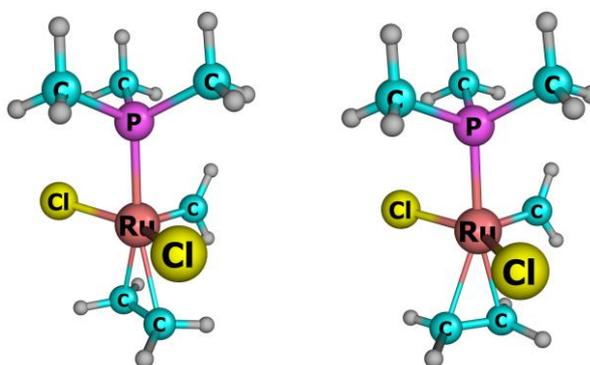
Figure 3.4 Two possible modes of ethylene binding to the Cl$_2$(PMe$_3$)Ru=CH$_2$ system.

Table 3.1 Stereoelectronic parameters of Cl$_2$(PR$_3$)Ru=CH$_2$ and V_{SE1}, V_{S1}, V_{E1} and E_1

values in kcal/mol.

PR$_3$ in Cl$_2$(PR$_3$)Ru=CH$_2$	V_{SE1}	V_{S1}	V_{E1}	S4' (^{o})	$^o\theta$	Ru-P distance d (Å)	Binding Energy (E_1)
PH$_3$	0.00	0.00	0.00	52.4	87	2.150	11.90
PMe$_3$	-6.39	3.47	-9.86	30.7	118	2.178	7.93
PEt$_3$	-12.71	4.82	-17.53	37.1	132	2.192	6.41
P(^{t}Bu)$_3$	-11.96	14.89	-26.85	11.4	182	2.255	1.21
P(^{i}Pr)$_3$	-14.54	7.76	-22.31	24.0	160	2.216	5.20
PEt$_2$Me	-10.70	4.22	-14.92	35.3	128	2.188	6.91
PMe$_2$Et	-8.84	3.84	-12.68	32.3	123	2.182	7.39
PMe$_2$(^{i}Pr)	-10.01	4.29	-14.30	35.8	132	2.188	6.65

PMeEt(^{i}Pr)	-12.28	4.84	-17.12	27.9	137	2.193	6.97
PEt$_2$(^{i}Pr)	-13.79	5.45	-19.24	31.1	141	2.197	6.27
PH$_2$Me	-3.54	0.51	-4.05	45.1	97	2.158	11.47
PHMe$_2$	-5.71	1.15	-6.85	40.7	108	2.172	10.71
PH$_2$Et	-6.51	0.77	-7.28	45.9	102	2.161	10.22
PHEt$_2$	-9.71	3.53	-13.24	41.3	117	2.176	7.39
P(^{i}Pr)(^{t}Bu)$_2$	-12.80	12.25	-25.05	21.0	175	2.238	2.17
PPh$_3$	-7.05	6.14	-13.19	28.9	145	2.192	5.98
PMePh$_2$	-6.51	5.13	-11.65	30.5	136	2.190	6.71
PMe$_2$Ph	-6.23	4.06	-10.29	29.6	122	2.180	7.63
PEtPh$_2$	-8.39	5.75	-14.14	34.5	140	2.191	5.78
PH$_2$Ph	-5.09	0.48	-5.57	46.7	106	2.160	11.02
PPh$_2$(^{i}Pr)	-9.54	6.47	-16.01	33.2	150	2.202	5.38

E_1 values showed a good linear correlation with V_{S1} (Figure 3.5). The steep negative slope of the correlation line indicates that a moderate increase in the steric effect can cause a large reduction in the binding energy. Interestingly, the MESP based electronic parameter V_{E1} also correlates linearly with E_1. However, the small positive value of the slope (Figure 3.5) indicates that an increase in the electron rich character of the phosphine can only cause a moderate reduction in the binding energy. From the relationships in Figure 3.5, the steric effect of the G1R systems can be estimated to be approximately 1.88 times more influential than the electronic effect in deciding the binding energy of the ethylene in metathesis catalysis.

$E_1 = 0.387V_{E1} + 12.41$
r = 0.9471

$E_1 = -0.727V_{S1} + 10.66$
r = 0.9677
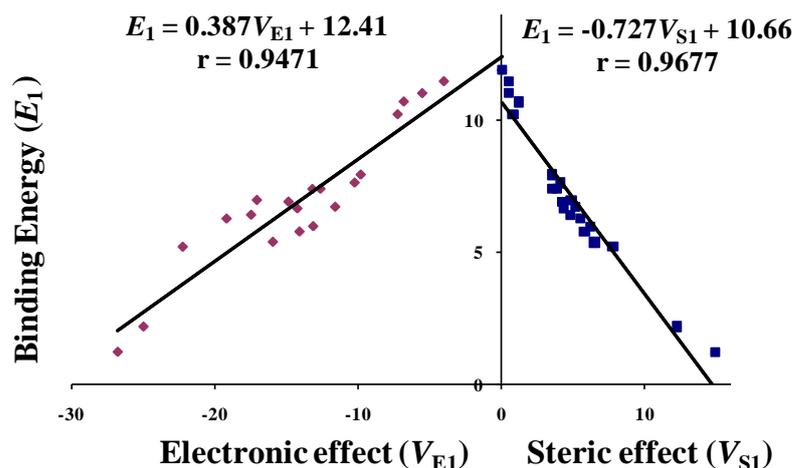
Figure 3.5 Correlation of V_{E1} with E_1 (in the left side) and V_{S1} with E_1 (in the right side).

The stereoelectronic parameters of the ethylene bound complex, *viz.* V_{SE2} (combined steric and electronic effects), V_{S2} (steric), and V_{E2} (electronic) can be evaluated by following a procedure very similar to that used for the active form of the catalyst. Thus, V_{SE2} can be calculated as the difference between the MESP value at the P nucleus of $Cl_2(PR_3)Ru=CH_2(CH_2CH_2)$ and $Cl_2(PH_3)Ru=CH_2(CH_2CH_2)$ while V_{S2} can be defined as the difference between the MESP of the P nucleus of $Cl_2(PH_3)Ru=CH_2(CH_2CH_2)$ and $Cl_2(PH'_3)Ru=CH_2(CH_2CH_2)$. It may be noted that $Cl_2(PH'_3)Ru=CH_2(CH_2CH_2)$ is derived from $Cl_2(PR_3)Ru=CH_2(CH_2CH_2)$, by replacing R with H and freezing all the other atoms. Hence, V_{E2} is the difference of V_{SE2} and $V_{S2.}$ The stereoelectronic parameters V_{SE2}, V_{S2} and V_{E2} along with the S4' values and Ru-P (*d*) distances are presented in Table 3.2. All V_{SE2} values are less negative (~1-3 kcal/mol) than V_{SE1} values of the active form, indicating a decrease in the electron accepting power of the metal from the phosphine when olefin coordinates to it, an expected result as the supply of electron from ethylene makes the metal more electron rich than the active form. Interestingly, the steric parameter V_{S2} of the olefin complex and V_{S1} of the active form are nearly the same. This does not mean that the steric effect of a PR_3 is almost the same in both the complexes because V_{S1} and V_{S2} are only relative values with respect to

the reference point 0.00 kcal/mol for the PH_3 coordinated system. A close examination of the olefin complexes shows that the olefin coordination leads to an increase in the Ru-P distance in every case compared to the active form. This suggests that, on the basis of the relationship $V_{S1} = 143.32d -308.92$, discussed earlier (Figure 3.3), the absolute steric effect of a PR_3 ligand has to be larger in the olefin complex than the active form. Thus, the similarity in V_{S1} and V_{S2} indicates that the olefin coordination exerts nearly equal amount of steric effect in every case. The electronic effect V_{E2} is not as strong as that of the active form because the phosphine is coordinated from a larger distance in $Cl_2(PR_3)Ru=CH_2(CH_2CH_2)$ than $Cl_2(PR_3)Ru=CH_2$. However, the relative ordering of V_{E1} and V_{E2} are very similar, the latter is always less negative than the former by 6 -12% in the case of alkyl substituted phosphines and 17 - 34% in the case of phenyl substituted phosphines.

The steric parameter V_{S2} showed good correlation with the S4' as well as with the θ values (Table 3.1) of the olefin complex (Figure 3.6). Since the MESP is a one electron property, it is felt that V_{S2} and V_{S1} can be used as a more sensitive descriptor to measure the steric effect than the geometric parameters such as the S4' and θ.

Table 3.2 Stereoelectronic parameters of $Cl_2(PR_3)Ru=CH_2(CH_2CH_2)$ and V_{SE2}, V_{S2}, V_{E2} and E_2 values in kcal/mol.

PR$_3$ in Ethylene complex	V_{SE2}	V_{S2}	V_{E2}	S4'	Ru-P distance d (Å)	Ru-CH$_2$ distance (Å)	Activation Energy (E_2)
PH$_3$	0.00	0.00	0.00	55.5	2.322	1.821	14.61
PMe$_3$	-5.40	3.31	-8.70	32.5	2.314	1.833	10.88
PEt$_3$	-10.94	4.46	-15.41	40.5	2.323	1.835	7.85
P(^{t}Bu)$_3$	-9.93	14.49	-24.41	14.1	2.534	1.828	4.57
P(^{i}Pr)$_3$	-12.59	7.86	-20.45	26.4	2.368	1.832	5.01

PEt$_2$Me	-9.14	3.99	-13.13	38.1	2.335	1.831	8.78
PMe$_2$Et	-7.44	3.83	-11.27	35.1	2.310	1.835	10.21
PMe$_2$(^{i}Pr)	-8.20	4.56	-12.76	38.6	2.318	1.835	9.29
PMeEt(^{i}Pr)	-10.67	4.59	-15.26	30.2	2.337	1.834	9.35
PEt$_2$(^{i}Pr)	-11.95	5.22	-17.17	34.0	2.335	1.834	7.70
PH$_2$Me	-2.73	0.89	-3.62	44.2	2.317	1.820	14.66
PHMe$_2$	-4.71	1.72	-6.43	37.1	2.329	1.819	13.34
PH$_2$Et	-5.37	1.03	-6.39	46.7	2.321	1.819	13.96
PHEt$_2$	-8.03	4.12	-12.15	41.0	2.310	1.833	10.40
P(^{i}Pr)(^{t}Bu)$_2$	-10.25	12.31	-22.55	26.7	2.447	1.831	5.19
PPh$_3$	-3.87	6.11	-9.97	31.2	2.338	1.838	10.30
PMePh$_2$	-4.05	4.56	-8.61	31.8	2.365	1.834	11.98
PMe$_2$Ph	-4.23	4.37	-8.59	30.4	2.306	1.835	8.99
PEtPh$_2$	-5.47	5.85	-11.33	37.1	2.329	1.837	10.68
PH$_2$Ph	-2.55	1.12	-3.67	46.7	2.323	1.820	13.05
PPh$_2$(^{i}Pr)	-6.65	6.40	-13.05	35.2	2.350	1.835	9.61
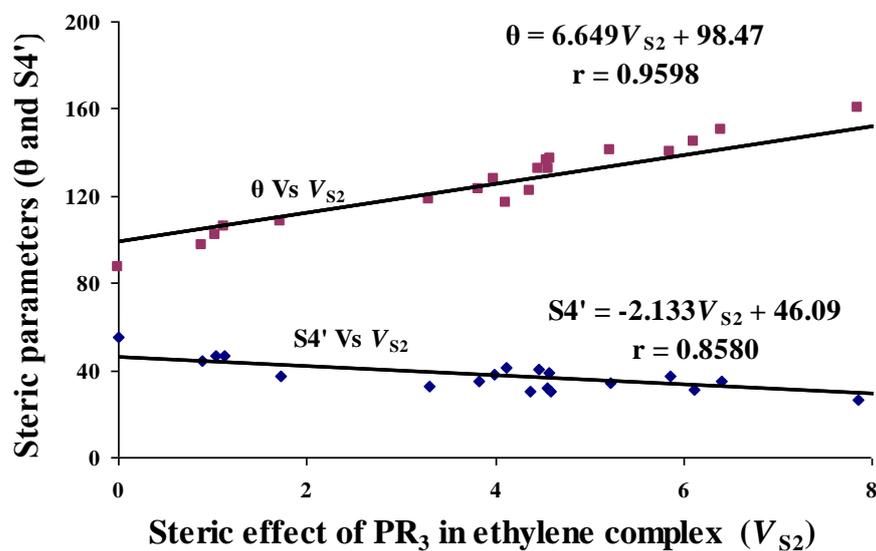
Figure 3.6 Correlation plots showing the relationship of θ with V_{S2} (top) and S4' with V_{S2}

(bottom).

The olefin complex must undergo C-C bond coupling reaction to form the metallacyclobutane which is the most important intermediate in olefin metathesis pathway. We have modeled the transition state for the formation of metallacyclobutane for all the twenty one cases studied herein to obtain the activation energy (E_2). The value of E_2 would depend on the stereoelectronic features of PR_3 in the olefin bound complex. In Figure 3.7, metathesis transformation of ethylene promoted by $Cl_2(PMe_3)Ru=CH_2$ is presented as a representative example along with two energy parameters E_1 and E_2. Since the metallacyclobutane is a key intermediate in olefin metathesis, E_2 serves as the most important energy parameter to study the activity of the catalyst. Recently, Jensen *et al.* [Occhipinti *et al.* 2006] have used energy terms (enthalpy) similar in definition to E_1 and E_2 to define a response variable named "productivity" in the QSAR study of ruthenium catalysts for olefin metathesis.
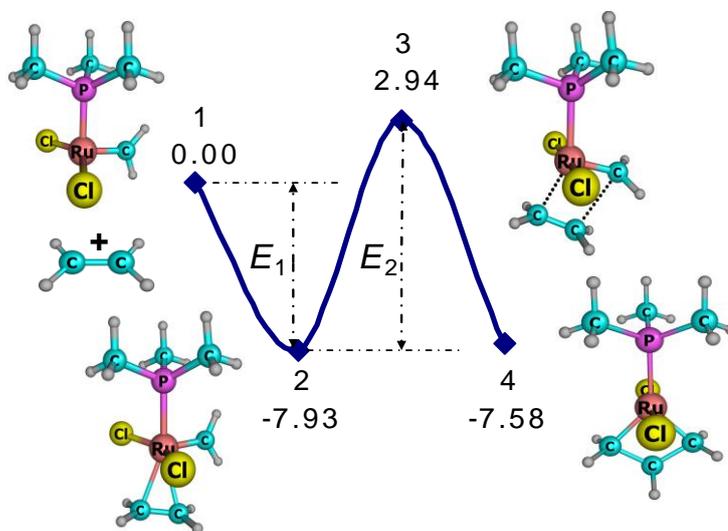
Figure 3.7 Metathesis transformation of ethylene in the presence of $Cl_2(PMe_3)Ru=CH_2$.

It may be noted that in the active form of the catalyst as well as in the ethylene bound complex (Figure 3.7), the plane of the carbene ligand and the plane containing the metal and chloro ligands are nearly orthogonal. In the formation of the transition state, the carbene ligand undergoes ~90° rotation to reach the plane of the metal and the chloro

ligands. This rotation yields more free space between the carbene and the phosphine ligands, leading to a reduction in the overall steric effect. In other words, due to the larger steric effect of PR_3 ligands in the olefin bound complex, more bulky ligands will force easy rotation of the carbene ligand to facilitate the formation the transition state. This is indeed observed in the correlation between the steric parameter V_{S2} and the activation barrier E_2 (r value is 0.872; Figure 3.8). Though the r value is not very impressive, the correlation line clearly suggests that an increase in the steric effect significantly decreases the activation barrier for the formation of metallacyclobutane. It may be noted that in most of the olefin complexes, the carbene is located between two of the R substituents of the P and they significantly affect the rotation barrier. In the correlation of E_2 versus V_{S2}, deviations of certain complexes might be resulted from the specific orientation of the substituents around the neighborhood of the carbene ligand (conformational issues). Interestingly, V_{E2} also showed a good linear relationship with the E_2 (r = 0.955; Figure 3.8) which indicates that an electron donating ligand will enhance the rotation of the carbene ligand in the transition state. In general, higher electron donating power of PR_3 ligand leads to an increase in the $Ru-CH_2$ bond length (Table 3.2) in the complex, suggesting easy rotation of the carbene moiety. The linear relationships in Figure 3.8 suggest that the steric effect is more dominating - approximately 1.62 times more powerful than electronic effect - in controlling the activation energy for the formation of metallacyclobutane in Grubbs first generation metathesis catalysis.

$E_2 = 0.456V_{E2} + 15.34$
$r = 0.9558$

$E_2 = -0.738V_{S2} + 13.56$
$r = 0.8725$
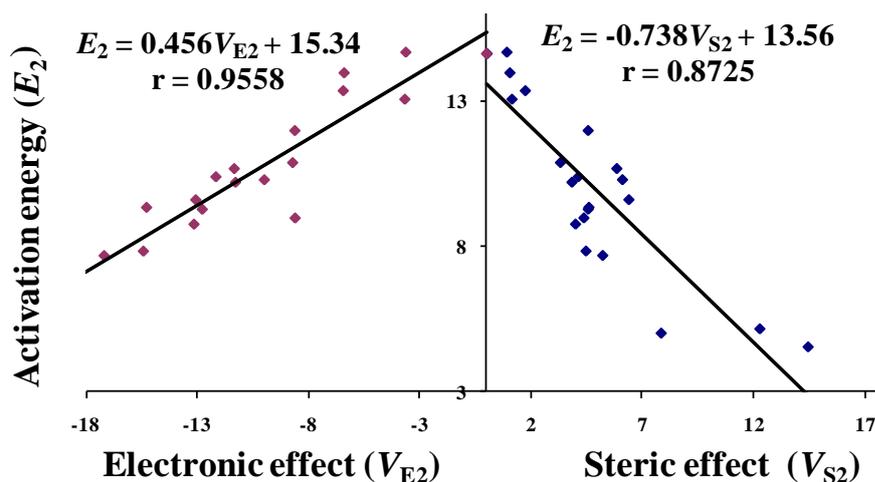
Figure 3.8 Correlation of V_{E2} with E_2 (in the left side) and V_{S2} with E_2 (in the right side).

3.4.2 Stereoelectronic Effects of N-Heterocyclic Carbenes in Second Generation Olefin Metathesis Catalysis

In this study, active form and the ethylene coordinated complex of nineteen G2R systems with saturated NHCs are considered (the abbreviations used for the names of NHC ligands are same as that used by Gusev [Gusev 2009]). The procedure for the naming of NHC ligands used by Gusev is as follows. NHCs with a double bond between C4 and C5 are represented by Im (imidazol-2-ylidene) and a saturated NHC ring is represented by sIm (4,5-dihydroimidazol-2-ylidene). The substituents 'R' on N are given as NR_2 after Im or sIm. For instance, saturated NHC with H substituents on N is given as sImNH$_2$ and the unsaturated NHC with H substituents on N is given as ImNH$_2$. If there are substituents at C4 and C5 positions, they will be given before N. Thus, the saturated NHC with CF$_3$ substituents on N and Me substituents on C4 and C5 positions are given as sImMe$_2N$(CF$_3$)$_2$. Figure 3.9 depicts the NHC ligands used in the second generation catalysts for the present study.

sIm*N*H₂ sIm*N*Me₂ sIm*N*Et₂ sIm*N*(ⁱPr)₂

sIm*N*(ᵗBu)₂ sIm*N*MeH sIm*N*EtH sIm*N*(ⁱPr)H

sIm*N*Me(ⁱPr) sIm*N*MeEt sIm*N*(ⁱPr)Et sIm*N*(CF₃)₂

sIm*N*Mes₂ sIm*N*Ph₂ sIm*N*Cy₂ sIm*N*Me(ᵗBu)

sIm*N*Et(ᵗBu) sImMe₂*N*Me₂ sImMe₂*N*(CF₃)₂
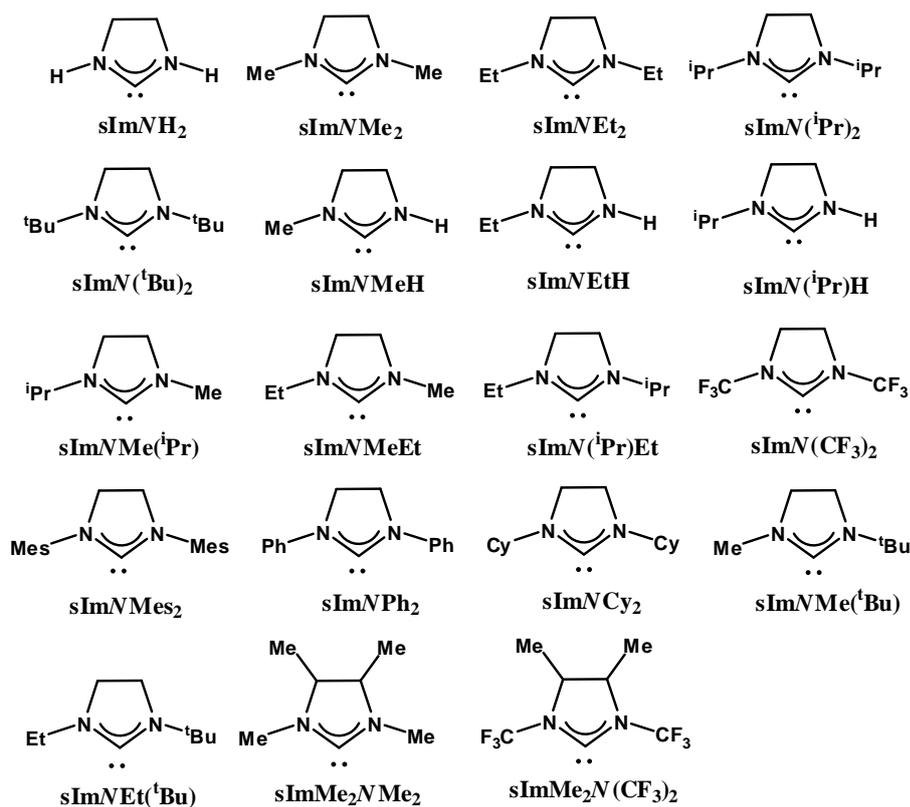
Figure 3.9 NHC ligands used in the second generation catalysts for the present study.

When unsymmetrical NHCs are involved, two conformers are possible and always the most stable active form and its ethylene complex are taken for the present study. A representative set of systems are presented in Figure 3.9. In the active form of sIm*N*H₂ coordinated system (this system where R = H is considered as the unsubstituted reference system), the two N–H bonds are directed more towards the chloro ligands (Figure 3.10). The angle between the plane of NHC and the plane of –CH₂ carbene is 56.5° which is measured in terms of the N–C–Ru–C dihedral angle, θ. As the size of N-R increases, the steric interaction of the R with chloro ligands forces the NHC to undergo a rotation around the Ru–C axis resulting to the closer approach of the alkylidene moiety to the N-substituents. Thus the θ value of a moderately bulky sIm*N*Me₂ coordinated complex is 38.8° and that of the most bulky sIm*N*(ᵗBu₂) coordinated is 0.9° (Figure 3.10). In the ethylene bound complexes (Figure 3.10), the θ value of sIm*N*H₂, sIm*N*Me₂ and sIm*N*(ᵗBu₂) coordinated systems are 70.9°, 35.8° and 0.1°, respectively, suggesting that

the steric effect due to the olefin can induce further structural changes. In fact, in the

sImN(^{t}Bu)$_2$ coordinated system, this effect from the olefin is maximum which forces the

−CH$_2$ to undergo rotation to lie in the plane of the Ru and two chloro ligands.
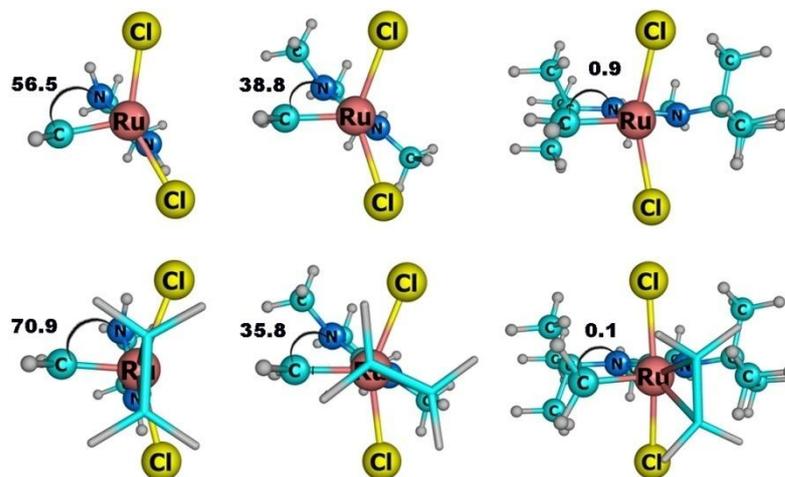
Figure 3.10 Active forms and ethylene bound complexes with sImNH$_2$, sImNMe$_2$ and

sImN(^{t}Bu)$_2$ ligands.

It may be noted that in G1R catalysts, the ligand PR$_3$ has a three dimensional

structure whereas in G2R the core of the NHC ligand is planar and rigid. Further, the N−

R bond of the NHC is oriented towards the metal center whereas the P–R bonds of the

G1R are oriented away from the metal center. Moreover, unlike the P-substituents of the

G1R, the N-substituents of the G2R are not directly bonded to the atom that coordinates

to the metal center. Thus, there is a fundamental difference in the way the steric effect of

NHC and PR$_3$ can act on the metal center. For instance, even with stericaly very bulky

P(^{t}Bu)$_3$, the orientation of the −CH$_2$ carbene is nearly unaffected in the active and

ethylene coordinated forms of G1R systems but even with a moderate increase in the

steric size, substantial structural changes can be observed around the carbene ligand in

G2R systems. In the previous section, the successful use of the MESP at the P nucleus of

the phoshine is described to assess the stereoelectronic profiles of PR$_3$ in G1R catalysis

[Mathew and Suresh 2011]. A good choice for the MESP based stereoelectronic

descriptor for G2R can be the MESP at the carbene carbon of the NHC [Mathew and Suresh 2010]. But this choice alone is not enough for G2R systems because the $-CH_2$ carbene also undergoes substantial structural changes which is also decisive to the selection of the reaction pathway. Therefore, we have chosen the combined value of the MESP at the NHC carbon nucleus (V_{C1}) and at the $-CH_2$ carbon nucleus (V_{C2}) as a descriptor to analyze the stereoelectronic features of G2R catalysis.

The V_{C1} and V_{C2} values are calculated for the active form of the catalyst, ($sImR_2NR_2$)$Cl_2Ru=CH_2$ (**1b**) and the ethylene bound complex, ($sImR_2NR_2$)$Cl_2Ru=CH_2(C_2H_4)$ (**2b**). For frozen geometries of **1b** and **2b**, the R substituents are replaced with H and fixed the N–H and C–H distances to that of $sImNH_2$ to generate the complexes ($sImH'_2NH'_2$)$Cl_2Ru=CH_2$ (**1b'**) and ($sImH'_2NH'_2$)$Cl_2Ru=CH_2(C_2H_4)$ (**2b'**) and determined their V_{C1}' and V_{C2}' values. The quantity ($V_{C1} + V_{C2}$) is used as the combined steric and electronic effects of ($sImR_2NR_2$)$Cl_2Ru=CH_2$. Since the electronic effect of R is not present in the frozen structures, **1b'** and **2b'**, the quantity ($V_{C1}' + V_{C2}'$) would reflect the steric only effect of R. We have considered **1b** and **2b** systems with R = H (unsubstituted systems) as reference systems. Therefore, for the active form of the catalyst, the relative value of ($V_{C1} + V_{C2}$) with respect to the reference system can be used as a measure of the combined steric and electronic effect, V_{SE3}. Similarly, the combined steric and electronic effect, V_{SE4} of the ethylene bound complex can be determined.

The steric effect of NHCs in the active form (designated as V_{S3}) as well as the ethylene bound complex (designated as V_{S4}) are calculated from the relative value of ($V_{C1}' + V_{C2}'$) for any R with respect to R = H systems. The Samb$V$ca, [Poater *et al*. 2009] a web application developed by Cavallo *et al*. is used to calculate the molecular volume based descriptor, the buried volume ($\%V_{Bur}$). The quantity ($V_{SE3} - V_{S4}$) represents the

electronic effect, V_{E3} of the active complex whereas the quantity ($V_{SE4} - V_{S4}$) represents the electronic effect, V_{E4} of the olefin bound complex. In Table 3.3, V_{SE3}, V_{S3}, V_{E3} and %V_{Bur} values of NHCs in the active form are presented. A good linear correlation between V_{S3} and %V_{Bur} is shown in Figure 3.11 (correlation coefficient, r = 0.961). The most deviated points in the correlation line correspond to systems with the sImNMes$_2$ and sImNPh$_2$ carbenes whose V_{S3} values are 8.15 and 8.30 kcal/mol, respectively. On the scale of %V_{Bur}, these systems are as bulky as the sImNEt(^{t}Bu) and sImNMe(^{t}Bu) ligands. It may be noted that the phenyl rings of the systems with sImNMes$_2$ and sImNPh$_2$ ligands are oriented perpendicular to the NHC ring plane which reduces their effective steric interactions with other ligands. It is felt that the volume based measure of the steric effect may not be adequate enough to represent such subtle variations in the structure as the rotation of substituent may not significantly alter the molecular volume.
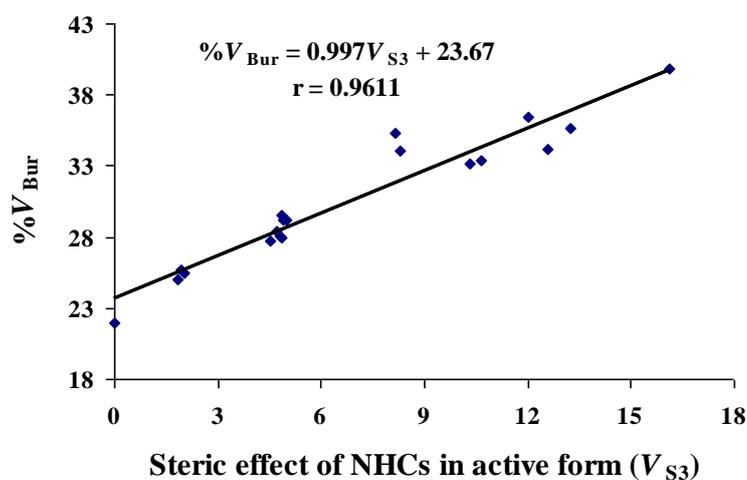
Figure 3.11 Correlation of %V_{Bur} with steric effect of NHCs in G2R active form (V_{S3}).

Coordination of ethylene to the active form can occur in three different modes, *viz.* A, B and C. In mode A, ethylene orients parallel to the Ru–CH$_2$ plane and in mode B, the orientation is perpendicular to the Ru-CH$_2$ plane. Mode C binding is observed only for the least bulky sImNH$_2$ coordinated system wherein the –CH$_2$ carbene orients like that of mode A while the ethylene adopts an orientation similar to that of mode B (Figure

3.12). Both mode A and B are possible with systems with moderately bulky NHCs and between the two modes, the preferred binding is mode A (entries 2 - 13 in Table 3.3). On the other hand, in all the systems with bulky NHCs (entries 14 to 19 in Table 3.3), ethylene showed only the mode B binding. When bulky NHCs are involved, the steric interaction of the N-substituents in **2b** forces the $-CH_2$ to rotate ~90º towards the plane containing the ruthenium and the chloro ligands (Figure 3.12). Interestingly, in $sImMe_2N(CF_3)_2$ and $sImN(CF_3)_2$ coordinated systems, though the V_{S3} values are high, the ethylene binding mode was very similar to that observed for less bulky systems. This discrepancy to the general trend can be attributed to the hydrogen bonding interaction between the N-substituent and $-CH_2$ as well as the Ru…F interaction (Figure 3.12).
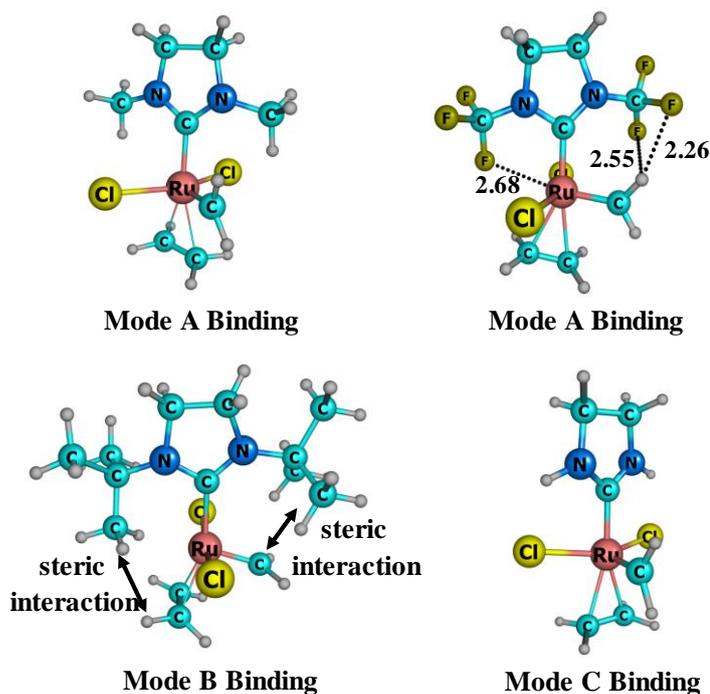
Figure 3.12 Ethylene coordinated systems of $sImNMe_2$, $sImN(CF_3)_2$, $sImN(^tBu)_2$ and $sImNH_2$ ligands. Ru-F, H-F distances are given in Å

Table 3.3 Stereoelectronic parameters of G2R active form complexes and their corresponding E_3 values.

NHC ligand in G2R active form	V_{SE3} kcal/mol	V_{S3} kcal/mol	V_{E3} kcal/mol	$\%V_{Bur}$	Binding Energy (E_3) kcal/mol
sImNH$_2$	0.00	0.00	0.00	22.0	10.78
sImNMeH	-1.66	1.86	-3.52	25.0	8.68
sImNEtH	-2.69	2.03	-4.73	25.5	8.47
sImN(^{i}Pr)H	-3.51	1.96	-5.46	25.7	8.33
sImNMe$_2$	-2.64	4.55	-7.19	27.7	6.99
sImNEt$_2$	-3.90	4.91	-8.82	29.2	6.61
sImN(^{i}Pr)$_2$	-5.58	5.02	-10.59	29.2	6.93
sImNMe(^{i}Pr)	-4.46	4.69	-9.15	28.4	7.13
sImNMeEt	-3.11	4.80	-7.91	28.1	6.90
sImN(^{i}Pr)Et	-4.61	4.88	-9.48	29.5	6.68
sImMe$_2$$NMe_2$	-5.55	4.86	-10.40	27.9	6.71
sImN(CF$_3$)$_2$	36.88	10.31	26.57	33.2	5.66
sImMe$_2$$N$(CF$_3$)$_2$	32.63	10.64	22.00	33.4	5.65
sImNMes$_2$	-8.13	8.15	-16.28	35.3	7.57
sImN(^{t}Bu)$_2$	-0.55	16.14	-16.68	39.8	10.95
sImNCy$_2$	-4.68	12.02	-16.70	36.4	10.61
sImNEt(^{t}Bu)	-1.19	13.22	-14.41	35.6	12.44
sImNPh$_2$	2.53	8.30	-5.78	34.1	6.59
sImNMe(^{t}Bu)	-1.73	12.57	-14.30	34.2	12.05

The binding energy (E_3) values of all the systems are presented in Table 3.3. Entries 2-13 are for mode A and entries 14-19 are for mode B binding. In mode A complexes, E_3 is in the range of 5.65 – 8.68 kcal/mol and the relationship of V_{S3} with the binding energy (E_3) is similar to that of G1R catalysts: E_3 decreases with increase in V_{S3} (Figure 3.13) [Mathew and Suresh 2011]. Interestingly, mode B complexes showed higher E_3 in the range of 6.59 – 12.44 kcal/mol and the relation of V_{S3} with E_3 is opposite

to that of mode A systems: E_3 increases with increase in V_{S3} (Figure 3.13). The sImN(^{t}Bu)$_2$ coordinated system is not agreeing to this trend because the ^{t}Bu, the bulkiest of all the substituents has exerted some steric influence on the coordinated ethylene (Figure 3.12), leading to a decrease in the binding energy than the expected value. E_3 value of sImNH$_2$ coordinated system (mode C binding) is 10.78 kcal/mol which is not fitting to any of the two general trends and hence this binding can be viewed as a hybrid of mode A and B bindings.
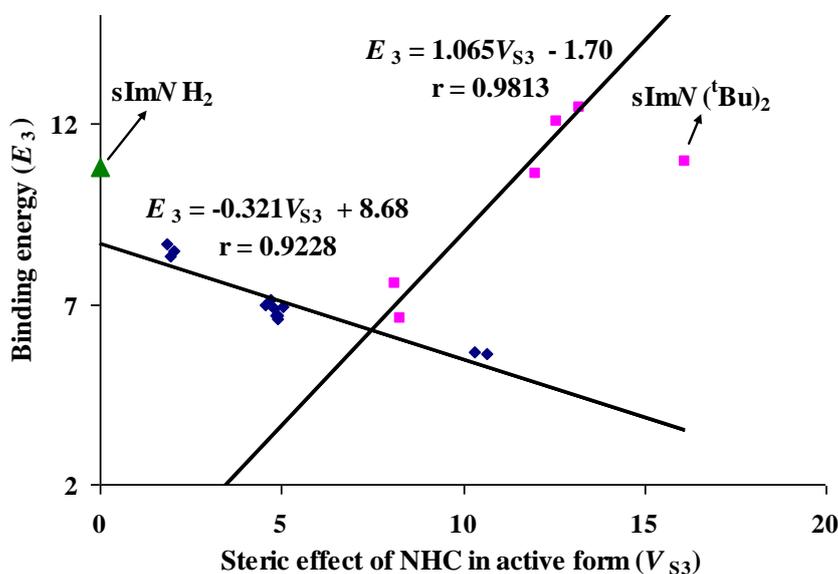
Figure 3.13 Correlation of binding energy (E_3) with steric effect (V_{S3}). ◆ Mode A complexes ■ Mode B complexes ▲ Mode C complex

The electronic effect (V_{E3}) also showed a good linear relationship to E_3 in mode A systems, except the sImN(CF$_3$)$_2$ and sImMe$_2$$N$(CF$_3$)$_2$ coordinated systems (Figure 3.14). This linear relationship suggests that an electron withdrawing NHC ligand enhances the binding affinity of the metal to the ethylene. In the case of sImN(CF$_3$)$_2$ and sImMe$_2$$N$(CF$_3$)$_2$ coordinated systems, the Ru–F distance of 2.68 Å in the former and 2.60 Å in the latter suggest significant Ru...F interaction (Figure 3.12). Moreover, the –CH$_2$ carbene showed hydrogen bonding interaction with the nearby F atom of the substituent.

This fact was supported by electron density analysis which showed the presence of a bond critical point for both the Ru…F and CH_2..F interactions (Figure 3.15) [[b]Ritter *et al*. 2006; Santiago *et al*. 2010]. Thus in these systems, the electron deficiency in the metal centre due to the high electron withdrawing power of NHC is largely compensated by the electron donation from the lone pair of F to the Ru *via* the Ru...F interaction and because of this E_3 of these systems deviated considerably from the general trend. In the case of mode B binding, except the case of sImNPh$_2$ coordinated system, the V_{E3} values lie in a small range of -14 to -16 kcal/mol and they did not show any correlation with E_3. It means that, irrespective of a high electron donating nature of NHC, the mode B binding is stronger in many cases than mode A binding. This result also points to the fact that mode B binding is almost fully controlled by the steric effect of the NHC ligand.

$$E_3 = 0.302V_{E3} + 9.68$$
$$r = 0.9093$$
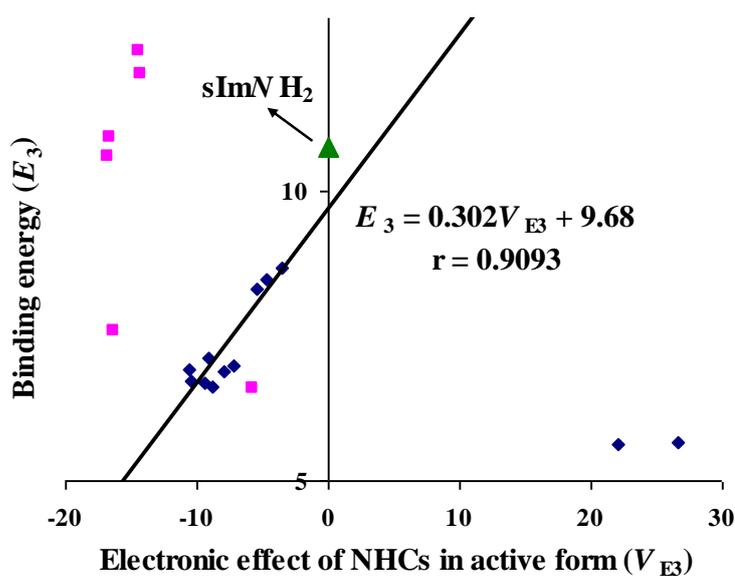
Figure 3.14 Correlation of binding energy (E_3) with electronic effect V_{E3}. ◆ Mode A complexes ■ Mode B complexes ▲ Mode C complex

$$\rho(r) = 0.019$$
$$\nabla^2\rho(r) = 0.083$$
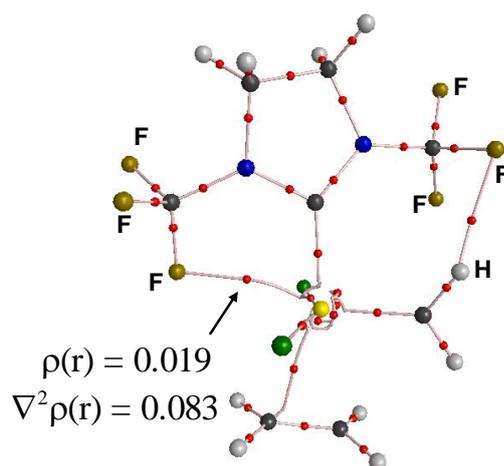
Figure 3.15 AIM topological plot of the ethylene complex of sImN(CF$_3$)$_2$ ligand. Charge density ($\rho(\mathbf{r})$) and the Laplacian ($\nabla^2\rho(\mathbf{r})$) at the Ru…F bond critical point is given in a. u.

The stereoelectronic parameters of NHCs in ethylene bound complexes, *viz.* V_{SE4}, V_{S4} and V_{E4} are summarized in Table 3.4 along with the %V_{Bur} values. The steric parameter, V_{S4} showed a good linear correlation the %V_{Bur} (r = 0.976; Figure 3.16). In the case of mode A binding, V_{S4} is nearly same as the corresponding steric parameter of **1b**, V_{S3} as the difference between V_{S4} and V_{S3} is in a small range of -0.72 to +1.72 kcal/mol. On the other hand, mode B binding showed drastic increase in the V_{S4} value compared to V_{S3} ((V_{S4} - V_{S3}) was in the range of 3.85 to 9.78 kcal/mol). The observed difference in the steric behavior of mode A and B binding is not surprising because in mode B, the ethylene coordination exerts significant structural changes to the active form whereas the structural features of the active form is largely retained in mode A.

Table 3.4 V_{SE4}, V_{S4}, V_{E4} and %V_{Bur} of the ethylene complexes along with the E_4 values

NHC ligand in G2R ethylene complex	V_{SE4} kcal/mol	V_{S4} kcal/mol	V_{E4} kcal/mol	%V_{Bur}	Activation energy (E_4) kcal/mol
sImNH$_2$	0.00	0.00	0.00	20.6	10.61
sImNMeH	6.04	1.19	4.85	23.8	9.77
sImNEtH	5.11	1.31	3.81	24.0	9.23

sImN(^{i}Pr)H	4.56	1.41	3.15	24.2	8.85
sImNMe$_2$	6.73	5.60	1.14	26.4	4.94
sImNEt$_2$	6.66	6.53	0.12	27.6	2.96
sImN(^{i}Pr)$_2$	4.74	6.47	-1.73	27.7	2.65
sImNMe(^{i}Pr)	5.49	5.88	-0.39	27.1	3.90
sImNMeEt	6.98	6.15	0.84	27.4	4.49
sImN(^{i}Pr)Et	5.92	6.60	-0.68	27.8	2.83
sImMe$_2$$NMe_2$	4.08	6.07	-1.99	26.6	4.50
sImN(CF$_3$)$_2$	45.55	11.15	34.41	31.6	1.56
sImMe$_2$$N$(CF$_3$)$_2$	41.45	11.86	29.59	32.1	0.88
sImNMes$_2$	10.68	16.59	-5.91	33.0	2.04
sImN(^{t}Bu)$_2$	10.86	19.99	-9.13	37.7	3.90
sImNCy$_2$	9.54	18.52	-8.98	35.9	3.89
sImNEt(^{t}Bu)	10.17	17.75	-7.59	33.8	3.61
sImNPh$_2$	16.06	18.08	-2.03	33.5	3.26
sImNMe(^{t}Bu)	10.20	17.71	-7.51	33.4	3.75

$$\%V_{Bur} = 0.667 V_{S4} + 22.88$$
$$r = 0.9764$$

Steric effect of NHC in ethylene complex (V_{S4})
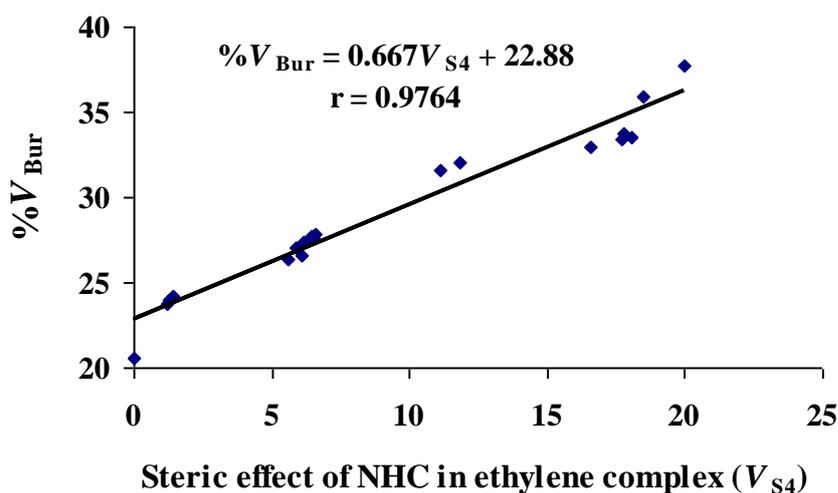
Figure 3.16 Correlation of %V_{Bur} with steric effect of NHCs in ethylene complex (V_{S4}).

In Figure 3.17, the metathesis pathway describing the metallacyclobutane formation is illustrated in the case of sImNMe$_2$ coordinated G2R catalyst along with a

representation of the binding energy, E_3 and the activation energy, E_4. For all the systems

studied herein, the E_4 are given in Table 3.4.
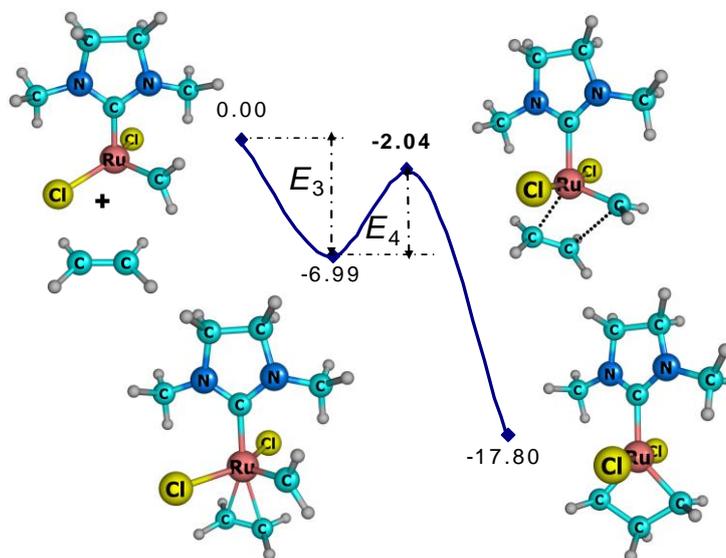
Figure 3.17 Metathesis transformation of ethylene in presence of sImNMe$_2$Cl$_2$Ru=CH$_2$.

In mode A systems, the transition state corresponds to the rotation of –CH$_2$

towards the π-face of the ethylene. The E_4 decreases with an increase in the steric effect,

V_{S4} and the correlation is depicted in Figure 3.18 (r = 0.942). It means that the rotation of

–CH$_2$ is more feasible when the steric effect of N-substituent increases in the complex. In

mode B systems, the –CH$_2$ group is coplanar with chloro ligands and therefore a rotation

of the coordinated ethylene towards the Ru–CH$_2$ plane will lead to the C–C bond

coupling. This rotation of ethylene is easy and E_4 falls in a range of 2 to 4 kcal/mol. In

general, a slight increase in E_4 is observed with an increase in the steric effect (Figure

3.18). The unsubstituted sImNH$_2$ coordinated system (mode C binding) is an exception

(E_4 = 10.61 kcal/mol) because in this case, both ethylene and –CH$_2$ must undergo

rotation to reach the transition state for the formation of metallacyclobutane.
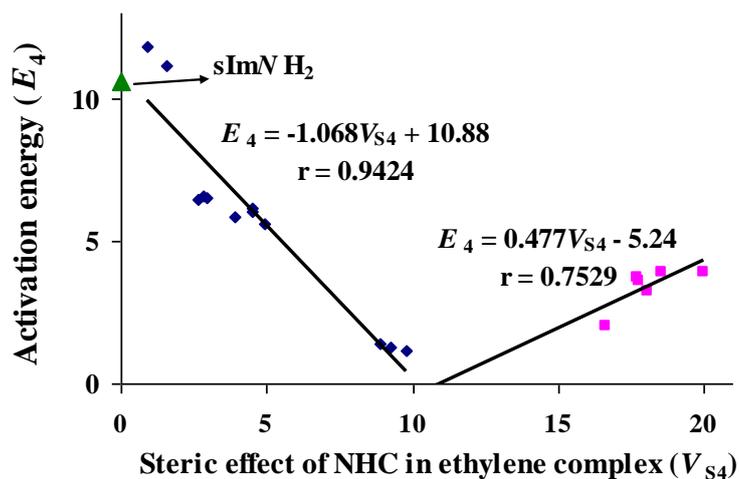
Figure 3.18 Relation E_4 with steric effect of NHCs in ethylene complexes (V_{S4}). ◆ Mode A complexes ■ Mode B complexes ▲ Mode C complex

In the case of mode A binding, the electronic effect V_{E4} can be correlated linearly with E_4 (r = 0.917): the activation energy decreases with increase in the electronic effect. The sImN(CF$_3$)$_2$ and sImMe$_2N$(CF$_3$)$_2$ coordinated systems are exceptions to this general trend which can be attributed to the already mentioned Ru...F and CH$_2$…F interactions (Figure 3.19). On the other hand, V_{E4} of the systems showing mode B binding is largely insensitive to the electronic effect.
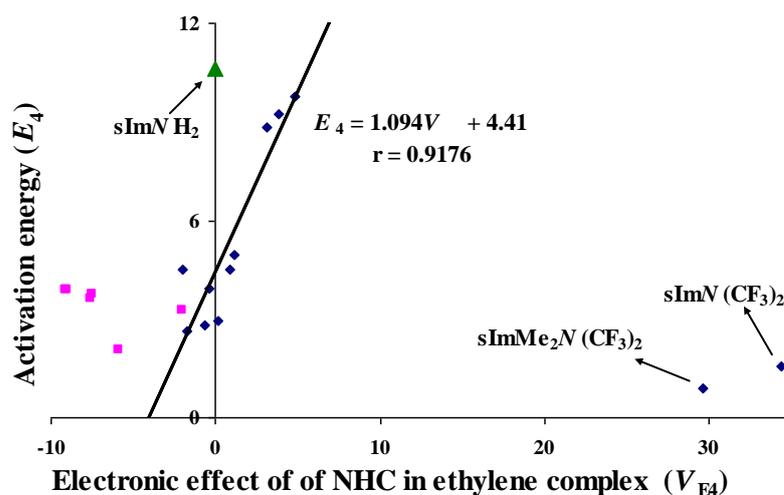
Figure 3.19 Relation of E_4 with electronic effect of NHCs in ethylene complexes (V_{E4}). ◆ Mode A complexes ■ Mode B complexes ▲ Mode C complex.

3.5 Conclusion

A simple method for assessing the steric and electronic effect of phosphines on the activity of Grubbs first generation olefin metathesis catalysts is described using the MESP-based quantum chemical descriptors. Steric parameter V_{S1} and electronic parameter V_{E1} are introduced for PR_3 ligand in the active form of the catalyst. Similarly, steric parameter V_{S2} and electronic parameter V_{E2} are defined for the ethylene coordinated form of the catalyst. Both V_{S1} and V_{S2} showed good linear relationships with structure based steric parameters, *viz.* the Tolman cone angle (θ) and the symmetric deformation coordinate (S4'). Further, the MESP approach to stereoelectronic features clearly showed that the steric contribution is 1.88 times more powerful than the electronic effect in controlling the binding of the ethylene to the active form of the catalyst. This aspect has come out nicely from V_{S1} versus E_1 and V_{E1} versus E_1 correlations. The binding energy of the olefin decreases with increase in the steric bulkiness as well as increase in the electron donating power of the PR_3 ligand. Further, the quantities V_{S2} and V_{E2} are found to be very useful for assessing the influence of stereoelectronic features of the PR_3 ligand on the activation energy for the metallacyclobutane formation as both parameters showed linear relationship to the activation barrier E_2. Sterically bulky ligands decrease the activation barrier considerably. This is due to the fact that bulky ligands enhance the twisting of the carbene ligand to adopt a favorable configuration for a C-C bond coupling with the coordinated olefin in the transition state. Compared to the olefin binding, the transition state formation is more influenced by the electronic effect. In general, electron rich ligands will show lower activation barriers than electron poor ligands. Thus, it can be said that a right balance of steric and electronic effects are required for making the most active catalyst. Most of the ligands used in olefin metathesis are electron rich which means that the activity of the catalyst is mainly tuned by increasing the steric effect of the

ligand. It is felt that the theoretical analysis on the dependency of steric and electronic effect of phosphines on the activity of first generation Grubbs olefin metathesis catalysts presented herein provides a useful strategy for the fine tuning of the stereoelectronic properties of ruthenium based olefin metathesis catalysts.

An approach based on the critical features of the molecular electrostatic potential (MESP) is developed for the quantification of steric and electronic properties of NHCs in Grubbs second-generation olefin metathesis catalysts. The MESP based steric parameters V_{S3} and V_{S4} showed impressive linear correlations to the molecular volume based quantity, $\%V_{Bur}$. The results presented in Figures 3.13, 3.14, 3.18 and 3.19 clearly suggest that the mode A binding of the olefin to the active form is preferred when the NHC is moderately bulky and the binding energy, E_3 as well as the activation barrier, E_4 shows strong dependency to both steric and electronic effects of the NHC. Both E_3 and E_4 show a decrease with an increase in the steric effect of the NHC while both show an increase with an increase in the electron withdrawing effect of the NHC. On the other hand, mode B binding of the olefin is preferred in the case of bulky NHC ligands and in such cases, the E_3 as well as E_4 showed an increase with an increase in the steric bulkiness of the NHC. However, electronic effect showed no correlation to either E_3 or E_4 in mode B binding. These results strongly suggest that the mode B biding of ethylene to the active form of the catalyst and the subsequent formation of the transition state for the C–C bond coupling are primarily controlled by the steric effect of the NHC. On the other hand, the electronic and steric effects have nearly equal importance in metathesis when the N-substituent is not very bulky. Secondary effects such as the lone pair interaction of halogen and metal center or hydrogen bond interaction from N-substituent to the carbene ligand can greatly influence the metathesis activity of the catalyst. The MESP is a powerful molecular descriptor to understand chemical reactivity and this work

illustrates the use of it in rationalizing an organometallic catalytic reaction in terms of the

stereoelectronic features and thermodynamic aspects.

Chapter 4

Mechanistic Analysis of the Deactivation Pathway of a Grubbs Second Generation Catalyst
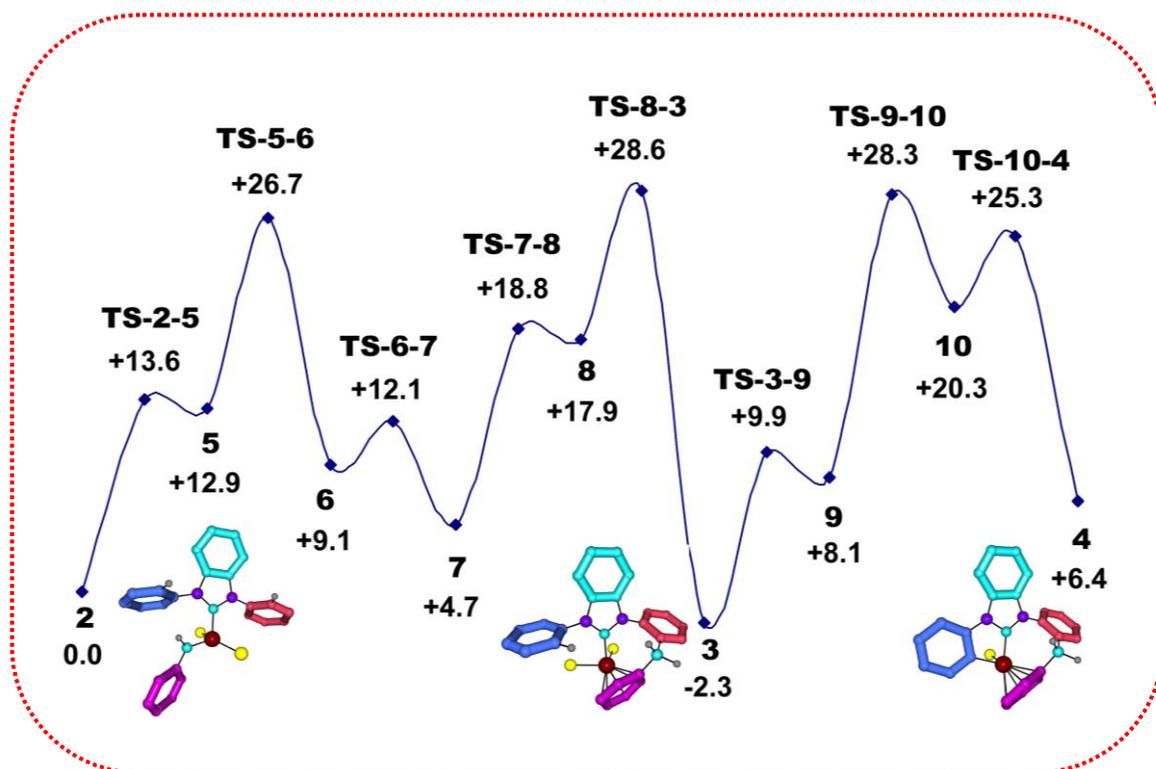
4.1 Abstract

*A mechanistic study has been carried out to explore the structural and energetic features leading to the decomposition pathways of Grubbs second generation olefin metathesis catalyst using density functional theory. The active form of the catalyst **2** has an inherent tendency to undergo intramolecular reactions as the highly electron deficient ruthenium centre is in the close proximity of the C-H bonds of the N-substituents. The theoretical results strongly suggest that the deactivation pathway initiates with the C–H activation rather than pericyclic cyclization suggested for related Grubbs-Hoveyda catalyst system by Blechert et al. The complex **2** passes through five transition states, viz. (i) formation of agostic complex through the activation of C–H bond of the N-heterocyclic carbene (NHC) -phenyl ring (ii) C–H σ bond metathesis with carbene moiety to form a benzyl complex (iii) two step rotational transformations of benzyl unit and (iv) carbene-arene bond formation to yield the first product **3**. The last step is the rate determining step with the highest activation barrier of 28.6 kcal/mol while the activation energy for the steps (i), (ii), and (iii) are 13.6 kcal/mol, 26.7 kcal/mol, and 18.8 kcal/mol, respectively. The transformation of the rigid carbene unit to a flexible benzyl unit facilitates the rotational transformations in step (iii) and the subsequent C–C bond formation in step (iv). The η^6 coordination of phenyl ring in **3** changes to η^2 to produce a less strained complex and the C–H activation of the second NHC-phenyl ring occurs easily with this transformation leading to a C–H agostic complex through a transition state with the activation barrier of 28.3 kcal/mol. The agostic interaction breaks up in*

*the next step leading to the ruthenium–carbon bond formation and the reductive elimination of HCl to second product **4**. The flexibility of all the three phenyl rings through their single bond connectivity plays a major role in the deactivation process of **2** as it leads to C-H agostic interaction with the ruthenium center. Therefore, the deactivation can be controlled by designing NHCs with rigid substituents which may not undergo agostic interactions.*

4.2 Introduction

N-heterocyclic carbenes (NHCs) are emerged as one of the most important family of ligands with their powerful σ-donating and weak π-accepting ability. Though the metal coordination chemistry of NHCs is reported by Öfele [Öfele 1968] and Wanzlick [Wanzlick and Schönherr 1968] in 1968, the isolation of first stable NHCs by Arduengo in 1991 [Arduengo *et al.* 1991] has made a significant impact in organometallic chemistry with the use of NHC ligands. The coordination of NHCs in metal complexes was found to impart major changes in its reactivity [Grubbs 2003; Scott and Nolan 2005; Crudden and Allen 2004] and in many organometallic systems NHCs are introduced as an analogue to phosphines. NHC ligands are getting wide attention in the designing of homogeneous catalytic systems [Herrmann 2002; Marion *et al.* 2006; Nolan 2006; Bourissou *et al.* 2000; Glorius 2007; Grubbs 2003]. For instance, the high catalytic efficiency observed in the second generation Grubbs olefin metathesis catalyst when a phosphine in the first generation Grubbs catalyst was replaced by an NHC has been attributed to the presence NHC ligands (Figure 4.1) [Chatterjee *et al.* 2000; Garber *et al.* 2000; Huang *et al.* 1999; Bielwaski and Grubbs 2000; Schwab *et al.* 1996; Scholl *et al.* 1999].
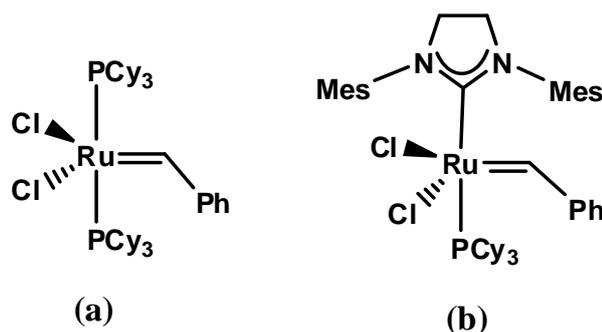
Figure 4.1 (a) First generation catalyst (b) second generation catalyst.

The role of steric and electronic effects of NHCs towards the enhanced activity of catalysts on replacing phosphines by NHCs have been proved both theoretically and experimentally [Bielwaski and Grubbs 2000; Scholl *et al.* 1999; Occhipinti *et al.* 2006; Scholl *et al.* 1999; Straub 2005; Straub 2007; Correa and Cavallo 2006; Tonner *et al.* 2007]. Catalyst activity can be improved by altering the substituents on the nitrogen of NHCs and there exists a number of modified second generation Grubbs catalyst systems have been reported [Bielwaski and Grubbs 2000; Scholl *et al.* 1999; Love *et al.* 2002; Chatterjee and Grubbs 1999]. It has been observed that the changes in the substituents on the nitrogen of NHC ring can change the activity of catalysts unusually in different types of metathesis reactions [Scholl *et al.* 1999; Love *et al.* 2002; Chatterjee and Grubbs 1999].

Since olefin metathesis has emerged as an important method in organic synthesis, the designing of catalyst with suitably substituted NHCs hold great importance. But the tendency of NHCs to undergo chemical transformations such as reductive elimination, decomplexation, and intramolecular reactions can cause the degradation of the system [Crudden and Allen 2004]. Phenyl and mesityl substituents on nitrogen was found to have a higher tendency to undergo C–H and C–C activation since the steric bulk keeps the C–H and C–C bonds close to the metal centre. The C–C and C–X (carbon-hetero atom) activation in ruthenium–NHC complexes were reported by Whittlesey *et al.* [Burling *et al.* 2004; [a]Diggle *et al.* 2008; [b]Diggle *et al.* 2008] (Scheme 4.1).
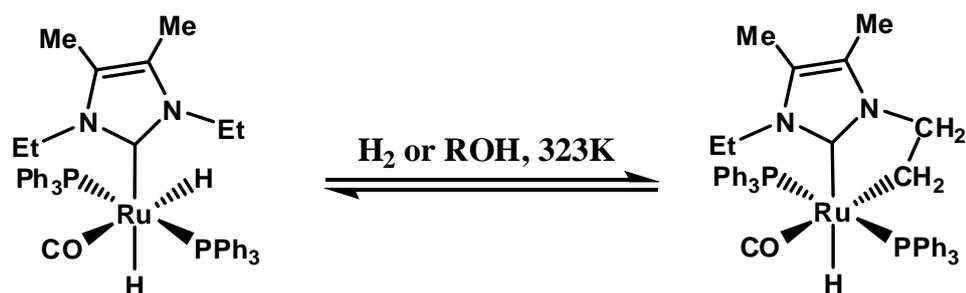
Scheme 4.1 Decomposition of an NHC coordinated complex (Burling *et al*. **2004**).

Grubbs *et al.* have observed the C–H activation in second generation Grubbs catalyst leading to the carbene-arene bond formation [Trnka *et al.* 2003; Hong *et al.* 2007]. Bletchert and co-workers reported the decomposition of a Grubbs-Hoveyda catalyst system and they proposed that the carbene–arene bond formation takes place directly through pericyclic cyclization [Vehlow *et al.* 2007] (Scheme 4.2). C–H activation in rhodium-NHC complexes [Huang *et al.* 2000; Dorta *et al.* 2004] and iridium-NHC complexes [Prinz *et al.* 2000; Corberán *et al.* 2006] were also reported.
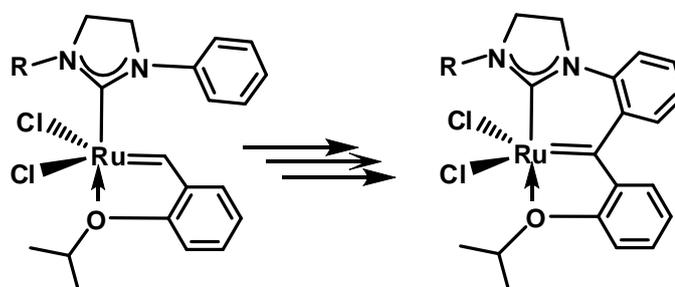
Scheme 4.2 Deactivation of Grubbs-Hoveyda catalyst (Vehlow *et al*. **2007**).

The mechanism of olefin metathesis with the assistance of Grubbs catalysts was already explored in both experimental and theoretical studies and the generally accepted Chauvin mechanism suggests that the reaction initiates with the dissociation of phosphine leading to the formation of a 14 electron complex followed by olefin coordination and metathesis steps from a metallacyclobutane [Hérisson and Chauvin 1970; Dias *et al.* 1997; Hinderling *et al.* 1998; Vyboishchikov *et al.* 2002; Aagaard *et al.* 1998; Fomine *et al.* 2003; Bernardi *et al.* 2003; Cavallo *et al.* 2003; Adlhart and Chen 2004; Suresh 2006

Suresh and Baik 2005; Suresh and Koga 2004]. Therefore, the 14-electron complex is the

species having catalytic activity or it can be considered as the active form of the catalyst

and the original 16-electron complex will act only as the pre-catalyst. In other words,

stability of the 14-electron species is directly related with the turnover number of the

catalytic process. Since the metal centre of the active form of the catalyst is highly

electron deficient it could undergo interaction even with σ bonds in the vicinity. Thus,

electron rich olefins can easily coordinate to the metal centre to undergo metathesis

reaction. But in the absence of a substrate to coordinate with the metal or in the absence

of enough concentration of the substrate, the 14-electron active form may get deactivated

either through intramolecular reactions or by the back coordination of phosphine. In a

recent article Grubbs *et al.* [Hong *et al.* 2007] reported such a deactivation reaction

observed in complex **2** leading to formation of complexes **3** and **4** in which new carbene-

arene and Ru–C bonds were formed (Figure 4.2).
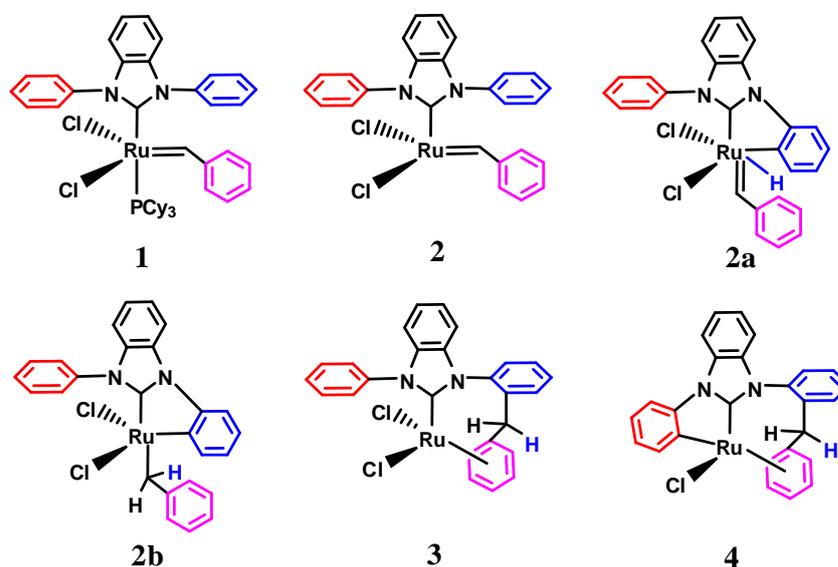
Figure 4.2 Grubbs second generation catalyst, the proposed intermediates and the

decomposition products.

The proposed mechanism [Hong *et al.* 2007] for the decomposition of Grubbs

second generation catalyst **1** involves the intermediacy of complex **2a**, a ruthenium

hydride complex formed by the oxidative addition of a C–H bond of a phenyl ring to the metal centre and the complex **2b** which is formed by α-H insertion to the benzylidene ligand (Figure 4.2). It is seen that all the three phenyl groups (red, blue and pink colored ones) in **2** are actively involved in the reaction and they undergo major changes. The present study will focus on this structural aspect and the complete mechanism of the transformations involved.

4.3 Computational Methods

All calculations were carried out using the Gaussian 03 [Frisch *et al.* Gaussian 03 2004] suite of programs. The optimizations, vibrational frequency and zero point energy (ZPE) calculations were performed using B3LYP hybrid functional [Becke 1988; Lee *et al.* 1988] and 6-31G(d,p) basis set for all atoms except for ruthenium which is treated with Lanl2DZ with extra f polarization functions [Hay and Wadt 1985; Ehlers *et al.* 1993] and the combined basis set is named as Gen1. LanL2DZ is a double zeta basis set which is a combination of Los Alamos National Laboratory (LANL) effective core potential (ECP) and double zeta valence basis set. All transition states were calculated using Synchronous Transit-Guided Quasi-Newton (STQN) method implemented in *Gaussian 03* program and transition states were characterized by a single imaginary frequency. Single point energy calculation of all geometries was done with the B3LYP/Gen2 method where Gen2 stands for Lanl2DZ+f functions for Ru and 6-311++G(d,p) for rest of the atoms. The single point energy values were also corrected with zero point energy obtained from the B3LYP/Gen1 frequency calculation. The ZPE corrected B3LYP/Gen2 level values were used through out for discussing the energetics.

4.4 Results and Discussion

The two probable pathways for the internal reaction to proceed from **2** can be envisaged, *viz.* (i) through the C–H activation of the phenyl ring via agostic interactions and (ii) a pericyclic cyclization leading to a direct C–C bond formation between carbene and arene.

4.4.1 C–H Activation through Agostic Interactions

The reaction initiates with the activation of a C–H bond in the phenyl substituent on the nitrogen leading to the formation of agostic complex. Since two phenyl rings are present on NHC ligand, the C–H bond of any of the phenyl ring can be activated first and the proposed mechanism considers the C–H bond of the phenyl ring (blue) which is near to the benzylidene ligand to undergo initial oxidative addition to form a ruthenium hydride complex **2a**. But the activation of a C–H bond in the phenyl ring (blue) which is near to the benzylidene ligand results the formation of an agostic complex **2c** (Figure 4.3) rather than the ruthenium hydride complex **2a** (Figure 4.2). In fact, this path is not energetically favorable since the energy difference between **2** and **2c** is ~42kcal/mol which implies the existence of a high activation barrier for this conversion (Figure 4.3).

Figure 4.3 Energy profile for the conversion of **2** to **2c** (All bond lengths are in Å and the relative energy values are in kcal/mol. All non participating hydrogen atoms are omitted for clarity)

The C–H bond of the phenyl ring which is in the opposite side of the benzylidene ligand (red) get activated more easily and subsequently force the flexible phenyl ring to rotate in **TS-2-5** and lead to further reaction (Figure 4.4). The interaction of the C–H bond with ruthenium forces the C–H bond to come close to an empty d orbital of ruthenium, leading to the formation of the agostic complex **5** where a bonding interaction exists between ruthenium and C–H σ bond. The C–H, Ru–C, and Ru–H bond lengths in complex **5** are 1.11 Å, 1.86 Å, and 2.50 Å, respectively. Further, Ru–H–C bond angle in **5** is 101° and a decrease in the Cl–Ru–Cl angle from 151° in **2** to 91° in **5** takes place during this transformation. It may be noted that the *trans* to *cis* transformation of chloro ligands in **TS-2-5** makes available a coordination site on ruthenium which is not *trans* to the strongly *trans*-influencing benzylidene ligand. This facilitates the phenyl C–H bond to easily reacts with electron deficient metal centre and form the agostic complex **5** (Figure 4.4).

Figure 4.4 Energy profile for the conversion of **2** to **5** (All bond lengths are in Å and the relative energy values are in kcal/mol. All non participating hydrogen atoms are omitted for clarity)

In the next step, a σ-bond metathesis [Hoyt *et al.* 2004] of the agostic C–H bond takes place in such a way that the phenyl carbon undergoes bonding with ruthenium and simultaneously the agostically bonded H migrates to the α carbon of the benzylidene ligand, leading to the formation the complex **6** wherein ruthenium is in +4 oxidation state. The ruthenium hydride transition state **TS-5-6** is very similar to the intermediate **2a** in the proposed mechanism and the high energy associated with this transition state can be assigned to the high oxidation state of the ruthenium (Ru–H distance in **TS-5-6** is 1.65 Å). The benzyl C–H, Ru–H and Ru–C bond lengths of 1.11 Å, 2.23 Å and 2.07 Å, respectively in **6** suggests the stabilizing agostic C–H bond interaction (Figure 4.5).

Figure 4.5 Energy profile for the conversion of **5** to **6** (All bond lengths are in Å and the relative energy values are in kcal/mol. All non participating hydrogen atoms are omitted for clarity)

Unlike the benzylidene ligand, benzyl ligand in **6** is more flexible due to the Ru–C single bond connection which enables the rotation of the phenyl (pink) group through **TS-6-7** to from **7** wherein the phenyl carbon is partially coordinated to ruthenium to stabilize the complex similar to an agostic C–H bond (Figure 4.6). Subsequent rotation of the benzyl group through **TS-7-8** gives the complex **8**. These internal rearrangements within the complex leads to closer approach of the benzyl group (pink) towards the coordinated phenyl (red) ring. In fact, the C–C distance of 2.45 Å in **8** is indicative of a possible interaction between the benzyl carbon and the coordinated phenyl ring. In addition, this rearrangement makes the phenyl group (pink) to interact strongly with the central metal atom (Ru-C distance is 2.40 Å).
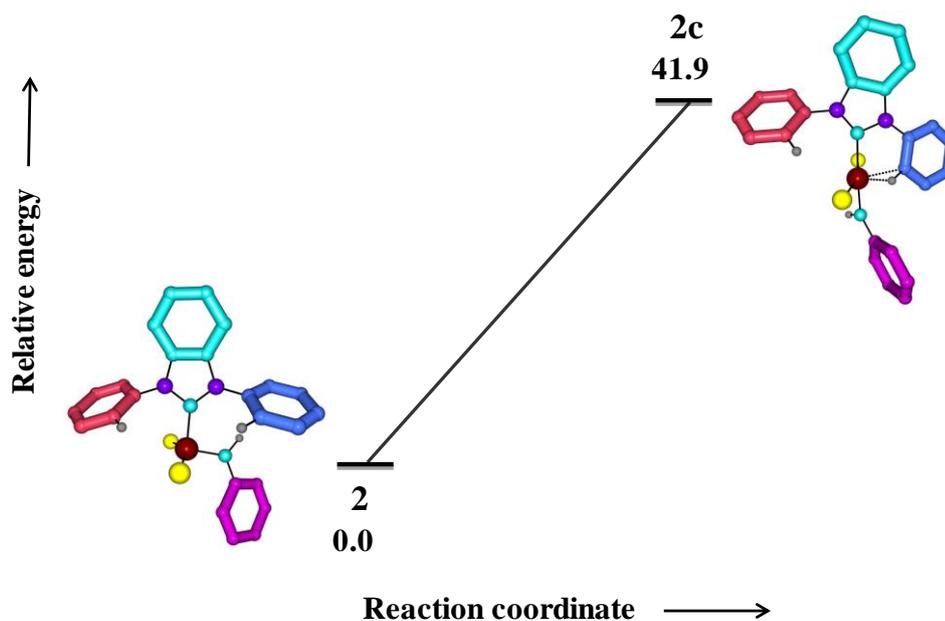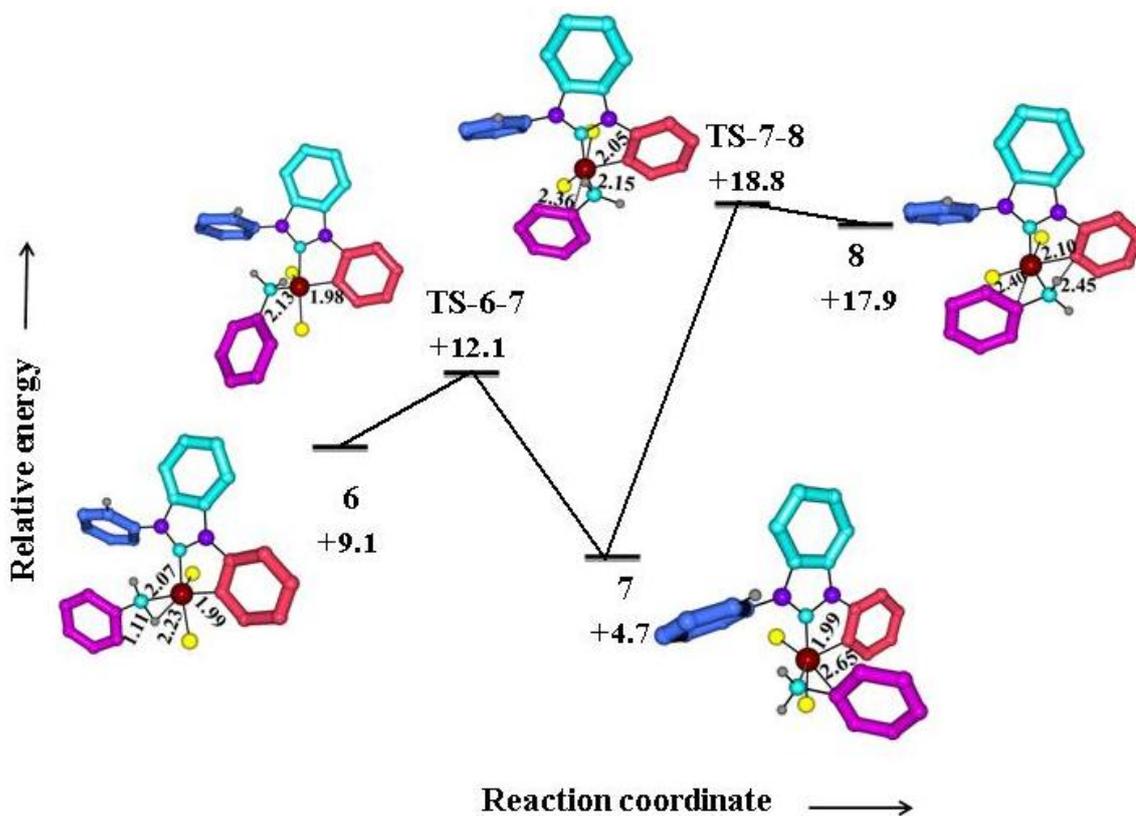
Figure 4.6 Energy profile for the conversion of **6** to **8** (All bond lengths are in Å and the relative energy values are in kcal/mol. All non participating hydrogen atoms are omitted for clarity).

A reductive elimination in **8** leads to subsequent C–C bond formation between benzyl group and the metallated phenyl carbon to form the first product **3** through a four centre transition state **TS-8-3** (Figure 4.7). In **3**, the phenyl ring (pink) on benzyl group is in η^6 coordination with ruthenium where the distance between ruthenium and the centre of the phenyl ring is 1.78 Å. This η^6 coordination makes the complex **3** stable and its relative energy value is -2.3 kcal/mol compared to **2** (Figure 4.7).
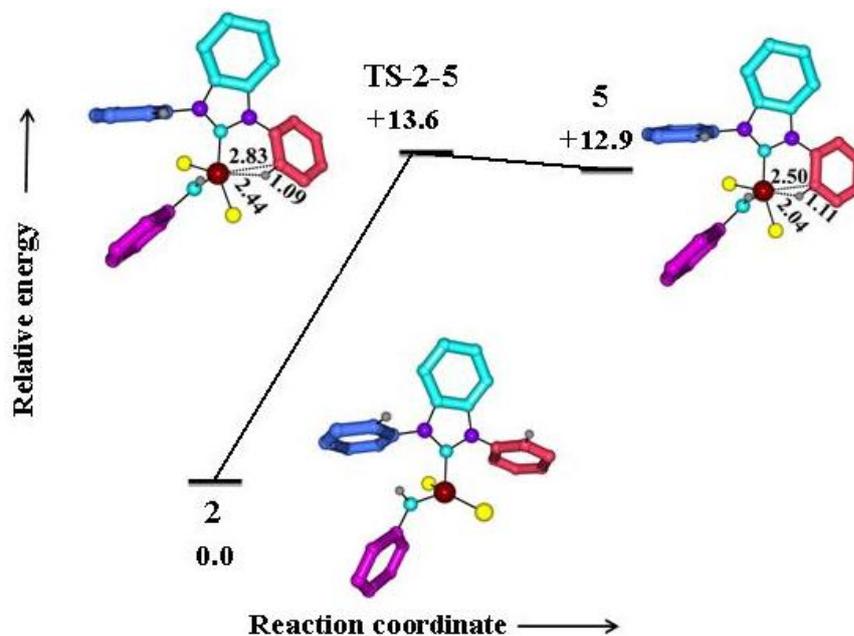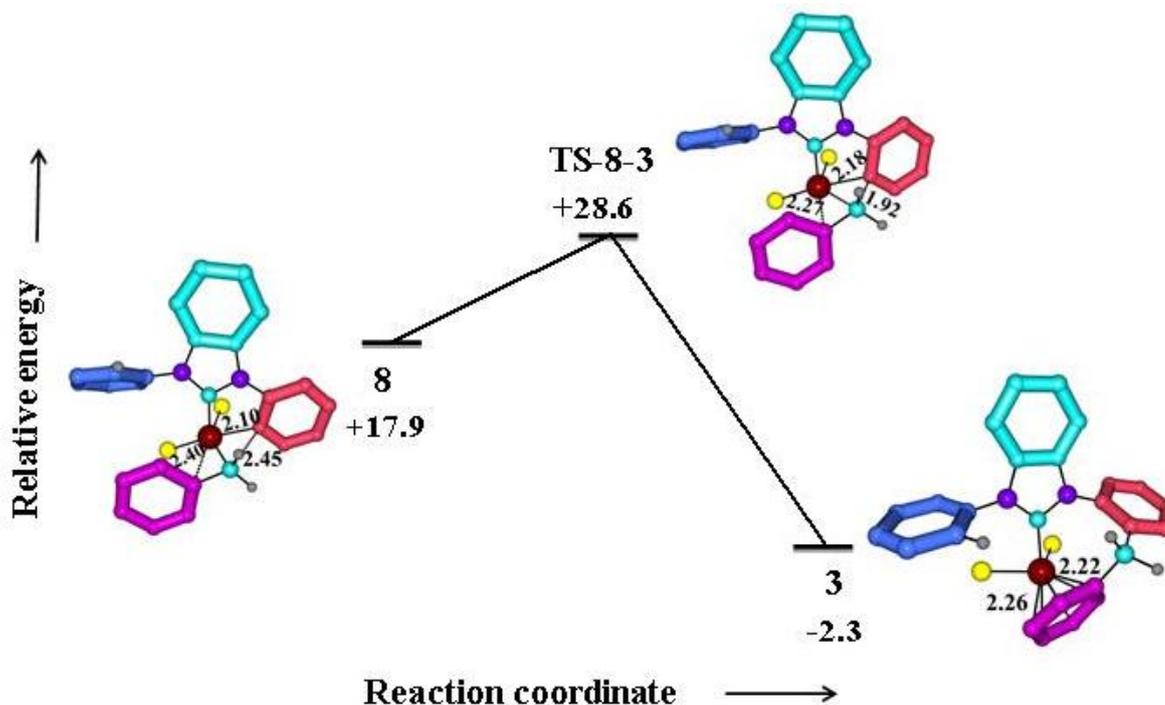
Figure 4.7 Energy profile for the conversion of **8** to **3** (All bond lengths are in Å and the relative energy values are in kcal/mol. All non participating hydrogen atoms are omitted for clarity).

The complex **3** acts as a precursor in the formation of the second product **4**. The η^6 coordinated phenyl ring changes to the η^2 state in **9** and this transformation may release some ring strain associated with methylene bridged region (CH_2 between the red and pink phenyl rings) and also opens up another coordination site on the metal centre. This enhances the activation of the C–H bond on the second phenyl ring (blue) and compels it to undergo rotation along the N–C σ-bond to form a new agostic complex **10** with C–H, Ru–H and C–H bond lengths of 1.16 Å, 1.75 Å and 2.20 Å, respectively through the transition state **TS-9-10**. The agostic bonding observed in the complex **10** is strong as the Ru–H–C bond angle is 95.5° and the C–H bond length is 1.16 Å (Figure 4. 8).
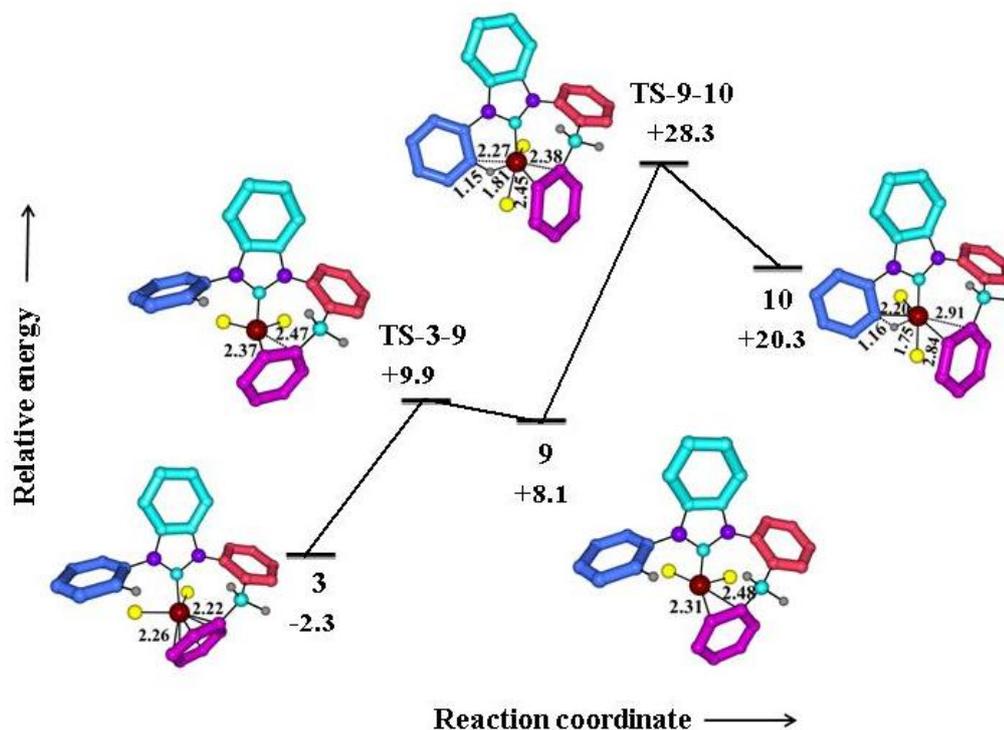
Figure 4.8 Energy profile for the conversion of **3** to **10** (All bond lengths are in Å and the relative energy values are in kcal/mol. All non participating hydrogen atoms are omitted for clarity).

The agostic bonding in **10** could increase the effective oxidation state of ruthenium from +2. The high energy associated with the less strained complex **10** can be attributed to the higher effective oxidation state of the metal centre. Similar agostic interactions were reported by Matsubara et al in ruthenium complexes [Matsubara *et al.* 1998; Matsubara *et al.* 2000]. Further, activation of the agostic C–H bond to the ruthenium produce another ruthenium hydride transition state **TS-10-4** wherein Ru has +4 oxidation state and this in turn leads to the reductive elimination of HCl to form the product **4** (Figure 4.9).
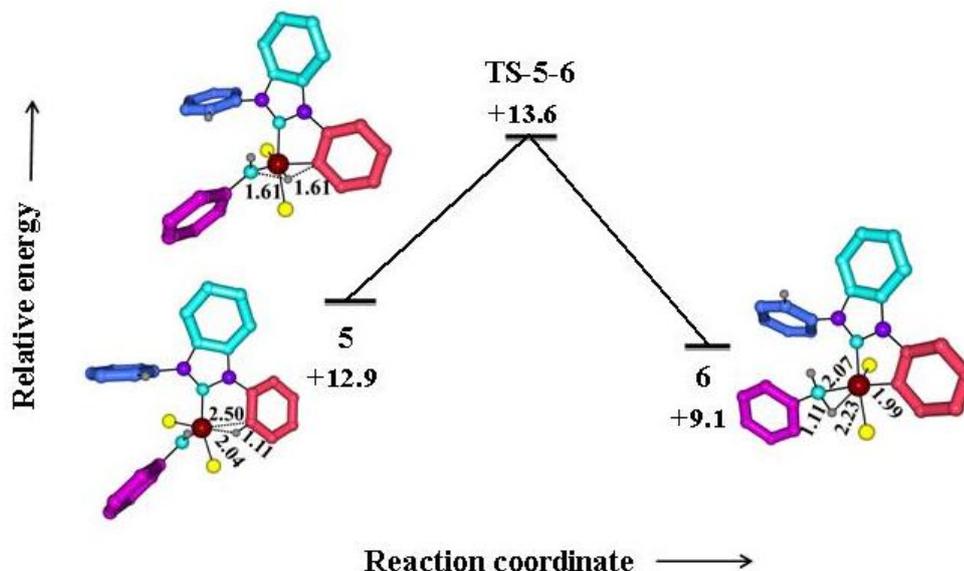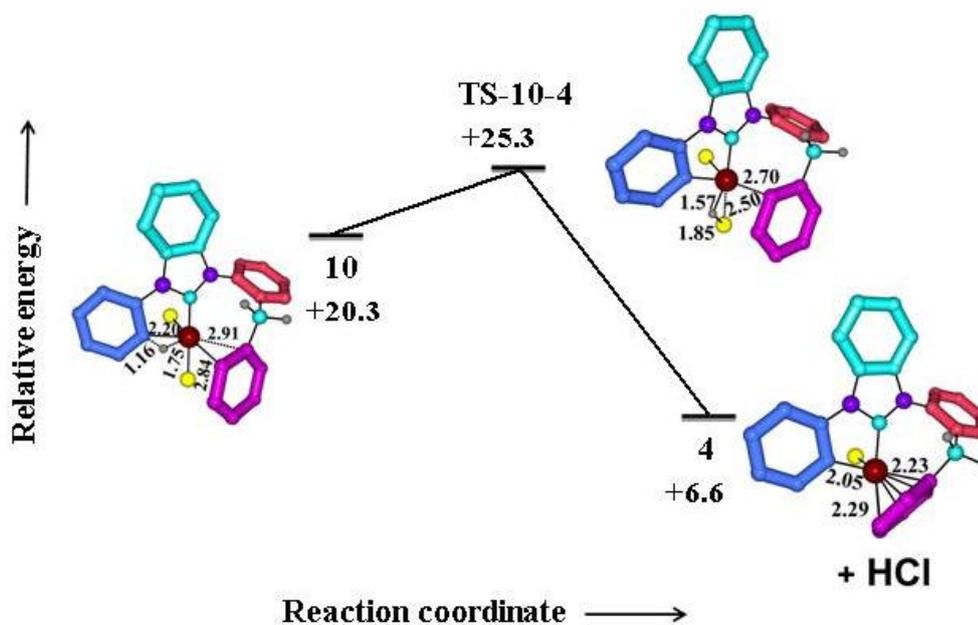
Figure 4.9 Energy profile for the conversion of **10** to **4** (All bond lengths are in Å and the relative energy values are in kcal/mol. All non participating hydrogen atoms are omitted for clarity).

Though the deactivation of the active complex **2** appears to be simple in the proposed mechanism, the theoretical results suggests the other way as it passes through five transition states to form the first product **3** and subsequently, **3** undergoes further reaction and forms the second product **4** by a three step mechanism. Figure 4.10 depicts all the intermediates and the transition states involved in the decomposition reaction via the C-H activation.
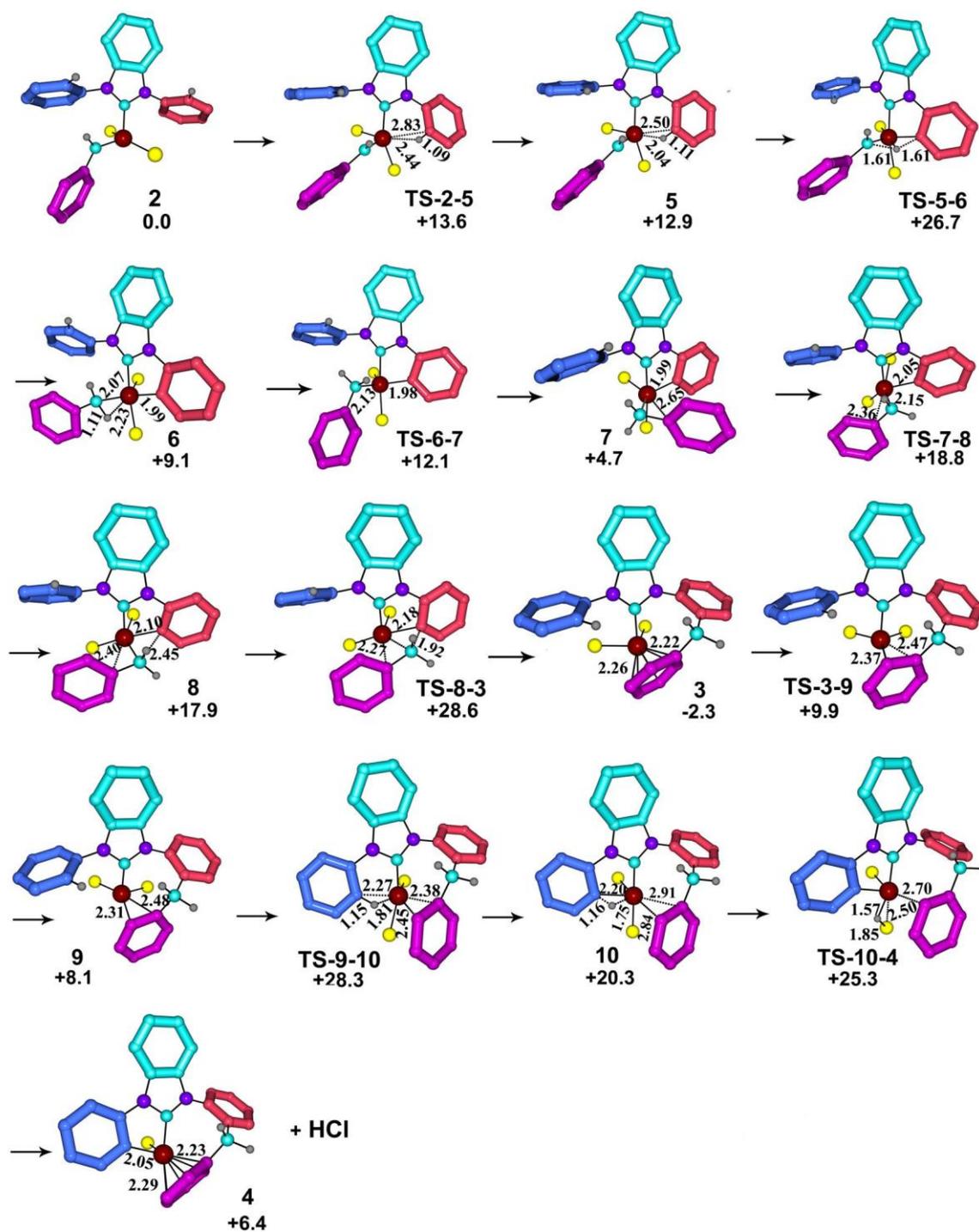
Figure 4.10 Intermediates and transition states involved in the reaction. (The relative energy values are in kcal/mol and bond length in Å. All non participating hydrogen atoms are omitted for clarity).

The major transformations involved in the entire reaction can be summarized as 1) the formation of C–H agostic complex with NHC-phenyl ring, 2) C–H σ-bond metathesis, 3) two step rotational transformations of benzyl ring, 4) carbene-arene bond formation, 5) transformation of arene coordination from η^6 to η^2, 6) formation of C–H agostic complex with second NHC-phenyl ring, 7) Ru–C bond formation, and 8) reductive elimination of HCl. In Figure 4.11, the energetics of the complete reaction is plotted. The rate determining step for the formation of **3** is **TS-8-3** (activation barier = 28.6 kcal/mol) while the that for the formation of product **4** is **TS-9-10** (activation barier = 28.3 kcal/mol).
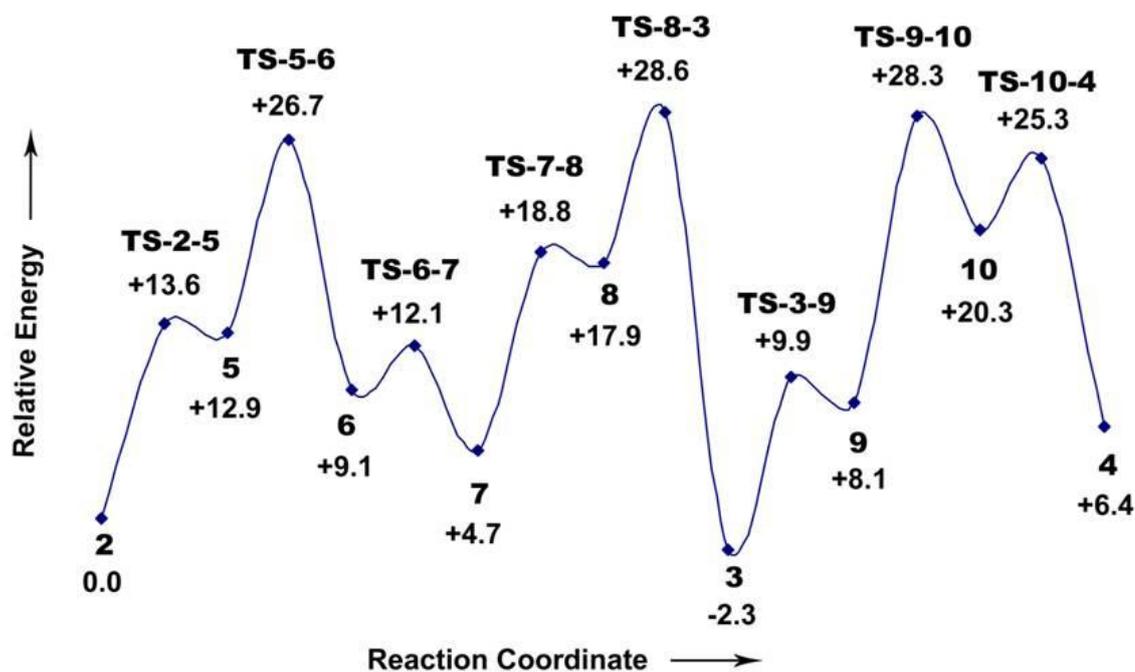
Figure 4.11 Energy profile diagram for the reaction. (The relative energy values are in kcal/mol.).

4.4.2 Pericyclic Cyclization Leading to Direct C–C Bond Formation

The second probable pathway for the deactivation of **2** is the pericyclic cyclization which is a direct carbene-arene bond formation reaction at the initial stage itself. Such a mechanism was proposed for the deactivation observed in a Grubbs-Hoveyda catalyst system by Blechert *et al.* [Vehlow *et al.* 2007]. The possibility of the cyclization reaction as the initial step is tested for the present case and the relative energy values of the transition state **TS-2-2d** and the cyclic product **2d** with respect to **2** along with their structural parameters are depicted in Figure 4.12.
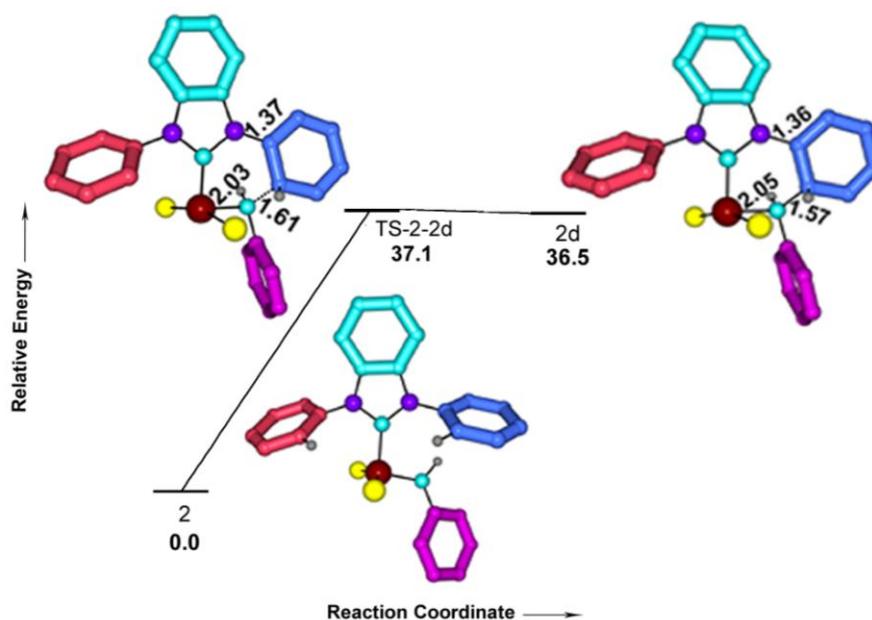
Figure 4.12 Energy profile diagram for the initial step of the pericyclic cyclization. (All bond lengths are in Å and the relative energy values are in kcal/mol. All non participating hydrogen atoms are omitted for clarity).

The activation barrier of 37.1 kcal/mol calculated for this transformation does not support the pericyclic cyclization as the initiation step for the deactivation of **2**. Further, the cyclic product **2d** is found to be stabilized only by 0.5 kcal/mol than the transition state **TS-2-2d** . These results also confirm that the C–H activation and subsequent

reactions (Figure 4.10) are responsible for the deactivation of **2.** In order to compare the second pathway (pericyclic cyclization) with the deactivation reaction in Grubbs-Hoveyda type catalyst, [Vehlow *et al.* 2007] we have also modeled the latter at the B3LYP/GenI level. The calculated mechanism for the Grubbs-Hoveyda system is given in Figure 4.13.
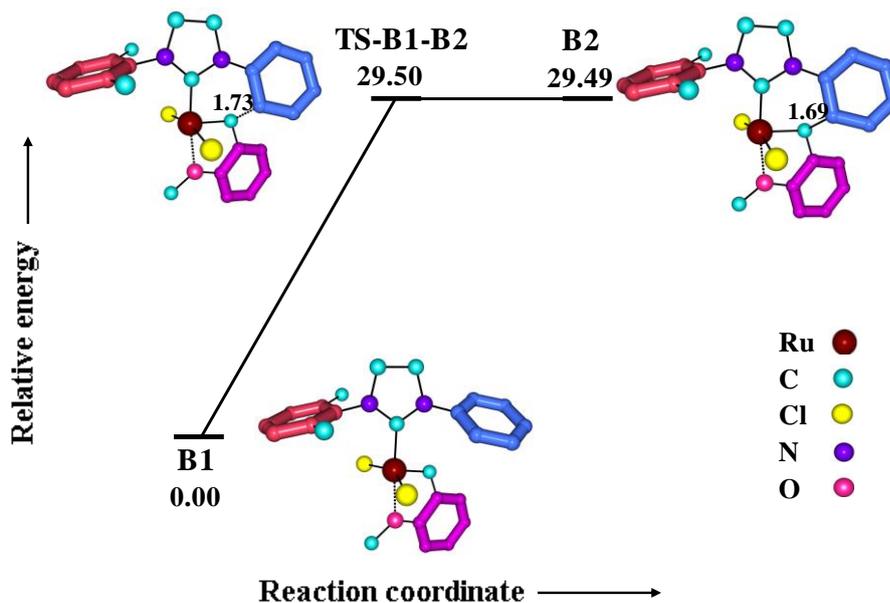
Figure 4.13 Energy profile diagram for the pericyclic cyclization in Grubbs-Hoveyda system. (All bond lengths are in Å and the relative energy values are in kcal/mol. All non participating hydrogen atoms are omitted for clarity).

The Grubbs-Hoveyda system showed low activation energy of 29.50 kcal/mol which is 7.50 kcal/mol smaller than the corresponding value observed in Grubbs system. This decrease in the activation energy may be attributed to the chelating oxygen in the system as it could keep the complex rigid and stable. However, the energy difference between the cyclic product and transition state is only 0.01 kcal/mol suggest that the formation of the product is not feasible as it will revert back to the original condition. In Blechert's reaction, [Vehlow *et al.* 2007] the prevention of the reversibility of the reaction is claimed on the basis of subsequent oxidation in the presence of formic acid.

In this reaction also the C–H bond activation pathway may be considered as another viable pathway than the initial C–C bond formation.

4. 5 Conclusions

The mechanistic study presented here proves that the deactivation of the Grubbs catalyst takes place through the C–H activation followed by C–H agostic interactions and σ-bond metathesis and the flexibility of the phenyl groups on the N-heterocyclic carbene plays the most important role in the initiation as well as the propagation of the reaction. The C–H bonds of the flexible phenyl substituents are vulnerable for agostic bonding with the highly electron deficient metal centre and this in turn will open up decomposition pathways of the active form of the catalyst. Further, the conversion of benzylidene to benzyl form is also vital since this provides flexibility to the third phenyl group (pink) which otherwise would have not interacted with the metal centre. Thus the results presented in this study suggest that the decomposition of the catalyst can be controlled by modifying the N-heterocyclic carbene ligand in such a way that the substituents on nitrogen atoms have limited flexibility.

List of publications

A) Articles in Journals

1. Quantitative Assessment of the Stereoelectronic Profile of Phosphine Ligands: **Jomon Mathew**, Tinto Thomas, and Cherumuttathu H. Suresh, *Inorg. Chem*., **2007**, *46*, 10800.

2. C-H Bond Activation through σ-Bond Metathesis and Agostic Interactions: Deactivation Pathway of a Grubbs Second-Generation Catalyst: **Jomon Mathew**, Nobuaki Koga and Cherumuttathu H. Suresh, *Organometallics*, **2008**, 27, 4666.

3. Use of Molecular Electrostatic Potential at the Carbene Carbon as a Simple and Efficient Electronic Parameter of N-heterocyclic Carbenes: **Jomon Mathew** and Cherumuttathu H. Suresh, *Inorg. Chem*., **2010**, 49, 4665.

4. Assessment of Stereoelectronic Effects in Grubbs First Generation Olefin Metathesis Catalysis Using Molecular Electrostatic Potential: **Jomon Mathew** and Cherumuttathu H. Suresh, *Organometallics* **2011**, 30, 1438.

5. Assessment of Stereoelectronic Effects in Grubbs Second Generation Olefin Metathesis Catalysis Using Molecular Electrostatic Potential: **Jomon Mathew** and Cherumuttathu H. Suresh, *Organometallics* **2011**, submitted.

B) Published contributions to academic conferences

6. Presented a poster entitled "Quantitative Assessment of the Stereoelectronic Profile of Phosphine Ligands" in the Indo-German Conference on "Modeling Chemical and Biological (Re)activity (MCBR)" held at IICT, Hyderabad during 26 – 29 September 2007.

7. Presented a poster entitled "Role of Steric effect on the Activity of Grubbs' First and Second Generation Olefin Metathesis Catalysts" in the National Conference on "Changing Paradigms in Theoretical and Computational Chemistry: From Atoms to Molecular Clusters" held at University of Pune, during 18-20 December 2009.

References

Aagaard, O. M.; Meier, R. J.; Buda, F. "Ruthenium-Catalyzed Olefin Metathesis: A Quantum Molecular Dynamics Study" *J. Am. Chem. Soc.* 120, **1998**, 7174.

Abel, E. W.; Bennett, M. A.; Wilkinson, G. "Substituted Carbonyl Compounds of Chromium, Molybdenum, Tungsten, and Manganese" *J. Chem. Soc.* **1959**, 2323.

Ackermann, L.; Furstner, A.; Weskamp, T.; Kohl, F. J.; Herrmann, W. A. "Ruthenium Carbene Complexes with Imidazolin-2-ylidene Ligands Allow the Formation of Tetrasubstituted Cycloalkenes by RCM" *Tetrahedron Lett.* 40, **1999**, 4787.

Adlhart, C.; Chen, P. "Mechanism and Activity of Ruthenium Olefin Metathesis Catalysts: The Role of Ligands and Substrates from a Theoretical Perspective" *J. Am. Chem. Soc.* 126, **2004**, 3496.

Allen, D.W.; Taylor, B.F. "The Chemistry of Heteroarylphosphorus Compounds. Part 15. Phosphorus-31 Nuclear Magnetic Resonance Studies of the Donor Properties of Heteroarylphosphines Towards Selenium and Platinum(II)" *J. Chem. Soc., Dalton Trans.* **1982**, 51.

Allen, F. H. "The Cambridge Structural Database: A Quarter of a Million Crystal Structures and Rising" *Acta Crystallogr.* B58, **2002**, 380.

Allen, L. C.; Karo, A. M. "Basis Functions for Ab Initio Calculations" *Rev. Modern Phys.* 32, **1960**, 275.

Allman, T.; Goel, R.G. "The Basicity of Phosphines" *Can. J. Chem.* 60, **1982**, 716.

Ananikov, V. P.; Szilagyi, R.; Morokuma, K.; Musaev, D. G. "Can Steric Effects Induce the Mechanism Switch in the Rhodium-Catalyzed Imine Boration Reaction? A Density Functional and ONIOM Study" *Organometallics* 24, **2005**, 1938.

Angelici, R.J. "Basicities of Transition Metal Complexes from Studies of Their Heats of Protonation: A Guide to Complex Reactivity" *Acc. Chem. Res*. 28, **1995**, 51.

Anton, D.R.; Crabtree, R.H. "Metalation-Resistant Ligands: Some Properties of Dibenzocyclooctatetraene Complexes of Molybdenum, Rhodium and Iridium" *Organometallics* 2, **1983**, 621.

Antonova, N. S.; Carb, J. J.; Poblet, J. M. "Quantifying the Donor-Acceptor Properties of Phosphine and N-Heterocyclic Carbene Ligands in Grubbs' Catalysts Using a Modified EDA Procedure Based on Orbital Deletion" *Organometallics* 28, **2009**, 4283.

[a]Arduengo, A. J., III; Harlow, R. J.; Kline, M. "A Stable Crystalline Carbene" *J. Am. Chem. Soc.* 113, **1991**, 361.

[b]Arduengo, A. J., III; Kline, M.; Calabrese, J. C.; Davidson, F. "Synthesis of a Reverse Ylide from a Nucleophilic Carbene" *J. Am. Chem. Soc.* 113, **1991**, 9704.

Baber, R. A.; Haddow, M. F.; Middleton, A. J.; Orpen, A. G.; Pringle, P. G."Ligand Stereoelectronic Effects in Complexes of Phospholanes, Phosphinanes, and Phosphepanes and Their Implications for Hydroformylation Catalysis" *Organometallics* 26, **2007**, 713.

Bader, R. F. W. *Atoms in Molecules: A Quantum Theory*. Clarendon Press: Oxford, U.K, **1990**.

Banks, R. L.; Bailey, G. C. "Olefin Disproportionation. A New Catalytic Process" *Ind. Eng. Chem. Prod. Res. Dev*. 3, **1964**, 170.

Bartholomew, J.; Fernandez, A.L.; Lorsbach, B.A.; Wilson, M.R.; Prock, A.; Giering, W.P. "Comments on Coupling Graphical and Regression Analyses of Ligand Effect Data" *Organometallics* 15, **1996**, 295.

Bartlett, R. J.; Silver, D. M. "Many-body Perturbation Theory Applied to Electron Pair Correlation Energies. I. Closed-Shell First-Row Diatomic Hydrides" *J. Chem. Phys*. 62, **1975**, 3258.

Becke, A. D. "Density-Functional Exchange-Energy Approximation with Correct Asymptotic Behavior" *Phys. Rev. A* 38, **1988**, 3098.

Becke, A. D. "Density-Functional Thermochemistry. III. The Role of Exact Exchange" *J. Chem. Phys*. 98, **1993**, 5648.

Bell, A.; Clegg, W.; Dyer, P. W.; Elsegood, M. R. J.; Gibson, V. C.; Marshall, E. L. J. "A Versatile Route to Well-Defined Molybdenum Metathesis Catalysts via Mixed Imido Precursors: The Molecular Structure of [Mo(N-2,6-$Pr^i_2C_6H_3$)(N-Bu^t)(CH_2CMe_3)$_2$]" *Chem. Soc., Chem. Commun.* **1994**, 2547.

Bellon, L.; Taft, R. W.; Abboud, J.- L. M. "Structural Effects on the Reactivity of Ethers in Donor-Acceptor Reactions" *J. Org. Chem*. 45, **1980**, 1166.

Berlin, J. M.; Goldberg, S. D.; Grubbs, R. H. "Highly Active Chiral Ruthenium Catalysts for Asymmetric Cross- and Ring-Opening Cross-Metathesis" *Angew. Chem., Int. Ed.* 45, **2006**, 7591.

Bernardi, F.; Bottoni, A.; Miscione, G. P. "DFT Sstudy of the Olefin Metathesis Catalyzed by Ruthenium Complexes" *Organometallics* 22, **2003,** 940.

Biefeld, C. G.; Eick, H. A.; Grubbs, R. H. "Crystal Structure of Bis(triphenylphosphine)tetramethyleneplatinum(II)" *Inorg. Chem.* 12, **1973**, 2166.

Bielawski, C. W.; Grubbs, R. H. "Highly Efficient Ring-Opening Metathesis Polymerization (ROMP) Using New Ruthenium Catalysts Containing N-Heterocyclic Carbene Ligands" *Angew. Chem., Int. Ed*. 39, **2000**, 2903.

Bigorgne, M. "Ĕtude de Spectre de Vibration de la Molécule de Nickel-carbonyle. Force et Nature des Liaisons" *J. Inorg. Nucl. Chem* 8**, 1958,** 113.

Bigorgne, M. "Sur Les Liaisons de Coordination Metal-Carbone des Derives des Metaux Carbonyle" *J. Organomet. Chem.* 1, **1963**, 101.

Binkley, J. S.; Pople, J.; Hehre, W. J. "Self-Consistent Molecular Orbital Methods. 21. Small Split-Valence Basis Sets for First-Row Elements" *J. Am. Chem. Soc.* 102, **1980**, 939.

Blosch, L. L.; Abboud, K.; Boncella, J. M. "Synthesis of an Air-Stable, Moisture-Stable, and Thermally Stable Tungsten(VI) Oxo Alkylidene Complex. Precursor to an Air- and Moisture-Stable ROMP Catalyst" *J. Am. Chem. Soc.* 113, **1991**, 7066.

[a]Bodner, G.M. "Fourier Transform Carbon-13 Nuclear Magnetic Resonance Study of Group VIB Transition Metal Carbonyl Complexes" *Inorg. Chem.* 14, **1975**, 2694.

[b]Bodner, G.M. "Fourier Transform Carbon-13 Nuclear Magnetic Resonance Sstudy of LnNi(CO)$_4$-n Derivatives" *Inorg. Chem.* 14, **1975**, 1932.

[c]Bodner, G.M.; Gaul, M. "A carbon-13 NMR Study of Phosphine, Phosphite, Arsine and Stibine Ligands and Their LNi(CO)$_3$, LCr(CO)$_5$ and η-(C$_5$H$_5$)Mn-(CO)$_2$L complexes" *J. Organomet. Chem.* 101, **1975**, 63.

Bodner, G.M.; May, M.P.; McKinney, L.E. "A Fourier Transform Carbon-13 NMR Study of the Electronic Effects of Phosphorus, Arsenic, and Antimony

Ligands in Transition-Metal Carbonyl Complexes" *Inorg. Chem.* 19, **1980**, 1951.

Bodner, G.M.; Todd, L.J. "Fourier-Transform Carbon-13 Nuclear Nagnetic Resonance Study of (Arene)tricarbonylchromium Complexes" *Inorg. Chem.* 13, **1974**, 360.

Bonaccorsi, R.; Pullman, A.; Scrocco, E.; Tomasi, J. "The Molecular Electrostatic Potentials for the Nucleic Acid Bases: Adenine, Thymine, and Cytosine" *Theor. Chim. Acta* 24, **1972**, 51.

Bonaccorsi, R.; Scrocco, E.; Tomasi, J. "Molecular SCF Calculations for the Ground State of Some Three-Membered Ring Molecules: $(CH_2)_3$, $(CH_2)_2NH$, $(CH_2)_2NH_2^+$, $(CH_2)_2O$, $(CH_2)_2S$, $(CH)_2CH_2$, and N_2CH_2" *J. Chem. Phys.* 52, **1970**, 5270.

Born, M.; Oppenheimer, J. R. "Zur Quantentheorie der Molekeln" *Ann. Phys*. 84, **1927**, 457.

Bourissou, D.; Guerret, O.; Gabbai, F. P.; Bertrand, G. "Stable Carbenes" *Chem. Rev.* 100, **2000,** 39.

Bowen, J. P.; Allinger, N. L. "Molecular Mechanics: The Art and Science of Parameterization" *Rev. Comp. Chem.* 2, **1991,** 81.

Boyd D. B.; Lipkowitz, K. B. "Molecular Mechanics: The Method and Its Underlying Philosophy" *J. Chem. Educ*. 59, **1982**, 269.

[a]Boys, S. F. "Electronic Wave Functions. I. A General Method of Calculation for the Stationary States of Any Molecular System" *Proc. Roy. Soc*. 200, **1950**, 542.

[b]Boys, S. F. "Electronic Wave Functions. II. A Calculation for the Ground State of the

Beryllium Atom" *Proc. Roy. Soc. (London)* 201, 1**950**, 125.

Brillouin, L. "Les Champs Self-Consistents de Hartrée et de Fock" *Actualities Sci. Ind.* 159, **1934**, 37.

Brown, T. L. "A Molecular Mechanics Model of Ligand Effects. 3. A New Measure of Ligand Steric Effects" *Inorg. Chem.* 31, **1992**, 1286.

Brown, T. L.; Lee, K. J. "Ligand Steric Properties" *Coord. Chem. Rev.* 128, **1993,** 89.

Bunten, K. A.; Chen, L. Z.; Fernandez, A. L.; Poë A. J. "Cone Angles: Tolman's and Plato's" *Coord. Chem. Rev.* 233, **2002**, 41.

Burling, S.; Mahon, M. F.; Paine, B. M.; Whittlesey, M. K.; Williams, J. M. J. "Reversible Intramolecular Alkyl C-H Bond Activation, Alcohol Dehydrogenation, and *trans-cis* Dihydride Isomerization in Ruthenium N-Heterocyclic Carbene Complexes" *Organometallics,* 23, **2004,** 4537.

Caffery, M. L.; Brown, T. L. "A Molecular Mechanics Model of Ligand Effects. 1. Binding of Phosphites to Pentacarbonylchromium" *Inorg. Chem.* 30, **1991**, 3907.

Cai, S.; Hoffman, D. M.; Wierda, D. A. "Rhenium(VII) Oxo-Alkyl Complexes: Reductive and α-Elimination Reactions" *Organometallics* 15, **1996**, 1023.

Calderon, N.; Chen, H. Y.; Scott, K. W. "Olefin metathesis - A Novel Reaction for Skeletal Transformations of Unsaturated Hydrocarbons" *Tetrahedron Lett.* 8, **1967**, 3327.

Calderon, N.; Ofstead, E. A.; Ward, J. P.; Judy, W. A.; Scott, K. W. "Olefin Metathesis. I. Acyclic Vinylenic Hydrocarbons" *J. Am. Chem. Soc.* 90, **1968**, 4133.

Carbo, J. J.; Maseras, F.; Bo, C.; van Leeuwen, P.W.N.M. "Unraveling the Origin of Regioselectivity in Rhodium Diphosphine Catalyzed Hydroformylation. A DFT QM/MM Study" *J. Am. Chem. Soc.* 123, **2001**, 7630.

Casey, C. P.; Burkhardt, T. J. "Reactions of (diphenylcarbene)pentacarbonyltungsten(0) with Alkenes. Role of Metal-Carbene Complexes in Cyclopropanation and Olefin Metathesis Reactions" *J. Am. Chem. Soc.* 96, **1974**, 7808.

Cavallo, L. "Mechanism of Ruthenium-Catalyzed Olefin Metathesis Reactions from a Theoretical Perspective" *J. Am. Chem. Soc.* 124, **2002**, 8965.

Cavallo, L.; Correa, A.; Costabile, C.; Jacobsen, H. "Steric and Electronic Effects in the Bonding of N-Heterocyclic Ligands to Transition Metals" *J. Organomet. Chem.* 690, **2005**, 5407.

Cavallo, L.; Sola, M. "A Theoretical Study of Steric and Electronic Effects in the Rhodium-Catalyzed Carbonylation Reactions" *J. Am. Chem. Soc.* 123, **2001**, 12294.

Chatt, J.; Hart, F. A. "Reactions of Tertiary Diphosphines with Nickel and Nickel Carbonyl" *J. Chem. Soc.* **1960**, 1378.

Chatterjee, A. K.; Grubbs, R. H. "Synthesis of Trisubstituted Alkenes via Olefin Cross-Metathesis" *Org. Lett.* 1, **1999,** 1751.

Chatterjee, A. K.; Morgan, J. P.; Scholl, M.; Grubbs, R. H. "Synthesis of Functionalized Olefins by Cross and Ring-Closing Metathesis" *J. Am. Chem. Soc.* 122, **2000,** 3783.

Chianese, A. R.; Li, X.; Janzen, M. C.; Faller, J. W.; Crabtree, R. H. "Rhodium and Iridium Complexes of N-Heterocyclic Carbenes via Transmetalation: Structure and Dynamics" *Organometallics* 22, **2003**, 1663.

Choi, C. H.; Gordon, M. S. "Cycloaddition Reactions of 1,3-Cyclohexadiene on the Silicon(001) Surface" *J. Am. Chem. Soc.* 121, **1999**, 11311.

Čizek, J. "On the Correlation Problem in Atomic and Molecular Systems. Calculation of

Wavefunction Components in Ursell-Type Expansion Using Quantum-Field Theoretical Methods" *J. Chem. Phys*. 45, **1966**, 4256.

[a]Clavier, H.; Correa, A.; Escudero-Adan, E. C.; Benet- Buchholz, J.; Cavallo, L.; Nolan, S. P. "Chemodivergent Metathesis of Dienynes Catalyzed by Ruthenium–Indenylidene Complexes: An Experimental and Computational Study" *Chem. Eur. J.* 15, **2009**, 10244.

[b]Clavier, H.; Urbina-Blanco, C. A.; Nolan, S. P. "Indenylidene Ruthenium Complex Bearing a Sterically Demanding NHC Ligand: An Efficient Catalyst for Olefin Metathesis at Room Temperature" *Organometallics* 28, **2009**, 2848.

Clementi, E. "Simple Basis Set for Molecular Wavefunctions Containing First- and Second-Row Atoms" *J. Chem.Phys*. 40, **1964**, 1944.

Collman, J. P.; Hegedus, L. S.; Norton, J. R.; Kinke, R. G. *Principles and Applications of Organotransition Metal Chemistry*. Mill Valey, CA, **1987**.

Conrad, J. C.; Amoroso, D.; Czechura, P.; Yap, G. P. A.; Fogg, D. E. "The First Highly Active, Halide-Free Ruthenium Catalyst for Olefin Metathesis" *Organometallics* 22, **2003**, 3634.

Cooney, K. D.; Cundari, T. R.; Hoffman, N. W.; Pittard, K. A.; Temple, M. D.; Zhao, Y. "A Priori Assessment of the Stereoelectronic Profile of Phosphines and Phosphites" *J. Am. Chem. Soc.* 125, **2003**, 4318.

Corberán, R.; Sanaú, M.; Peris, E. "Aliphatic and Aromatic Intramolecular C-H Activation on Cp*Ir(NHC) Complexes" *Organometallics* 25, **2006,** 4002.

Correa A.; Cavallo, L. "The Elusive Mechanism of Olefin Metathesis Promoted by (NHC)Ru-Based Catalysts: A Trade between Steric, Electronic, and Solvent Effects" *J. Am. Chem. Soc.* 128, **2006**, 13352.

Cramer, C. J. *"Essentials of Computational Chemistry"*. John Wiley & Sons, Chichester, **2004**.

Crudden, C. M.; Allen, D. P. "Stability and Reactivity of N-Heterocyclic Carbene Complexes" *Coord. Chem. Rev.* 248, **2004**, 2247.

Cundari, T. R. *Computational Organometallic Chemistry*. Marcel Dekker, New York, **2001**.

Dapprich, S.; Komaromi, I.; Byun, K. S.; Morokuma, K.; Frisch, M. J. "A New ONIOM Implementation in Gaussian 98. Part I. The Calculation of Energies, Gradients, Vibrational Frequencies and Electric Field Derivatives" *J. Mol. Struct. (Theochem)* 462, **1999**, 1.

de la Mata, F. J.; Gómez, J.; Royo, P. "Synthesis and Reactivity of Cyclopentadienyl Chloro, Imido and Alkylidene Tungsten (VI) Complexes" *J. Organomet. Chem.* 564, **1998**, 277.

de la Mata, F. J.; Grubbs, R. H. "Synthesis and Reactions of Tungsten Oxo Vinylalkylidene Complexes: Reactions of $WCl_2(O)(PX_3)$ (X = OMe, R) Precursors with 3,3-Diphenylcyclopropene" *Organometallics* 15, **1996**, 577.

Deshmukh, M. M,; Gadre, S. R.; Tonner R.; Frenking G. "Molecular Electrostatic Potentials of Divalent Carbon(0) Compounds" *Phys. Chem. Chem. Phys*. 10, **2008**, 2298.

Dias, E. L.; Nguyen, S. T.; Grubbs, R. H. "Well-Defined Ruthenium Olefin Metathesis Catalysts: Mechanism and Activity" *J. Am. Chem. Soc.* 119, **1997**, 3887.

[a]Diggle, R. A.; Kennedy, A. A.; Macgregor, S. A.; Whittlesey, M. K. "Computational Studies of Intramolecular Carbon-Heteroatom Bond Activation of N-Aryl Heterocyclic Carbene Ligands" *Organometallics* 27, **2008**, 938.

[b]Diggle, R. A.; Macgregor, S. A.; Whittlesey, M. K. "Computational Study of C-C Activation of 1,3-Dimesitylimidazol-2-ylidene (IMes) at Ruthenium: The Role of Ligand Bulk in Accessing Reactive Intermediates" *Organometallics* 27, **2008**, 617

Dimitrova, M.; Galabov, B. "Predicting the Acidities of Substituted Phenols Using Electrostatic Potential at Nuclei" *Croat. Chem. Acta.* 82, **2009**, 21.

Dinur, U.; Hagler, A.T. "New Approaches to Empirical Force Fields" *Rev. Comp. Chem.* 2, **1991**, 99.

Ditchfield, R.; Hehre, W. J.; Pople, J. "Self-Consistent Molecular-Orbital Methods. IX. An Extended Gaussian-Type Basis for Molecular-Orbital Studies of Organic Molecules" *J. Chem. Phys.* 54, **1971**, 724.

Diver, S. T.; Giessert, A. J "Enyne Metathesis (Enyne Bond Reorganization)" *Chem. Rev.* 104, **2004**, 1317.

Dölker, N.; Frenking, G. "Two Possible Reaction Pathways for the Formation of a Ruthenium Carbene Complex by Addition of Acetylene to $[RuH_2Cl_2(PH_3)_2]$: A Quantum Chemical Study" *J. Organomet. Chem.* 617-618, **2001**, 225.

Doll, J.; Freeman, D.L. "Monte Carlo Methods in Chemistry" *IEEE Comput. Sci. Eng.* 1, **1994**, 22.

Dorta, R.; Stevens, E. D.; Hoff, C. D.; Nolan, S. P. "Steric and Electronic Properties of N-Heterocyclic Carbenes (NHC): A Detailed Study on Their Interaction with $Ni(CO)_4$" *J. Am. Chem. Soc.* 125, **2003**, 10490.

Dorta, R.; Stevens, E. D.; Nolan, S. P. "Double C-H Activation in a Rh-NHC Complex Leading to the Isolation of a 14-Electron Rh(III) Complex" *J. Am. Chem. Soc.* 126, **2004,** 5054.

Dorta, R.; Stevens, E. D.; Scott, N. M.; Costabile, C.; Cavallo, L.; Hoff, C. D.; Nolan, S. P. "Steric and Electronic Properties of N-Heterocyclic Carbenes (NHC): A Detailed Study on Their Interaction with Ni(CO)$_4$" *J. Am. Chem. Soc.* 127, **2005**, 2485.

Dubois, J.-E.; Mouvier, G. "Essai de Correlation Reactivite-Structuren Relative aux Vitesses D'addition du Brome sur les Olefines Aliphatiques" *Tetrahedron Lett.* 4, **1963**, 1325.

Dunne, B. J.; Morris, R. B.; Orpen, A. G. "Structural Systematics. Part 3. Geometry Deformations in Triphenylphosphine Fragments: a Test of Bonding Theories in Phosphine Complexes" *J. Chem. Soc., Dalton Trans.* **1991**, 653.

Dunning Jr., T. H. "Gaussian Basis Functions for Use in Molecular Calculations. I. Contraction of (9s5p) Atomic Basis Sets for the First-Row Atoms" *J. Chem. Phys.* 53, **1970**, 2823.

Dunning Jr., T. H. "Gaussian Basis Sets for Use in Correlated Molecular Calculations. I. The atoms Boron through Neon and Hydrogen" *J. Chem. Phys.* 90, **1989**, 1007.

Dyker, C. A., Lavallo, V., Donnadieu, B. and Bertrand, G., "Synthesis of an Extremely Bent Acyclic Allene (A "Carbodicarbene"): A Strong Donor Ligand" *Angew. Chem., Int. Ed. Engl.* 47, **2008**, 3206.

Dykstra, C.E. *Ab Initio Calculation of the Structures and Properties of Molecules*, Elsevier, Amsterdam, **1988**.

Ehlers, A. W.; Bohme, M.; Dapprich, S.; Gobbi, A.; Hollwarth, A.; Jonas, V.; Kohler, K. F.; Stegmann, R.; Veldkamp, A.; Frenking, G. "A Set of f-Polarization Functions for Pseudo-Potential Basis Sets of the Transition Metals Sc…Cu, Y…Ag and La…Au" *Chem. Phys. Lett.* 208, **1993,** 111.

Eriks, K.; Giering, W.P.; Liu, H.-Y.; Prock, A. "Applications of the Quantitative Analysis of Ligand Effects (QALE). Steric Profiles for Reactions Involving "Spectator" Phosphorus(III) Ligands" *Inorg. Chem.* 28, **1989**, 1759.

Feller, D.; Davidson, E. R. "Basis Sets for Ab Initio Molecular Orbital Calculations and Intermolecular Interactions" *Rev. Comp. Chem1*, **1990**, 1.

Fermi, E. "Eine statistiche Methode zur Bestimmung einiger Eigenschaften des Atomes und ihre Anwendung auf die Theorie des periodischen Systems der Elemente" *Z. Phys*. 48, **1928**, 73.

Fermi, E. "Un Metodo Statistice per la Determinazione di Alcune Oroprieta Dell'atomo" *Rend. Acad. Lincei* 6, **1927**, 602.

Fernandez, A. L.; Lee, T. Y.; Reyes, C.; Prock, A.; Giering, W. P. "A Thermodynamically Based and Definitive Demonstration of the Inadequacy of the ECW Model for Phosphorus(III) Ligands" *Organometallics* 17, **1998**, 3169.

Fernandez, A.L.; Wilson, M.P.; Prock, A.; Giering, W.P. "Evaluation of the Stereoelectronic Parameters of Fluorinated Phosphorus(III) Ligands. The Quantitative Analysis of Ligand Effects (QALE)" *Organometallics* 20, **2001**, 3429.

Fey, N. "The Contribution of Computational Studies to Organometallic Catalysis: Descriptors, Mechanisms and Models" *Dalton Trans.* **2010**, 296.

Fey, N.; Haddow, M. F.; Harvey, J. N.; McMullin, C. L.; Orpen, A. G. "A Ligand Knowledge Base for Carbenes (LKB-C): Maps of Ligand Space" *Dalton Trans.* **2009**, 8183.

Fey, N.; Harvey, J. N.; Lloyd-Jones, G. C..; Murray, P.; Orpen, A. G.; Osborne. R.; Purdie, M. "Computational Descriptors for Chelating P,P- and P,N-Donor Ligands" *Organometallics* 27, **2008**, 1372.

Fey, N.; Howell, J. A. S.; Lovatt, J. D.; Yates, P. C.; Cunningham, D.; McArdle, P.; Gottlieb, H. E.; Coles, S. J. "A Molecular Mechanics Approach to Mapping the Conformational Space of Diaryl and Triarylphosphines" *Dalton Trans.* **2006**, 5464.

Fey, N.; Orpen, A. G.; Harvey, J. N. "Building Ligand Knowledge Bases for Organometallic Chemistry: Computational Description of Phosphorus(III)-Donor Ligands and the Metal–Phosphorus Bond" *Coord. Chem. Rev.* 253, **2009**, 704.

Fey, N.; Tsipis, A. C.; Harris, S. E.; Harvey, J. N.; Orpen, A. G.; Mansson, R. A. "Development of a Ligand Knowledge Base, Part 1: Computational Descriptors for Phosphorus Donor Ligands" *Chem. Eur. J.* 12, **2006**, 291.

Field, M. J.; Bash, P. A.; Karplus, M. "A Combined Quantum Mechanical and Molecular Mechanical Potential for Molecular Dynamics Simulations" *J. Comput. Chem.* 11, **1990**, 700.

Flükiger, P.; Lüthi, H. P.; Portmann, S.; Weber, J. MOLEKEL, 4.0; Swiss Center for Scientific Computing: Manno, Switzerland: **2000**.

Fock,V. "Näherungsmethode zur Lösung des Quantenmechanischen Mehrkörper Problems" *Z. Phys.* 61, **1930**, 126.

Fomine, S.; Vargas, S. M.; Tlenkopatchev, M. A. "Molecular Modeling of Ruthenium Alkylidene Mediated Olefin Metathesis Reactions. DFT Study of Reaction Pathways" *Organometallics* 22, **2003,** 93.

Foresman, J. B.; Head-Gordon, M.; Pople, J. A.; Frisch, M. J. "Toward a Systematic Molecular Orbital Theory for Excited States" *J. Phys. Chem.* 96, **1992**, 135.

Fournier, P.-A.; Collins, S. K. "A Highly Active Chiral Ruthenium-Based Catalyst for Enantioselective Olefin Metathesis" *Organometallics* 26, **2007**, 2945.

Fox, H. H.; Lee, J.-K.; Park, L. Y.; Schrock, R. R. "Synthesis of Five- and Six-Coordinate Alkylidene Complexes of the Type $Mo(CHR)(NAr)[OCMe(CF_3)_2]_2Sx$ and Their Use as Living ROMP Initiators or Wittig Reagents" *Organometallics* 12, **1993**, 759.

Frisch, M. J.; Trucks, G. W.; Schlegel, H. B.; Scuseria, G. E.; Robb, M. A.; Cheeseman, J. R.; Montgomery, J. A.; Vreven, T.; Kudin, K. N.; Burant, J. C.; Millam, J. M.; Yengar, S. S.; Tomasi, J.; Barone, V.; Mennucci, B.; Cossi, M.; Scalmani, G.; Rega, N.; Petersson, G. A.; Nakatsuji, H.; Hada, M.; Ehara, M.; Toyota, K.; Fukuda, R.; Hasegawa, J.; Ishida, M.; Nakajima, T.; Honda, Y.; Kitao, O.; Nakai, H.; Klene, M.; Li, X.; Knox, J. E.; Hratchian, H. P.; Cross, J. B.; Bakken, V.; Adamo, C.; Jaramillo, J.; Gomperts, R.; Stratmann, R. E.; Yazyev, O.; Austin, A. J.; Cammi, R.; Pomelli, C.; Ochterski, J. W.; Ayala, P. Y.; Morokuma, K.; Voth, G. A.; Salvador, P.; Dannenberg, J. J.; Zakrzewski, V. G.; Dapprich, S.; Daniels, A. D.; Strain, M. C.; Farkas, O.; Malick, D. K.; Rabuck, A. D.; Raghavachari, K.; Foresman, J. B.; Ortiz, J. V.; Cui, Q.; Baboul, A. G.; Clifford, S.; Cioslowski, J.; Stefanov, B. B.; Liu, G.; Liashenko, A.; Piskorz, P.; Komaromi, I.; Martin, R. L.; Fox, D. J.; Keith, T.; Al-Laham, M. A.; Peng,

C. Y.; Nanayakkara, A.; Challacombe, M.; Gill, P. M. W.; Johnson, B.; Chen, W.; Wong, M. W.; Gonzalez, C.; Pople, J. A. Gaussian 03, Revision E.01. Gaussian, Inc: Wallingford, CT, **2004**.

Froese, R. D. J.; Morokuma, K. "Accurate Calculations of Bond-Breaking Energies in C60 Using the Three-Layered ONIOM Method" *Chem. Phys. Lett.* 305, **1999**, 419

Fu, G. C.; Nguyen, S. T.; Grubbs, R. H. "Catalytic Ring-Closing Metathesis of Functionalized Dienes by a Ruthenium Carbene Complex" *J. Am. Chem. Soc.* 115, **1993**, 9856.

Fürstner, A., Alcarazo, M., Goddard, R., Lehmann, C.W. "Coordination Chemistry of ene-1,1-diamines and a Prototype "Carbodicarbene" *Angew. Chem., Int. Ed. Engl.* 47, **2008**, 3210.

Furstner, A.; Ackermann, L.; Gabor, B.; Goddard, R.; Lehmann, C. W.; Mynott, R.; Stelzer, F.; Thiel, O. R. "Comparative Investigation of Ruthenium-Based Metathesis Catalysts Bearing N-Heterocyclic Carbene (NHC) Ligands" *Chem. Eur. J.* 7, **2001**, 3236.

Gadre, S. R.; Bhadane, P. K.; Pundlik, S. S.; Pingale, S. S. in *Molecular Electrostatic Potential: Concepts and Applications*. Ed: J. S. Murray and K. D. Sen, Elsevier, Amsterdam, **1996**.

Gadre, S. R.; Kulkarni, S. A.; Shrivastava, I. H. "Molecular Electrostatic Potentials: A Topographical Study" *J. Chem. Phys*. 96, **1992**, 5253.

Gadre, S. R.; Kulkarni, S. A.; Suresh, C. H.; Shrivastava, I. H. "Basis Set Dependence of the Molecular Electrostatic Potential Topography. A Case Study of Ssubstituted Benzenes" *Chem. Phys. Lett.* 239, **1995**, 273.

Gadre, S. R.; Pathak, R. K. "Maximal and Minimal Characteristics of Molecular

Electrostatic Potentials" *J. Chem. Phys*. 93, **1990**, 1770.

Gadre, S. R.; Shirsat, R. N. *Electrostatics of Atoms and Molecules*. Universities Press: Hyderabad, India, **2000**.

Gadre, S. R.; Shrivastava, I. H. "Topography Driven Electrostatic Charge Models for Molecules" *Chem. Phys. Lett.* 205, **1993**, 350.

Gadre, S. R.; Suresh, C. H. "Electronic Perturbations of the Aromatic Nucleus: Hammett Constants and Electrostatic Potential Topography" *J. Org. Chem.* 62, **1997**, 2625.

Galabov, B.; Ilieva, S.; Hadjieva, B.; Atanasov, Y.; Schaefer, H. F. "Predicting Reactivities of Organic Molecules. Theoretical and Experimental Studies on the Aminolysis of Phenyl Acetates" *J. Phys. Chem. A* 112, **2008**, 6700

Galabov, B.; Ilieva, S.; Schaefer, H. F. "An Efficient Computational Approach for the Evaluation of Substituent Constants" *J. Org. Chem.* 71, **2006**, 6382.

Gao, J. "Methods and Applications of Combined Quantum Mechanical and Molecular Mechanical Potentials" *Rev. Comp. Chem.* 7, **1996**, 119.

Garber, S. B.; Kingsbury, J. S.; Gray, B. L.; Hoveyda, A. H. "Efficient and Recyclable Monomeric and Dendritic Ru-Based Metathesis Catalysts" *J. Am. Chem. Soc.* 122, **2000**, 8168.

Gessler, S.; Randl, S.; Blechert, S. "Synthesis and Metathesis Reactions of a Phosphine-Free Dihydroimidazole Carbene Ruthenium Complex" *Tetrahedron Lett.* 41, **2000**, 9973.

Getty, K.; Delgado-Jaime, M. U.; Kennepohl, P. "An Electronic Rationale for Observed Initiation Rates in Ruthenium-Mediated Olefin Metathesis: Charge

Donation in Phosphine and N-Heterocyclic Carbene Ligands" *J. Am. Chem. Soc.* 129, **2007**, 15774.

Glorius, F. *N-Heterocyclic Carbenes in Transition Metal Catalysis*. Springer-Verlag: Berlin, Germany, **2007**.

Gonsalvi, L.; Adams, H.; Sunley, G. J.; Ditzel, E.; Haynes, A. "A Dramatic Steric Effect on the Rate of Migratory CO Insertion on Rhodium" *J. Am. Chem. Soc.* 121, **1999**, 11233.

Goto, K.; Ohzu, Y.; Sato, H.; Kawashima, T. "Synthesis of Novel Triarylphosphines Bearing a m-terphenyl-Based Dendrimer-Type Framework" *Phosphorus, Sulfur, Silicon Relat. Elem.* 177, **2002**, 2179.

Grubbs, R. H. *Handbook of Metathesis*. Wiley-VCH: Weinheim, Germany, **2003**.

Grubbs, R. H.; Coates, G. W. "α-Agostic Interactions and Olefin Insertion in Metallocene Polymerization Catalysts" *Acc. Chem. Res.* 29, **1996**, 85.

Gusev, D. G. "Electronic and Steric Parameters of 76 N-Heterocyclic Carbenes in $Ni(CO)_3(NHC)$" *Organometallics* 28, **2009**, 6458.

Hall, G. G. "The Molecular Orbital Theory of Chemical Valency. VIII. A Method of Calculating Ionization Potentials" *Proc. Roy. Soc. (London)* A205, **1951**, 541.

Hartree, R. R. "The Wave Mechanics of an Atom with a Non-Coulomb Central Field. Part I. Theory and Methods" *Proc. Cambridge Phil. Soc*. 24, **1928,** 89.

Hay, P. J.; Wadt, W. R. "Ab Initio Effective Core Potentials for Molecular Calculations. Potentials for the Transition Metal Atoms Sc to Hg" *J. Chem. Phys.* 82, **1985,** 270.

Hehre, W. J.; Ditchfield, R.; Pople, J. "Self-Consistent Molecular Orbital Methods. XII.

Further Extensions of Gaussian-Type Basis Sets for Use in Molecular Orbital Studies of Organic Molecules" *J. Chem. Phys.* 56, **1972**, 2257.

Hehre, W. J.; Stewart, R. F.; Pople, J. A. "Self-Consistent Molecular-Orbital Methods. I. Use of Gaussian Expansions of Slater-Type Atomic Orbitals" *J. Chem. Phys*. 51, **1969**, 2657.

Herisson, J. L.; Chauvin, Y. "Catalysis of Olefin Transformations by Tungsten Complexes. II. Telomerization of Cyclic Olefins in the Presence of Acyclic Olefins" *Makromol. Chem.* 141, **1971**, 161.

Herrmann, W. A. "N-heterocyclic Carbenes: A New Concept in Organometallic Catalysis" *Angew. Chem., Int. Ed.* 41, **2002,** 1290.

Herrmann, W. A.; Köcher, C. "N-Heterocyclic Carbenes" *Angew. Chem. Int. Ed.* 36, **1997**, 2162.

Hillier, A. C.; Sommer, W. J.; Yong, B. S.; Petersen, J. L.; Cavallo, L.; Nolan, S. P. "A Combined Experimental and Theoretical Study Examining the Binding of N-Heterocyclic Carbenes (NHC) to the Cp*RuCl (Cp* = η5-C_5Me_5) Moiety: Insight into Stereoelectronic Differences between Unsaturated and Saturated NHC Ligands" *Organometallics* 22, **2003**, 4322.

Hinderling, C.; Adlhart, C.; Chen, P. "Olefin Metathesis of a Ruthenium Carbene Complex by Electrospray Ionization in the Gas Phase" *Angew. Chem., Int. Ed.* 37, **1998,** 2685.

Hirota, M.; Sakakibara, K.; Komatsuzaki, K.; Akai, I. "A New Steric Substituent Constant Ωs Based on Molecular Mechanics Calculations" *Computers Chem.* 15, **1991**, 241.

Hohenberg, P.; Kohn, W. "Inhomogeneous Electron Gas" *Phys. Rev*. 136, **1964,** B864.

Hong, S. H.; Chlenov, A.; Day, M. W.; Grubbs, R. H. "Double C-H Activation of an N-Heterocyclic Carbene Ligand in a Ruthenium Olefin Metathesis Catalyst" *Angew. Chem., Int. Ed.* 46, **2007,** 5148.

Hong, S. H.; Grubbs, R. H. "Highly Active Water-Soluble Olefin Metathesis Catalyst" *J. Am. Chem. Soc.* 128, **2006**, 3508.

Horrocks, Jr. W. D.; Taylor, R. C. "Infrared Spectroscopic Study of Derivatives of Cobalt Tricarbonyl Nitrosyl " *Inorg. Chem.* 2, **1963**, 723.

Hoyt, H. M.; Michael, F. E.; Bergman, R. G. "C-H Bond Activation of Hydrocarbons by an Imidozirconocene Complex" *J. Am. Chem. Soc.* 126, **2004,** 1018.

[a]Huang, J. K.; Schanz, H. J.; Stevens, E. D.; Nolan, S. P. "Influence of Sterically Demanding Carbene Ligation on Catalytic Behavior and Thermal Stability of Ruthenium Olefin Metathesis Catalysts" *Organometallics* 18, **1999**, 5375.

[b]Huang, J. K.; Stevens, E. D.; Nolan, S. P.; Petersen, J. L. "Olefin Metathesis-Active Ruthenium Complexes Bearing a Nucleophilic Carbene Ligand" *J. Am. Chem. Soc.* 121, **1999**, 2674.

Huang, J.; Schanz, H.-J.; Stevens, E. D.; Nolan, S. P. "Stereoelectronic Effects Characterizing Nucleophilic Carbene Ligands Bound to the Cp*RuCl (Cp* = η5-C_5Me_5) Moiety: A Structural and Thermochemical Investigation" *Organometallics* 18, **1999**, 2370.

Huang, J.; Stevens, E. D.; Nolan, S. P. "Intramolecular C-H Activation Involving a Rhodium-imidazol-2-ylidene Complex and Its Reaction with H_2 and CO" *Organometallics* 19, **2000,** 1194.

Humbel, S.; Sieber, S.; Morokuma, K. "The IMOMO method: Integration of Different

Levels of Molecular Orbital Approximations for Geometry Optimization of Large Systems: Test for n-butane Conformation and SN2 Reaction: RCl$^+$Cl$^-$ " *J. Chem. Phys.* 105, **1996**, 1959.

Irle, S.; Rubin, Y.; Morokuma, K. "ONIOM Study of Ring Opening and Metal Insertion Reactions with Derivatives of C$_{60}$: Role of Aromaticity in the Opening Process" *J. Phys. Chem. A* 106, **2002**, 680.

Ivin, K. J; Mol, J. C. "*Olefin Metathesis and Metathesis Polymerization*" Academic Press: San Diego, CA, **1997**.

Jacobsen, H. "P-Heterocyclic Carbenes as Potential Ligands in the Design of New Metathesis Catalysts. A Computational Study" *Dalton Trans.* **2006**, 2214.

Jafarpour, L.; Stevens, E. D.; Nolan, S. P. "A Sterically Demanding Nucleophilic Carbene:1,3-bis(2,6-diisopropylphenyl)imidazol-2-ylidene. Thermochemistry and Catalytic Application in Olefin Metathesis" *J. Organomet. Chem.* 606, **2000**, 49.

Jensen, F. *Introduction to computational chemistry*, Wiley, Chichester, **1999**.

Jørgensen, P.; Simons, J. and North Atlantic Treaty Organization, Scientific Affairs Division, *Geometrical Derivatives of Energy Surfaces and Molecular Properties*, Reidel, Dordrecht, **1986**.

Jover, J.; Fey, N.; Harvey, J. N.; Lloyd-Jones, G. C.; Orpen, A. G.; Owen-Smith, G. J. J. ; Murray, P.; Hose, D. R. J.; Osborne, R.; Purdie, M. "Expansion of the Ligand Knowledge Base for Monodentate P-Donor Ligands (LKB-P)" *Organometallics* 29, **2010**, 6245.

Katz, T. J.; McGinnis, J. "Mechanism of the Olefin Metathesis Reaction" *J. Am. Chem. Soc.* 97, **1975**, 1592.

Kaufhold, O., Hahn, F.E. "Carbodicarbenes: Divalent Carbon(0) Compounds" *Angew. Chem., Int. Ed. Engl.* 47, **2008**, 4057.

Kelly III, R. A.; Clavier, H.; Giudice, S.; Scott, N. M.; Stevens, E. D.; Bordner, J.; Samardjiev, I.; Hoff, C. D.; Cavallo, L.; Nolan, S. P. "Determination of N-Heterocyclic Carbene (NHC) Steric and Electronic Parameters Using the [(NHC)Ir(CO)$_2$Cl] System" *Organometallics* 27, **2008**, 202.

Kelly, H. P. *Advances in Chemical Physics* John Wiley & Sons, New York, **1969**.

Kerdcharoen, T.; Morokuma, K. "ONIOM-XS: An Extension of the ONIOM Method for Molecular Mimulation in Condensed Phase" *Chem. Phys. Lett.* 355, **2002**, 257.

Kingsbury, J. S.; Harrity, J. P. A.; Bonitatebus, P. J., Jr.; Hoveyda, A. H. "A Recyclable Ru-Based Metathesis Catalyst" *J. Am. Chem. Soc.* 121, **1999**, 791.

Kingsbury, J. S.; Hoveyda, A. H. "Regarding the Mechanism of Olefin Metathesis with Sol-Gel-Supported Ru-Based Complexes Bearing a Bidentate Carbene Ligand. Spectroscopic Evidence for Return of the Propagating Ru Carbene" *J. Am. Chem. Soc.* 127, **2005**, 4510.

Kohn, W.; Sham, L. J. "Self-Consistent Equations Including Exchange and Correlation Effects" *Phys. Rev.* 140, **1965**, A1133.

Koleva, G.; Galabov, B.; Wu, J. I.; Schaefer, H. F.; Schleyer, P. v. R. "Electrophile Affinity: A Reactivity Measure for Aromatic Substitution" *J. Am. Chem. Soc.* 131, **2009**, 14722.

Komatsuzaki, T.; Sakakibara, K.; Hirota, M. "A New Method for Evaluating the Steric Hindrance by Substituent" *Tetrahedron Lett.* 30, **1989**, 3309.

Komatsuzaki, T.; Sakakibara, K.; Hirota, M. "A New Steric Substituent Parameter Ωs. Sophistication of Calculation and Correlation with the Kinetic Data of Several Reactions" *Chem. Lett.* **1990**, 1913.

König, F. B.; Schönbohm, J.; Bayles, D. "AIM2000" *J. Comput. Chem.* 22, **2001**, 545.

Krishnan, R.; Pople, J. A. "Approximate Fourth-Order Perturbation Theory of the Electron Correlation Energy" *Int. J. Quantum Chem*. 14, **1978**, 91.

Kühl, O. "Predicting the Net Donating Ability of Phosphines-Do We Need Sophisticated Theoretical Methods?" *Coord. Chem. Rev.* 249, **2005**, 693.

Kümmel, H. G. "*A biography of the coupled cluster method*". Ed: R.F. Bishop, T. Brandes, K.A. Gernoth, N.R. Walet, Y. Xian, Recent Progress in Many-Body Theories Proceedings of the 11th International Conference. World Scientific Publishing. Singapore, **2002**.

La, D. S.; Alexander, J. B.; Cefalo, D. R.; Graf, D. D.; Hoveyda, A. H.; Schrock, R. R. "Mo-Catalyzed Asymmetric Synthesis of Dihydrofurans. Catalytic Kinetic Resolution and Enantioselective Desymmetrization through Ring-Closing Metathesis" *J. Am. Chem. Soc*. 120, **1998**, 9720.

[a]Ledoux, N.; Allaert, B.; Linden, A.; Van der Voort, P.; Verpoort, F. "Bis-coordination of N-(Alkyl)-N'-(2,6-diisopropylphenyl) Heterocyclic Carbenes to Grubbs Catalysts" *Organometallics* 26, **2007**, 1052.

[b]Ledoux, N.; Allaert, B.; Vander Mierde, H.; Verpoort, F. "Comparative investigation of Hoveyda-Grubbs catalysts bearing modified N-heterocyclic carbene ligands" *Adv. Synth. Catal.* 342, **2007**, 1692.

Lee, C. T.; Yang, W. T.; Parr, R. G. "Development of the Colle-Salvetti Correlation-Energy Formula into a Functional of the Electron Density" *Phys. Rev. B* 37, **1988**, 785.

Lever, A. B. P. "Electrochemical Parametrization of Metal Complex Redox Potentials, Using the Ruthenium(III)/Ruthenium(II) Couple to Generate a Ligand Electrochemical Series" *Inorg. Chem.* 29, **1990**, 1271.

Lever, A. B. P. "Electrochemical Parametrization of Rhenium Redox Couples" *Inorg. Chem.* 30, **1991**, 1980.

Limaye, A. C.; Gadre, S. R. "UNIVIS-2000: An Indigenously Developed Comprehensive Visualization Package" *Curr. Sci.* 80, **2001**, 1296.

Lippstreu, J. J.; Straub, B. F "Mechanism of Enyne Metathesis Catalyzed by Grubbs Ruthenium-Carbene Complexes: A DFT Study" *J. Am. Chem. Soc*. 127, **2005**, 7444.

Liu, S.; Pedersen, L. G. "Estimation of Molecular Acidity via Electrostatic Potential at the Nucleus and Valence Natural Atomic Orbitals" *J. Phys. Chem. A* **2009**, 113, 3648.

Liu, Z.; Torrent, M.; Morokuma, K. "Molecular Orbital Study of Zinc(II)-Catalyzed Alternating Copolymerization of Carbon Dioxide with Epoxide" *Organometallics* 21, **2002**, 1056.

Love, J. A.; Morgan, J. P.; Trnka, T. M.; Grubbs, R. H. "A Practical and Highly Active Ruthenium-Based Catalyst that Effects the Cross Metathesis of Acrylonitrile" *Angew. Chem., Int. Ed.* 41, **2002,** 4035.

Luque, F. J.; Orozco, M.; Bhadane, P. K.; Gadre, S. R. "Effect of Solvation on the Shapes, Sizes and Anisotropies of Polyatomic Anions via Molecular Electrostatic Potential Topology: an Ab Initio Self Consistent Reaction Field Approach" *J. Chem. Phys*. 100, **1994**, 6718.

M. I. Kabachnik, Dokl. Akad. Nauk. *SSSR*, 110, **1956**, 393.

Mansson, R. A.; Welsh, A. H.; Fey, N.; Orpen, A. G. "Statistical Modeling of a Ligand Knowledge Base" *J. Chem. Inf. Model.* 46, **2006**, 2591.

Marion, N.; Navarro, O.; Mei, J.; Stevens, E. D.; Scott, N. M.; Nolan, S. P. "Modified (NHC)Pd(allyl)Cl (NHC = N-Heterocyclic Carbene) Complexes for Room-Temperature Suzuki-Miyaura and Buchwald-Hartwig Reactions" *J. Am. Chem. Soc.* 128, **2006**, 4101.

Martin, D.; Baceirdo, A.; Gornitzka, H.; Schoeller, W. W.; Bertrand, G. "A Stable P-Heterocyclic Carbene" *Angew. Chem., Int. Ed.* 44, **2005**, 1700.

Martorell, A.; Naasz, R.; Feringa, B. L.; Pringle, P. G. "Phosphonite Ligands for Enantioselective Copper(I)-Catalysed Conjugate Addition of Diethylzinc to Enones" *Tetrahedron: Asymmetry* 12, **2001**, 2497.

Maseras, F.; Morokuma, K. "IMOMM: A New Integrated Ab Initio + Molecular Mechanics Geometry Optimization Scheme of Equilibrium Structures and Transition States" *J. Comput. Chem.* 16, **1995**, 1170.

Mathew, J.; Koga, N.; Suresh, C. H. "C-H Bond Activation through σ-Bond Metathesis and Agostic Interactions: Deactivation Pathway of a Grubbs Second-Generation Catalyst" *Organometallics* 27, **2008**, 4666.

Mathew, J.; Suresh, C. H. "Use of Molecular Electrostatic Potential at the Carbene Carbon as a Simple and Efficient Electronic Parameter of N-heterocyclic Carbenes" *Inorg. Chem.* 49, **2010**, 4665.

Mathew, J.; Thomas, T.; Suresh, C. H. "Quantitative Assessment of the Stereoelectronic Profile of Phosphine Ligands" *Inorg. Chem.* 46, **2007**, 10800.

Matsubara, T.; Koga, N.; Musaev, D. G.; Morokuma, K. "Density Functional Study on Activation of *ortho*-CH Bond in Aromatic Ketone by Ru Complex. Role of

Unusual Five-Coordinated d^6 Metallacycle Intermediate with Agostic Interaction" *J. Am. Chem. Soc.* 120, **1998,** 12692.

Matsubara, T.; Koga, N.; Musaev, D. G.; Morokuma, K. "Density Functional Study on Highly *ortho*-Selective Addition of an Aromatic C-H Bond to Olefins Catalyzed by a Ru(H)$_2$(CO)(PR$_3$)$_3$ Complex" *Organometallics* 19, **2000,** 2318.

Matsumoto, T.; Kasai, T.; Tatsumi,K. "Chiral Crystallization of a Linear Two-Coordinated Palladium(0) Complex Bearing Propeller-Shaped Bulky Phosphine Ligands" *Chem. Lett.* 31, **2002**, 346.

McLain, S. J.; Wood, C. D.; Schrock, R. R. "Preparation and Characterization of Tantalum(III) Olefin Complexes and Tantalum(V) Metallacyclopentane Complexes Made from Acyclic α Olefins" *J. Am. Chem. Soc*. 101, **1979**, 4558.

Meriwether, L. S.; Fiene, M. L. "Bonding in Ni(0) Complexes. I. Phosphine Exchange Kinetics and Infrared Spectra of Nickel-Carbonyl-Phosphine Complexes" *J. Amer. Chem. Soc.* 81, **1959**, 4200.

Michelotti, F. W.; Keaveney, W. P. "Coordinated Polymerization of the bicyclo-[2.2.1]-heptene-2 ring System (norbornene) in Polar Media" *J. Polym. Sci.* A3, **1965**, 895.

Michrowska, A.; Bujok, R.; Harutyunyan, S.; Sashuk, V.; Dolgonos, G.; Grela, K. "Nitro-Substituted Hoveyda-Grubbs Ruthenium Carbenes: Enhancement of Catalyst Activity through Electronic Activation" *J. Am. Chem. Soc*. 126, **2004**, 9318.

Møller, C.; Plesset, M. S. "Note on an Approximation Treatment for Many-Electron

Systems" *Phys. Rev.* 46, **1934**, 618.

Mordasini, T. Z.; Thiel, W. "Combined Quantum Mechanical and Molecular Mechanical Approaches" *Chimia* 52, **1998**, 288.

Movassaghi, M.; Piizzia, G.; Siegela, D. S.; Piersantia, G. "Observations in the Synthesis of the Core of the Antitumor Illudins via an Enyne Ring Closing Metathesis Cascade" *Tetrahedron Lett.* 50, **2009**, 5489.

Murdzek, J. S.; Schrock, R. R. "Well-Characterized Olefin Metathesis Catalysts that Contain Molybdenum" *Organometallics* 6, **1987**, 1373.

Murray, J. S.; Lane, P.; Brinck, T.; Politzer, P. "Electrostatic Potentials on the Molecular Surfaces of Cyclic Ureides" *J. Phys. Chem.* 95, **1991**, 844.

Murray, J. S.; Politzer, P. "Electrostatic Potentials of Amine Nitrogens as a Measure of the Total Electron-Attracting Tendencies of Substituents" *Chem. Phys. Lett.* **1988**, 364.

Murray, J. S.; Sen, K. *Molecular Electrostatic Potentials*. Elsevier: Amsterdam, **1996**.

Natta, G.; Dall'Asta, G.; Motroni, G. "Coordinated Polymerization of Cyclobutene in the Presence of the Aqueous $RhCl_3$ Catalytic System" *J. Polymer Sci., Polymer Lett.* B2, **1964**, 349.

Nguyen, S. T.; Grubbs, R. H. "Syntheses and Activities of New Single-Component, Ruthenium-Based Olefin Metathesis Catalysts" *J. Am. Chem. Soc.* 115, **1993**, 9858.

Nguyen, S. T.; Johnson, L. K.; Grubbs, R. H. "Ring-Opening Metathesis Polymerization (ROMP) of Norbornene by a Group VIII Carbene Complex in Protic Media" *J. Am. Chem. Soc.* 114, **1992**, 3974.

Nolan, S. P. *N-Heterocyclic Carbenes in Synthesis* Wiley-VCHM: Weinheim, **2006**.

Nozaki, K.; Sato, N.; Tonomura, Y.; Yasutomi, M.; Takaya, H.; Hiyama, T.; Matsubara, T.; Koga, N. "Mechanistic Aspects of the Alternating Copolymerization of Propene with Carbon Monoxide Catalyzed by Pd(II) Complexes of Unsymmetrical Phosphine-Phosphite Ligands" *J. Am. Chem. Soc.* 119, **1997**, 12779.

Occhipinti, G.; Bjørsvik, H.-R.; Jensen, V. R. "Quantitative Structure-Activity Relationships of Ruthenium Catalysts for Olefin Metathesis" *J. Am. Chem. Soc.* 128, **2006**, 6952.

Öfele, K "1,3-Dimethyl-4-imidazolinyliden-(2)-pentacarbonylchrom ein Neuer übergangsmetall-carben-komplex" *J. Organomet. Chem.* 12, **1968**, 42.

Ohta, H.; Tokunaga, M.; Obora, Y.; Iwai, T.; Iwasawa, T.; Fujihara, T.; Tsuji, Y. "A Bowl-Shaped Phosphine as a Ligand in Palladium-Catalyzed Suzuki-Miyaura Coupling of Aryl Chlorides: Effect of the Depth of the Bowl" *Org. Lett.* 9, **2007**, 89.

Ohzu, Y.; Goto, K.; Kawashima, T. "A Bowl-Shaped Triarylphosphane with a Large Cone Angle: Synthesis and Crystallographic Analysis of a $[(PdX_2)_3(PR_3)_2]$-Type Complex" *Angew. Chem., Int. Ed.* 42, **2003**, 5714.

Oskam, J. H.; Fox, H. H.; Yap, K. B.; McConville, D. H.; O'Dell, R.; Lichtenstein, B. J.; Schrock, R. R. "Ligand Variation in Alkylidene Complexes of the Type Mo(CHR)(NR')(OR")$_2$ "*J. Organomet. Chem.* 459, **1993**, 185.

Parr, R. G.; Yang,W. *Density Functional Theory of Atoms and Molecules*, Oxford University Press, New York, **1989**.

Pathak, R. K.; Gadre, S. R. "Nonexistence of Local Maxima in Molecular Electrostatic Potential Maps" *Proc. Ind Acad. Sci. (Chem. Sci.)* 102, **1990**, 189.

Pauli Jr. W. "Über den Zusammenhang des Abschlusses der Elektronengruppen im Atom

mit der Komplexstruktur der Spektren" *Z. Phys.* 31, **1925**, 765.

Peng, C.; Ayala, P. Y.; Schlegel, H. B.; Frisch, M. J. "Using Redundant Internal Coordinates to Optimize Equilibrium Geometries and Transition States" *J. Comp. Chem.* 17, **1996**, 49.

Perdew, J. P. "Density-Functional Approximation for the Correlation Energy of the Inhomogeneous Electron Gas" *Phys. Rev. B* 33, **1986**, 8822.

Perdew, J. P.; Chevary, J. A.; Vosko, S. H.; Jackson, K. A.; Pederson, M. R.; Singh, D. J.; Fiolhais, J. C. "Atoms, Molecules, Solids, and Surfaces: Applications of the Generalized Gradient Approximation for Exchange and Correlation" *Phys.Rev.B.* 46, **1992**, 6671.

Perrin, L.; Clot, E.; Eisenstein, O.; Loch, J.; Crabtree, R. H. "Computed Ligand Electronic Parameters from Quantum Chemistry and Their Relation to Tolman Parameters, Lever Parameters, and Hammett Constants" *Inorg. Chem.* 40, **2001**, 5806.

Phukan, A. K.; Kalagi, R. P.; Gadre, S. R.; Jemmis, E. D. "Structure, Reactivity and Aromaticity of Acenes and Their BN Analogues: A Density Functional and Electrostatic Investigation" *Inorg. Chem.* 43, **2004**, 5824.

Poater, A.; Cosenza, B.; Correa, A.; Giudice, S.; Ragone, F.; Scarano, V.; Cavallo, L. "SambVca: A Web Application for the Calculation of the Buried Volume of N-Heterocyclic Carbene Ligands" *Eur. J. Inorg. Chem.* **2009**, 1759.

Poilblanc, R., Bigorgne, M. "A Discussion on the Assignment of the C-O Vibration Bands of Metal Hexacarbonyl Derivatives" *J. Organomet. Chem.* 5, **1966**, 93.

Politzer, P. "Atomic and Molecular Energies as Functionals of the Electrostatic Potential" *Theor. Chem. Acc.* 111, **2004**, 395.

Politzer, P.; Murray, J. S. "The Fundamental Nature and Role of the Electrostatic Potential in Atoms and Molecules" *Theor. Chem. Acc.* 108, **2002**, 134.

Politzer, P.; Murray, J. S. "Relationships between Dissociation Energies and Electrostatic Potentials of $C-NO_2$ Bonds: Applications to Impact Sensitivities" *J. Mol. Struct.* 376, **1996**, 419.

Politzer, P.; Truhlar, D. G. *Chemical Applications of Atomic and Molecular Electrostatic Potentials*. Plenum Press: New York, **1981**.

Pople, J. A.; Beveridge, D. L. *Approximate Molecular Orbital Theory*, McGraw-Hill, New York, **1970**.

Pople, J. A.; Binkley, J. S.; Seeger, R. "Theoretical Models Incorporating Electron Correlation" *Int. J. Quantum Chem. Symp.* 10, **1976**, 1.

Prinz, M.; Grosche, M.; Herdtweck, E.; Herrmann, W. A. "Unsymmetrically Substituted Iridium(III)-Carbene Complexes by a CH-activation Process" *Organometallics* 19, **2000,** 1692.

Pulay, P. *Modern Electronic Structure Theory*, World Scientific, Singapore, **1995**.

Rahman, M.M.; Liu, H.-Y.; Eriks, K.; Prock, A.; Giering, W.P. "Quantitative Analysis of Ligand Effects. Part 3. Separation of Phosphorus(III) Ligands into Pure .Sigma.-Donors and .Sigma.-Donor/.Pi.-Acceptors. Comparison of Basicity and .Sigma.-Donicity" *Organometallics* 8, **1989**, 1.

Rahman, M.M.; Liu, H.Y.; Prock, A.; Giering, W.P. "Quantitative Analysis of Lligand Effects. 2. Steric and Electronic Factors Influencing Transition-Metal-Phosphorus(III) Bonding" *Organometallics* 6, **1987**, 650.

Ramirez, F., Desai, N. B., Hansen, B.; McKelvie, N. Hexaphenylcarbodiphosphorane, $(C_6H_5)_3PCP(C_6H_5)_3$ *J. Am. Chem. Soc.* 83, **1961**, 3539.

Rapaport, D. C. *The Art of Molecular Dynamics Simulation*, Cambridge University Press, Cambridge, **2004**.

Rappé, A. K.; Casewit, C. J.; Colwell, K. S.; Goddard, W. A., III.; Skiff, W. M. "UFF, a Full Periodic Table Force Field for Molecular Mechanics and Molecular Dynamics Simulations" *J. Am. Chem. Soc.* 114, **1992**, 10024.

Re, S.; Morokuma, K. "ONIOM Study of Chemical Reactions in Microsolvation Clusters: $(H_2O)_nCH_3Cl + OH^-(H_2O)_m$ (n + m = 1 and 2)" *J. Phys. Chem. A* 105, **2001**, 7185.

Renaud, J.; Graf, C-D.; Oberer, L. "Ruthenium-Catalyzed Enyne Metathesis of Acetylenic Boronates: A Concise Route for the Construction of Cyclic 1,3-Dienylboronic Esters" *Angew. Chem., Int. Ed.* 39, **2000**, 3101.

Rinehart, R. E.; Smith, H. P. "The Emulsion Polymerization of the Norbornene Ring System Catalyzed by Noble Metal Compounds" *J. Polym. Sci. Polym. Lett.* 3, **1965**, 1049.

[a]Ritter, T.; Hejl, A.; Wenzel, A. G.; Funk, T. W.; Grubbs, R. H. "A Standard System of Characterization for Olefin Metathesis Catalysts" *Organometallics* 25, **2006**, 5740.

[b]Ritter, T.; Day, M. W.; Grubbs, R. H. "Rate Acceleration in Olefin Metathesis through a Fluorine-Ruthenium Interaction" *J. Am. Chem. Soc.* 128, **2006**, 11768.

Rocklage, S. M.; Fellmann, J. D.; Rupprecht, G. A.; Messerle, L. W.; Schrock, R. R. "Multiple Metal-Carbon Bonds. 19. How Niobium and Tantalum Complexes of the Type $M(CHCMe_3)(PR_3)_2Cl_3$ Can be Modified to Give Olefin Metathesis Catalysts" *J. Am. Chem. Soc.* 103, **1981**, 1440.

Roothaan, C. C. J. "New Developments in Molecular Orbital Theory" *Rev. Mod. Phys.* 23, **1951**, 69.

Samojłowicz, C.; Bieniek, M.; Grela, K. "Ruthenium-Based Olefin Metathesis Catalysts Bearing N-Heterocyclic Carbene Ligands" *Chem. Rev.* 109, **2009**, 3708.

Sanford, M. S.; Love, J. A.; Grubbs, R. H. "Mechanism and Activity of Ruthenium Olefin Metathesis Catalysts" *J. Am. Chem. Soc.* 123, **2001**, 6543.

Santiago, A. A.; Vargas, J.; Fomine, S.; Gaviño, R.; Tlenkopatchev, M. A. "Polynorbornene with Pentafluorophenyl Imide Side Chain Groups: Synthesis and Sulfonation" *J. Polym. Sci. A: Polym.Chem.* 48, **2010**, 2925.

Sayyed, F. B.; Suresh, C. H. "An Electrostatic Scale of Substituent Resonance Effect" *Tetrahedron Lett.* 50, **2009**, 7351.

Schaverien, C. J.; Dewan, J. C.; Schrock, R. R. "Multiple Metal-Carbon Bonds. 43. Well-Characterized, Highly Active, Lewis Acid Free Olefin Metathesis Catalysts" *J. Am. Chem. Soc.* 108, **1986**, 2771.

Schlick, T. *Molecular Modeling and Simulation*, Springer-Verlag, New York, **2002**.

Schmidbaur, H.; Nusstein, P. "Synthesis of the First Carbodiarsorane and Related Arsenic Ylides" *Organometallics* 4, **1985**, 344.

Schoeller, W. W.; Schroeder, D.; Rozhenko, A. B. "On the Ligand Properties of the P-versus the N-heterocyclic Carbene for a Grubbs Catalyst in Olefin Metathesis" *J. Organomet. Chem.* 690, **2005**, 6079.

Schofield, M. H.; Schrock, R. R.; Park, L. Y. "Rhenium(VII) Monoimido Alkylidene Complexes: Synthesis, Structure, and Lewis-Acid-Cocatalyzed Olefin Metathesis" *Organometallics* 10, **1991**, 1844.

Scholl, M.; Ding, S.; Lee, C. W.; Grubbs, R. H. "Synthesis and Activity of a New Generation of Ruthenium-Based Olefin Metathesis Catalysts Coordinated with 1,3-Dimesityl-4,5-dihydroimidazol-2-ylidene Ligands" *Org. Lett.* 1, **1999**, 953.

Scholl, M.; Trnka, T. M.; Morgan, J. P.; Grubbs, R. H. "Increased Ring Closing Metathesis Activity of Ruthenium-Based Olefin Metathesis Catalysts Coordinated with Imidazolin-2-ylidene Ligands" *Tetrahedron Lett.* 40, **1999,** 2247.

Schrock, R. R. "High-Oxidation-State Molybdenum and Tungsten Alkylidyne Complexes" *Acc. Chem. Res.* 19, **1986**, 342.

Schrock, R. R. "The Alkoxide Ligand in Olefin and Acetylene Metathesis Reactions" *Polyhedron* 14, **1995**, 3177.

Schrock, R. R.; Crowe, W. E.; Bazan, G. C.; DiMare, M.; O'Regan, M. B.; Schofield, M. H. "Monoadducts of Imido Alkylidene Complexes, Syn and Anti Rotamers, and Alkylidene Ligand Rotation" *Organometallics* 10, **1991**, 1832.

[a]Schrock, R. R.; Depue, R. T.; Feldman, J.; Yap, K. B.; Yang, D. C.; Davis, W. M.; Park, L.; DiMare, M.; Schofied, M.; Anhaus, J.; Walborsky, E.; Evitt, E.; Kruger, C.; Betz, P. "Further Studies of Imido Alkylidene Complexes of Tungsten, Well-Characterized Olefin Metathesis Catalysts with Controllable Activity" *Organometallics* 9, **1990**, 2262.

[b]Schrock, R. R.; Murdzek, J. S.; Bazan, G. S.; Robbins, J.; DiMare, M.; O'Regan, M. "Synthesis of Molybdenum Imido Alkylidene Complexes and Some Reactions Involving Acyclic Olefins" *J. Am. Chem. Soc.* 112, **1990**, 3875.

Schrock, R. R.; Depue, R. T.; Fellmann, J. D.; Schaverien, C. J.; Dewan, J. C.; Liu, A. H. "Preparation and Reactivity of Several Alkylidene Complexes of the Type $W(CHR')(N-2,6-C_6H_3-iso-Pr_2)(OR)_2$ and Related Tungstacyclobutane Complexes. Controlling Metathesis Activity through the Choice of Alkoxide Ligand" *J. Am. Chem. Soc.* 110, **1988**, 1423.

Schrock, R. R.; Rocklage, S. M.; Wengrovius, J. H.; Rupprecht, G.; Fellmann, J. "Preparation and Characterization of Active Niobium, Tantalum and Tungsten Metathesis Catalysts" *J. Mol. Catal.* 8, **1980**, 73.

Schrödinger, E. "Quantisierung als Eigenwertproblem" *Ann. Phys*. 79, **1926**, 361.

Schubert, U.; Kappenstein, C.; Milewski-Mahrla, B.; Schmidbaur, H. "Molekül- und Kristallstrukturen zweier Carbodiphosphorane mit PCP-Bindungswinkeln nahe 120°" *Chem. Ber.* 114, **1981**, 3070.

Schwab, P.; France, M. B.; Ziller, J. W.; Grubbs, R. H. "A Series of Well-Defined Metathesis Catalysts–Synthesis of [$RuCl_2$(=CHR')(PR_3)$_2$] and Its Reactions" *Angew. Chem.,Int. Ed. Engl.* 34, **1995**, 2039.

Schwab, P.; Grubbs, R. H.; Ziller, J. W. "Synthesis and Applications of $RuCl_2$(=CHR')(PR_3)$_2$: The Influence of the Alkylidene Moiety on Metathesis Activity" *J. Am. Chem. Soc.* 118, **1996**, 100.

Scott, N. M.; Nolan, S. P. "Stabilization of Organometallic Species Achieved by the Use of N-Heterocyclic Carbene (NHC) Ligands" *Eur. J. Inorg. Chem.* 2005, **2005,** 1815.

Seiders, T. J.; Ward, D. W.; Grubbs, R. H. "Enantioselective Ruthenium-Catalyzed Ring-Closing Metathesis" *Org. Lett.* 3, **2001**, 3225.

Shavitt, I. *Methods in Computational Physics* Academic Press, New York, **1963**.

Shirsat, R. N.; Bapat, S. V.; Gadre, S. R. "Molecular electrostatics: A Comprehensive Topographical Approach" *Chem. Phys. Lett*. 200, **1992**, 373.

Singh, U. C.; Kollman, P. A. "A Combined Ab Initio Quantum Mechanical and Molecular Mechanical Method for Carrying out Simulations on Complex Molecular Systems: Applications to the CH_3Cl + Cl^- Exchange Reaction and Gas Phase Protonation of Polyethers" *J. Comput. Chem.* 7, **1986**, 718.

Slater, J. C. "Atomic Radii in Crystals" *J. Chem. Phys.* 41, **1964**, 3199.

Slater, J. C. "A Simplification of the Hartree-Fock Method" *Phys. Rev.* **1951**, 81, 385.

Slater, J. C. "Note on Hartree's Method" *Phys. Rev.* 35, **1930**, 210.

Sowa Jr. J.R..; Zanotti, V.; Angelici, R.J. "Effect of Tridentate Phosphine Ligand Structure on the Basicities of Tungsten Tricarbonyl Complexes" *Inorg. Chem.* 30, **1991**, 4108.

Sowa Jr. J.R..; Zanotti, V.; Facchin, G.; Angelici, R.J. "Calorimetric Studies of the Heats of Protonation of the Metal in $Fe(CO)_3$(Bidentate Phosphine, Arsine) Complexes: Effects of Chelate Ligands on Metal Basicity" *J. Am. Chem. Soc.* 114, **1992**, 160.

Stewart, J. J. P. "Semiempirical Molecular Orbital Methods" *Rev. Comp. Chem.* 1, **1990**, 45.

Stewart, R. F. "Small Gaussian Expansions of Slater-Type Orbitals" *J. Chem. Phys.* 52, **1970**, 431.

Straub, B. F. "Origin of the High Activity of Second-Generation Grubbs Catalysts" *Angew. Chem., Int. Ed.* 44, **2005**, 5974.

Straub, B. F. "Ligand Influence on Metathesis Activity of Ruthenium Carbene Catalysts: A DFT Study" *Adv. Synth. Catal.* 349, **2007,** 204.

Strohmeier, W.; Muller, F. J. "Klassifizierung Phosphorhaltiger Liganden in Metallcarbonyl-Derivaten nach der p-Acceptorstärke" *Chem. Ber.* 100, **1967**, 2812.

Suresh, C. H. "Molecular Electrostatic Potential Approach to Determining the Steric Effect of Phosphine Ligands in Organometallic Chemistry" *Inorg. Chem.* 45, **2006**, 4982.

Suresh, C. H. "Nature of α, β-CCC Agostic Bonding in Metallacyclobutanes" *J. Organomet. Chem.* 691, **2006,** 5366.

Suresh, C. H.; Baik, M. H. "α, β-(C–C–C) Agostic Bonds in Transition Metal Based Olefin Metathesis Catalyses" *Dalton Trans.* **2005**, 2982.

Suresh, C. H.; Gadre, S. R. "A Novel Electrostatic Approach to Substituent Constants: Doubly Substituted Benzenes" *J. Am. Chem. Soc.* 120, **1998**, 7049.

Suresh, C. H.; Gadre, S. R. "Electrostatic Potential Minimum of the Aromatic Ring as a Measure of Substituent Constant" *J. Phys. Chem. A.* 111, **2007**, 710.

Suresh, C. H.; Koga , N. "Orbital Interactions in the Ruthenium Olefin Metathesis Catalysts*" Organometallics* 23, **2004**, 76.

Suresh, C. H.; Koga, N. "Quantifying the Electronic Effect of Substituted Phosphine Ligands via Molecular Electrostatic Potential" *Inorg. Chem.* 41, **2002,** 1573.

Suresh, C. H.; Koga, N. "Orbital Interactions in the Ruthenium Olefin Metathesis Catalysts" *Organometallics* 23, **2004,** 76.

Suresh, C. H.; Koga, N.; Gadre, S. R. "Molecular Electrostatic Potential and Electron Density Topography: Structure and Reactivity of (substituted arene)Cr(CO)$_3$ Complexes" *Organometallics* 19, **2000**, 3008.

[a]Svensson, M.; Humbel, S.; Froese, R. D. J.; Matsubara, T.; Sieber, S.; Morokuma, K. "ONIOM: A Multilayered Integrated MO + MM Method for Geometry Optimizations and Single Point Energy Predictions. A Test for Diels-Alder

Reactions and Pt(P(t-Bu)$_3$)$_2$ + H$_2$ Oxidative Addition" *J. Phys. Chem.* 100, **1996**, 19357.

[b]Svensson, M.; Humbel, S.; Morokuma, K. "Energetics Using the Single Point IMOMO (Integrated Molecular Orbital+Molecular Orbital) Calculations: Choices of Computational Levels and Model System" *J. Chem. Phys.* 105, **1996**, 3654.

Szabo, A.; Ostlund, N. S. *Modern Quantum Chemistry Introduction to Advanced Electronic Structure Theory*, Dover, New York, **1996**.

Taft, R. W. *Steric Effects in Organic Chemistry*. Wiley: New York, **1956.**

Tebbe, F. N.; Harlow, R. L. "Titanacyclobutenes" *J. Am. Chem. Soc.* 102, **1980**, 6149.

Tebbe, F. N.; Parshall, G. W.; Ovenall, D. W. "Titanium-Catalyzed Olefin Metathesis" *J. Am. Chem. Soc.* 101, **1979**, 5074.

Tebbe, F. N.; Parshall, G. W.; Reddy, G. S. "Olefin Homologation with Titanium Methylene Compounds" *J. Am. Chem. Soc.* **1978**, 100, 3611.

Thomas, L. H. "The Calculation of Atomic Fields" *Proc. Cambridge Phil. Soc*. 23, **1927**, 542.

Tolman, C. A. "Electron Donor-Acceptor Properties of Phosphorus Ligands. Substituent Additivity" *J. Am. Chem. Soc.* 92, **1970**, 2953.

Tolman, C. A. "Steric Effects of Phosphorus Ligands in Organometallic Chemistry and Homogeneous Catalysis" *Chem. Rev.* 77, **197**7, 313.

Tonner, R.; Frenking, G. "C(NHC)$_2$: Divalent Carbon(0) Compounds with N-Heterocyclic Carbene Ligands—Theoretical Evidence for a Class of Molecules with Promising Chemical Properties" *Angew. Chem., Int. Ed*. 46, **2007**, 8695.

Tonner, R.; Frenking, G. "Carbodiphosphoranes: The Chemistry of Divalent Carbon(0)" *Angew. Chem. Int. Ed.* 46, **2007**, 8695.

Tonner, R.; Heydenrych, G.; Frenking, G. "Bonding Analysis of N-Heterocyclic Carbene Tautomers and Phosphine Ligands in Transition-Metal Complexes: A Theoretical Study" *Chem. Asian J.* 2, **2007**, 1555.

Tonner, R.; Öxler, F.; Neumüller, B.; Petz, W.; Frenking, G. "Carbodiphosphoranes: The Chemistry of Divalent Carbon(0)" *Angew. Chem., Int. Ed.* 45, **2006**, 8038.

Torrent, M.; Vreven, T.; Musaev, D. G.; Morokuma, K.; Farkas, O.; Schlegel, H. B. "Effects of the Protein Environment on the Structure and Energetics of Active Sites of Metalloenzymes. ONIOM Study of Methane Monooxygenase and Ribonucleotide Reductase" *J. Am. Chem. Soc.* 124, **2002**, 192.

Trnka, T. M.; Grubbs, R. H. "The Development of $L_2X_2Ru=CHR$ Olefin Metathesis Catalysts: An Organometallic Success Story" *Acc. Chem. Res.* 34, **2001**, 18.

Trnka, T. M.; Morgan, J. P.; Sanford, M. S.; Wilhelm, T. E.; Scholl, M.; Choi, T.; Ding, S.; Day, M. W.; Grubbs, R. H. "Synthesis and Activity of Ruthenium Alkylidene Complexes Coordinated with Phosphine and N-Heterocyclic Carbene Ligands" *J. Am. Chem. Soc.* 125, **2003,** 2546.

Tsipis, A. C.; Orpen, A. G.; Harvey, J. N. "Substituent Effects and the Mechanism of Alkene Metathesis Catalyzed by Ruthenium Dichloride Catalysts" *Dalton Trans.* **2005**, 2849.

Ujaque, G.; Cooper, A. C.; Maseras, F.; Eisenstein, O.; Caulton, K. G. "Computational Evidence of the Importance of Substituent Bulk on Agostic Interactions in $Ir(H)_2(P^tBu_2Ph)_2+$ " *J. Am. Chem. Soc.* 120, **1998**, 361.

van Hecke, G. R.; Horrocks, Jr. W. D. "Approximate Force Constants for Tetrahedral Metal Carbonyls and Nitrosyls" *Inorg. Chem.* 5, **1966**, 1960.

van der Eide, E. F.; Piers, W. E. "Mechanistic Insights into the Ruthenium-Catalyzed Diene Ring-Closing Metathesis Reaction" *Nat. Chem.* 2, **2010**, 571.

van Veldhuizen, J. J.; Campbell, J. E.; Giudici, R. E.; Hoveyda, A. H. "A Readily Available Chiral Ag-Based N-Heterocyclic Carbene Complex for Use in Efficient and Highly Enantioselective Ru-Catalyzed Olefin Metathesis and Cu-Catalyzed Allylic Alkylation Reactions" *J. Am. Chem. Soc.* 127, **2005**, 6877.

Vaughan, W. M.; Abboud, K. A.; Boncella, J. M. "Mechanism of the Formation of a Tungsten(VI) Alkylidene Complex Which Undergoes Reversible Metalation of an Ancillary Ligand" *J. Am. Chem. Soc.* 117, **1995**, 11015.

Vehlow, K.; Gessler S.; Blechert S. "Deactivation of Ruthenium Olefin Metathesis Catalysts through Intramolecular Carbene-Arene Bond Formation" *Angew. Chem., Int. Ed.* 46, **2007,** 8082.

Vehlow, K.; Maechling, S.; Blechert, S. "Ruthenium Metathesis Catalysts with Saturated Unsymmetrical N-Heterocyclic Carbene Ligands" *Organometallics* 25, **2006**, 25.

Vougioukalakis, G. C.; Grubbs, R. H. "Ruthenium-Based Heterocyclic Carbene-Coordinated Olefin Metathesis Catalysts" *Chem. Rev.* 110, **2010**, 1746.

Vougioukalakis, G.C., Grubbs, R. H. "Ruthenium Olefin Metathesis Catalysts Bearing an N-Fluorophenyl-N-Mesityl-Substituted Unsymmetrical N-Heterocyclic Carbene" *Organometallics* 26, **2007**, 2469.

Vreven, T.; Mennucci, B.; da Silva, C. O.; Morokuma, K.; Tomasi, J. "The ONIOM-PCM method: Combining the Hybrid Molecular Orbital Method and the Polarizable Continuum Model for Solvation. Application to the Geometry

and Properties of a Merocyanine in Solution" *J. Chem. Phys.* 115, **2001**, 62.

Vreven, T.; Morokuma, K. "On the Application of the IMOMO (Integrated Molecular Orbital + Molecular Orbital) Method" *J. Comput. Chem.* 21, **2000**, 1419.

Vyboishchikov, S. E.; Bühl, M.; Thiel, W. "Mechanism of Olefin Metathesis with Catalysis by Ruthenium Carbene Complexes: Density functional Studies on Model Systems" *Chem.Eur. J.* 8, **2002,** 3962.

Wanzlick, H. W.; Schönherr, H. J. "Direct Synthesis of a Mercury Salt-Carbene Complex" *Angew. Chem., Int. Ed. Engl.* 7, **1968**, 141.

Warshel, A.; Levitt, M. "Theoretical Studies of Enzymatic Reactions: Dielectric, Electrostatic and Steric Stabilization of the Carbonium Ion in the Reaction of Lysozyme" *J. Mol. Biol.* 103, **1976**, 227.

Weigend, F.; Ahlrichs, R. "Balanced Basis Sets of Split Valence, Triple Zeta Valence and Quadruple Zeta Valence Quality for H to Rn: Design and Assessment of Accuracy" *Phys. Chem. Chem. Phys.* 7, **2005**, 3297.

Weiner, P. K.; Kollman, P. A. "AMBER: Assisted Model Building with Energy Refinement. A General Program for Modeling Molecules and Their Interactions" *J. Comput. Chem.* 2, **1981**, 287.

Weskamp, T.; Kohl, F. J.; Hieringer, W.; Gleich, D.; Herrmann, W. A. "Highly Active Ruthenium Catalysts for Olefin Metathesis: The Synergy of N-Heterocyclic Carbenes and Coordinatively Labile Ligands" *Angew. Chem., Int. Ed.* 38, **1999**, 2416.

Weskamp, T.; Schattenmann, W. C.; Spiegler, M.; Herrmann, W. A. "A Novel Class of Ruthenium Catalysts for Olefin Metathesis" *Angew. Chem., Int. Ed. Engl.* 37, **1998**, 2490.

White, D.; Coville, N. J. "Quantification of Steric Effects in Organometallic Chemistry" *Adv. Organomet. Chem*. 36, **1994**, 95.

Wilson, M. R.; Liu, H. Y.; Prock, A.; Giering, W. P. "Reinvestigation of the Oxidative Addition of Methyl Iodide, Hydrogen, and Oxygen to Ir(CO)(Cl)L$_2$. Quantitative Analysis of Ligand Effects (QALE)" *Organometallics*. 12, **1993**, 2044.

Wilson, M. R.; Prock, A.; Giering, W. P.; Fernandez, A. L.; Haar, C. M.; Nolan, S. P.; Foxman, B. M. " Effects Involving Rh-PZ$_3$ Compounds. The Quantitative Analysis of Ligand Effects (QALE)" *Organometallics*. 21, **2002**, 2758.

Woon, D. E.; Dunning Jr., T. H. "Gaussian Basis Sets for Use in Correlated Molecular Calculations. III. The Atoms Aluminum through Argon" *J. Chem. Phys*. 98, **1993**, 1358.

Zhao Y, Truhlar DG. "Density Functionals with Broad Applicability in Chemistry" *Acc. Chem. Res.* 41, **2008**, 157.

Zhao, Y.; Schultz, N. E.; Truhlar, D. G. "Exchange-Correlation Functional with Broad Accuracy for Metallic and Nonmetallic Compounds, Kinetics, and Noncovalent Interactions" *J. Chem. Phys.* 123, **2005**, 161103.

Zhu, S. S.; Cefalo, D. R.; La, D. S.; Jamieson, J. Y.; Davis, W. M.; Hoveyda, A. H.; Schrock, R. R. "Chiral Mo-Binol Complexes: Activity, Synthesis, and Structure. Efficient Enantioselective Six-Membered Ring Synthesis through Catalytic Metathesis" *J. Am. Chem. Soc*. 121, **1999**, 8251.

Ziegler, K.; Holzkamp, E.; Breil, H.; Martin, H. "The Mühlheim Low-Pressure Polyethylene Process" *Angew. Chem., Int. Ed.* 67, **1955**, 541.